DESIGN OF RECONFIGURABLE ANTENNAS FOR MULTIBAND RADIOS

A THESIS SUBMITTED TO AUCKLAND UNIVERSITY OF TECHNOLOGY
IN FULFILMENT OF THE REQUIREMENTS FOR THE DEGREE OF
DOCTOR OF PHILOSOPHY

Adnan Ghaffar
School of Engineering, Computer and Mathematical Sciences

December 2020

Attestation of Authorship

I hereby declare that this submission is my own work and that, to the best of my knowledge and belief, it contains no material previously published or written by another person nor material which to a substantial extent has been accepted for the qualification of any other degree or diploma of a university or other institution of higher learning.

Signature of candidate

Acknowledgements

First of all, many thanks to **ALLAH ALMIGHTY**, who has provided me this opportunity and give me strength with patience during this hard time of study. I would not able to complete this research work without the blessings of **ALLAH ALMIGHTY**.

I wish to express my deepest thanks to my primary supervisor **Dr. Xue Jun Li** Associate Professor, School of Engineering, Computer Science and Mathematical Science, Auckland University of Technology, New Zealand for his excellent support, scientific guidelines, encouragement, critical review, and motivation, which helps me to uplift my knowledge and polish my skills. My profound appreciation for my secondary supervisor **Dr. Boon-Chong Seet** for his kind and valuable suggestion to improve my research work. I am also thankful to **Jian Huang** for helping to perform the experiment testing in Communication Laboratory.

Last but not least, I would like to acknowledge the efforts of my parents in spiritual and financial ways. I will also thanks to my sweet wife Aneeqa Kiran for her care, love, and emotional support.

Adnan Ghaffar

December 2020

Abstract

In recent years, telecommunication technologies have witnessed exponential growth, especially in the cellular communications and wireless sensor networks. To meet the demand of increasing transmission capacity, it is necessary to improve the signal to noise ratio of cellular communication channels and enable multiple frequency bands operations. It is difficult to design a mobile device with multi-standard antennas.

Passive antennas have reached their limit, and the use of a frequency reconfigurable antenna to extend operational bandwidth is a promising solution. A reconfigurable antenna can be considered as one of the key elements in future wireless communication transceivers. By using reconfigurable antennas, the total antenna volume can be reused, thus leading to a compact system design.

Due to advancement in modern communication systems, mobile devices are becoming more compact. Motivated by this requirement, we propose a new design for compact reconfigurable antennas. These antennas operate in different bands and shows good agreement results. A novel dual band reconfigurable antenna with horizontal and vertical polarization was demonstrated. Its frequency and polarization reconfigurability has useful applications in tracking, sending and radar, etc. The current distribution and mathematical analysis of different mode justify the proposed concept.

Compact size along with the multi-band functionality is the great need of current electronic and communication industry. For this purpose, different novel frequency reconfigurable monopole antennas are proposed. One antenna offers a wideband mode

of 3-8GHz along with narrow bands at various frequencies of 2.1 GHz, 2.25 GHz, 2.45 GHz, 3.3 GHz, 3.5 GHz, and 8 GHz. Other antennas are proposed for 5G sub-6-GHz band, which make it suitable candidate for 2.1 GHz 4G-LTE band, 2.45 GHz ISM band, 5G-sub-6-GHz band and S-band satellite applications.

Flexible antenna have gained much attention in wearable electronics industry. To cover this, a hybrid frequency and pattern reconfigurable antenna is presented. The frequency of the proposed antenna can be shifted from 2.1 GHz to 1.8 GHz by switching the state of both diodes in OFF and ON-state, respectively. For the ISM band applications, another capacitor loaded DGS flexible antenna is explored. The strong agreement between simulated and measured results for both conformal and non-conformal conditions makes the proposed work a promising candidate for the applications operating in 3G, 4G, LTE, GSM, and ISM bands.

Contents

List of Tables

List of Figures

Glossary and Notations

Glossary

DGS	Defected Ground Structure
RA	Reconfigurable Antenna
WiMAX	Worldwide Interoperability for Microwave Access
WLAN	Wireless local Area Network
GPS	Global Positioning System
UMTS	Universal Mobile Telecommunications System
RF	Radio Frequency
MEMS	Micro-Electromechanical System
FET	Field-Effect Transistor
CP	Circular Polarization
LC	Liquid Crystal
SIW	Substrate Integrated Waveguide
CR	Cognitive Radio
RHCP	Right Hand Circular Polarization ,
LHCP	Left Hand Circular Polarization
ME	Magneto-Electric
BTFB	Back-to-Back F
EBG	Electromagnetic Bandgap
AR	Axial Ratio

MS	Metasurface
BLC	Branch Line Coupler
PIFA	Planar Inverted-F Antenna
MIMO	Multiple-input and Multiple-output
QHA	Quadrifilar Helical Antenna
SIW	Substrate Integrated Waveguide
PTH	Plated-through Hole
ST-SRR	Slot-type Split Ring Resonator
SPDT	Single-pole Double-throw
AMC	Artificial Magnetic Conductor
SAR	Specific Absorption Rate
PDMS	Polydimethylsiloxane
IoT	Internet of Things
CPW	Co-planar Waveguide
FEM	Finite Element Method
HFSS	High-frequency Structure Simulator
UWB	Ultra Wideband
ISM	Industrial, Medical and Medical
VNA	Vector Network Analyzer

Notation

Z_L	Load Impedance
Z_R	Radiating Mode Impedance
Z_B	Impedance of Short Circuit Transmission
ε_r	Relative Permittivity
ε_{eff}	Efective Dielectric Constant
h	Thickness of Substrate
λ	Free Space Wavelength
c	Speed of the Light
f_o	Central Resonating Frequency
x_o	Expression Coefficient
L_{eq}	Equivlent Inductance
C_{eq}	Total Equivalent Capacitance
S_{11}	Return Loss
E	Finite Lenght
L_{Si}	Inductance for Radiating Mode
C_{Si}	Capacitance
R_{Si}	Resistance
Φ	Phase Difference

Chapter 1

Introduction

1.1 Background

Antenna plays an important role in the performance of any wireless communication system. An antenna can be defined as a structure, which is associated with the transition region between free space and guiding medium that transmits and receives the electromagnetic waves. It functions as a transducer, which transforms the electric signals into radio waves at the transmitting end and converts the radio waves back into the electric current at the receiving end. The antenna carries an altering current, which generates an EM field around the wire that varies in the same manner as the current does. If another conducting wire is placed near the antenna, the electromagnetic field will induce a weaker electric current in the wire.

Antennas finds their applications in radios, television, RADAR, cell phones, and spacecraft. Antennas can be classified according to different applications: radio antennas, television antennas or vehicle antennas. Antennas vary in terms of coverage. Antenna may also be classified according to installation location, such as: indoor antennas and outdoor antennas.

In the last few decades, the ever-increasing demand for high data rate communication

has made the wireless systems the fastest growing sector of the communication industry. As the name suggests, wireless communications refer to the transmission of data without using wires, cables or any other type of conducting materials. Initially, the minor portion of EM spectrum was utilized in optical devices but with the advancement in technology, the communication systems are also utilizing the electromagnetic spectrum outside the visible region. For example, the cellular systems have evolved from the first generation (1G) analogue system to the fifth generation (5G) high-speed digital system. Antenna is a vital part of the communication system and a wireless communication. It helps not only to transmit the message but also to receive it. Since the advent of the wireless technology, the compact size, high performance (in terms of coverage, capacity, and transmission quality) and low cost antenna has huge demand in the market.

Incorporating several communication standards within a single system is the major necessity of modern wireless communication to operate at multiple frequencies for different applications. A straightfoward solution is to use multiple antennas, each for a frequency band. However, this solution will increase the cost and the complexity of the communication system. In addition, it creates the mutual coupling problem, which in turn degrades the performance of the antenna. Dual-band antennas mitigate the effects of electromagnetic interference and distortion, thus offering preferred usage over single-band antennas. Dual-band antennas are indispensable in order to simplify the communication structures for multi-standard operation, high data rate, saving cost, reducing size and eliminating undesirable coupling between antennas.

1.2 Motivation

With the recent advancement in the telecommunication industry, there is ever-increasing demand of compact, high speed mobile devices. Antenna is the vital part of every wireless communication system and electronic device, and it has vast applications like

vehicular communication, Internet of Things (IoTs), global positioning systems (GPS), global system for mobile communication (GSM), Bluetooth, wireless local area network (WLAN), and satellite communications. Mostly antennas designed for a specific application have constant functional properties (fixed polarization, radiation pattern, and frequency). However, to cope with modern wireless communication networks that requires the integration of multiple radios into a single device, the implementation of fixed frequency band antenna can lead to several problems , e.g. very large volume, complex circuitry, and low efficiency. To address these problems, multiband and smart antennas are required. However, it remains challenging to support multiple wireless standards with the limitation of mobile devices in size and circuit complexity.

To address the current and future demands of the increasing number of mobile subscribers and their high data rate multimedia applications, it is of great interest to design flexible, small size, controllable, and easily adjustable antenna. Reconfigurable antennas have become a promising solution. They can support multiple frequency band and improve the spectrum utilisation efficiency. Increasing attention is being drawn to reconfigurable antennas due to their compact size, low cost, less complex, more feasible, and planar design. Reconfigurable antennas can be achieved by changing the frequency, polarization, and radiation pattern properties according to the requirement.

1.3 Objectives

The objective of this doctoral work is to proposed reconfigurable antennas from their actual state as a conceptual structure into a practical reconfigurable antenna architecture. The specific goals pursued in this work focus on defining new geometries to reduce the antenna complexity and also on the performance evaluation of the antenna reconfigurability. These goals range from the conceptualization of the reconfigurable antenna geometry and new technological approaches, to experimental characterization

techniques and the theoretical derivation of figures-of-merit, and are listed below:

1. Propose novel antenna geometries and new conceptual architectures to improve the antenna reconfigurability while reducing the required number of switches and/or the overall complexity of the antenna. These geometries must remove the high level of redundancy of the existing reconfigurable antennas. Alternative conceptual architectures must explore new roles of reconfigurable antenna, for instance as patch slot antenna.

2. Explore switching and reconfiguration technologies for novel reconfigurable antennas. Analyze the capabilities of existent semiconductor switches and develop new reconfiguration technologies to reduce insertion losses, increase isolation, decrease actuation power and in general to improve the switch and the reconfigurable antenna performances

3. Enhance the knowledge about the maximum reconfiguration capabilities of patch slot antennas. Existing publications explore specific optimized configurations, but leave unexplored the full reconfiguration properties of the antenna. The full frequency reconfiguration range and the complete diversity of radiation patterns must be characterized to properly judge the reconfiguration level of reconfigurable antennas.

4. Derive figures-of-merit to evaluate the reconfiguration level of monopole antennas and its impact over the system-level performance. Specific figures-of-merit to quantify antenna reconfigurability are not yet available in the current literature, even though being crucial to compare and determine which reconfigurable antenna designs provide higher performance.

1.4 Research Questions

The inappropriate feeding network, larger antenna size, complex reconfigurable mechanism in current research on reconfigurable antennas motivate us to further reduce the antenna size to cope up with modern wireless communication standards. The research questions are given below:

1. Is it possible to design simple and low profile antenna design?
2. What are the most accurate,less complex and simple biasing techniques that will not affect the radiation pattern and overall antenna efficiency?
3. What are best possible methods for flexible materials fabrication and the integration of the lumped components with wearable devices?
4. Is it possible to integrate multiple reconfigurability techniques into one design ?

1.5 Original Contribution

The main contribution of this thesis is as follows:

- **Compact Reconfigurable PIFA Antennas for Mobile Devices**.

  This work is comprised of frequency reconfigurable microstrip planar inverted-F antenna (PIFA) antenna. The compact antenna size 44mm $\times$ 14mm is mounted on FR4-substrate. Two PIN diodes are used to resonate the antenna at GSM 850/900, GLONASS 1616, DCS 1800, PCS 1900, and UMTS 2100 frequency bands. The antenna achieves omnidirectional radiation pattern for different frequencies.

  The second design presents the design of a compact PIFA with reconfigurable dual resonance frequency of 800 MHz and 1.4 GHz, and switchable horizontal and vertical polarization for mobile devices. By controlling the ON/OFF states

of two PIN diodes, four operation modes (combinations of two frequencies and two polarizations) can be achieved. The proposed antenna has a gain of 3.7 dBi, efficiency of up to 92%, and a reflection coefficient of less than -10 dB over the resonant bands for both horizontal and vertical polarization.

- **Design of Reconfigurable Antenna for Multiple Band Applications**

  The proposed multiband multi-mode frequency reconfigurable antenna comprises of a simple geometrical structure along with compact overall size of 15mm $\times$ 30mm $\times$ 1.6mm. The proposed compact size antenna could be a potential candidate for portable devices operating inside Wi-Max, WLAN, 5G-sub-6GHz, S-band, and X-band.

  Another frequency reconfigurable antenna is proposed to cover sub 6 GHz. By changing the states of two PIN diodes, resonance in the sub 6 GHz band (2.5 GHz, 3.5 GHz, and 3.7-4.2 GHz) is achieved. When both diodes are ON, it resonate at 2.18-2.36 GHz, 2.68-3.32 GHz, and 3.75-4.50 GHz. In dual-band case, when both diodes are OFF, the resonance frequency is 2.25-2.58 GHz, and 3.5-4.46 GHz.

  Next, an 8-band frequency reconfigurable antenna is presented. The antenna can operate in four dual-band modes. The antenna has a size of 18mm $\times$ 18mm $\times$ 1.6mm.

- **Flexible Frequency and Radiation Pattern Reconfigurable Antenna**

  For hybrid reconfigurable antennas, this thesis presents a compact frequency and pattern reconfigurable flexible antenna for heterogeneous applications. A triangular monopole antenna with a semicircular stub is made frequency and pattern tunable by connecting and disconnecting two inverted L-shaped stubs utilizing PIN diodes. The antenna features a compact size of 40mm $\times$ 50mm

$\times$ 0.254mm, while the operational bandwidth is from 1.65 GHz to 2.51 GHz with pattern reconfigurability of 180° in the E-plane. The antenna is a promising candidate for heterogeneous applications including the GSM band (1800 and 1900 MHz) and ISM band (2.4 GHz) along with well-known cellular communication bands of 3G, 4G, and LTE bands ranging from 1700-2300 MHz around the globe.

The last antenna presented in this thesis features a compact dual-band flexible antenna. The antenna geometry consists of serpentine shaped to achieve a compact size antenna and defected ground structure (DGS) was used to improve matching for the lower resonance band. Furthermore, an additional capacitor is loaded in the DGS to achieve the higher resonance band. The antenna geometry consists of simple structure and shows a compact size of 78mm $\times$ 40mm $\times$ 0.254mm. To validate the design, an antenna prototype is fabricated, and a comparison of various performance parameters is presented.

1.6 List of Publication

Journal Paper

1 . **Adnan Ghaffar**, Wahaj Abbas Awan, Abir Zaidi, Niamat Hussain, Syed Muhammad Rizvi, Xue Jun Li, "Compact Ultra Wide-Band and Tri-Band Antenna for Portable Device." In *Radioengineering*, 29(4), 2020.

2 . **Adnan Ghaffar**, Xue Jun Li, Wahaj Abbas Awan, Syeda Iffat Naqvi, Niamat Hussain, Bong Chong Seet, Mohammad Alibakhshikenari, Francisco Falcone, Ernesto Limiti. "Design and Realization of a Frequency Reconfigurable Multimode Antenna for ISM, 5G-sub-6-GHz and S-band Applications." In *MPDI Applied Sciences*, 11(4),p. 1635, 2021.

3 . **Adnan Ghaffar**, Xue Jun Li, Wahaj Abbas Awan, Aqeel Hussain Naqvi, Niamat Hussain, Mohammad Alibakhshikenari, Ernesto Limiti. "A Flexible and Pattern Reconfigurable Antenna with Small Dimensions and Simple Layout for Wireless Communication Systems Operating over 1.65–2.51 GHz." In *MPDI Electronics*, 10(5), p. 601, 2021.

4 . **Adnan Ghaffar**, Xue Jun Li, Wahaj Abbas Awan, Amir Hossein Nazeri, Niamat Hussain, Boon-Chong Seet, "Compact Multiband Multimode Frequency Reconfigurable Antenna for Heterogeneous Wireless Applications". In *RF and Microwave Computer-Aided Engineering*, e22659, 2021.

Conference Paper

1. **Adnan Ghaffar**, Xue Jun Li, and Boon-Chong Seet, "Dual frequency band and polarization reconfigurable antenna for mobile devices." In IEEE 17^{th} International Conference on Communication Technology (ICCT), pp. 696-700, 2017.

2. **Adnan Ghaffar**, Xue Jun Li, and Boon-Chong Seet, "Compact Dual-Band Broadband Microstrip Antenna at 2.4 GHz and 5.2 GHz for WLAN Applications." In IEEE 7^{th} Asia-Pacific Conference on Antennas and Propagation (APCAP), pp. 198-199, 2018.

3. **Adnan Ghaffar**, Xue Jun Li, Boon-Chong Seet, Wahaj Abbas Awan, and Niamat Hussain, "Compact Multiband Frequency Reconfigurable Antenna for 5G Communications." In IEEE 29^{th} International Telecommunication Networks and Applications Conference (ITNAC), pp. 1-3, 2019.

4. **Adnan Ghaffar**, Xue Jun Li, Niamat Hussain, and Wahaj Abbas Awan, "Flexible Frequency and Radiation Pattern Reconfigurable Antenna for Multi-Band Applications." In IEEE 4^{th} Australian Microwave Symposium (AMS), pp. 1-2, 2020.

5. **Adnan Ghaffar**, Xue Jun Li, Wahaj Abbas Awan, and Niamat Hussain, "A Compact Dual-Band Antenna Based on Defected Ground Structure for ISM Band Applications." In WSA 24^{th} International ITG Workshop on Smart Antennas, pp. 1-2. VDE, 2020.

6. **Adnan Ghaffar**, Xue Jun Li, Wahaj Abbas Awan, and Niamat Hussain, "A Compact Multiband Multi-Mode Frequency Reconfigurable Antenna for Portable Devices." In IEEE 5^{th} International Conference on The UK-China Emerging Technologies (UCET), pp.1-4, 2020.

7. **Adnan Ghaffar**, Xue Jun Li, Wahaj Abbas Awan, and Niamat Hussain, " Capacitor Loaded Dual-band Flexible Antenna for ISM Band Applications." In IEEE 9^{th} Asia-Pacific Conference on Antennas and Propagation (APCAP), pp.1-2, 2020.

8 . **Adnan Ghaffar**, Xue Jun Li, Tanveer Ahmad, Niamat Hussain, Mohammad Alibakhshikenari, and Ernesto Limiti, "Circulary Polarized Pattern Reconfigurable Flexible Antenna for 5G-sub-6-GHz Applications." In IEEE Asia-Pacific Microwave Conference (APMC), pp.625-627 2020.

9 . **Adnan Ghaffar**, Xue Jun Li, Tanveer Ahmad, " A Compact Frequency Reconfigurable PIFA Antenna for Heterogeneous Applications." In IEEE Asia-Pacific Microwave Conference (APMC), pp.628-630, 2020.

Book Chapter

1. **Adnan Ghaffar**, Xue Jun Li, Wahaj Abbas Awan, and Niamat Hussain," Reconfigurable Antennas: Analysis and Applications." Wideband, Multiband and Smart Antenna Systems by SPRINGER. (Accepted).

Contribution to other Related Works

1. Awan, Wahaj Abbas, **Adnan Ghaffar**, Niamat Hussain, and Xue Jun Li, "A Frequency Reconfigurable Flexible Antenna for Multiple Mobile Applications." In IEEE Asia-Pacific Microwave Conference (APMC), pp. 813-815, 2019.

2. Awan, Wahaj Abbas, Niamat Hussain, **Adnan Ghaffar**, Abir Zaidi,Syeda Iffat Naqvi, and Xue Jun Li, "Compact Flexible Frequency Reconfigurable Antenna for Heterogeneous Applications." In IEEE 9^{th} Asia-Pacific Conference on Antennas and Propagation (APCAP), pp.1-2, 2020.

3. Awan, Wahaj Abbas, Niamat Hussain **Adnan Ghaffar**, Abir Zaidi , and Xue Jun Li, "A Compact Flexible Antenna for ISM and 5G Sub-6-GHz band Application." In WSA 24^{th} International ITG Workshop on Smart Antennas, pp. 1-3. VDE, 2020.

4. Ahmad, Tanveer, Xue Jun Li, Jiang Wenchao, **Adnan Ghaffar**, " Frugal Sensing: A Novel approach of Mobile Sensor Network Localization based on Fuzzy-Logic." In ACM Proceeding of MobiArch, The 15^{th} Workshop on Mobility in the Evolving Internet Architecture, pp. 8-15, 2020.

5. Niamat Hussain,Awan, Wahaj Abbas, Syeda Iffat Naqvi, **Adnan Ghaffar**, Abir Zaidi,Syed Aftab Naqvi, Adnan Iftikhar, and Xue Jun Li, "A Compact Flexible Frequency Reconfigurable Antenna for Heterogeneous Applications." In IEEE Access, pp.173298-173307, 2020.

6. Adamu Halilu Jabire, **Adnan Ghaffar**, Xue Jun Li, Anas Abdu, Sani Saminu, Abubakar Muhammad Sadiq, and Adamu Mohammad Jajere, " Design of A Compact UWB/MIMO Antenna with High Isolation and Gain." In IEEE Workshop on Microwave Theory and Techniques in Wireless Communications (MTTW), pp. 72-75, 2020.

7. Awan, Wahaj Abbas, **Adnan Ghaffar**, Niamat Hussain, and Xue Jun Li, "CPW-Fed Dual-Band Antenna for 2.4/5.8 GHz Applications." In IEEE 8^{th} Asia-Pacific Conference on Antennas and Propagation (APCAP), 2019.

8. Awan, Wahaj Abbas, Niamat Hussain, **Adnan Ghaffar**,Syeda Iffat Naqvi, Abir Zaidi, Musa Hussain, and Xue Jun Li, "A Low Profile Frequency Reconfigurable Antenna for mmWave Applications." In Springer 6^{th} International Conference on Wireless Technologies, Embedded and Intelligent Systems (WITS), 2020. (Accepted).

9. Awan, Wahaj Abbas, Syed Iffat Naqvi, Niamat Hussain, **Adnan Ghaffar**, Abir Zaidi, and Xue Jun Li, "A miniaturized UWB Antenna for Flexible Electronics." In IEEE AP-S Symposium on Antenna and Propagation (CNC/USNC-URSI),2020.

10. Adamu Halilu Jabire, **Adnan Ghaffar**, Xue Jun Li, Sani Saminu, Mohammad Alibakhshikenari, Ernesto Limiti, and Fransisco Falcone, "Metamaterial-Based Desing of Compact UWB/MIMO Monopoles Antenna with Characteristic Mode Analysis." In MDPI Applied Sciecne, 11(4), p. 1542, 2021.

1.7 Thesis Organization

The rest of the thesis is organized as follows:

Chapter 2 starts with the history of the reconfigurable antennas, then explains the current research on the different reconfigurable techniques. From physical to optical reconfiguration techniques, including electrical and material-based methods to attain the reconfigurability, are explained in detail. Reconfigurable properties like frequency, radiation pattern, polarization are investigated with examples. The importance of the reconfigurable antenna in wearable technology, band-notching and some other latest

applications in modern communications systems like MIMO, SDR, and wireless sensing are also included at the end of the chapter.

Chapter 3 presents the frequency reconfigurable PIFA antennas. First, a compact frequency reconfigurable antenna using two PIN diodes were designed to cover GSM 850/ 900 and UMTS 2100 frequency bands. The measurement results show the good agreement with simulated results. In second design, hybrid reconfigurable PIFA antenna was presented. The antenna by using four PIN diodes operates at 800 MHz and 1.4 GHz frequency by switching between horizontal and vertical polarization. The antenna design and working principle is also explained in detail.

Chapter 4 presents three frequency reconfigurable antennas for different wireless applications. It starts with the monopole frequency reconfigurable antenna, which consists of two stubs that are connected with the help of PIN diodes. Next, microstrip patch antenna is designed. It is based on a wideband antenna, subsequently is converted into frequency reconfigurable antenna. Two V-shaped slots are etched on the triangle patch, and PIN diodes are inserted to get the required frequency. In third design, a compact octaband monopole frequency reconfigurable antenna was presented in detail. The proposed antennas were also compared with state-of-the-art-works.

Chapter 5 demonstrates two reconfigurable antennas on flexible material. The antenna consists of semicircular patch on the triangular radiator with two L-shaped stubs. PIN diodes are used to connect between stubs and radiator. With a fabricated antenna, the measurement results are verified against simulated results, and good agreement was achieved. The bending analysis in X & Y axis direction is also studied. In second work, the serpentine and DGS shape radiator loaded with capacitor is design. The proposed antenna resonates at 850 MHz and 2520 MHz frequency.

Chapter 6 concludes the whole research work and provides recommendations for the future work in reconfigurable antenna designs.

Chapter 2

Literature Review

2.1 History of Reconfigurable Antenna

The concept of reconfigurable antennas was investigated since the late 1990s, and recently it gained much attention in industry and research due to the advancement in modern wireless communication systems. In the early 1920s, some antenna with reconfigurable properties were designed to tune the frequency and to steer the beam. However, the shifting between the frequencies and their characteristics parameters were controlled by external parameters.

The initial work related to the frequency reconfigurability was presented in a patent by Norton in 1926 [1], and the frequency shifting was achieved by using variable inductive loading. In the early 1930s, another reconfigurable antenna consists of the nulls in the form of the two-element array was explained in [2], and it was steered by using a calibrated variable phase changer to determine the direction of arrival of a signal. The radiation pattern reconfigurable antenna was presented in [3] as shown in Figure 2.1. It is rhombic-wire antenna and motor with counterweights was used to change the dimension and angles of the proposed antenna. The multiple-unit steerable antenna (MUSA) was the combination of a six-element array of rhombic antennas with phase

shifters [4], and the beams were steered in the elevation plane.

The development of antennas with radiation pattern agility took place towards the 1940s,which was mainly driven by the World War II when beam-scanning antennas played a key role in radar applications. The main techniques to achieve beam scanning were movable, multi-feed reactors and phased-arrays. However, one can argue that these designs are not reconfigurable antennas since there is not a clear interaction between the reconfiguration and the radiation mechanism. Another example of a frequency tunable antenna was found in a patent by E. Werndl in 1942, where it is proposed to adjust the length of the dipole antenna by using a liquid metal [5]. This array had 13 rotary phase changers for beam steering [6].

The combination of reconfiguration and radiation was explained by Rotman and Maestri in 1960, and it behave as reconfigurable antennas [7]. In this technique, the modes of the radiation waveguide were switched electromechanically to get the different radiation beams. Some years after the first frequency tunable antennas, the first design of antennas with steerable radiation pattern appeared. In 1979, "*reconfigurability*"was defined as "*the ability to adjust beam shapes upon the command*" [8]. The authors used a six-beam antenna to dynamically change the coverage area for a communications satellite. Several additional papers reported other reconfigurable space-based arrays. Moreover, the first patent on frequency tunning and polarization switching antenna was claimed by Schaubert in [9]. The mostly early design reconfigurable antennas lack of few functions with huge physical control, but they opened new paths for the research on antenna reconfigurability.

In the 1990s, the advancement in the cellular networks, vast development of wireless sensor networks, and telecommunication-based services open a new era of modern communication systems. To make the wireless system robust and portable was the priority at that time. Additionally, in the following years, other wireless standards (e.g. Worldwide Interoperability for Microwave Access (WiMAX), Wireless local area

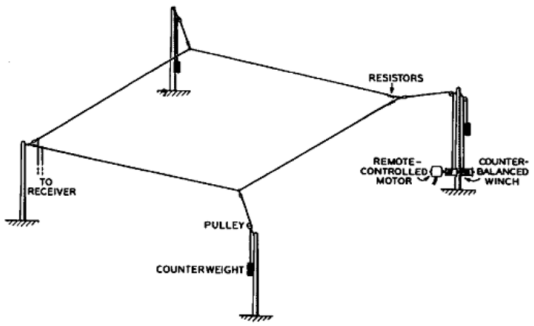

Figure 2.1: Beam steerable rhombic antenna [3]

network (WLAN), Bluetooth, Global Positioning System (GPS), Universal Mobile Telecommunications System (UMTS) were introduced in the market to fulfil the desire of modern communication systems. To support different wireless standards and cover the wide area to for quality service, a single wireless device must be powerful to provide the high data rate, strong reliability, and high efficiency. To address that, multiple fixed frequency antennas create a big challenge for hand-held mobile devices.

In the 2000s, many reconfigurable antennas were reported on the different designs of frequency shifting, radiation pattern and polarization switching applications [10, 11]. Due to the recent development in the modern communication systems, the pace of the research of reconfigurable antenna has been speed up.

As mentioned previously, the physical modification technique is not always reliable. Electronic switching is a promising technology, which was implemented in many of the latest designs. Smart materials were also incorporated in the recent designs [12, 13, 14]. Furthermore, other novel designs investigated the printed antenna technology, which can be easily integrated with switching / tuning elements. Many antenna types like monopole, patch, Yagi-Uda, and dipole have been explored in the last few decades. However, it remains a significant challenge to create a multi-mode, multi-functional integrated antenna to cope up with the latest wireless communication systems.

2.2 Reconfigurable Techniques

The concept of reconfigurability in the context of an antenna refers to the capability to change its characteristic antenna electrical parameters through electric or mechanic mechanisms. Ideally, a reconfigurable antenna is designed to change the resonant frequency, input impedance, bandwidth, polarization, and radiation pattern as a function of the required systems. Broadly speaking, there are five different mechanisms to reconfigure an antenna, which are discussed as follows.

2.2.1 Physical Reconfigurable Antenna

Physical reconfiguration is one basic and classic technique that was used in the early designs. Under this category, the antenna characteristics can be modified by changing the antenna structure by mechanical systems. Over time, innovative ideas were developed by implementing the actuation methods, and this helps to change the antenna structure by shifting radiation parts to get the reconfigurable antenna parameters. For example, devices like stepper motors, linear actuators were implemented to fully or partially modify the antenna dimension. The motor-control based [15], and rotatable antennas [16] were successfully demonstrated. Moreover, reconfigurable antennas based on electrostatic/magnetic actuator were also presented in [17], and they achieved satisfactory results. A frequency reconfigurable antenna consisting of parasitic elements was presented in [18] as shown in Figure 2.2 (a), and frequency is tuned with the help of a piezoelectric actuator. In another example, as shown in Figure 2.2 (b), where frequency reconfiguration is obtained by adjusting the inclination angle, and it was magnetically controlled to get the required resonant frequency [17]. Besides these, physical adjustment by using the liquid metals can also be used to attain the reconfigurability in the form of the stretchable antennas [19] as shown in Figure 2.2 (c).

Although physical modification has been presented successfully in many designs, it has

some drawbacks like slow speed, less life cycle and dependence on the antenna physical dimensions. Despite these, it is still a promising technology for higher frequency band application where other technologies are limited due to some electrical characteristics.

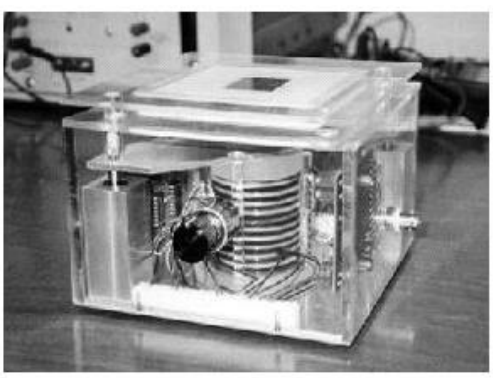

(a)

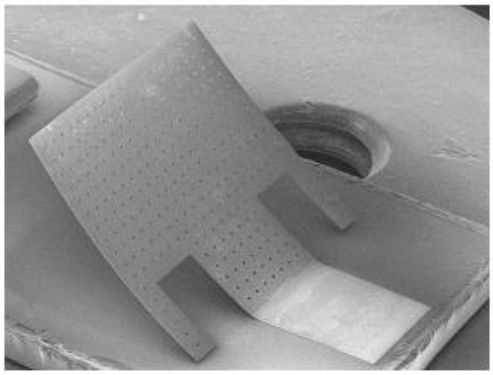

(b)

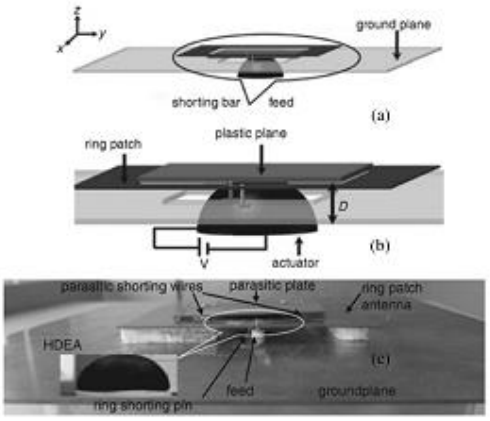

(c)

Figure 2.2: (a) peizoelectric actuator [18] (b) magnetic actuator [17] (c) electromechanical system [19]

2.2.2 Electrical Switching Reconfigurable Antenna

The electrical mechanism is the most promising technology for antenna reconfiguration as it is easily integrable and highly compatible with low profile antenna technology. In this technique, no physical adjustment technology is required to change the antenna parameter to get the required frequency/radiation pattern/ polarization. Some lumped

elements are inserted at the strategic locations of an antenna for the reconfiguration purpose. There are two types of electrical reconfiguration technology-one is using radio frequency (RF) switch like PIN diode, RF micro-electromechanical system (MEMS) and GaAs field-effect transistor (FET) [20], and the other one is using tunable capacitors through varactor diodes. These switching elements can produce the change in impedance matching, surface current distribution and electrical behaviour of an antenna [21].

A PIN diode consists of heavily doped p-type and n-type regions, which are separated by lightly doped intrinsic region. It behaves as good RF-switch by shifting between forward and reverse biasing states. It has a very low resistance at high frequencies in forward biasing and behaves as an open circuit in the reverse-biased state. In addition, it is current-controlled, so it takes very few milliwatts power to turn on the diodes. They are widely used in practice due to their properties like high reliability, low insertion loss, ability to control large RF signal power and fast switching speed.

The counterparts of PIN diodes are the RF-MEMS, which are considered as tiny mechanical switch. The RF-MEMS uses low power consumption, low insertion loss, high isolation and better linear properties. The polarization reconfigurable antenna using RF-MEMS switches were explained in [22]. The antenna consists of the ring slot and feeds with coupled ring slot aperture. A stub is added to generate the circular polarization (CP), and RF-MEMS switches are inserted to switch the polarization between linear and circular as shown in Figure 2.3. The measurement results show that antenna impedance bandwidth is of 22.90% and 3dB axial ratio bandwidth is 13.07%. However, it is not a good candidate for microwave and millimeter wave (mmWave) frequencies due to bad power handling capabilities and expensive packing process to protect it against the environment.

Despite the numerous advantages, RF switches have some issues like the non-linearity of the switches, signal loss and interference due to biasing circuit, which disturb the impedance matching and reduce the antenna efficiency. The coupling between the

biasing circuit and antenna radiation elements can degrade the antenna performance parameters as well. Techniques to reduce the coupling include minimizing the length of biasing line, and if possible, using the available biasing circuit, putting biasing lines on the less intense near field (e.g. on the ground plane). Another method is to load the biasing line inductively or on a high resistive material.

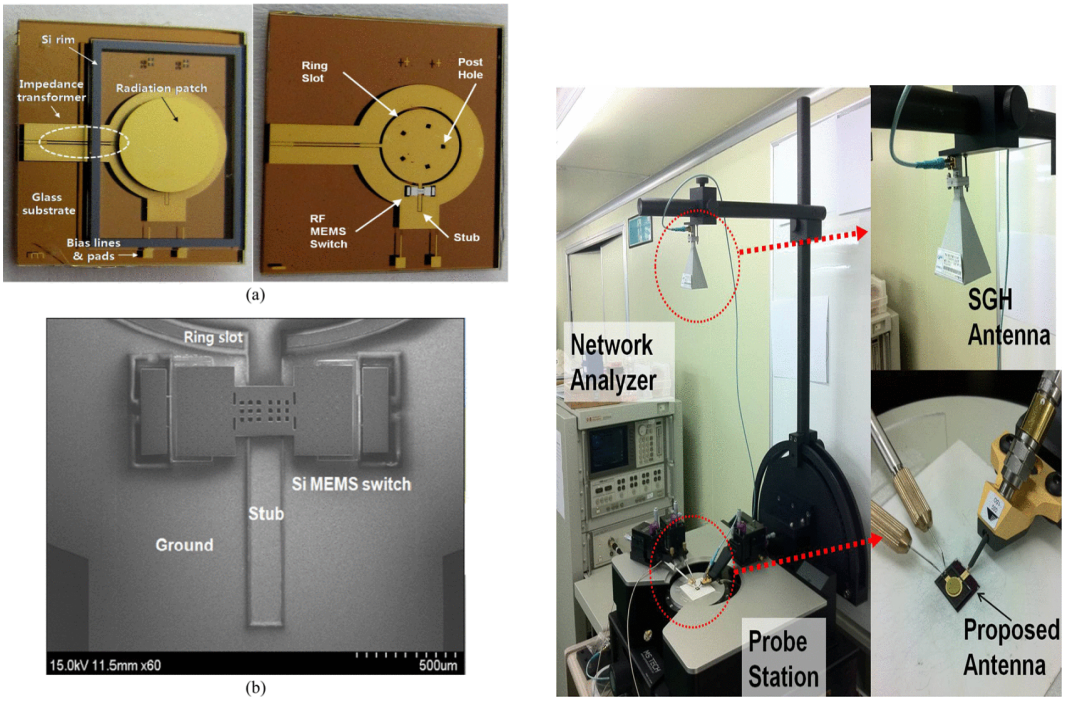

Figure 2.3: (a) Antenna prototype with integration of RF-MEMS (b) setup for radiation pattern measurement [22]

2.2.3 Material Based Reconfigurable Antenna

The smart material with tunable properties is another prominent technology for antenna reconfiguration. The changes in the material characteristics contribute to shifting the antenna frequency. For example, these material permittivity changes are used to modify the electrical antenna length. The electromagnetic property (permittivity, ε_r and permeability, μ_r) of the material has a great impact on the properties of antennas and

other RF microwave devices [23, 24]. A static electric field can be used to change the permittivity of a ferroelectric material, while the permeability of ferrite material can be changed by applying the magnetic field [25, 26]. These materials have been used in many novel research works to achieve the antenna reconfigurability [27]. The frequency reconfigurable microstrip patch antenna based on the ferrite material was presented in [25]. The required tuning frequency is obtained by changing the DC magnetic field. The reconfigurable microstrips antennas [24, 26] based on ferrite material show nonuniformity in the biasing and multi-field distribution, which limits their practical usage.

Beam steering antennas have been exclusively explored by the industry and academia. A leaky-wave antenna with stub array was explained in [28], and the phase shift can be tuned by changing the material properties. Another leaky wave slot array antenna was designed in [29]. The ferroelectric base was used for this design. The permittivity of the material can be changed by varying the biasing voltage between the top conducting layer and bottom ground substrate, which will change the permittivity of the ferro material and hence the beam direction.

Liquid crystal (LC) is another type of reconfigurable smart material, whose properties are affected by its molecular direction, and characteristics also changed by applying the electric or magnetic field [30]. The beam-switchable reflection-array antenna based on the LC substrate was explained in [31]. By varying the applied voltage, the beam of the antenna can be tuned. Recently, some work has been done on this technology [32, 33]. Another material called vanadium dioxide (V_{O2}) was also used for antenna reconfiguration [34] by applying the thermal induction as shown in Figure 2.4.

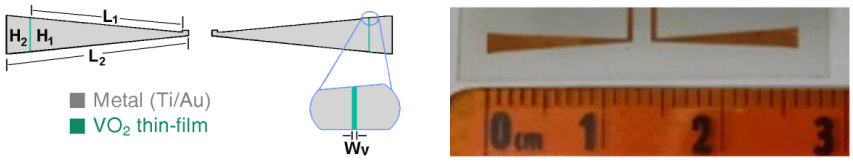

(a) (b)

Figure 2.4: (a) layout of the reconfigurable bowtie antenna with V_{O2} (b) fabricated bowtie antenna [34]

Smart materials can achieve continuous reconfigurability with a simple control system; however, they are lossy and can only provide reconfigurability for a limited range. Additionally, several challenges remain notable, which include proper modelling in the design process and reliability, sensitivity in the antenna operation. By overcoming these limitations, this technology could unleash its great potential for antenna reconfiguration at both lower and higher frequency bands.

2.2.4 Optical Switching Reconfigurable Antenna

Optical reconfiguration has also gained much attention in recent years [35, 36, 37]. It deals with the photo-conductive switches and does not need any complex biasing circuit and physical modification. Optical fibres are used for this purpose, and light source is required for photo-switching [38]. When the laser is ON, the charge density is increased in the material, which also increases the conductivity of the semiconductor devices.This technique has been implemented successfully in many designs [39, 40]. This optical switching technique has a complex structure and needs costly fibre. Although they have low distortion, lossy behaviour and slow switching speed as compare to lumped element switching technology.

The frequency reconfigurable annual ring circular patch antenna using the photo-conductive switches was designed in [39] as shown in Figure 2.5. These switches were activated by using the laser light and dual frequency band operations were achieved.

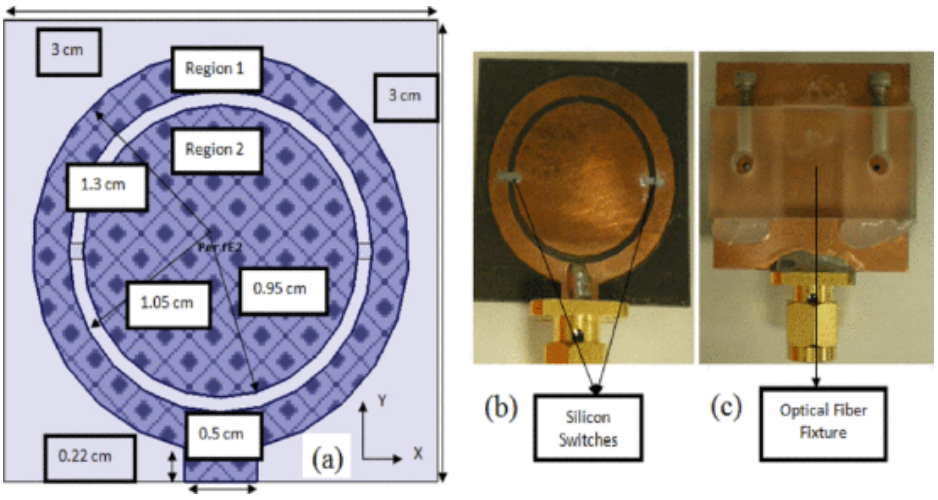

Figure 2.5: (a) antenna dimensions (b) antenna top layer (c) bottom view [39]

The frequency and beam reconfigurable antenna based on CPW to CPS (coplanar stripline) feed was explained in [40]. Two silicon switches are used in this printed dipole antenna as shown in Figure 2.6. The antenna prototype shows good agreement, and there is a frequency shift of 40%.

The extensive research was not done on optical switching antennas, but some attempts were made to further investigate technology in the form of frequency reconfigurable patch antenna [37] and notch-band UWB antenna [35] by using optical switching.

2.2.5 Software-based Reconfigurable Antenna

Controlling a reconfigurable antenna with software can be done using many platforms such as Field Programmable Gate Arrays (FPGAs), Microcontroller, or Arduino Boards [41]. The frequency reconfigurable antenna based on FPGA was explained in [42]. In this work as shown in Figure 2.7, the FPGA is used to turn ON/OFF the PIN diodes, which further connect and disconnect the different portions of an antenna to get the required frequency.

In another work [16], the LabVIEW is used to control the rotation of the stepper motor, which is used for antenna reconfiguration purpose. The software control using LabVIEW

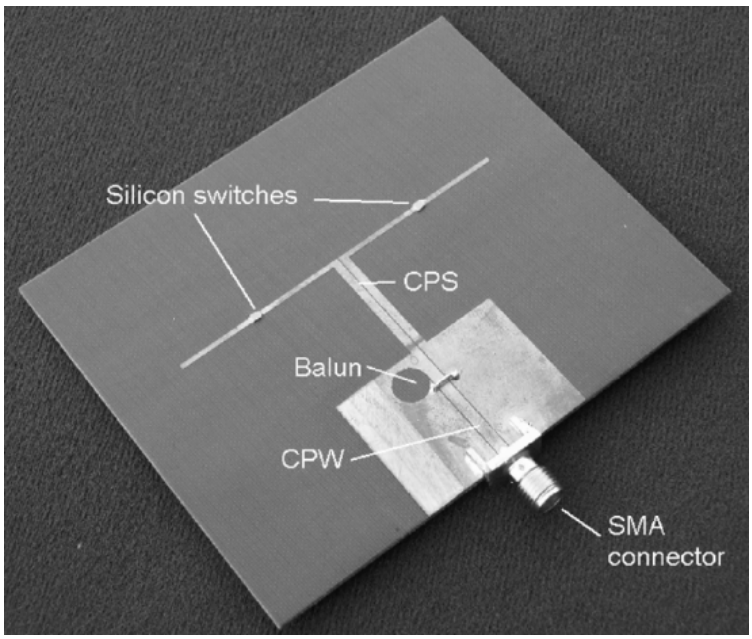

Figure 2.6: The switched dipole antenna [40]

and FPGA is a simple approach, eliminating the need for complicated programming skills for antenna designer. Arduino boards are also used for antenna reconfigurability. In [43], one can control the antenna movement, and determine when and how to change the antenna parts as per the requirement as shown in Figure 2.8.

The surrounding activities may also affect the antenna's operation. Such an example was explained in [44], where temperature sensors activate the thermal switches on the antenna structure. Motion detection is another technique, which behaves as an active part for the biasing of the antenna reconfiguration. An infrared motion detector sensor [45] was used in the biasing circuit of varactor diode as shown in Figure 2.9. It detected the motion and change the voltage level of varactor diode to perform the different frequency tuning.

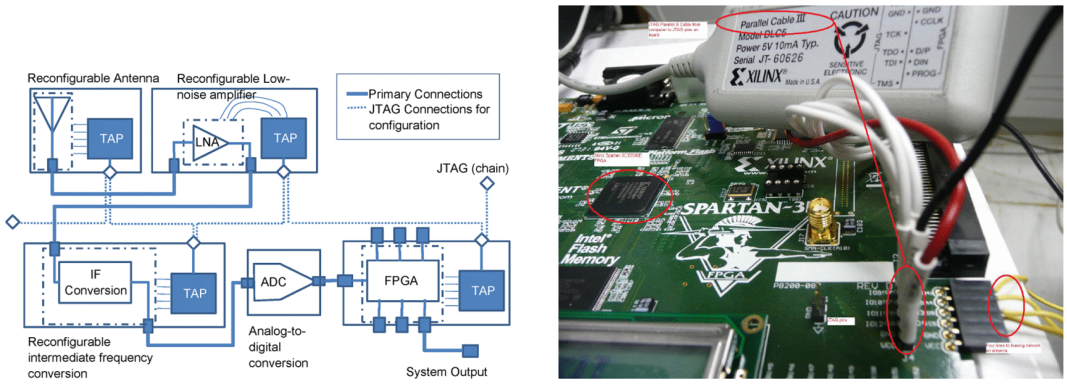

(a) (b)

Figure 2.7: (a) Reconfigurable antenna system (b) The paralleled III cable with FPGA board [42]

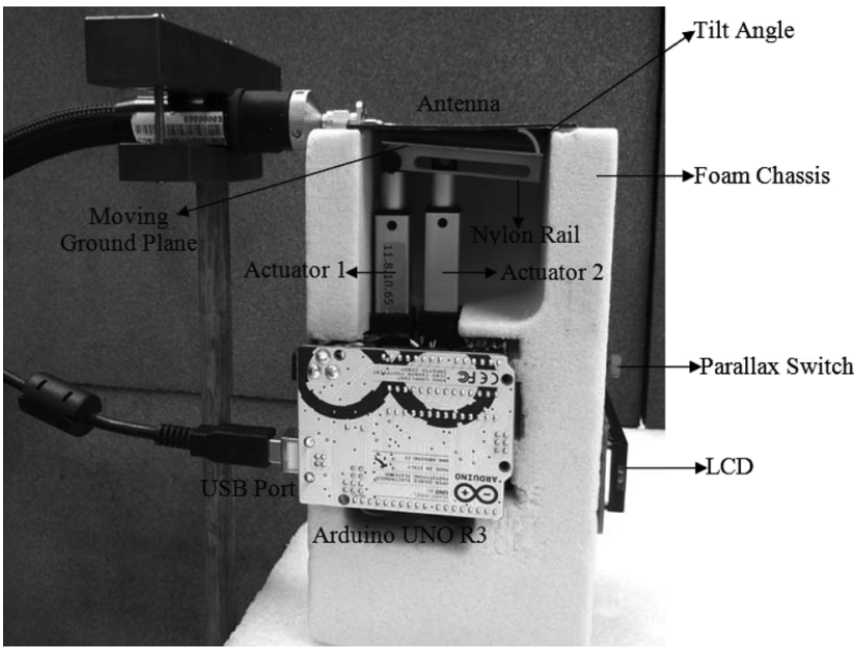

Figure 2.8: Antenna prototype with controlling circuit [43]

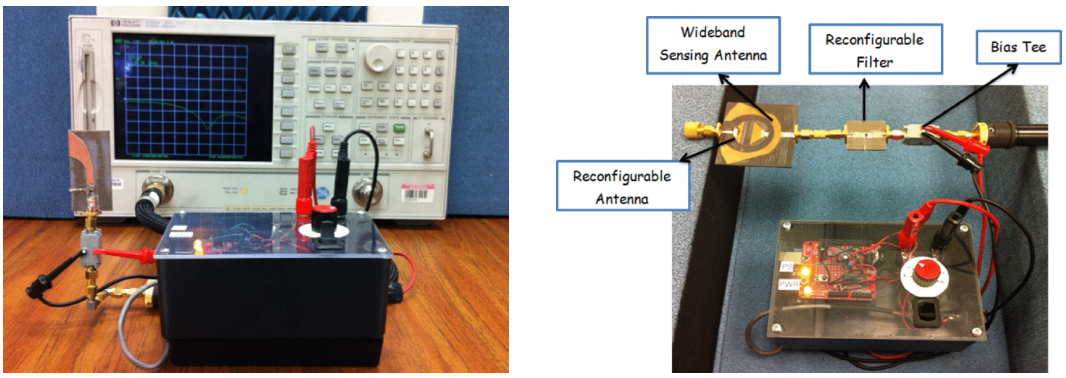

(a) (b)

Figure 2.9: (a) Measurement setup of the filtenna with surrounding (b) Reconfigurable filter with the wideband antenna awareness [45]

2.3 Properties of Reconfigurable Antenna

The term '*reconfigurable antenna*' is defined as an antenna with the capability to change its performance parameters (frequency, radiation pattern and polarization) by physically or electrically changing the structure of an antenna. By reconfiguration, the fundamental parameters of an antenna are changed, leading to the varied electric field distribution to get the required results.

2.3.1 Types of Reconfigurability

Reconfigurability of an antenna is generally described as the ability to purposely change its fundamental properties. By definition, three basic characteristics of an antenna are important , namely, frequency, radiation pattern, and polarization. Accordingly, the reconfigurable antenna can be categorised into four types.

2.3.2 Frequency Reconfigurable Antenna

An antenna that can change its resonating frequency is called a frequency reconfigurable antenna. Frequency reconfigurability can be achieved by physical modification or

electrical switching to change the length of an antenna.

One way to support multiple frequency bands is to integrate multiple single band antennas. Consequently, the overall size and complexity of the communication system increased gradually. As shown in Figure 2.10 (a), multiple antennas are designed for different wireless standards, thus occupying the large size of the portable device. On the contrary, if frequency reconfigurable antenna is adopted, it can reduce the device size, thus the related cost. This is important for modern wireless communications and mobile devices.

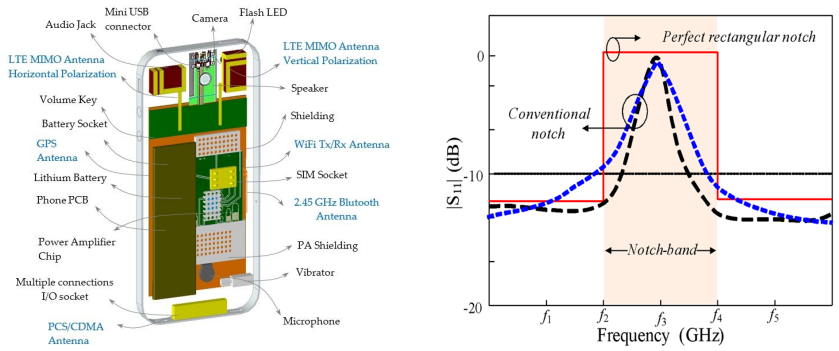

(a) (b)

Figure 2.10: (a) Multiple antenna used in portable devices (b) Band-notch scenario [46]

Band-notch can also be achieved by using the frequency reconfigurable antenna as shown in Figure 2.10 (b). Filters are used to reject the unnecessary band, which creates the interference and reduces the overall efficiency of the communication system. The reconfigurable antennas behave as band-notching for wideband antennas, where multiple wireless bands overlap. Frequency reconfigurable antennas can eliminate filters.

Recently, cognitive radio (CR) has gained much attention in communication technology, as it can achieve better spectrum utilisation. CR helps to detect the available spectrum, and allocates idle frequency bands (in which primary users are not transmitting) to secondary users. The successful applications by changing the effective radiation length can be found in dipole [47, 48] , monopole/ patch [49, 50] and slot antenna [51, 52, 53].

Moreover, the effective length of an antenna can be varied by changing the material property of the antenna without any physical alteration. The resonant frequency can be modified by changing the dielectric constant of the material. An antenna can operate at lower or higher resonant frequency with higher or lower permittivity, respectively. The printed antenna with dielectric variation was designed in [54, 55].

In the reactive method, the input impedance of the antenna can be changed by connecting the reactive parts so as to get the required impedance matching to resonate at normal frequency. To get the continuous tunning of frequency, varactor diode is used to achieve the required impedance matching. The reconfigurable antenna with varactor tunability for the notched band was proposed in [56, 57, 58].

To better understand the working principle of frequency reconfigurability, let us look at an antenna proposed in [59] as shown in Figure 2.11, where a new technique substrate integrated waveguide (SIW) was introduced for low-cost fabrication and high-speed communication applications. The proposed antenna consists of right/left-handed transmission line, which is a combination of capacitance, inductance and shunt capacitance. The operation frequency can be modified by changing the capacitance of varactor diode embedded on the meander line. The resonance frequency is changed from 4.13 GHz to 4.50 GHz by varying the biasing voltage from 0 to 36 V. The proposed antenna showed good agreement between simulated and measured results, indicating a promising candidate for the front end of the RF component and cognitive radio (CR) applications.

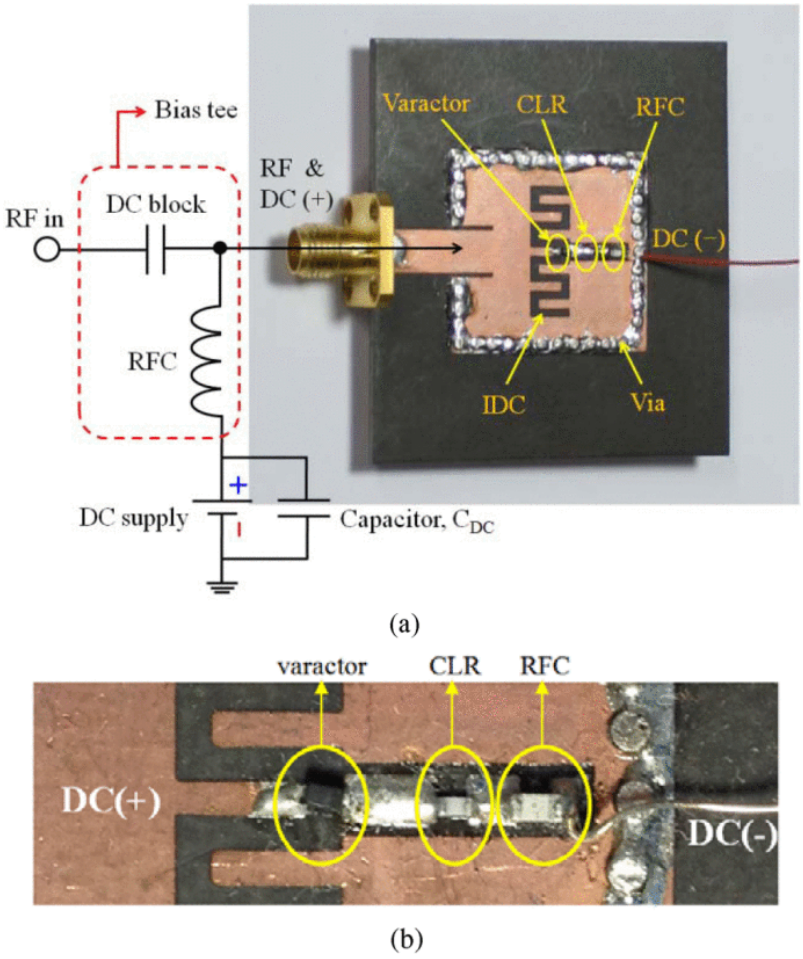

Figure 2.11: (a) SIW-IDC antenna prototype (b) Bias network section [59]

Similarly, another frequency reconfigurable antenna with miniaturized wideband and multi-band properties was presented in [60]. As shown in Figure 2.12, the antenna shape consists of a triangle patch connected with the microstrip transmission line. The main radiating patch relates to two serpentine-shape stubs at the edges with the help of two PIN diodes. The biasing circuit is designed on the backside to avoid affecting the radiation pattern and connected with serpentine stubs with the help of shorting vias. The biasing circuit was the combination of the resistor to provide reasonable voltage and inductor. The proposed antenna resonates at eight different frequencies by choosing the different states of the PIN diodes. The antenna prototype is shown in Figure 2.13. In summary, frequency reconfigurable antennas are particularly useful in situations

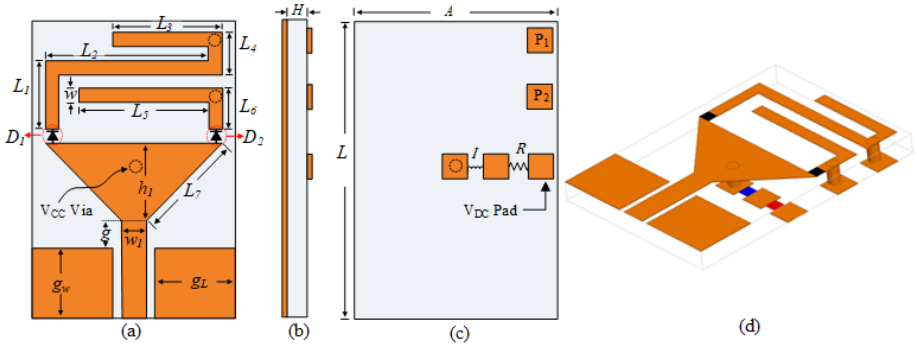

Figure 2.12: Antenna schematic (a) Top side (b) Side view (c) Bottom side (d) Perspective view [60]

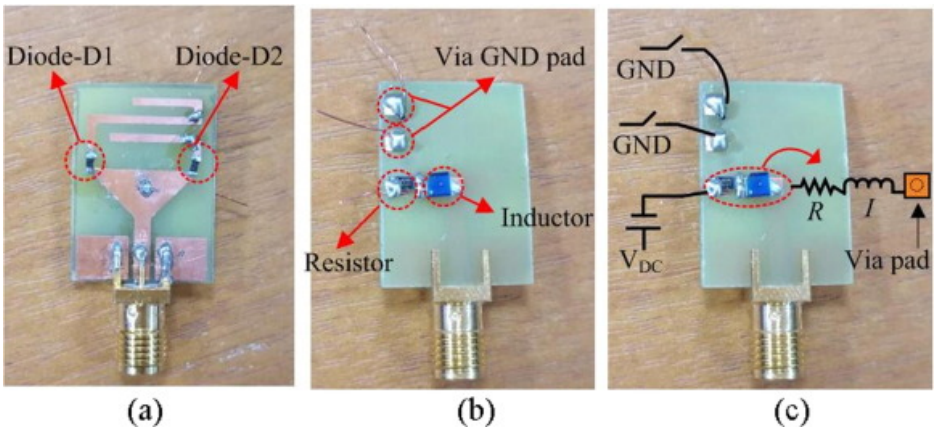

Figure 2.13: Antenna prototype (a) Top-view (b) Bottom-view (c) Bottom view with biasing circuit [60]

where several communication systems converge because the multiple antennas can be replaced with a single reconfigurable antenna. An exemplar application of this type of antenna is CR. Frequency reconfiguration is generally achieved by modifying antenna's dimensions physically, electrically using RF-switches, impedance loading, or tunable materials.

2.3.3 Polarization Reconfigurable Antenna

In this category, the polarization of an antenna can be switched among linear, horizontal or circular polarization (RHCP/LHCP). It can be obtained by controlling the feed arrangement or changing the material property.

Polarization reconfigurable antennas are used to reduce the adverse effect of the multipath fading and mostly used in multiple input multiple output (MIMO) channels. Figure 2.14 illustrates the effect of polarization reconfigurable antennas in multi-path wireless channels, where single circularly polarized (CP) antenna is communicating with other antennas using the right hand circular polarization (RHCP) and left hand circular polarization (LHCP). In case, if the transmitting antenna is linearly polarized, then polarization mismatch will occur.

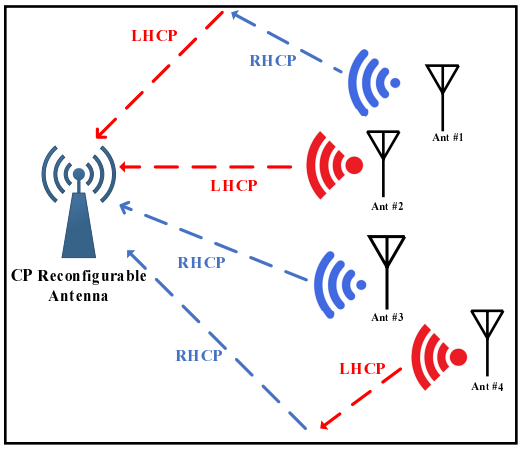

Figure 2.14: Multipath wireless channel

The capability of switching among horizontal, vertical, and circular polarization can be used to reduce polarization mismatch losses, suppress interference signal strength and reduce multipath fading in portable devices. For example, the antenna can change from vertical to left-hand circular polarization [61]. Different design techniques like slits, slots, cross on the ground plane, truncated corner of main radiation patch parasitic, and addition of electrical switches are employed to get the polarization reconfigurability [62, 63]. Additionally, reconfigurability in impedance matching network [64] also help to switch between linear (vertical/horizontal) and circular (right hand circular polarization (RHCP), left hand circular polarization (LHCP)) polarization at resonate frequency.

A novel wideband tri-polarization reconfigurable dipole antenna based on magneto-electric (ME) for WLAN application was designed in [65]. The proposed antenna operates in one linear polarization mode and two circular polarization modes, which are achieved by using four PIN diodes. The linear polarization is obtained by using T-probe fed on dipole antenna having four-sectional structure. The antenna prototype shows impedance bandwidth of 31 %, axial ration BW of 7.9 % and high efficiency of 80%-90% for all polarizations. As shown in Figure 2.15 (a), tri-polarization antenna was investigated in [66]. The antenna design features a multi-layer PCB and consists of the radiation patch, ground plane and cross-probe fed with the PIN diodes. On the bottom side of the radiation patch, there are horizontal and vertical metallic posts that form the L-shaped coupled fed, which helps to increase the bandwidth. PIN diodes and biasing circuit are designed on the ground plane, and the different states of PIN diodes can shift the polarization between linear and circular (RHCP/LHCP) polarization. The measurement results showed good agreement with the simulated results, illustrating a promising candidate for the WLAN and satellite communication applications.
In [62], the authors proposed compact size, low profile, wideband omnidirectional patch antenna with polarization reconfigurability for wireless communication. The antenna geometry combines a circular patch and a ground plane as shown in Figure 2.15 (b). The radiation patch and the ground plane are connected via nine shorting pins. The annular slot and six radial slots are etched on the bottom side.

2.3.4 Radiation Pattern Reconfigurable Antenna

The radiation pattern reconfigurable antenna is able to change its radiation pattern, while maintaining other parameters of an antenna. In this category, the reconfigurability can be achieved by changing the shape, orientation or gain of an antenna.
The radiation pattern reconfigurable antenna serves as the promising candidate in

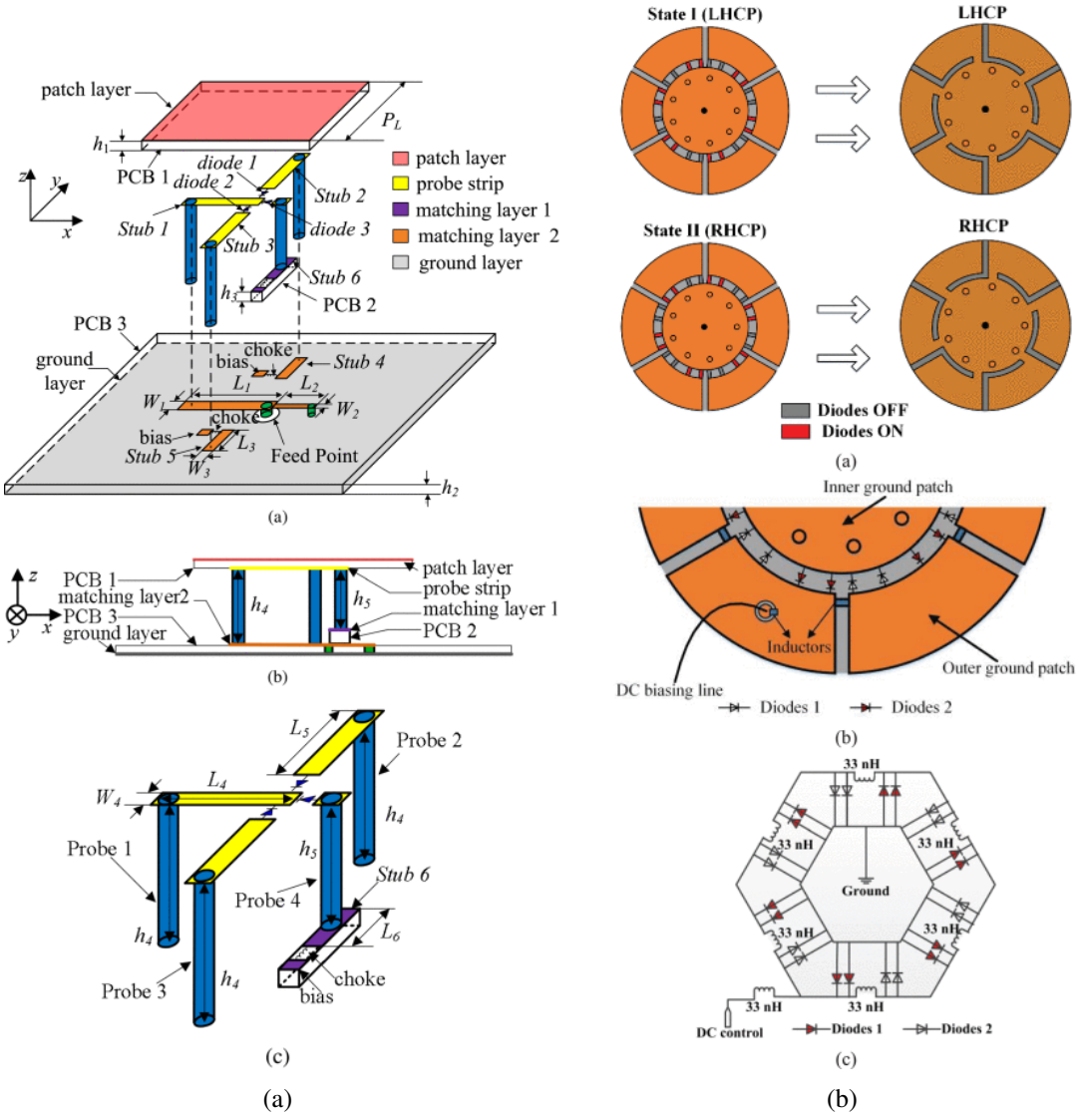

Figure 2.15: (a) Geometry of the proposed antenna [66] (b) Proposed antenna structure [62]

several wireless applications like tracking, surveillance, remote sensing, 5G mobile communications and vehicle-to-vehicle communications. Beam steering antennas have high gain, which is an important factor to maintain the stable communication link. Reconfigurable antennas can be used to the main lobe toward the incoming signal, reducing co-channel interference.

Another application is to create the best communication link between moving vehicles. By mounting the antenna on the roof of a vehicle, and beamforming can help to maintain a reliable communication link, while they are moving. Like this, the overall efficiency of the system is increased.

Radiation pattern reconfigurable antennas can also be used in biomedical applications. For example, the value of the specific absorption rate (SAR) can be decreased by redirecting the beams of the antenna away from the patient's body.

Beam steering changes the direction of maximum radiation to maximize the antenna gain in a link with mobile devices. In this technique, impedance matching is kept constant while changing the current distribution. Conventional methods for beam steering include rotating the arms of a dipole or rotating the whole antenna in the orthogonal plane [67, 68]. One of the most frequently used methods is using tunable elements as parasitic with other main radiators. They behave as the coupled current and do not disturb the impedance matching as they do not have any electrical connection. This technique was implemented with dipole/ Yagi-dipole [69, 70], monopole antenna [41], slot antenna [71, 72, 73], patch antenna [74, 75, 76], and Yagi antenna [77, 78].

Another method of pattern reconfiguration is multi-mode excitation, which is obtained by activating the mode of an antenna [79, 80], though it has very limited applications. The electronic reconfiguration method was applied in many designs using SIW configuration, water grating and periodic structure to control the mode and phase properties [81, 82, 83, 84]. Leaky wave antennas are famous for larger beam-steering, but it is still challenging to increase their beam-scanning range.

The most attractive application of the pattern reconfigurable antenna is surveillance and tracking because they provide different beam direction with same resonate frequency [85]. Mobile antenna systems are the example of pattern reconfigurable antenna.

2.3.5 Hybrid Reconfigurable Antenna

This technique features the combination of any of the previous three types. The hybrid reconfigurable antennas are also referred as compound reconfigurable antenna. For example, one can tune the frequency as well as change the beam streering or switch among the polarization of an antenna simultaneously. It is quite challenging to control the one parameter without affecting other parameters. However, hybrid reconfigurability makes antenna more robust in various applications. The most common application of compound reconfiguration is the combination of frequency agility and beam scanning to provide improved spectral efficiencies.

2.3.5.1 Frequency and Radiation Pattern Reconfigurable Antenna

In this category, the frequency and the radiation pattern of a antenna can be changed simultaneously. One can switch the radiation pattern among omnidirectional, broad-side and end-fire modes. A dual-band frequency and radiation pattern reconfigurable antenna was explained in [86]. The antenna has a simple patch shape with a row of shorting vias in the centre. The antenna shows monopolar and broadside radiation pattern for its lower and upper frequency, respectively. The presence of the shorting vias do not disturb the conventional mode of the microstrip patch antenna but helps to create another mode for radiation reconfigurability. Two separate biasing voltages and four varactor diodes were used for the independent switching of the resonant frequency.

An antenna array for frequency and radiation pattern was designed in [87]. The proposed antenna consists of two patches, open stubs and varactor diode with independent biasing

voltage. A T-junction power divider was used to connect and feed the two patches antenna array as shown in Figure 2.16. The resonant frequency tunning range is from 2.15 GHz to 2.38 GHz and beams steering was ± 23 across the broadside.

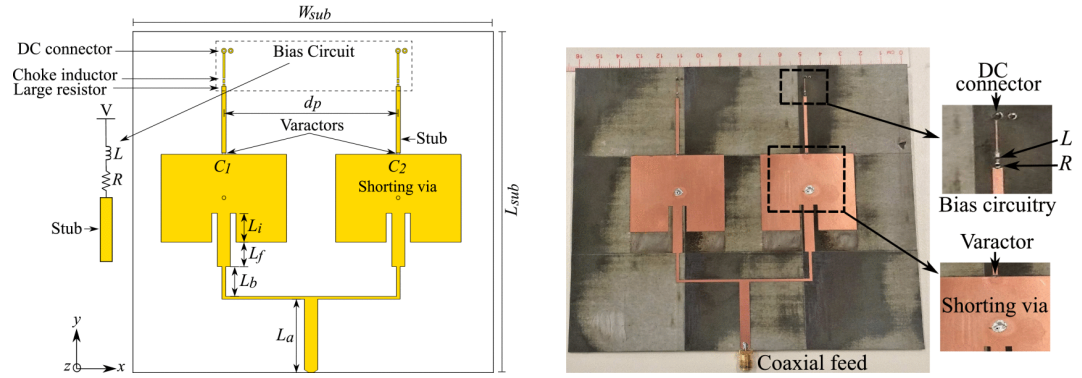

(a) (b)

Figure 2.16: (a) Two antenna element arrays with T-junction power divider (b) Antenna prototype [87]

The combination of monopole and patch antennas was studied in [88] to get the radiation pattern and frequency reconfigurable antenna. It consists of a patch antenna on the front side and a monopole antenna on the bottom side with the defected ground plane as shown in Figure 2.17. The monopole and patch antennas were used to resonate at a lower and higher frequency, respectively. To get the omnidirectional radiation pattern, the substrate was truncated at the far end from the feed. By changing the states of two diodes, the proposed antenna behaves in omnidirectional pattern mode at 2.21 GHz-2.79 GHz, unidirectional pattern mode of higher frequency at 5.27 GHz-5.56 GHz, and both modes working, simultaneously.

To cover the S-band and C-band, a microstrip antenna was presented in [89]. The reconfigurable antenna has a patch with inset feed on the front side, while it has two rectangular-shaped slots on the ground plane. The six PIN diodes were inserted in the slots on the ground plane. The different states of the PIN diodes resonate antenna at 3 frequencies of the S-band and 8 different frequencies of C-band.

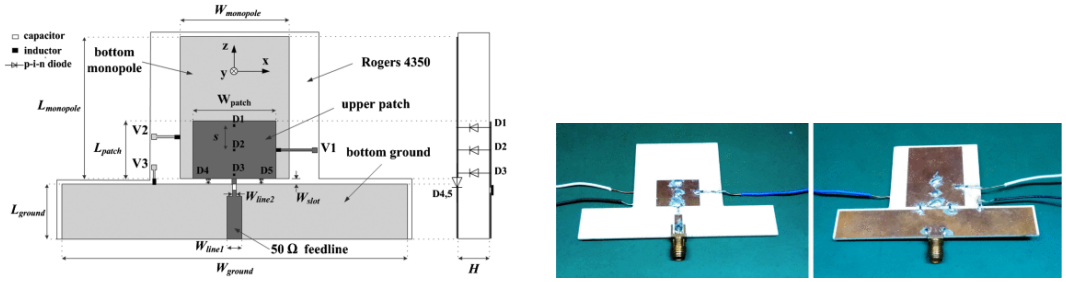

(a) (b)

Figure 2.17: (a) Dimension of the proposed antenna design (b) Antenna prototype [88]

A wideband slot antenna for LTE and C-band applications was investigated in [90]. The substrate has a sickle-shaped slot with a ground plane on one side and fork-shaped microstrip line on the other side. Two PIN diodes were inserted into sickle-shaped slot for frequency reconfigurability, while two diodes were used for the connection of vertical and horizontal arms of the fork-shaped feed line for pattern reconfigurability. Good agreement was shown between the simulated and the measurements results, and antenna shows 25 degree and 20 degree beam steering at 3.4 – 3.8 GHz and 3.7-4.2 GHz, respectively.

Another slot antenna to switch between three different frequencies (1.8,1.9, 2.1 GHz) and beam steering for three angles (0, ± 15) were presented in [91]. The proposed antenna consists of a main radiator slot on the front side and (upper,lower) slits on the ground plane. Two switches were placed on the main radiator, while three switches in each slit. To produce the directional radiation pattern, an aluminum reflector was placed behind the antenna as slotted antennas normally have bidirectional radiation pattern.

In [92], frequency and radiation pattern reconfigurable antenna was proposed, which consists of the centre fed patch and four identical back-to-back F (BTFB) elements.

2.3.5.2 Frequency and Polarization Reconfigurable Antenna

For this type of antennas, the frequency can tune for available band, and polarization switching helps to reduce the multipath effect and increase the channel capacity. Recently, it has gained much attention due to its useful application like tracking, sensing and radar, etc. and some design examples are explained as follows. A novel frequency and polarization reconfigurable antenna based on electromagnetic bandgap (EBG) for satellite navigation was explained in [93]. The proposed antenna consists of EBG surface, which has same metallic rectangular patches array on both side of the thin substrate. It has active biasing circuit on each surface, which helps to rotate the reflection phase orthogonally concerning the incident waves. A CPW was used to feed the proposed antenna and provide good impedance matching for the frequency tuning and switching the circular polarization (RHCP/LHCP). Measurement results showed the good agreement with simulated and mathematical analysis, and antenna prototype achieved the measured 3dB axial ratio (AR) bandwidth of 40 %.

Another low profile antenna based on EBG structure was presented in [94] for frequency tuning and shifting between linear and circular polarization. The proposed antenna has a three-layer structure. The EBG pattern is on the top layer, which has 12 $\times$ 12-unit cells square patch at the centre and four strips at the edges. The central patch has a gap that was used for loading of PIN diodes. By controlling the biasing voltage of PIN diodes, the proposed antenna achieves frequency tuning and polarization switching.

A high gain antenna with the combination of the metasurface, a planar slot, and the metallic reflector was investigated in [95] as shown in Figure 2.18. The metasurface consists of 64 identical patches. Due to the symmetry of the structure, the equivalent circuit of the metasurface (MS) is considered as a symmetry RLC circuit because the diagonal corner of the unit cell is not cut in a zigzag shape.

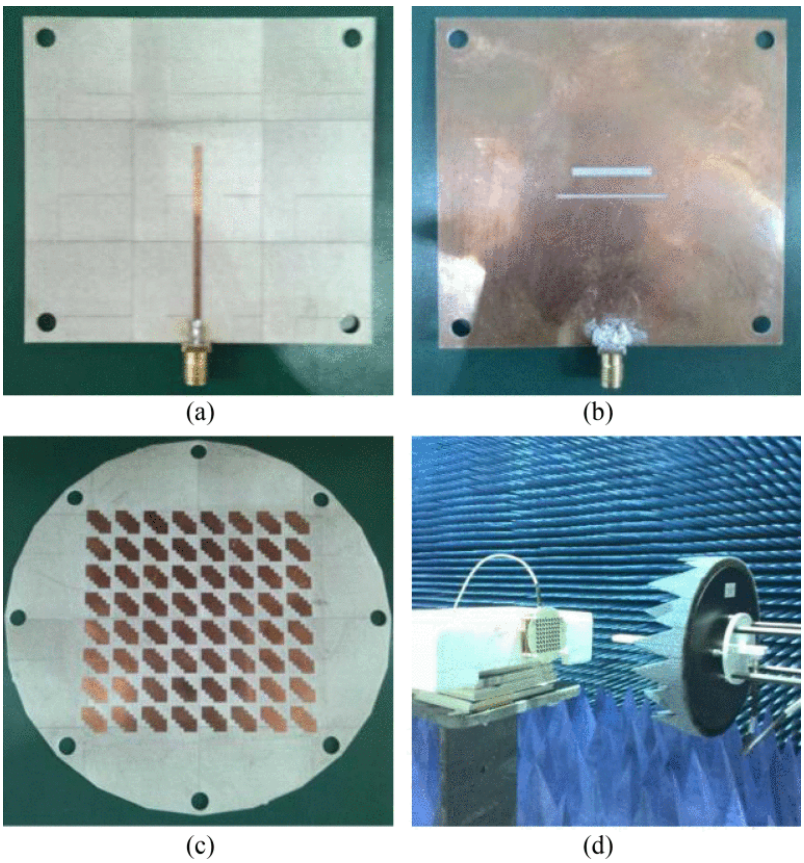

Figure 2.18: (a) Feedline of proposed antenna (b) Surface of slot antenna (c) MS (d) Measurement setup [95]

For a wider bandwidth, the slot antenna is converted to the double-slot structure. The polarization reconfiguration of the proposed antenna can be achieved by rotating the metasurfaces around the centre of the slot structure, and frequency can be tuned by the adjustment of the spacing among slot, MS, and metallic reflector. The measured gain for the proposed antenna was 16.5 dBi with a fractional bandwidth of 33.33 %.

A stub loaded patch antenna microstrip patch antenna for smart communications was designed in [96]. The antenna consists of square microstrip patch and 12 identical stubs at the four edges of the patch. The varactor diodes were used for the connection between stubs and the patch as shown in Figure 2.19. The biasing circuit was at the other end of the stub and consists of a resistor and a choke inductor. The 12 varactors and stubs were divided into two groups and provide independent DC-bias voltage. The

antenna prototype showed the wide fractional bandwidth of 40 %.

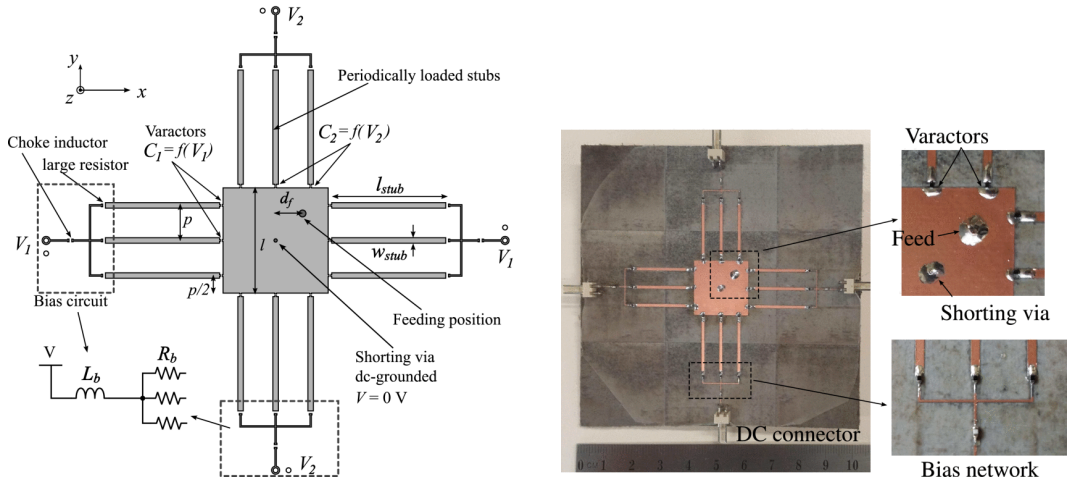

(a) (b)

Figure 2.19: (a) Dimension of the proposed antenna design (b) Antenna prototype [96]

The reconfigurable antenna with frequency and polarization capability was presented in [97], which consists of monopole structure, defected ground plane, and reflector. Two slots were etched, and PIN diodes were inserted on the ground plane with the addition of metal vias along with the slots. The antenna showed four different modes by changing the different states of the PIN diodes. It showed linear polarization in two modes, while shows circular polarization with LHCP and RHCP in the other modes, respectively.

The frequency reconfigurability [98] can also be achieved by truncated the square patch at the corner as shown in Figure 2.20. The truncated square patch is separated from the corner by a narrow slot and it behaved as radiation patch, and a diode was inserted in the slot to change the circular polarization at different frequencies to make it suitable for modern communication systems.

A dual-probe feed reconfigurable antenna was explained in [99]. The antenna consists of circular-shaped microstrip patch on the top layer and branch line coupler feed etched on ground plane at the bottom layer. The varactor diodes were inserted in the gaps of

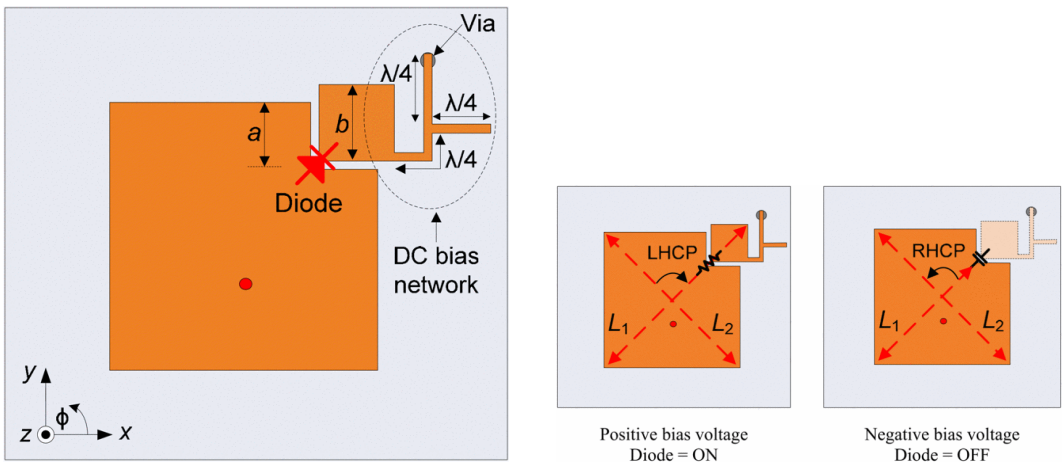

(a) (b)

Figure 2.20: (a) Schematic of the proposed antenna (b) Biasing operation mechanism [98]

the circular patch at the top layer, and a reverse bias voltage was applied with the help of biasing pad at the bottom side of the patch. An additional branch line coupler (BLC) feed network was used to simultaneously tune the frequency from 2.05 GHz to 3.13 GHz along with circular polarization.

2.3.5.3 Radiation Pattern and Polarization Reconfigurable Antenna

The reconfiguration in radiation pattern along with polarization supports beam steering and multiple polarization shifting on a single antenna radiator. They increase the capacity of modern communication systems, improve signal strength and radiation coverage.

In [100], the authors presented an omnidirectional patch that operates at two orthogonal ± 45 linear polarization and produces a dipole-like radiation pattern for convening both polarization and radiation pattern reconfigurability. The proposed antenna consists of two back-to-back coupled patches with common ground. The antenna has four input ports, and polarization can be achieved by the port selection, while the phase difference between the ports was utilized for radiation pattern reconfigurability. It is consider

promising candidate for the MIMO applications.

A compact-size, low cost and smart antenna for beam switching and polarization reconfiguration was designed in [101]. The antenna has dual port inset fed patch, parasitic elements and driven elements as shown in Figure 2.21. The driven element is the combination of square patch antenna with simple feeding network, and parasitic element consists of the printed dipole with PIN diodes. The radiation pattern can be obtained by placing reconfigurable parasitic elements around the driven antenna over the three polarization states.

A simple, low profile PIFA antenna for radiation pattern along with polarization reconfiguration for WLAN application was presented in [102]. The antenna consists of the printed inverted-F antenna on the top left corner, and another printed inverted F parasitic element for pattern reconfiguration on the bottom right corner. The antenna prototype showed a good gain of 1.2 dBi and 4.2 dBi for the ON and OFF states, respectively. A circularly polarized switchable feed network antenna with reconfigurable beam pattern for the wireless system was expressed in [103] as shown in Figure 2.22. In this research work, the switchable L-probe feed base feeding network, and slot augmented circualr patch were explained in detail. The measured bandwidth was of 7.8 % from 2.4 to 2.65 GHz, and the radiation pattern swtich between the broadside and the conical modes. A high gain radiation pattern and polarization reconfigurable antenna using metasurface was explained in [104]. The antenna structure consists of three layers. The top layer consists of metasurface formed by a combination of $4\times$ 4 nonuniform rectangular metal films. The PIN diodes were inserted between these films and used to get the pattern reconfiguration between ± 20 in the direction of the Z-axis. The middle layer was the ground plane and PIN diodes were also used between the slots to get the polarization reconfiguration. The proposed antenna resonated between 4.95 GHz to 5.05 GHz and the gain of the main lobe was 7-8 dBi.

A compact size cuboid quadrifilar helical antenna (QHA) to operate at 0.9 GHz with

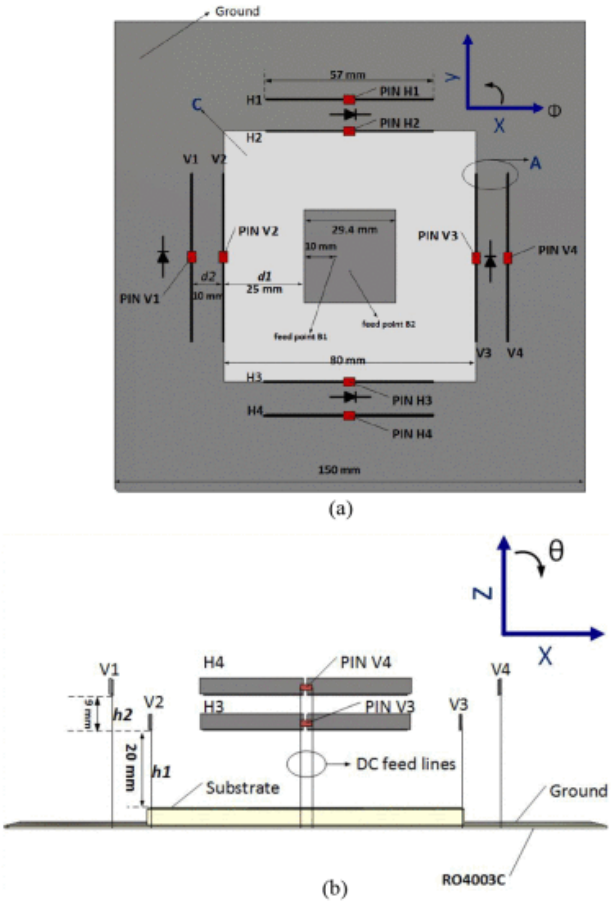

(a)

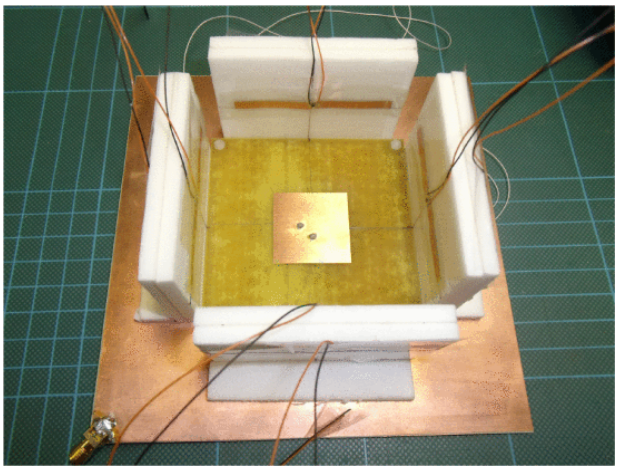

(b)

Figure 2.21: (a) Plane view (b) Antenna prototype [101]

radiation pattern and polarization reconfigurability was explained in [105]. The proposed antenna was the combination of a reconfigurable radiator and switchable feeding network. The reconfigurable radiator consists of folded thin substrate, which behaves like a cuboid, and the radiation arms on the surface. The switchable feeding network consists of out of phase power divider and two reconfigurable couplers. The proposed antenna prototype resonates between two orthogonal CP and switch radiation pattern between broadside and backfire modes. Another frequency and radiation pattern reconfigurable low profile antenna was explained in [106]. The antenna consists of simple patch radiator and parasitic elements related to the PIN diodes.

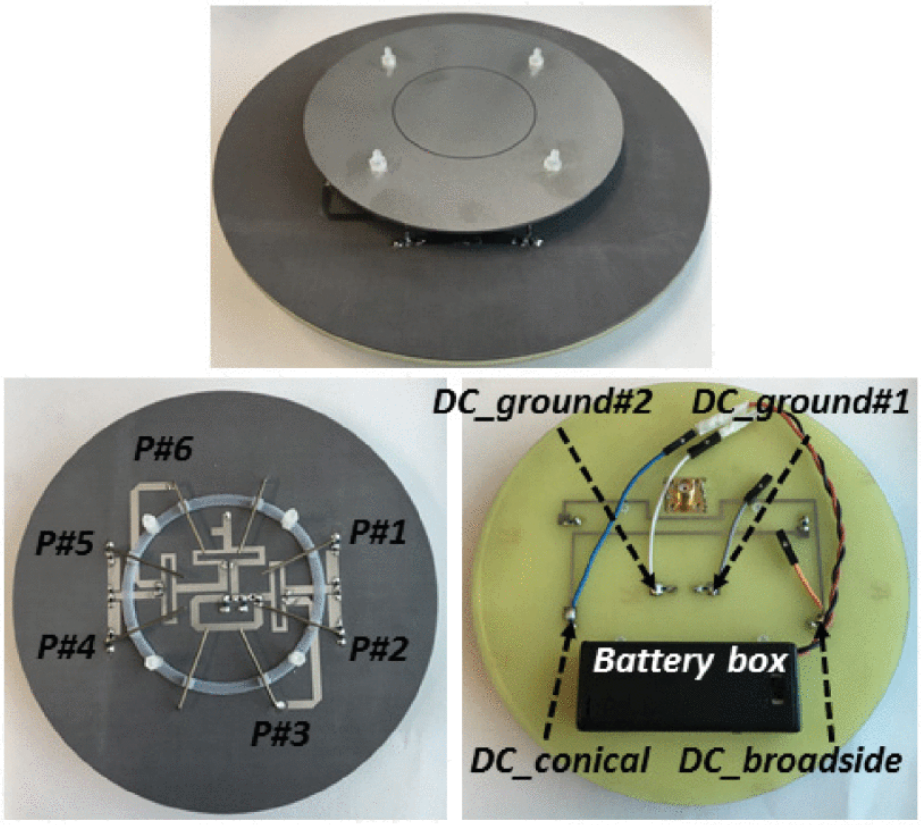

Figure 2.22: Proposed antenna prototype [103]

2.3.5.4 Frequency, Radiation Pattern, and Polarization Reconfigurable Antenna

Most of the aforementioned examples are either single or dual-characteristics reconfigurable antennas. Besides that, one can tune the antenna parameters (frequency, radiation pattern, polarization) simultaneously. Little work was done on this category. One such multiple-property reconfigurable antenna was presented in [107]. This antenna consists of small metallic patches known as pixel surface, radiation patch and 60 PIN diode switches as shown in the Figure 2.23. The antenna prototype shows the frequency tuning over a fractional bandwidth of 25 % range, beam steering over ± 30 in two principal plane and switching between four different polarization.

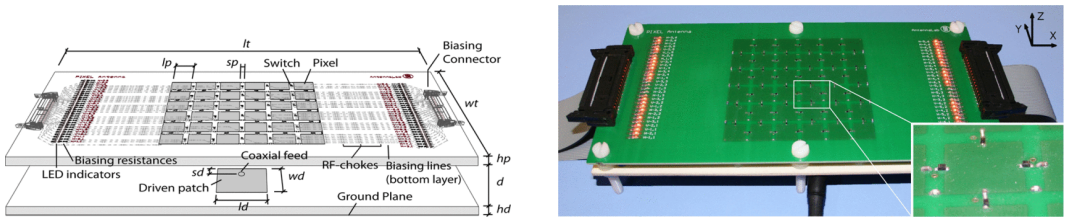

(a) (b)

Figure 2.23: (a) Schematic of the parasitic pixel layer (b) Pixel antenna prototype [107]

Another example was explained in [108]. The antenna structure was the combination of a rhombus-shaped radiator, three excitation lines at different angles and a common feedline. The required configuration can be obtained by changing the biasing states of three pairs of PIN diodes. The proposed antenna can tune frequency between 5.2/5.8 GHz, linear/ circular/ ± 45 polarization with beam titled at 30 degree in right and left-hand direction. A novel cavity-based slot antenna for frequency, radiation pattern, and polarization reconfiguration was investigated in [109] as shown in Figure 2.24. The reconfigurability can be obtained controlling the states of the switches between the two cross slots etched on the surface of the substrate integrated waveguide (SIW) cavity.

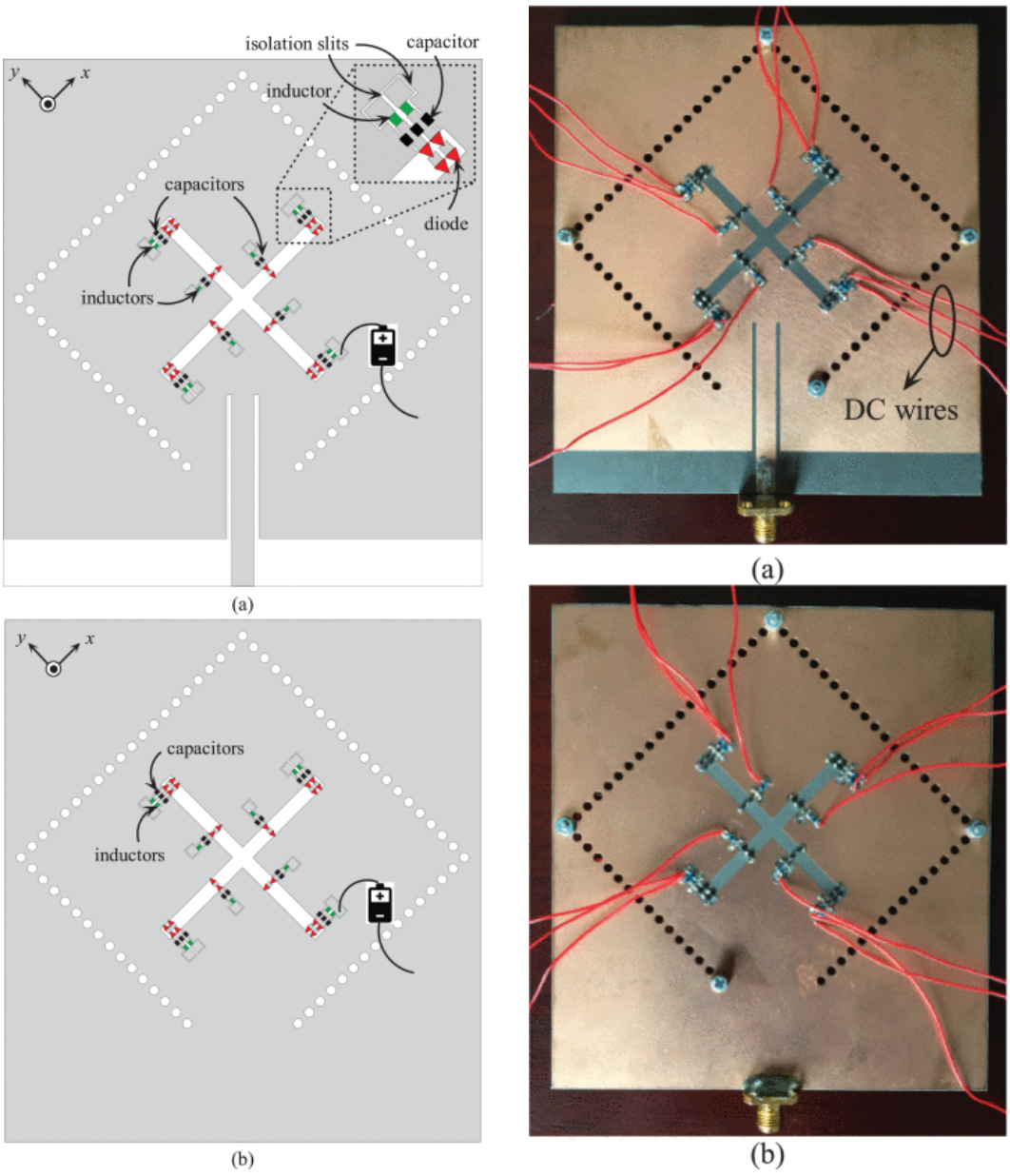

Figure 2.24: Antenna dimension with the prototype [109]

Table 2.1 shows the summary of reconfigurable techniques for different designs.

Table 2.1: Summary of the Reconfigurable techniques

Reference	**Reconf. Type**	**Reconf. Means**	**Frequency (GHz)**	**No. of Switches**
[59]	Frequency	SIW-IDC Varactor Diode	4.13-4.50 GHz	1
[60]	Frequency	PIN Diode	2.4, 3.0, 3.3 4.1 4.6, 5.6, 6.2 GHz	2
[65]	Polarization	PIN Diode	2.4 GHz	4
[66]	Polarization	PIN Diode	2.4 GHz	3
[79]	Rad. Pattern	PIN Diode	2.3 GHz	2
[80]	Rad. Pattern	RF-MEMS	1-10GHz	4
[89]	F/R	PIN Diode	S & C Band	6
[90]	F/R	PIN Diode	LTE & C Band	4
[97]	F/P	PIN Diode	2.02-2.95 GHz	2
[98]	F/P	PIN Diode	5.65, 5.78 GHz	1
[104]	R/P	PIN Diode	5GHz	4
[105]	R/P	PIN Diode	0.9 GHz	8
[108]	F/R/P	PIN Diode	5.2/5.8 GHz	5
[109]	F/R/P	PIN Diode	2.29-2.38 GHz	48

2.4 Reconfigurable SIW Antenna

The invention of SIW provides low loss, good power handling capacity and effective functionality with planar circuits [110]. The structure of SIW is similar to conventional cavity slot and provides a low profile, flexibility and simple integration with planar circuits [111, 112]. The SIW is composed of fittingly divided vias with a similar

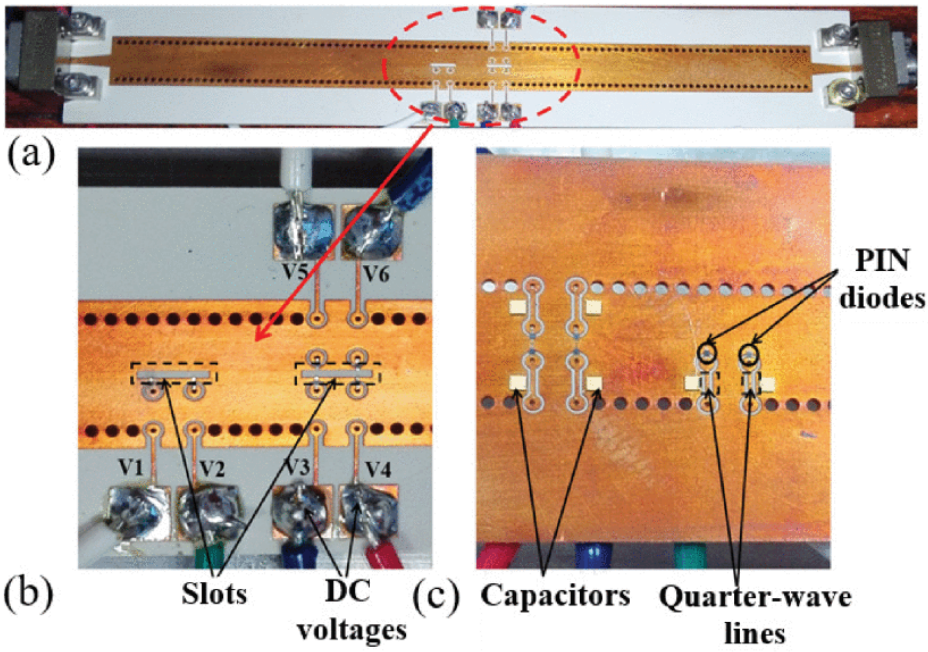

Figure 2.25: (a) Prototype overview (b) Front view (c) Back view [115]

distance between them, engendering with least radiation loss. The dispersion between the vias controls the field spillage of the waveguide. The SIW technology is an elective strategy for the minimal effort of waveguide like the parts integrated with simple PCB standards [113, 114]. It is much better in comparison with existing technologies as for lightweight, ease of integration and straightforward designs. A novel leaky-wave antenna with fixed frequency and switchable beam steering for the 5G applications was explained in [115]. In this work, the PIN diodes were used to control the phase shift angle and position of the feeding slots as shown in Figure 2.25. A new technique of central excitation based on four coupling plated-through hole (PTH) was introduced. The holes relate to the ground plane and top wall as well. The reconfigurable feeding method is applied by using the PIN diodes.

2.5 Reconfigurable Band-notch UWB Antenna

In the last few years, UWB technology gained much attention due to its advantages like low power consumption, wide bandwidth, low cost, less complexity, and high data rate transmission [116, 117]. Due to these properties, UWB technology is widely used in many application like indoor communication, cognitive radio, radar, localization, and automotive etc. [118, 119, 120]. There are several other narrow bands standard coexist within the UWB like IEEE 802.16 WiMAX (3.3–3.6 GHz; 5.25–5.825 GHz), IEEE 802.11a wide local area network (WLAN) (5.15–5.35 GHz; 5.725–5.825 GHz), and ETSI HiperLAN /2 (5.15–5.35 GHz, 5.47–5.725 GHz). This overlap band creates the electromagnetic interfaces with UWB technology when they are operating at the same time in other wireless devices [121, 122, 123]. Normally, filters are used to reject the unwanted band and increase the communication efficiency, but the addition of the filters increases the overall size, cost, complexity, and the insertion losses [124, 125]. Currently, much research is going on to design the UWB antenna with band-notch characteristics. UWB antennas with band-notch characteristics were developed by using slot or slit [126, 127, 128], slots in the feeding network [129, 130, 131], slot in the ground plane [132, 133, 134], and parasitic patches [135, 136]. Hence, they are fixed band notched UWB antennas, and they are not applicable when coverage of all frequency ranges of UWB technology is required. By using the reconfigurable band-notching technique, one can use the required frequency band as per system requirement.

As shown in Figure 2.26, the low profile reconfigurable UWB antenna with single or dual-band rejection was expressed in [137]. The proposed antenna is the combination of monopole structure, PIN diode, biasing circuit, partial ground plane along with arc-shaped slot and open-ended L-shaped stubs for band rejection. The antenna operates in four modes: full UWB (3.1-10.6GHz), single-band rejection of WiMAX or WLAN, and dual band (WiMAX, WLAN) band rejection. The dual-band reconfigurable notched

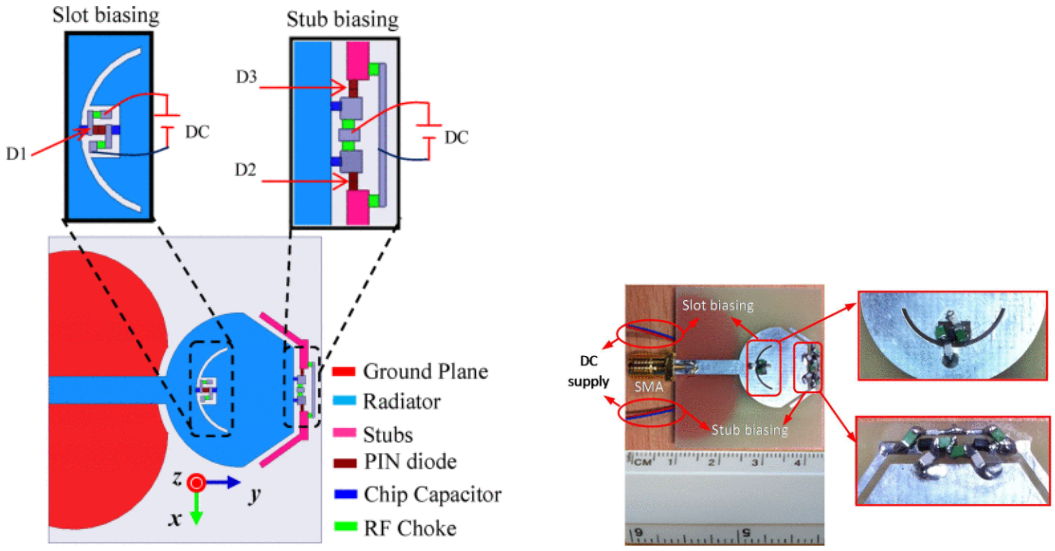

(a) (b)

Figure 2.26: (a) Antenna dimension (b) Antenna prototype [137]

slot-type split ring resonator (ST-SRR) antenna for WiMAX and WLAN applications was explained in [138]. The defected ground plane was used for impedance matching, and ST-SRR is used in the feed to get the required band-notch for UWB antenna. The measurement results showed that antenna gains a fractional bandwidth of 138.63%. A novel compact triple band-notched reconfigurable fractal antenna was explained in [139]. By using the fractal technique, the overall size of the proposed antenna was reduced to 53% as shown in Figure 2.27. The proposed antenna consists of circular patch, slots, PIN diodes and split ring resonator (SRR). The proposed antenna operates at notched frequency at WiMAX, WLAN, and X bands.

2.6 Reconfigurable Metamaterial Antenna

The advancement in metamaterial and metasurface has brought more opportunities in the field of microwave devices. By definition, metamaterials have artificial and unusual characteristics such as negative permittivity and permeability that do not occur in natural

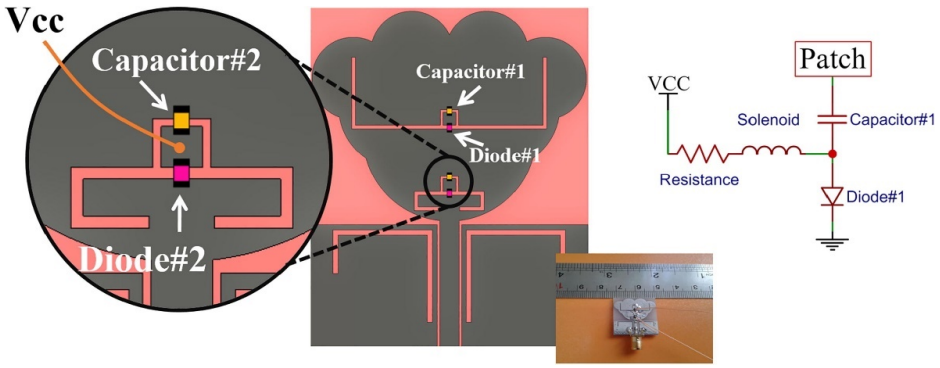

Figure 2.27: Antenna structure with biasing circuit [139]

materials [140]. Except for low profile, metamaterials also provide more flexibility in the design of microwave device and more functionality for the control. Metasurface (MS) is two dimensional equivalent of metamaterials and it helps to improve the return loss and gain along with the polarization of an antenna [141]. The frequency and polarization reconfigurable antenna using double-layer metasurface was explained in [142]. The polarization reconfigurable metasurface (PRMS) was in the uppermost layer on the side face to the middle layer, while frequency reconfigurable metasurface (FRMS) was on the opposite side of the patch antenna. The proposed antenna shows the resonant frequency between 4 GHz and 5 GHz, and the polarization switching between LP, RHCP, and RHCP.

A wideband polarization reconfigurable antenna was presented in [143]. The metasurfaces are the combination of 4 $\times$ 4 periodic metal plates. The proposed antenna consists of square patch radiation, metasurface, and four tunable switching feeding probes. The switchable feeding network is the combination of a 2-way power divider and single-pole double-throw (SPDT) switches using PIN diodes as shown in Figure 2.28. By changing the biasing voltage, the proposed antenna was tuned between x & y direction, linear polarization and RHCP/LHCP. The beam switching reconfigurable antenna was expressed in [144]. The reconfigurable metasurface was the combination of double-slit square ring and PIN diodes.

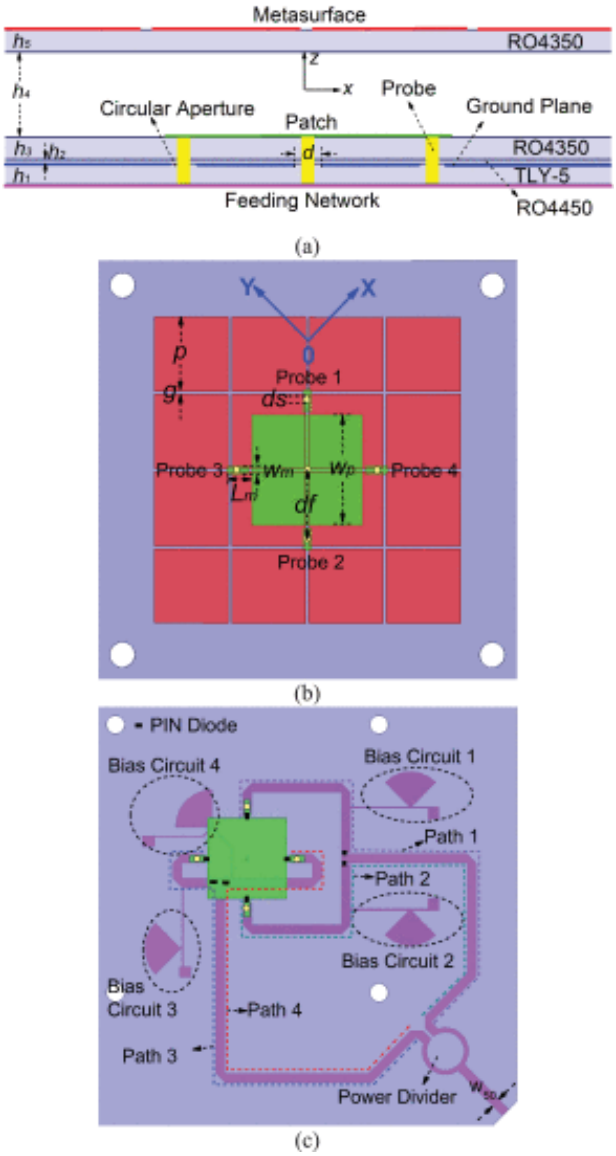

Figure 2.28: (a) antenna dimension (b) antenna prototype [143]

2.7 Reconfigurable Antenna for Flexible Material

In recent years, wearable antenna technology has gained much attention in industry and academia due to its attractive features like lightweight, flexible, low cost and easily integrable with modern communication systems. In the medical field, wearable antennas are used to monitor the critical health condition of a patient, check the sugar level, investigate the inner intestinal system, blood pressure, heartbeat and temperature of the body. In the recreation side, they can be applied in augmented reality glasses, touchscreen computer, and smartwatches. The flexible antenna with reconfigurable technique provides the small size and low-cost solution for modern electronics and advanced wireless communication systems. There are some challenges related to the integration of reconfigurable components such as switches, biasing circuits and mechanical stability. Extensive antenna types have been developed on the conventional rigid substrate in the last few decades. The requirement of the flexible antenna with reconfigurable technique has been increased as they are the main component of the wearable technology and cope up with the advance wearable devices.

The CPW-fed based quad-band and penta-band flexible reconfigurable antenna were presented in [145], [21] and [146], respectively. The copper tape was used in these antenna prototypes, making it difficult to predict the exact behaviour of PIN diodes for practical applications. The flexible reconfigurable antenna on PET film for WLAN/ WiMAX wireless applications was presented in [147]. The antenna has folded slot and CPW-fed but with large antenna volume. The dual-band CPW fed flexible reconfigurable antenna was explained in [148]. It was monopole antenna incorporated with U-shape slot to get the required frequency. The frequency and polarization reconfigurable flexible antenna was investigated in [149]. The antenna consists of a folded slot, stub, and artificial magnetic conductor (AMC) surface to reduce the specific absorption rate (SAR) value. The antenna prototype shows good agreement in a flat and curved

situation, and measurement on the human body as well. A robust, flexible and frequency reconfigurable antenna was presented in [150]. The antenna consists of conductive fibre on polydimethylsiloxane (PDMS) substrate as shown in Figure 2.29. The antenna prototype and other lumped component were encapsulated with an additional layer of PDMS. The antenna bending characteristics were investigated in free space, on body phantom, and in the household washing machine. These tests show that antenna working order is normal even in extreme bending (radius 28 mm) and after washing. An inkjet-printed frequency reconfigurable antenna on a paper substrate for wireless applications was explained in [151]. The antenna consists of a main radiator, L-shape, U-shaped radiators and the ground plane. With a PIN diode, the proposed antenna can tune between 1.5 GHz and 4 GHz.

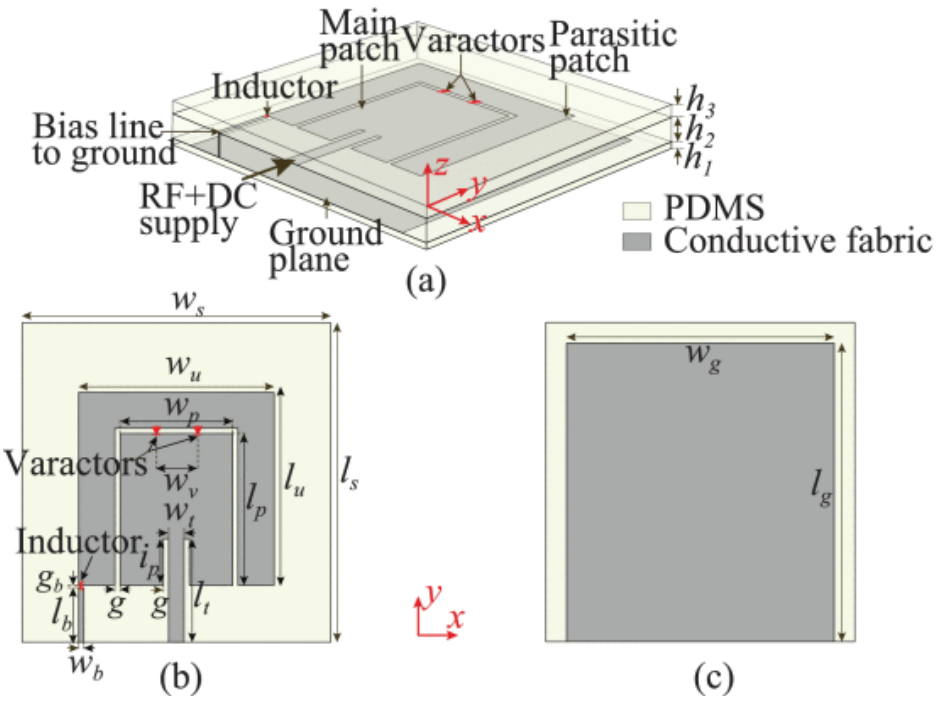

Figure 2.29: Antenna configuration (a) Cross-sectional view (b) Patch layer (c) Ground Layer [150]

2.8 Application of Reconfigurable Antenna

The new era of antenna design must generate an antenna that is cognitive and adjust to the environment and ever-changing conditions. Also, there is a need for antennas that can overcome failure and swiftly respond to new developments. Cognitive radio, massive multiple-input-multiple-output (MIMO), wireless body area networks, satellite, and space communication platforms are all possible applications for the integration of highly, reliable, and efficient reconfigurable antenna.

2.8.1 Reconfigurable Antenna for MIMO Communication System

To fulfil the requirements of current and future modern communication systems, MIMO system plays a vital role to cover the high data rate and signal strength requirements within a defined bandwidth. The MIMO technology depends on the multiple antennas which are implemented on both sides of the communication systems. The implementation of MIMO reconfigurable antenna at the front end will improve the data capacity and directivity, significantly.

A frequency reconfigurable antenna for MIMO applications was explained in [152]. The single element of an antenna was the combination of 4×4 MIMO antenna, and it was designed to operate 2.4 GHz and 2.6 GHz frequency. The single element MIMO antenna was either two 2×2 MIMO antenna or a single 4×4 array as shown in Figure 2.30. The proposed antenna was coaxially fed, and PIN diodes were inserted on the backside. The different states of the PIN diodes were controlled by a microcontroller module. To get the high gain, an air gap was introduced between the radiation patch and the ground plane.

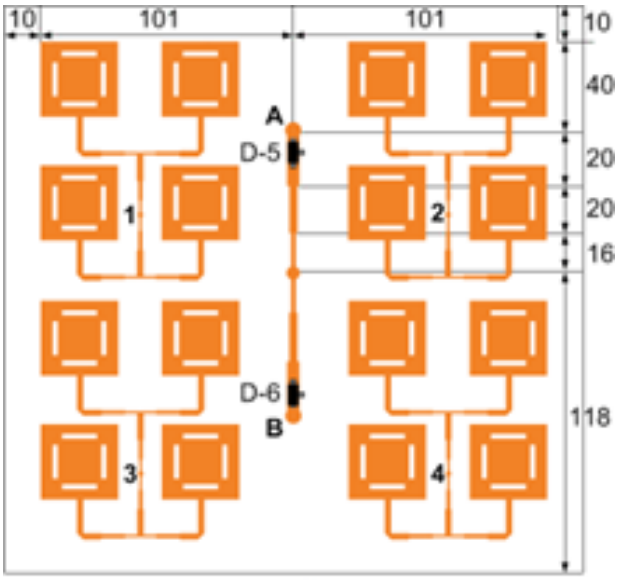

(a)

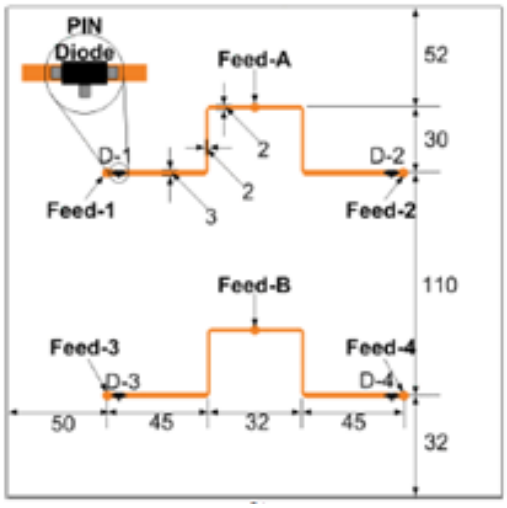

(b)

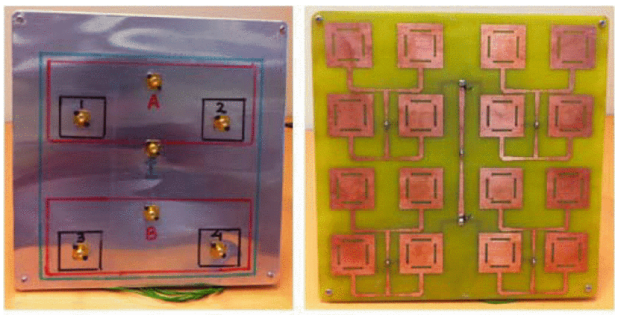

(a)

(c)

Figure 2.30: . (a) Front view (b) back view (c) antenna prototype [152]

2.8.2 Reconfigurable Antenna for Cognitive Radio Applications

It is a big challenge to provide a high data rate and fast browsing speed for the ever-increasing number of mobile subscribers. Secondly, the distribution of the band spectrum is not uniform, which also adversely affect the overall efficiency of the system. To overcome this limitation, a new technique named Cognitive Radio was introduced that use the unoccupied/idle band spectrum for communication and increase the system efficiency. Wideband and reconfigurable antennas are a promising candidate for cognitive radio communication. Additionally, compact size antennas are the requirements for portable mobile devices.

A compact novel broadband antenna was presented in [153]. In this work, both the discrete and continuous tunning was implemented to get a large frequency range. The antenna consists of UWB monopole antenna with reconfigurable impedance matching network as shown in Figure 2.31. The proposed design has two independent paths to cover the 430 MHz and 5GHz frequency. The first path was directly connected with a UWB antenna that covers the 1-5 GHz frequency range. The second path was controlled through a varactor diode based matching network. Two discrete switches were used to move between wideband and reconfigurable mode.

2.8.3 Reconfigurable Antenna for mmWave Communication

5G is proposed to explore higher operating frequency bands, which includes the millimeter wave (mmWave) band. The mmWave band lies between 30 and 300 GHz frequency ranges. While using the higher frequency, new challenges arise like an increase in patch loss and complexity of the system including antennas, filter, and amplifiers. The compact reconfigurable antenna with tunable radiation pattern is of great interest to maintain the user requirements in an atmosphere dependent scenario. Figure 2.32 shows a polarization reconfigurable antenna, consisting of square radiation

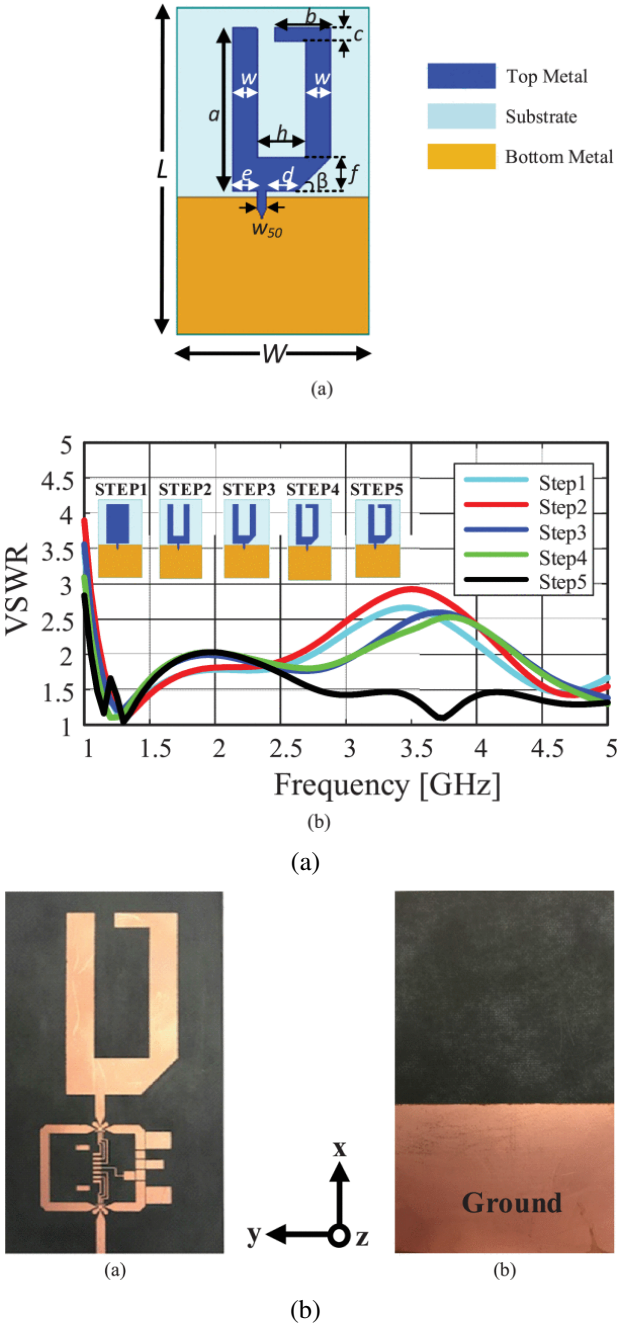

Figure 2.31: (a) Proposed antenna geometry (b) antenna prototype [153]

patch, microstrip line and two PIN diodes [154]. The proposed antenna can switch between RHCP and LHCP by changing the states of PIN diodes. The antenna shows impedance bandwidth from 27.6 GHz to 28.6 GHz. A good axial ration was also achieved between 27.65 to 28.35 GHz.

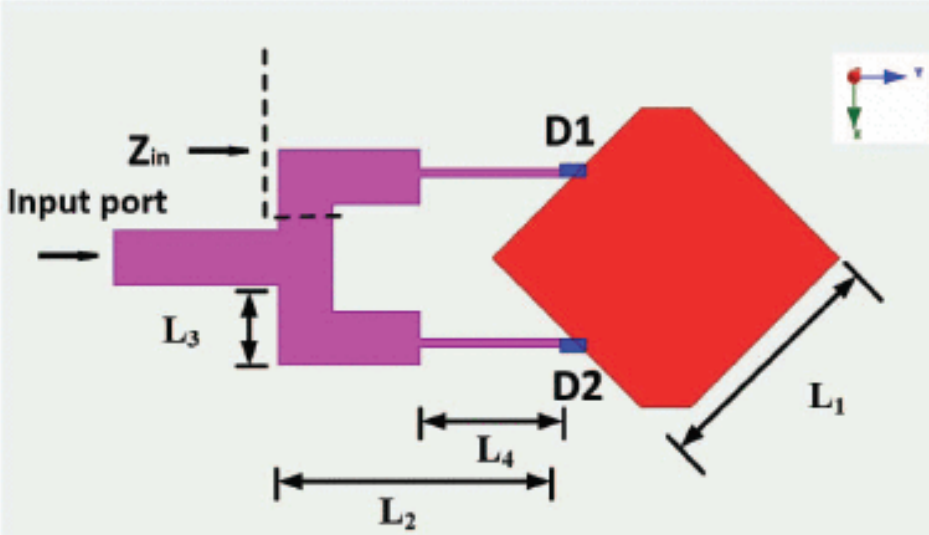

Figure 2.32: Dimension of the proposed antenna [154]

2.9 Summary

This chapter starts with the brief history of reconfigurable antenna. The techniques and properties for the reconfiguration of an antenna were explained in detail. Some existing proposed reconfigurable antenna designs, methods, and their constraints are also discussed. In addition, the applications and the benefits of the reconfigurable antennas are highlighted.

Chapter 3

Reconfigurable PIFA Antenna for Mobile Devices

3.1 Introduction

With the recent advancement in telecommunication industry, there is high demand of compact, high speed, planar, and easily integrate able devices. Antenna is the vital part of every wireless communication systems and electronic devices, and it has vast applications like vehicular communication, Internet of Things (IoTs), global positioning systems (GPS), global system for mobile communication (GSM), Bluetooth, wireless local area network (WLAN), and satellite communications. Mostly antennas used in above mentioned applications have constant functional properties (fixed polarization, radiation pattern, and frequency). However, to cope up with modern wireless communication networks, and the integration of multiple radios into single device, the implementation of fixed operation antenna in one device can lead to some problems , e.g. very large volume, complex circuitry, and low efficiency. To support the advanced wireless network systems, there is requirement of multi-functional and smart antennas that is capable to handle the systems trade-off, and take action accordingly.

It is also challenging to provide more services without increasing the system size, and circuit complexity. Additionally, future development in communication, and new ways to interconnect with other devices will create new challenges to meet large data rate requirement, high-speed, and more data services. To address the current and future demands of electronics and wireless communication networks, it is of great interest to design flexible, small size, controllable, and easily adjustable antenna.

3.2 Frequency Reconfigurable PIFA Antenna

3.2.1 Introduction

Reconfigurable antenna has become an effective and promising solution for system adaptability due to their changing scenarios. They can play an important role in overcoming the above mentioned problems, and help to improve system efficiency. Additionally, they have got attention in recent days due to their properties like compact size, low cost, low complexity, easy configuration and planar design. Reconfigurable antenna can be achieved by changing the frequency, polarization, and radiation pattern properties according to the the requirement.

3.2.2 Related Work

The existing research on reconfigurable antenna has highlighted shortcoming such as numerous feeding networks and multiple impedance matching circuits, which lead to large antenna size and adversely affect the antenna efficiency. There are a lot of single-band, dual-band [155] and multi-band antennas reported in the literature. A compact reconfigurable antenna for four-band with the help of two varactor diode was presented in [156]. This design shows low bandwidth for higher frequency. The combination of PIN diode and varactor diode was explained in [157] for the reconfiguration of PIFA

antenna. The antenna resonates at four different frequencies by changing the states of RF switches. However, it has limited bandwidth. The mixture of different switches also makes the biasing circuit more complex. A 3D compact loop-inverted F reconfigurable antenna was designed in [158]. One PIN diode controlled the loop antenna mode and inverted F-mode (IFA). Although this antenna covers multiple bands, but it has return loss less than -6dB for all bands. A microstrip slot antenna to cover six frequencies was presented in [159]. Six PIN diodes are used to resonate at frequencies between 2.2 GHz to 4.75 GHz. But this antenna has narrow bandwidth with large antenna size.

To cover the 3G/4G applications, a compact penta-band antenna was designed in [160] with two slits, and ground plane. To fully cover the LTE band (low frequency and high frequency LTE), two PIN diodes and additional ground was used. The reconfigurable antenna for the 4G LTE applications was described in [161]. The antenna consists of long strip, short strip, and PIN diodes. Although, proposed antenna covers the low band (LTE700, GSM 850/900) band, and high band (GSM 1800/1900, LTE 2300/2500) band, and its measurements results shows 6dB of return loss over all bands.

To cover three different modes (single-band mode, dual-band mode, and triple-band mode), a frequency reconfigurable monopole antenna was presented in [162]. The antenna consists of an arrow shaped radiation element with stubbed ground plane on the bottom side. An optimized biasing circuit was designed on the ground side of antenna with resistors and inductor connected via holes. Copper strip was used as a switch in simulation, which shows ideal performance as compare to equivalent circuit of PIN diode.

Frequency and pattern reconfigurable antenna with five PIN diodes was investigated in [163]. The antenna behaves as planar monopole or microstrip patch by changing the states of switches and operates in three different radiation pattern modes, like omnidirectional at lower frequency band of 2.21-2.79 GHz, unidirectional mode at higher frequency of 5.27-5.56 GHz, and a hybrid mode. But it has a large antenna size.

A T-shaped feeding strip with T-shaped parasitic shorted element to cover low bands (GSM 850/ 900) and high bands (GSM 1800 / 1900 / UMTS 2100 / LTE 2300 / 2500 bands) was presented in [164]. However, the authors used copper strip as a switch in the simulation that could not address the exact behavior of PIN diode. Moreover, the results showed greater than -10dB impedance matching for lower bands.

A frequency reconfigurable antenna was presented in [165]. Two PIN diodes were used to cover three operating modes like inverted F-antenna (IFA), monopole, and loop-mode. A frequency reconfigurable PIFA antenna using defected ground structure was proposed in [166]. Three PIN diodes were used, and their positions are optimized using the genetic algorithm (GA). The antenna operates in three different frequencies (2.1 GHz, 2.4 GHz, and 3.5 GHz), but it has small bandwidth with large antenna size. The microstrip patch antenna with slots in the ground plane to cover frequencies between 2.2 GHz and 6 GHz was designed in [167]. The authors used SPICE model of PIN diode in CST software to analyze the real impact of voltage on the antenna performance. Although, the proposed antenna resonates at ten frequencies, but the antenna size was quite large. A cedar-shaped frequency reconfigurable antenna was designed in [168]. The combination of PIN diode and three pairs of varactor diodes were used. The bulky antenna becomes lossy due to the large number of varactor diodes. A coupled-fed loop antenna to cover octa-band was proposed in [169]. Low frequency mode was achieved with the combination of loop mode of 0.5λ and chip capacitor. The antenna operates at high band by the combination of 1λ frequency mode, 1.5λ mode, and 2λ mode with 0.5λ mode of coupling loop. But the antenna shows -6dB reflection coefficient for lower mode.

A compact frequency reconfigurable PIFA antenna based on nested slot was designed in [170]. First, multi-band antenna was achieved without any RF switch with larger antenna volume. Then two PIN diodes were used for frequency reconfiguration with 60% reduction in the size. The antenna resonates between 0.77 GHz to 3.55 GHz, but the

S_{11} is higher than -6dB for all frequencies. The E-shaped wearable dipole antenna was designed in [171]. The antenna presents robustness performance on different bending conditions. But it has a larger antenna size. A CPW-fed frequency reconfigurable antenna was designed in [172]. Four PIN diodes were used to cover frequency between 2 GHz to 10 GHz. It mentioned that biasing line was used for PIN diodes, capacitor, and inductor. However, copper strip was used as a lumped switch instead of real PIN diodes in the antenna prototype.

3.2.3 Proposed Antenna Design

The proposed frequency reconfigurable antenna is shown in Figure 3.1. The antenna consists of F-shaped and I-shaped radiation elements. The antenna is designed on an FR-4 substrate with a dielectric constant (ϵ_r) of 4.4, and loss tangent $(tan\delta)$ 0.02. The ground plane is printed on the back side of substrate, and it is connected with radiation element through multiple vias for better ground. A second ground plane is used (connected with main ground plane) for better impedance matching. The antenna is fed with a 50Ω SMA connector. The outer part of SMA is connected with ground plane. The shorting vias, ground plane and radiation elements adopt copper material with thickness of 0.035mm. All parameters of the proposed antenna are shown in Table 3.1.

Detailed dimensions of the proposed antenna are shown in Figure 3.1 (a), including radiation part, PIN diodes, capacitors, and ground plane. Two PIN diodes are located on the radiation elements. The different states of PIN diodes are used for frequency reconfigurability. The first diode (D1) is inserted between the long radiation strip and L-shaped strip that is connected with ground plane by multiple vias. The second diode (D2) is placed in the I-shaped strip that is also connected with shorting vias and long strip. A small size of wire 0.5mm is connected on the both side of D1. By changing

the states of the PIN diodes "ON" and "OFF", the antenna operates in four different states, among which three states are considered. When the D1 is ON and D2 is OFF, the radiation elements have a length 65 mm and cover GSM 850/900 bands. When D1 is OFF, and D2 is ON, the antenna operates in the loop mode, and covers GLONASS 1616, DCS 1800, PCS 1900, and UMTS 2100 bands. When both diodes are OFF, the antenna resonates to cover UMTS 2100 and GSM 900 with -6dB return loss.

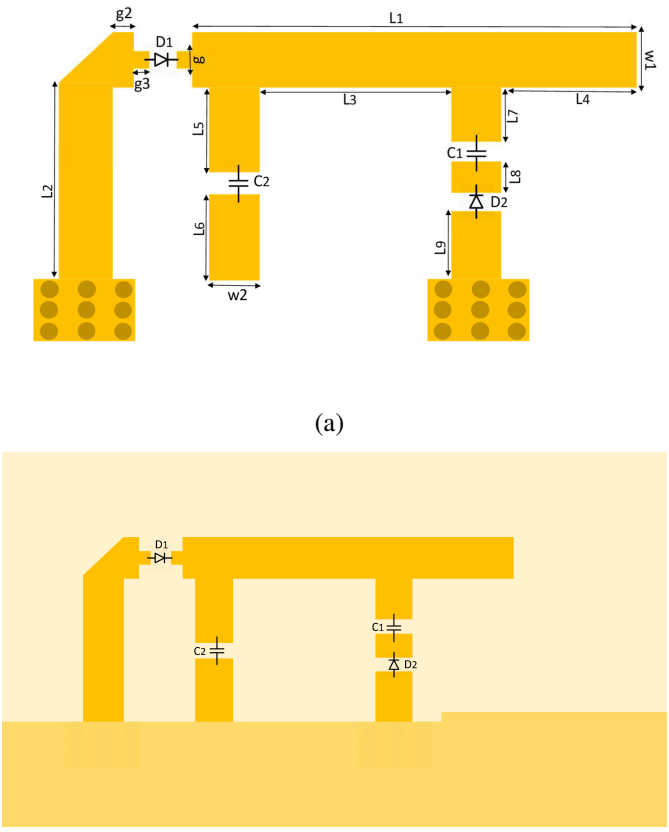

(a)

(b)

Figure 3.1: Prototype of proposed antenna design (a) Detailed dimensions (b) Antenna structure

3.2.3.1 Switching Techniques

While PIN diodes have unique advantages like fast switching speed, good isolation, low power consumption, excellent repeatability, and high operating life as compared to

other RF switches like RF MEMS, and varactor diodes. It behaves as current-controlled resistor for radio and microwave frequencies. When it is forward biased, it behaves like conventional PN diode to pass current in one direction. When it is reverse biased, it functions as an open circuit to stop current. We used SMP-1345 PIN diode from SKYWORKS with frequency range from 10 MHz to 6 GHz. When the PIN diode is forward biased, there is an inductance of 0.7nH in series with a resistance of 1.5 Ω. The low low resistance allows currents to flow in the radiation elements. When the diode is reverse biased, a parallel capacitance of 0.15pF with (5kΩ) resistance is in series with an inductance of 0.7nH. A capacitor of value 100pF is used between diode D1 and feeding for DC blocking. Similarly, another capacitor is used between D2 and I-shaped radiation element. A biasing voltage of 0.89 V and 0 V is applied to PIN diode for ON and OFF states, respectively.

Table 3.1: Dimensions of the Proposed Antenna

Parameter	**Values (mm)**	**Parameter**	**Values (mm)**
L	120	L_1	37.6
W	60	L_2	12.65
L_g	120	L_3	16.5
W_g	43.25	L_4	17.2
W_1	2	L_5	6.65
W_2	2	L_6	2.3
g	0.5	L_7	3.25
g_2	0.4	L_8	0.5
g_3	0.7	L_9	2.4
g_4	0.4		

3.2.3.2 Parametric Studies

To better understand the functionality and optimized the different parameters of reconfigurable antenna, a parametric study was conducted.

Figure 3.2 shows the simulated return loss of antenna with respect to variation in radiation element width (D) of diode D1 on both sides. It can be shown in Figure 3.2 (a) that the proposed antenna shows a narrow bandwidth and does not resonate at GSM 950 frequency band; when D1 is ON and D2 is OFF, and width is changed from 1mm to 2mm, while other parameters remain same. On the contrary, when D1 is OFF, and D2 is ON; the bandwidth is narrow at 1 mm and does not cover the UMTS 2100 band. It also shows lossy behavior as shown in Figure 3.2 (b)- when the width is 2 mm. Finally, when both diodes are OFF; the higher frequency is shifted to a lower band as shown in Figure 3.2 (c).

The simulated return loss for the proposed antenna relative to change the length of longer strip, while other parameters remain the same is shown in Figure 3.3. As the frequency and the wavelength are inversely proportional, so when the length is decreased, the frequency is shifted to higher band. In case, when D1 is ON and D2 is OFF, the proposed antenna does not cover GSM 850 and GSM 900 band at the lengths of 32.6mm and 27.6mm, respectively. Both bands are covered, when the length is 37.6mm, and it can be shown in Figure 3.3(a). In other case, when D1 is OFF and D2 is ON, the proposed antenna shows narrow bandwdith at 27.6mm, and does not cover the upper and lower band. It still shows narrow bandwidth when the length is 32.6mm. The antenna shows wide bandwidth of 600 MHz at the length of 37.6mm as shown in Figure 3.3-(b). Finally, as shown in Figure 3.3-(c), the lower frequency band is marginally shifted, and shows good return loss with different lengths, when both diodes are in OFF-state.

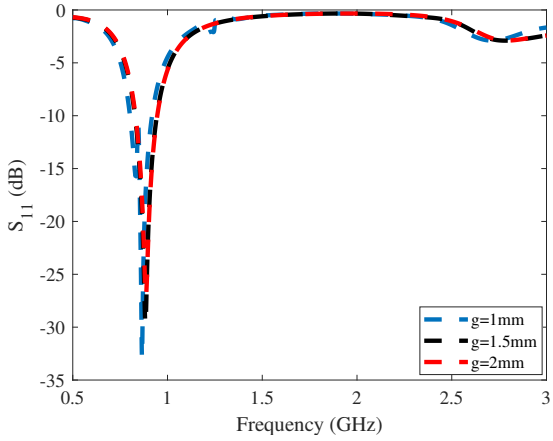

(a)

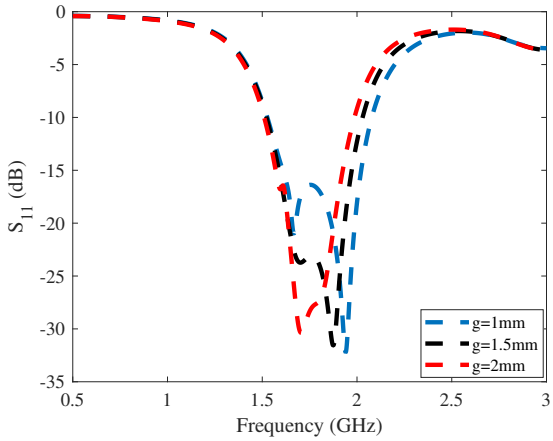

(b)

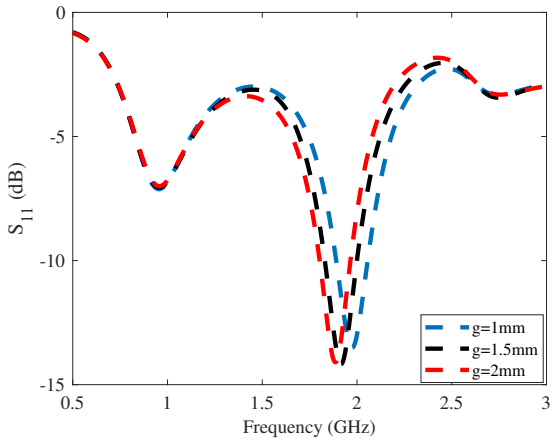

(c)

Figure 3.2: Width size (g) for both sides of D1 when: (a) When D1 ON, D2 OFF; (b) D1 OFF, D2 ON; (c) Both diodes OFF

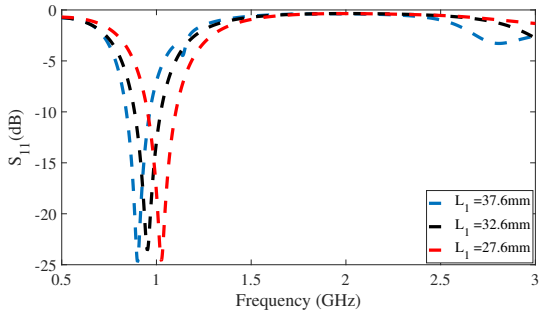

(a)

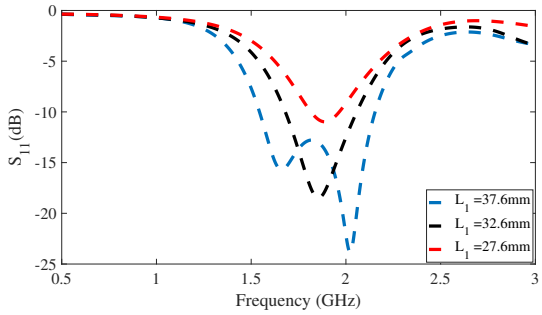

(b)

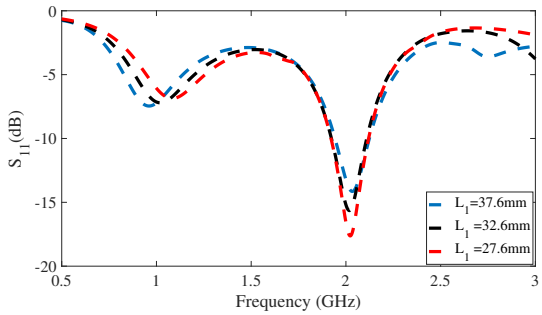

(c)

Figure 3.3: Variation of long strip L_1: (a) D1 is ON, D2 OFF; (b) D1 OFF, D2 ON; (c) Both diodes OFF

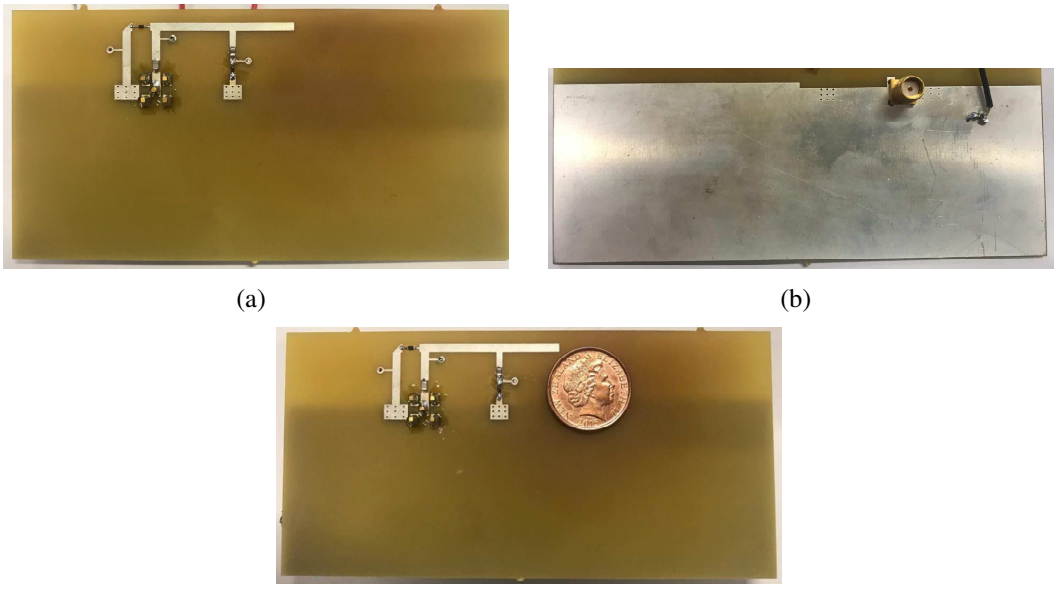

(a) (b)

(c)

Figure 3.4: Proposed Antenna Prototype: (a) Front side (b) Back side (c) Compact antenna structure

3.2.4 Results and Discussion

The fabricated prototype of front and back side for the proposed antenna is shown in Figure 3.4 (a) & (b), and comparison of compact antenna size can be seen in Figure 3.4 (c). A portable vector network analyzer (VNA) was used to measure the return loss of the proposed antenna. The radiation pattern was measured by using ME1310 from Keysight Technologies. The voltage is provided to the PIN diode with a power supply. The connecting wires were connected on the ground plane to avoid the disturbance of radiation pattern. The PIN diode in forward bias maximally consumed 10 mA current with 0.89 V. 0V is used to turn off the PIN diodes.

The simulated and measured return loss of the proposed antenna is shown in Figure 3.5. According to the simulation results, as shown in Figure 3.5 (a), when both diodes are OFF, the antenna operates at 1.94 GHz to 2.12 GHz (the UMTS 2100 band). The antenna also cover GSM 900/950, but in this case the return loss is around 6dB. When D1 is ON and D2 is OFF, the frequency is shifted to a lower band. The proposed antenna

resonates at frequencies from 0.841 GHz to 0.964 GHz and covers GSM 850/900 band as shown in Figure 3.5 (b). When D1 is OFF and D2 ON, the antenna behaves as wideband as shown in Figure 3.5 (c). The impedance bandwidth is almost 600 MHz, and covers GLONASS 1616, DCS 1800, PCS 1900, and UMTS 2100 bands. Both the simulated and measured results show a return loss more than 10dB for all bands. Although- there is negligible variance between the measured and simulated results, it should be due to the parasitic effects of PIN diodes, variance of electrical property of FR4 substrate, and the solder mask.

To understand the operation of reconfigurable antenna, it is important to study the current distribution on radiation elements. Figure 3.6- shows the HFSS simulation results of PIFA antenna surface current distribution at 0.85/0.90, 1.6, 1.8, 1.9, and 2.1 GHz, respectively. As shown in Figure 3.6 (a), when D1 is ON, and D2 is OFF, the current flows in F-shaped radiation element to feed, and it is close to the quarter-wave length of GSM 850/GSM 900. When D1 is OFF , and D2 is ON, the surface current flows in I-shaped and longer-strip radiation element to the the feed as can be seen in Figure 3.6 (b). It covers the 4 different frequencies from 1.54 GHz to 2.13 GHz. Finally, the surface current distribution for both diodes in OFF states is shown in Figure 3.6 (c). The current mainly flows in the longer strip and some part of I-shaped radiation element.

The simulated and measured 2D radiation pattern of proposed reconfigurable antenna is plotted in Figure 3.7. The radiation patterns were measured in anechoic chamber. As shown in Figure 3.7 (a) and (b), the radiation pattern in E-plane as well as in H-plane shows an omnidirectional characteristics. On the contrary, the antenna behaves like a dipole in E-plane-when D1 is OFF and D2 is ON as shown in Figure 3.7 (c), but shows omnidirectional behaviour as shown in Figure 3.7 (d). Finally, when D1 is ON and D2 is OFF, the proposed antenna shows dipole-like characteristics for both planes as shown in Figure 3.7 (e) and (f). The results of all configurations are summarized in Table 3.2.

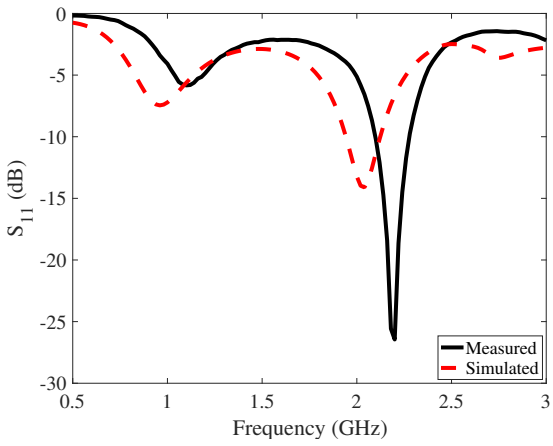

(a)

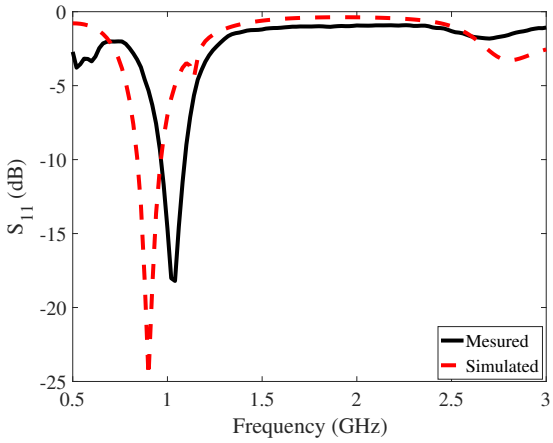

(b)

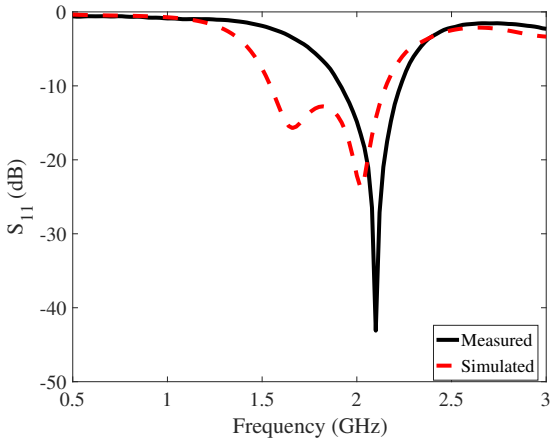

(c)

Figure 3.5: Simulated and measured return loss for different states of PIN diodes when: (a) Both diodes are off (b) D1 on, D2 off (c) D1 off, D2 on

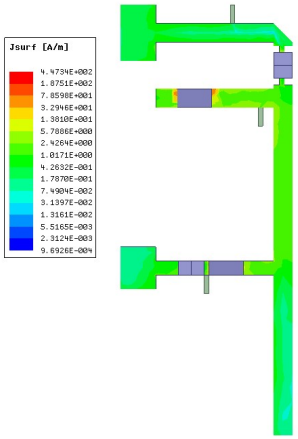

(a)

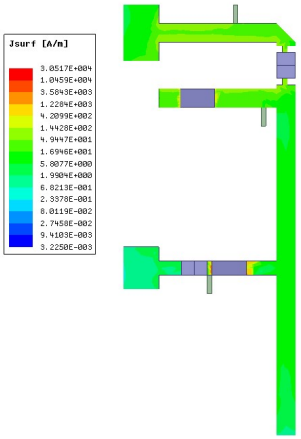

(b)

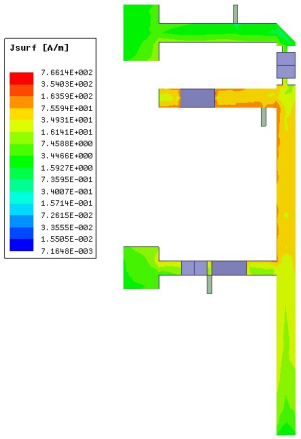

(c)

Figure 3.6: Current distribution when: (a) D1 on, D2 off (b) D1 off, D2 on (c) Both diodes off

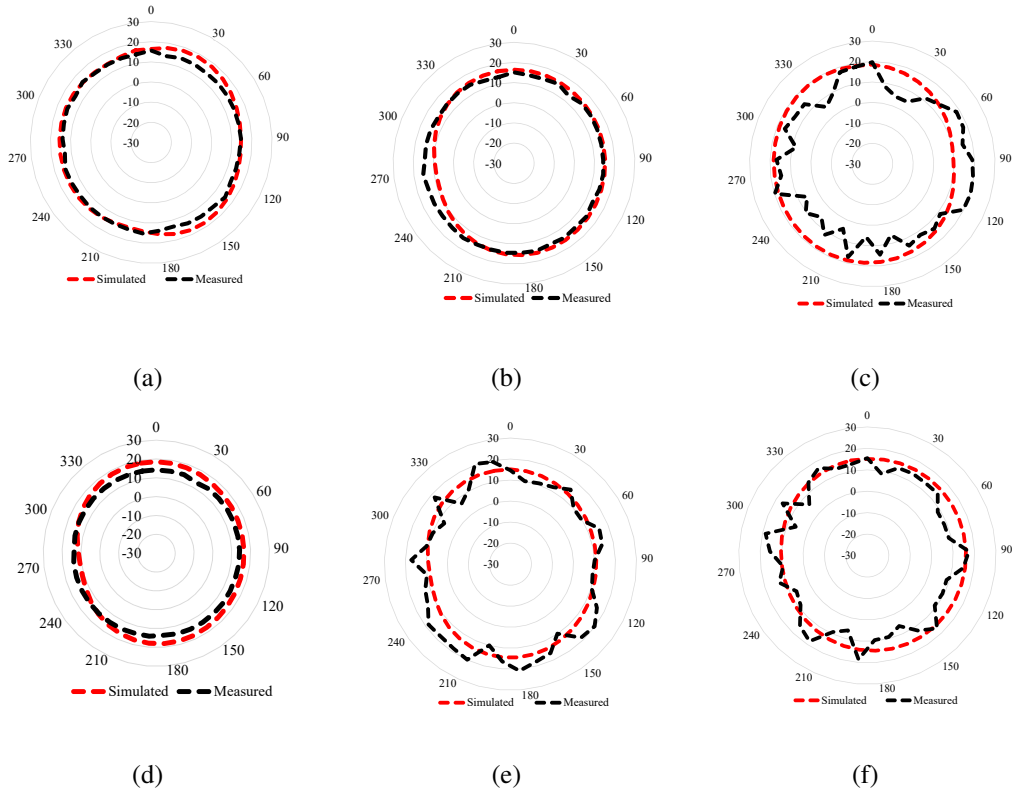

Figure 3.7: Simulated and measured 2-D radiation pattern of proposed antenna design when: (a,b) Both diodes are OFF; (c,d) D1 is OFF, D2 is ON; (e,f) D1 is ON, D2 is OFF

Table 3.2: Performance parameters of the Proposed Antenna

Configuration	**Bandwidth**	**Gain (dBi)**	**Efficiency**
D1 ON, D2 OFF	0.84-0.964 GHz	2.12	84%
D1 OFF, D2 ON	1.54-2.13 GHz	1.95	82%
Both OFF	$1.94 - 2.12$ GHz 0.865-1.07 GHz (-6dB)	1.89	87%

3.2.5 Comparison with state-of-the-art-work

Table 3.3 compared the proposed frequency reconfigurable antenna with existing works in terms of antenna size, substrate, resonant frequencies and the number of switches.

Table 3.3: Comparison with other Designs

Reference	**Antenna Size (mm^3)**	**No. of Frequencies**	**No of Switches**	**Substrate**
[156]	$31.5 \times 30.5 \times 1.57$	0.7 GHz, 1.90 GHz 3.5 GHz, 5.2 GHz	2	FR-4
[157]	$30 \times 70 \times 1$	USPCS, WCDMA,m-WiMAX, and WLAN	2	FR-4
[159]	$50 \times 46 \times 1.52$	3.12 GHz, 3.42 GHz 3.75 GHz, 4.06 GHz 4.42 GHz, 4.77 GHz	5	Taconic RF 35
[160]	$8 \times 62 \times 5$	LTE Band, GSM850 /900 Bands	2	FR-4
[162]	$40 \times 43 \times 1.6$	WLAN, WiMAX, C-Band, ITU Bands	4	FR-4
[163]	$80 \times 25.1 \times 1.5$	2.21 - 2.79 GHz 5.27 - 5.56 GHz	5	Rogers 4350
[166]	$63.5 \times 33.5 \times 1.6$	2.1 / 2.4 / 3.5 GHz	3	FR-4
[167]	$50 \times 45 \times 1.6$	2.2 - 6 GHz	2	FR-4
[168]	$65 \times 60 \times 1.55$	1.45 - 4.6 GHz	6	FR-4
[171]	$62 \times 46 \times 3$	2.45 / 5.25 / 5.75 GHz	N/A	Denim
[172]	$40 \times 60 \times 1.6$	2 - 10 GHz	4	FR-4
This Work	$44 \times 14 \times 3.2$	GSM 850/ 900, and UMTS 2100	2	FR-4

3.3 Polarization Reconfigurable Dual-Band PIFA Antenna

3.3.1 Introduction

A number of reconfigurable and multiband antennas have been reported in the literature, but most of them could not cover the 800 MHz and 1400 MHz with dual polarization capability, as the antenna required significant space due to the quarter-wavelength at 800 MHz [173]. To implement compact wideband antenna, coupling feed and short circuiting techniques are used to achieve different frequency ranges [174, 175]. Most multiband antennas reported in the literature for mobile devices have a size of under 500 mm^2 [176, 177]. However, they have poor efficiencies(<40%) for the lower frequency band. It is also noted that the compact antenna proposed in [4] has a relatively high return loss of -6dB for the desired band. In [178], a C-shaped ground monopole antenna with dimensions $35 \times 10 \times 0.8mm^3$ was designed to improve the bandwidth, but it did not support dual polarizations . Nowadays, a number of reconfigurable antennas have been studied by using PIN diodes, Micro-Electro-Mechanical Systems (MEMS), varactor diodes, and smart material for different communication applications. Up to now, limited attention has been paid to cover horizontal and vertical polarizations for 800 MHz and 1.4 GHz [179, 180, 181]. Through a careful analysis of the literature, it is noticed there are indeed trade-offs between antenna gain, operating frequency band, input impedance and reduction in the antenna size [182].

With the rapid development in wireless technologies, there is a strong demand for compact size antenna design. As single-band and multiband antennas do not fulfil this requirement, they are not suitable for wireless handheld devices or MIMO applications. Mutual coupling is the critical issue in MIMO as multiple antennas are used at receiver and transmitter side [183]. Due to the complexity in the antenna structure and operation

of multiband antennas, it is hard to achieve antenna miniaturization [184]. The possibility of strong co-channel interference increased due to poor isolation [185, 186, 187]. Increased antenna complexity, small size, low cost fabrication, easy integration with communication device, and reduced coupling between antennas elements are the major design challenges. Reconfigurable antennas play an important role in addressing the challenges of single-band and multiband antennas. They can provide good impedance match for multiple frequency bands with less space. This section proposes a new design of a dual frequency and polarization reconfigurable antenna. The proposed antenna features a total size of 950 mm^2, an efficiency of higher than 88% in both considered frequency bands, and a small ground clearance of less than 15 mm, which is rare among the antennas for mobile devices reported in the literature. This design has high gain, stable radiation, and high impedance matching. The structure of the antenna is suitable for different applications like portable mobile devices.

3.3.2 Proposed Antenna Design and Configuration

Two orthogonal planar inverted-F antennas (PIFA) [188] are designed as shown in Figure 3.8, with two PIN diodes used to switch between horizontal and vertical polarization. Another two PIN diodes in antenna branches are used to tune the antenna to resonate at either 800 MHz or 1.4 GHz.

Figure 3.9 (a) shows the layout of the proposed PIFA, which is fabricated using FR-4 dielectric substrate. The permittivity and thickness of FR-4 is 4.4, and 0.8 mm, respectively. The antenna consists of two elements, each with a compact size of $32 \times 15mm^2$. The proposed antenna differs from a conventional PIFA in that instead of connecting the short directly to the feeding element, it is connected to the end of an electromagnetically coupled strip that is parallel to the feeding element. The main parts of the antenna are the PIN diodes (NXP BAP64-03) and radiation elements. For

reconfigurability, two PIN diodes are used to alter the length of shorted strip. A ground plane of size $105 \times 45mm^2$ acts as a system ground for the mobile device. For compact size, the shorted strip and ground plane are placed near the substrate.

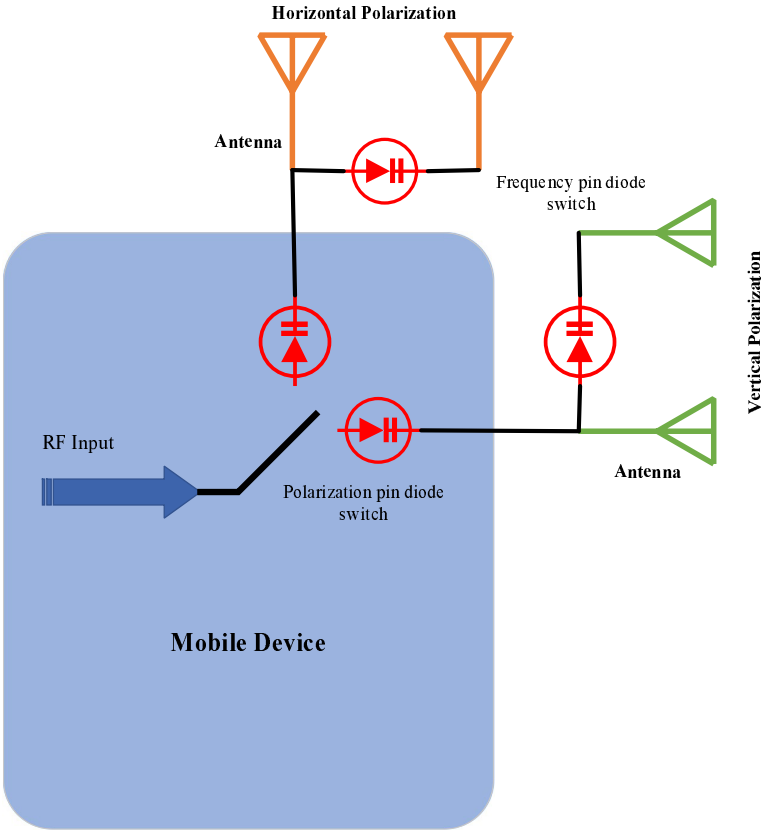

Figure 3.8: Design concept of frequency and polarization reconfigurable antenna

The antenna dimensions are shown in Figure 3.9 (b). Two PIN diodes are fabricated at points E and H to control the resonance frequency and another two PIN diodes are placed at points B and C to control the antenna polarization. The operating voltage and current for PIN diodes is +5 V and 3 mA, respectively. The antenna structure is composed of two independent elements. The overall length (58 mm) of this structure is equal to about a quarter-wavelength at 1.4 GHz. An additional resonance is created from an electromagnetically coupled strip (93 mm) using a shorted parasitic element, which is attached with ground plane through a planar inverted via. The microstrip line

with 50 Ω is connected with feeding strip on the top side. The shorted and the feeding strips have coupling gap of 0.5 mm between them. The longer shorted strip behaves as second radiator. The length of feeding strip is about 93 mm (a quarter-wavelength at 800 MHz), thus generates the lower resonance frequency of 800 MHz with return loss larger than 10 dB. The antenna operating mode and PIN diodes functions are listed in Table 3.4.

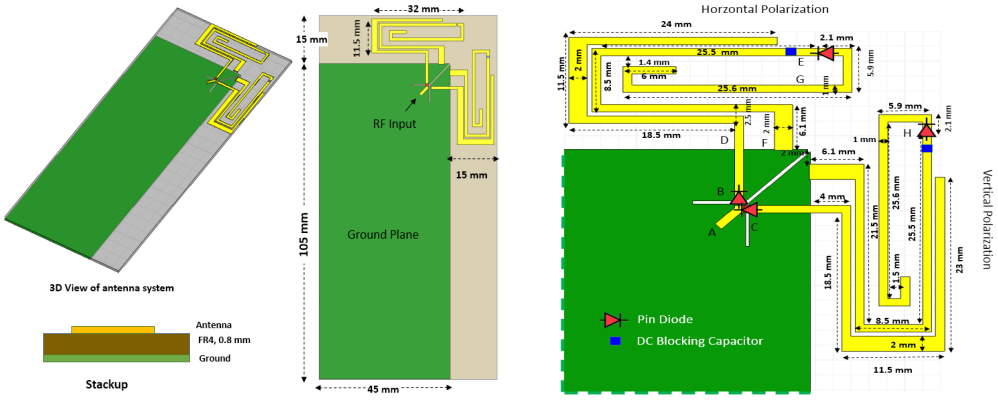

(a) (b)

Figure 3.9: Layout of proposed antenna: (a) 3-D structure; (b) Antenna Dimensions (Top view)

Table 3.4: Antenna Operating Modes and PIN Diode Function

Antenna Mode	**Polarization**	**Resonant Frequency**	**PIN Diodes**			
			B	**C**	**E**	**H**
1	Horizontal	1400 MHz	ON	OFF	OFF	OFF
2	Horizontal	800 MHz	ON	OFF	ON	ON
3	Vertical	1400 MHz	OFF	ON	OFF	OFF
4	Vertical	800 MHz	OFF	ON	ON	ON

3.3.3 Antenna Operational Principal

The higher resonant frequency of 1.4 GHz can cover the Long Term Evolution (LTE) 1.4 GHz bands. This resonant frequency is achieved by section A-B-D-E shown in Figure 3.9, by setting PIN diode E to OFF. The lower resonant frequency of 800 MHz is obtained by section A-D-E-F-G. The first resonant frequency mode is centered at 1.4 GHz. By adding an electromagnetically coupled shorted strip to the feeding element (with antenna in ON-state), the antenna resonant mode is shifted to 800 MHz.

The PIN diodes are placed inside the inner strip. To turn the PIN diode "ON", a DC bias (Vcc) of +5V is applied through the inner strip, and its electrical path is tuned to 800 MHz. On the other hand, the electrical path is tuned to 1.4 GHz if the PIN diode is "OFF". To match the impedance to the desired band and reduce the RF signal coupled to the DC source, a 100 pF DC blocking capacitor is used.

The type of PIN diode used is NXP BAP64-03, whose equivalent circuit for "ON" and "OFF" states is shown Figure 3.10. The PIN diode in "ON" state is equivalent to a lump element circuit with 0.8Ω resistor and 1.68 nH inductor in series. Similarly, the equivalent circuit of the PIN diode in "OFF" state consists of a 1.68 nH inductor in series with a parallel circuit of 10 $k\Omega$ resistor and 0.35 pF capacitor. When the diode is in "OFF" state, the current will flow along the smaller strip, causing the antenna to resonate at the higher frequency. On the contrary, when the PIN diode is in "ON" state, most of the current will flow along the larger strip and cause the antenna to resonate at the lower frequency. By changing the path of current flow, different resonant frequency can be achieved.

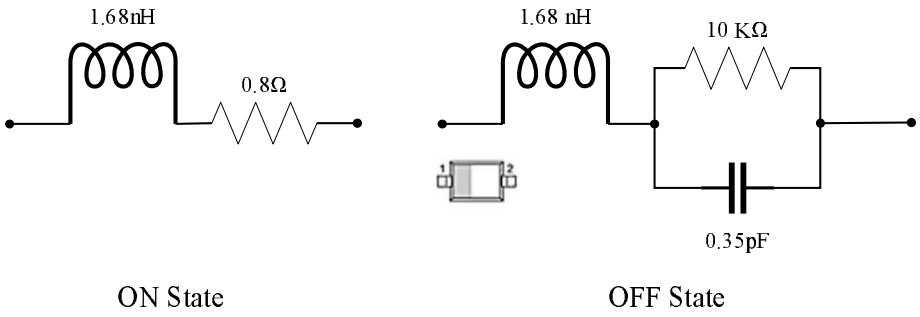

Figure 3.10: Equivalent circuit of BAP64-03 PIN diode ON/OFF states

3.3.4 Antenna Mathematical Modeling

A PIFA and its supporting PCB is shown diagrammatically in Figure 3.11. This configuration can be decomposed into radiating and balanced modes. The input impedance is given by:

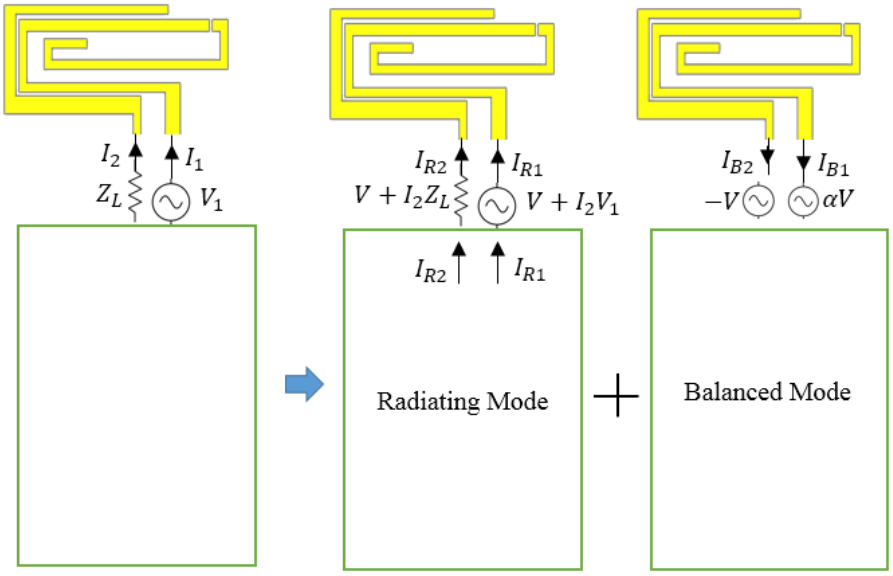

Figure 3.11: Antenna Radiating and Balanced Mode Operations

$$Z_1 = \frac{(1+\alpha)^2 Z_R(Z_L + Z_B) + \alpha^2 Z_L Z_B}{(1+\alpha)^2(Z_L + Z_R) + Z_B} \tag{3.1}$$

Where Z_L is the load impedance applied to the un-fed side of the strip, Z_R is the

radiating mode impedance, and Z_B is the impedance of the short circuit transmission line formed by the strip, derived from the balanced mode. The current sharing factor,α is given by:

$$\alpha = \frac{I_{R2}}{I_{R1}} \tag{3.2}$$

I_{R1} and I_{R2} are the radiating mode currents at the feed and load, respectively. For the case of $Z_L = 0$ (3.1) can be simplified to:

$$Z_1 = \frac{(1+\alpha)^2 Z_R Z_B}{(1+\alpha)^2 (Z_R) + Z_B} \tag{3.3}$$

This is like the well-known expression for a folded dipole—the radiating mode is impedance transformed by a factor $(1+\alpha)^2$ and adds in parallel with the balanced mode. The equivalent circuit is illustrated in Figure 3.12. It should be noted that the impedance transformation in this mode is high, since I_{R2} is greater than I_{R1} due to the position of the slot. This tends to produce an impedance that is too high. It is noteworthy that the bandwidth can be enhanced if Z_B and Z_R are resonant at the same frequency (when becomes a double-tuning circuit).

For open circuit case, setting $Z_L = \infty$ gives:

$$Z_1 = Z_R + (\frac{\alpha}{1+\alpha})^2 Z_B \tag{3.4}$$

The balanced mode impedance is transformed by a factor $(\alpha/(1+\alpha))^2$, and adds in series with the radiating mode.

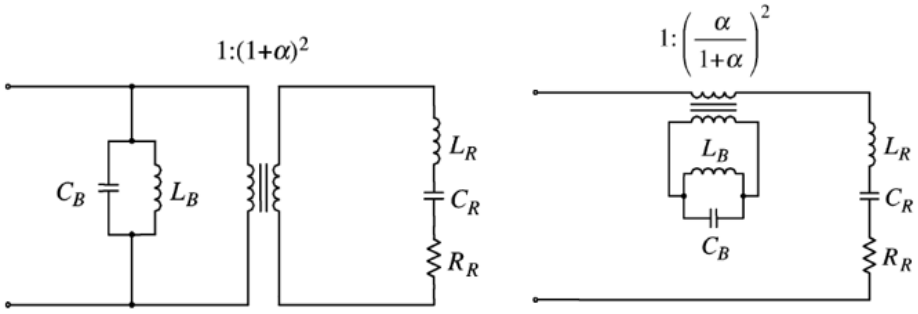

Figure 3.12: Equivalent circuit with a short circuit load and open circuit load

The balanced mode causes the antenna to resonate twice at lower and higher frequencies than determined by the radiating mode (controlled by L_R and C_R). The low and high frequency resonances occur when the radiating mode capacitance and inductance are cancelled by the inductance and capacitance of the transformed balanced mode respectively. There is no impedance transformation with an open circuit load, which tends to produce an impedance that is too low. With a reactive load, the antenna can be tuned over a wide range of impedance- from below the first resonance up to the second resonance of the open circuit mode. And $Z_B = -j\omega L_B/(1 - \omega L_B C_B)$ and $Z_R = R_R + j\omega L_R + (1/j\omega C_R)$.

Equivalent antenna circuit is validated using circuit simulation as shown in Figure 3.13 for 1.4 GHz. Values those used in the subsequent detailed design are: $\omega = 1, R_R = 8.8\Omega, L_R = 4.6nH, C_R = 1.9pF, L_B = 2.3nH, C_B = 0.46pF$. Using these values, the S-parameter for open and short circuit load is shown in Figure 3.13.

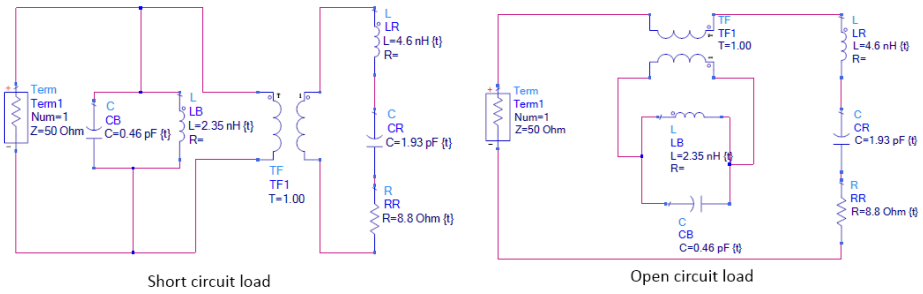

(a)

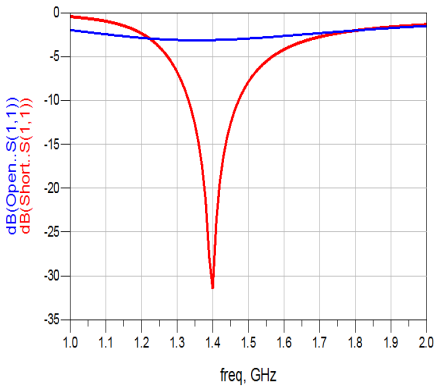

(b)

Figure 3.13: Implementation of Equivalent circuit for open and short circuit load

With inductive loading, any frequency between the first resonance of the open circuit mode and the resonance of the short circuit mode can be achieved. Capacitive tuning allows frequencies between the resonance of the short circuit mode and the second resonance of the open circuit mode to be covered. From the equivalent circuits with open and short circuit loads, the open circuit mode exhibits resonance at a lower resistance than the short circuit mode.

3.3.5 Results and Discussion

The proposed antenna is designed and optimized using Finite Element Method (FEM) for best return loss performance. The Ansys HFSS software is used for the simulation. Figure 3.14 shows the simulated return loss. By controlling the state of all four PIN

diodes, the proposed antenna can be successfully tuned to 800 MHz or 1400 MHz with horizontal or vertical polarization. For horizontal polarization, the obtained bands are 760–850 MHz and 1.38-1.47 GHz, while for vertical polarization, they are 760–810 MHz and 1.31–1.47 GHz. At these frequencies and polarizations, the reflection coefficient is found to be less than -10 dB.

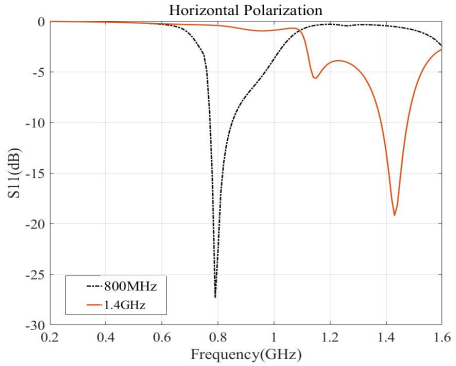

(a)

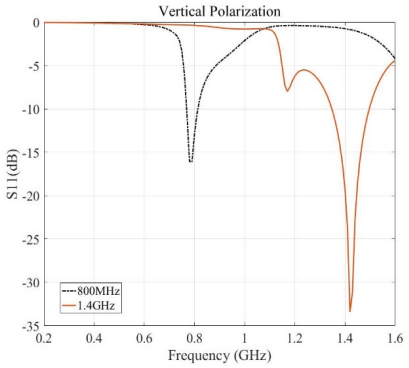

(b)

Figure 3.14: Return loss for (a) horizontal; (b) vertical polarization resonances

Figure 3.15 shows the simulated 3D radiation patterns at 800 MHz and 1.4 GHz for horizontal and vertical polarizations. The simulated gain is found to vary between 2.13-3.7 dBi and the efficiency between 88-92%. The 2D radiation pattern of the proposed antenna for different states of PIN diodes is shown in Figure 3.16.

Table 3.5: Antenna Simulation Results

Antenna Mode	**Polarization**	**Resonant Frequency**	**Antenna Results**		
			Gain (dB)	**Efficiency**	**Bandwidth (-10 dB)**
1	Horizontal	1.4 GHz	3.69	91	90 MHz
2	Horizontal	800 MHz	2.13	90	90 MHz
3	Vertical	1.4 GHz	2.58	92	50 MHz
4	Vertical	800 MHz	2.14	88	150 MHz

To further verify the antenna's performance and clearly show which sections of antenna are responsible for radiation in different bands, the E-Field distribution is studied. As observed from Figure 3.17, the 1.4 GHz resonant frequency mode is the result of feeding strip in OFF-state and the current is mainly located on the feeding monopole element. Similarly, strong surface currents are observed on the shorted strip and on the coupled monopole at about 800 MHz. Antenna polarization is characterized by the directions of the electric fields. To validate the antenna polarization, vector E-field is plotted both for horizontal and vertical antenna as shown in Figure 3.18.

3.3.6 Comparison with state-of-the-art-work

Table 3.6 compared the proposed frequency reconfigurable antenna with existing works in terms of antenna size, substrate, resonant frequencies and the number of switches.

3.4 Summary

In this chapter, a simple and compact frequency reconfigurable antenna by using two PIN diodes were designed to resonate at GSM 850/ 900 and UMTS 2100 bands. In first

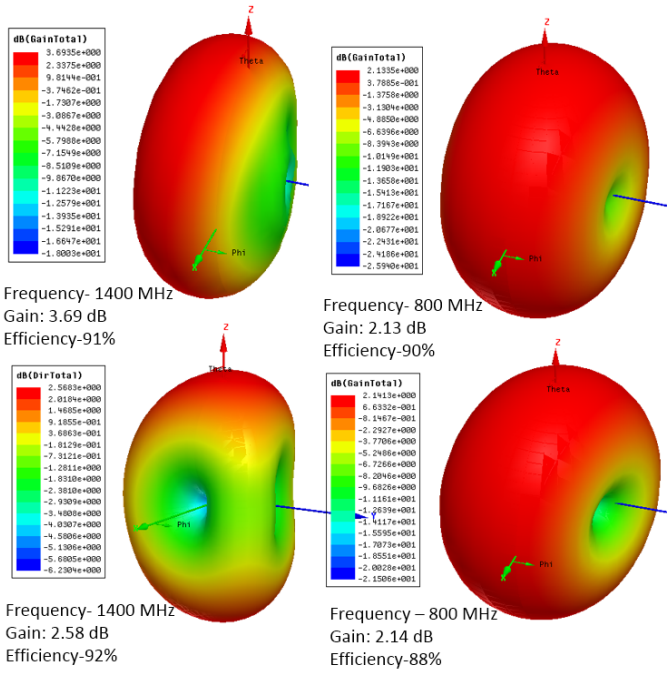

Figure 3.15: Simulated 3D radiation pattern of proposed antenna

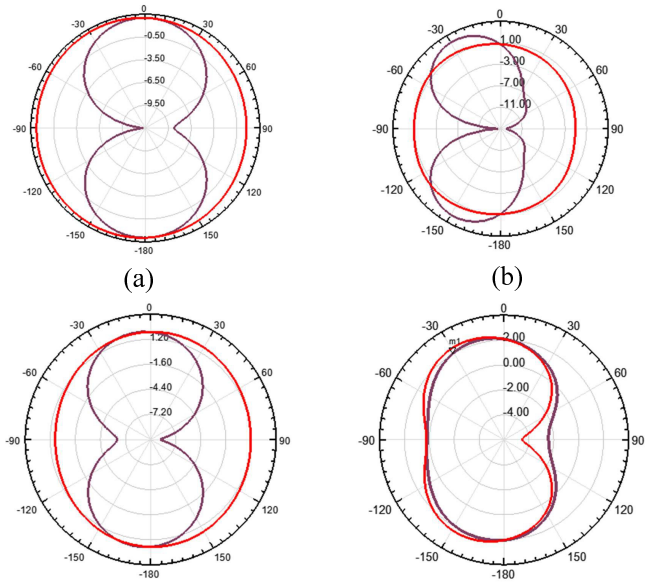

Figure 3.16: 2.D radiation pattern at 1.4 GHz and 800 MHz (a) Horizontal polarization at 1.4GHz, (b)Horizontal polarization at 800MHz, (c)Vertical polarization at 1.4 GHz, (d)Vertical polarization at 800MHz

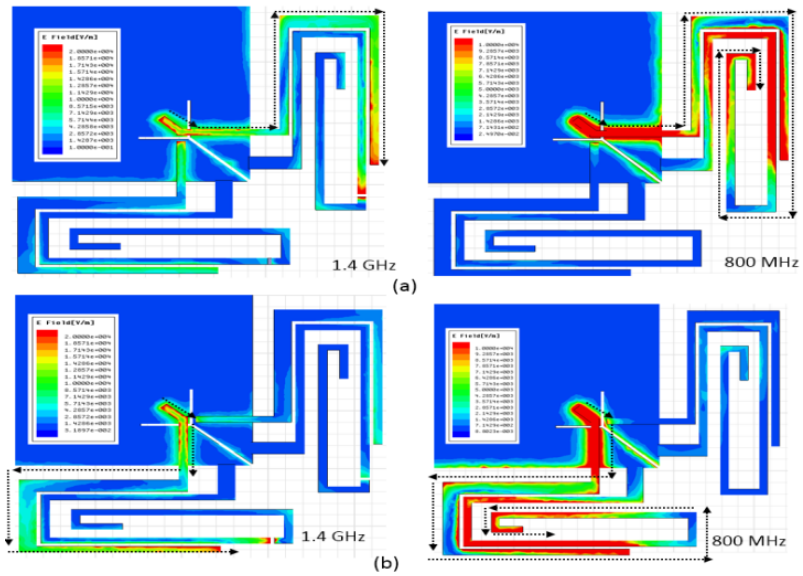

Figure 3.17: E-Field distribution in all four operating modes

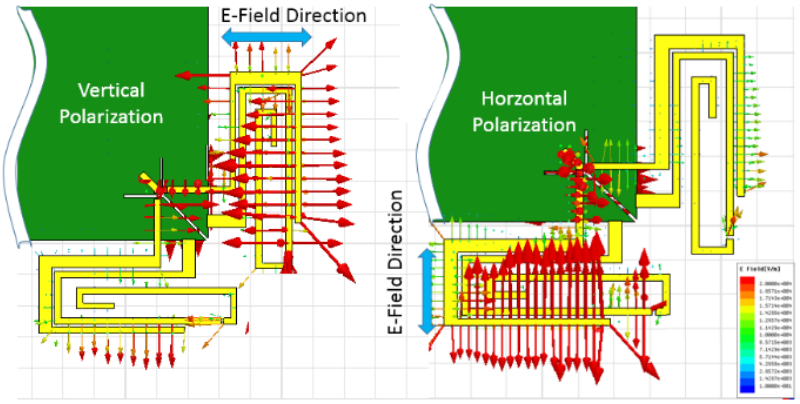

Figure 3.18: E-Field plot of horizontal and vertical polarized antenna

Table 3.6: Comparison with other Designs

Reference	**Antenna Size** (mm^3)	**No. of Frequencies**	**No of Switches**	**Substrate**
[179]	$7 \times 50 \times 4.8$	GSM 850/900, DCS PCS, UMTS, LTE2300 LTE2500	1	FR-4
[180]	$100 \times 60 \times 1$	LTE, GSM850/900 DCS, PCS, UMTS	1	FR-4
[181]	$27.8 \times 10 \times 1.6$	GSM, DCS, PCS UMTS2100 Bands	1	FR-4
[184]	$18 \times 20 \times 0.5$	WLAN, WiMAX LTE Bands,	2	Nelco N4000
[185]	$42 \times 100 \times 0.508$	GSM, DCS, PCS UMTS, Bluetooth WLAN	2	Rogers 4003
[186]	$45 \times 11 \times 6$	GSM900/1800/1900 UMTS Bands	2	FR-4
This Work	$32 \times 15 \times 0.8$	0.8 GHz, 1.4 GHz Horizontal/Vertical Polarization	4	FR-4

part, simple and compact PIFA antenna was presented. In second part, reconfigurable antenna with polarization was explained. The main feature of the first design is its highly compact size, while retaining a performance comparable with existing designs. The second design is a novel dual frequency and polarization-reconfigurable antenna. The proposed antenna resonates at 800 MHz and 1.4 GHz intended frequencies, and switch between horizontal and vertical polarization.

Chapter 4

Reconfigurable Antenna for 5G Applications

4.1 Frequency Reconfigurable Printed Monopole Antenna

4.1.1 Introduction

Rapid advancement in wireless communication systems leads to modern applications like internet of things (IoT), the fifth generation mobile communications (5G), and internet of medical things (IoMT). As a result, the number of mobile users increases exponentially, which forces these technologies to adopt multiple frequency bands to accommodate the user requirements [189]. Among the frequency bands, the Industrial Scientific and Medical (ISM) band is being adopted in Wireless Local Area Networks (WLAN), Worldwide Interoperability for Microwave Access (WiMAX), Bluetooth, and Zigbee [190]. The overcrowded allocations of various wireless applications lead to undesired channel interference problem, thus necessitating the usage of frequency reconfigurable antennas [191].

Being the indispensable component of any wireless system, antenna plays a vital role in achieving compactness in overall size of communication system [192]. Therefore, a frequency reconfigurable antenna, owing the advantage of the compact size, becomes necessary for modern wireless systems. In addition, it can mitigate the band congestion problem with multimode frequency reconfigurable antennas [193]. Operating band can be reconfigured by embedding various electrical and mechanical components in the radiator, which may include radio frequency (RF) positive-intrinsic-negative (PIN) diodes [194], optical switches, micro-electro-mechanical systems (MEMS), and micro-fluids [195].

Researchers have made tremendous efforts in designing frequency reconfigurable antennas for multiple applications [196, 197, 198, 199, 200, 201, 202, 203, 204]. A narrow-band reconfigurable microstrip slot antenna was presented in [196], the antenna achieves five narrow bands in single band operational mode at the cost of five PIN-diodes and large antenna size of 2300 mm^2. In [197], a compact slotted patch antenna was presented, operating in single, dual and triband operating bands. Although the antenna comprises of simple structure and compact size, but it only covers narrow bands. A low-profile frequency reconfigurable antenna with dual band operating bands was presented in [198]. Three PIN-diodes were utilized to achieve four different states. However, the antenna possess narrow bands along with single mode of operation. In [199, 200], the researchers proposed dual band to single band frequency reconfigurable antennas for WLAN applications. Although the presented work posesses a compact size, the adoption of ideal switches (copper tape) limits their usage in practical applications. In [201], the authors proposed a frequency reconfigurable antenna by utilizing just two PIN diodes, and achieved operation modes in either dual band mode or triband mode by changing the states of the diodes. Although the presented antenna offers two dual band and two triband modes by utilizing just two PIN-diodes, it had a fairly large size of 2250 mm^2. In [202], four PIN-diodes were adopted in radiating circuitry to achieve tri,

quad, and penta-band operational modes. However, the presented work is not suitable for practical applications due to the usage of copper tape for measurements. Moreover, the size of 2400 mm^2 also prevents its adoption in mobile applications. A slotted patch antenna with six varactors was designed in [203] with dual and tri-band operational mode. However, the antenna size is 3900 mm^2 along with its poor agreement between simulated and measured results. In [204], a compact frequency reconfigurable antenna with single and dual band operational mode was presented. However, no solution to achieve any wideband mode with concurrent multiple bands was presented.
Through the literature review, we noticed that it is still desired to have a compact antenna with multimode operation, simple geometrical structure, utilizing a smaller number of diodes and better radiation characteristics. This motivates us to propose a compact multimode antenna for heterogeneous wireless applications. The major contribution of this chapter is as follow:

1. The presented multimode antenna offers a smaller ratio of the numbers of operating bands to the numbers of PIN-diodes than any of the existing frequency configurable antennas in the literature.

2. The proposed antenna consists of a simple geometrical configuration, thus leading to significantly reduced fabrication error.

3. The proposed antenna achieves excellent agreement between the simulated results and the measured ones, while presenting an overall better performance as compared to any of the state-of-the-art frequency reconfigurable antennas.

4.1.2 Design Methodology

4.1.2.1 Antenna Configuration

Figure 4.1 presents the top, bottom, and side view of systematic geometry of the proposed frequency reconfigurable antenna. An FR4-epoxy dielectric (ε_r = 4.4, tanδ = 0.002, h = 1.6 mm) is used as the antenna substrate. The antenna is fabricated using standard copper cladding of 0.035 mm thickness. The antenna consists of rectangular radiator of dimension $L_p \times W_p$, whose bottom corners are truncated using slots triangular slots of dimension $L_m \times W_m$ to enhance the narrow bandwidth of the conventional monopole antenna. Two symmetric rectangular sleeves having dimension $S_{L1} \times S_w$ are utilized to achieve lower resonant mode, while a middle sleeve of length S_{L1} is connected to another triangular radiator having dimension of $L_R \times W_R$, to achieve a dual band antenna. Thereafter, three slots of $1mm \times 1mm$ are etched to insert diodes between stubs and main radiator. On the backside of the substrate, biasing circuit is connected to provide a DC voltage, as shown in Figure 4.1 (b). The presented antenna exhibits a compact size of $15mm \times 30mm \times 1.6mm$ which corresponds to $0.11\lambda_o \times 0.23\lambda_o \times 0.012\lambda_o$, where λ_o is free space wavelength at the lowest resonance of 2.3 GHz. The optimized parameters of the proposed antenna are as follow: $A_L = 30mm; A_W = 15mm; H = 1.6mm; C_W = 6mm; C_L = 5mm; d = 0.5mm; g = 1.5mm; W_m = 14mm; L_p = 5.5mm; L_m = 8.5mm; W_p = 6mm; S_{L1} = 8.5mm; S_{L2} = 9.5mm; S_w = 1mm; W_R = 14mm; L_R = 5.5mm.$

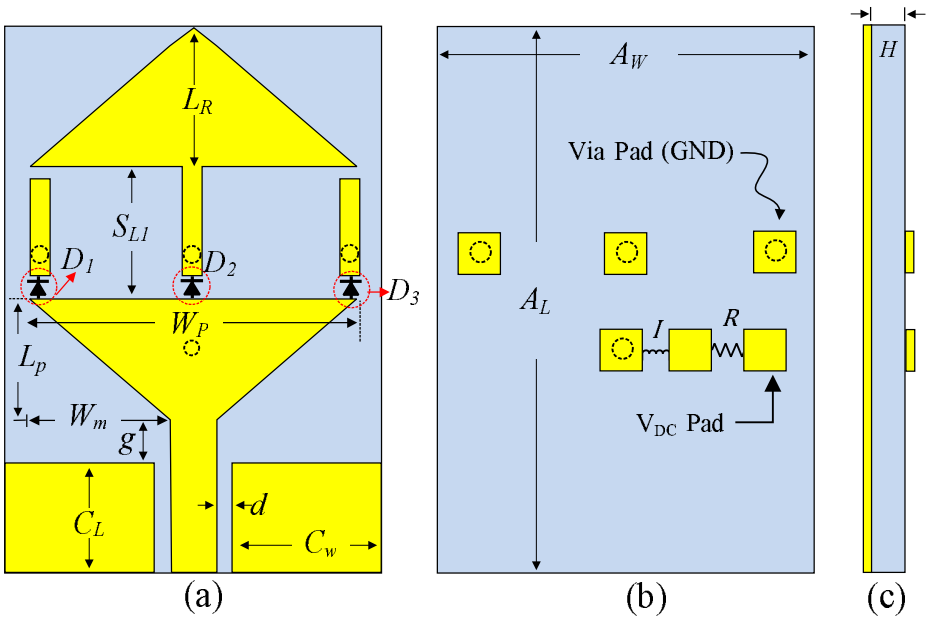

Figure 4.1: Geometrical configuration (a) top view (b) back view (c) side view

4.1.2.2 Design Characterization

The proposed antenna is extracted from a conventional monopole antenna, where the length L_p of the antenna is kept approximately equals $\lambda/4$ to attain a quarter-wave monopole antenna, where λ is the free space wavelength of the desire frequency. For the resonating frequency of 5.2 GHz, the dimension of the quarter-wave monopole antenna can be found by [205]:

$$L_T = \frac{c}{4f_o\sqrt{\epsilon_e}} \tag{4.1}$$

Where L_T is the total effective length of the monopole, which is given by $L_T = g + L_p$; where L_p is the length of the monopole, g is the gap between radiator and CPW feed, $c = 3 \times 10^8 ms^{-1}$ is the speed of the light in free space and f_o is the central resonating frequency which is chosen to be 5.2 GHz, and ε_e is the effective dielectric constant which is necessary to find instead of ε_r because field components are restricted to the substrate. The value of ε_{eff} can be extracted as:

$$\varepsilon_{eff} = \frac{\varepsilon_r + 1}{2} + \frac{\varepsilon_r + 1}{2}(1 + 12\frac{w}{h})^{-0.5} \tag{4.2}$$

The conventional monopole antennas show narrow bandwidth. An appropriate way to enhance the bandwidth of a coplanar waveguide antenna is truncating the radiating structure [206]. Recently, many of the researchers have adopted various techniques including fractal geometries [207], stub loading [208] and defected ground structure (DGS) [209] to overcome this challenging drawback. Here, we adopted the technique of truncating the radiator corner to enhance bandwidth. By tuning the dimension of the slot and gap between the radiator with feeding structure, maximum wideband can be achieved. In other words, the insertion of this slot also increases the effective length of the antenna, which results in good impedance matching over a wideband. The dimension of this modified patch can be calculated by (4.2), however, the effective length (L_T) for this modified patch is given as $L_T = g + L_m$; where L_m is the hypotenuse of the triangular slot.

For maximum achievable bandwidth, the length (L_m) and width (W_m) of slot and the gap of radiator from co-planar waveguide (CPW)-fed (g) can be calculated by [210]:

$$L_m = \frac{x_1 c}{f_o\sqrt{\varepsilon_e}} \tag{4.3}$$

$$g = \frac{x_3 c}{f_o\sqrt{\varepsilon_e}} \tag{4.4}$$

Where x_1, x_2, and x_3 are constants, which correspond to the fraction of free space wavelength at f_o where the values can be obtained through going detailed experimental studies. For the presented case, the optimum values of x_1, x_2, and x_3 are found to be 0.15, 0.18 and 0.045, respectively. Figure 4.2 depicts the comparison of S-parameters among the conventional rectangular monopole and the modified triangular-shaped

monopole antenna. Conventional monopole shows the impedance bandwidth of 1.31 GHz (4.59-5.9 GHz) while triangular antenna exhibits a wideband of 3.03 GHz (4.15-7.18 GHz) for S_{11} < -10dB.

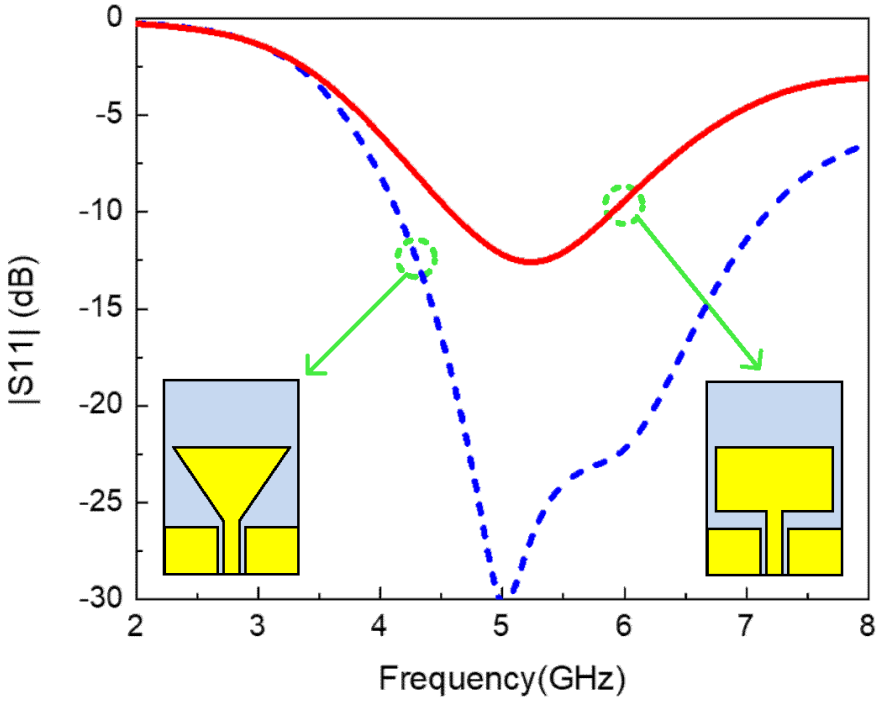

Figure 4.2: Simulated return loss comparison among rectangular monopole and modified triangular shaped monopole

Insertion of sleeves in radiating patch to lower the resonant frequency is a well-known technique to design compact size antennas [60]. At the first step, the resonant frequency of the triangular monopole antenna is shifted from 5 GHz to 3.5 GHz by inserting a rectangular sleeve, the resonant frequency (f_L) due to this sleeve can be calculated by [211]:

$$f_L = \frac{c}{x_o L_T}\left(\frac{\varepsilon_r + 1}{2}\right)^{-1/2} \tag{4.5}$$

Where L_T can be determined by using the relation of $L_T = g + L_m + S_{L1}$, ε_r is the relative permittivity of the substrate while x_o is the expression coefficient which is the

fractional part of the resonating frequency f_L. Thus, a dual-band antenna is extracted from a wideband antenna, as shown in Figure 4.3. Then, a symmetric sleeve is inserted at the other side of the radiator, and the insertion of this open-ended stub mitigates the higher resonance and antenna becomes a single band antenna, as shown in Figure 4.3. This phenomenon can be explained by observing the current densities at 6 GHz for both prototypes. It can be seen from Figure 4.4 (a) , when a single stub is connected to the radiator, the current density has the maximum value,which is responsible for higher resonance mode. On the contrary, when two sleeves are connected to the monopole antenna, the maximum current density is along joining point of the sleeve with radiator, as depicted in Figure 4.4 (b), which causes the mitigation of higher resonance.

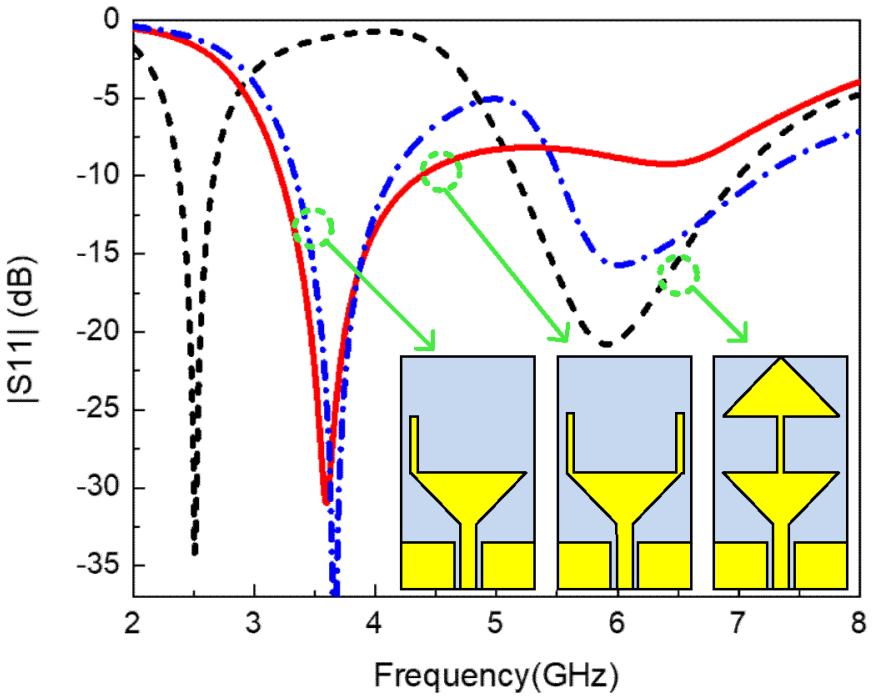

Figure 4.3: Simulated return loss comparison among triangular-shaped monopole antenna loaded with various stubs.

(a) (b)

Figure 4.4: Surface charge distribution at 6 GHz of (a) antenna loaded with a single stub (b) antenna loaded with two stub

Besides, it is observed by numerical analysis that the position of stub has a great impact on resonant frequency due to the increase of L_T. At the midpoint of triangular radiator L_T attain the maximum value of $L_{T(max)} = L_T + W_p/2 - S_{L1}/2$, thus results in shifting of resonant frequency toward the lower side. Therefore, another prototype was constructed to achieve a lower resonant at 2.45 GHz along with higher operational mode. An inverted triangular radiator is inserted at the top of the sleeve, which results in an increase of L_T. For this case the value of $L_T = g+L_m+W_p/2-S_{L1}/2+S_{L2}+W_R+L_R$, the optimized value of L_T for 2.45 GHz is 37.3 mm which is nearly equal to numerically calculated value of 37.1mm, using (4.5), whereas $x_o = 2$. The resulting S-parameters are depicted in Figure 4.3. In the last step, prototype-I and prototype-II are integrated to form a single antenna whereas three diodes were inserted between the sleeves and triangular monopole to achieve the frequency reconfigurability. Due to the insertion of diodes, the length of sleeves was optimized to obtain the desired frequencies, while the overall antenna size remains unchanged. Figure 4.5 depicts the design methodology of the proposed antenna by the integration of two different mode antennas.

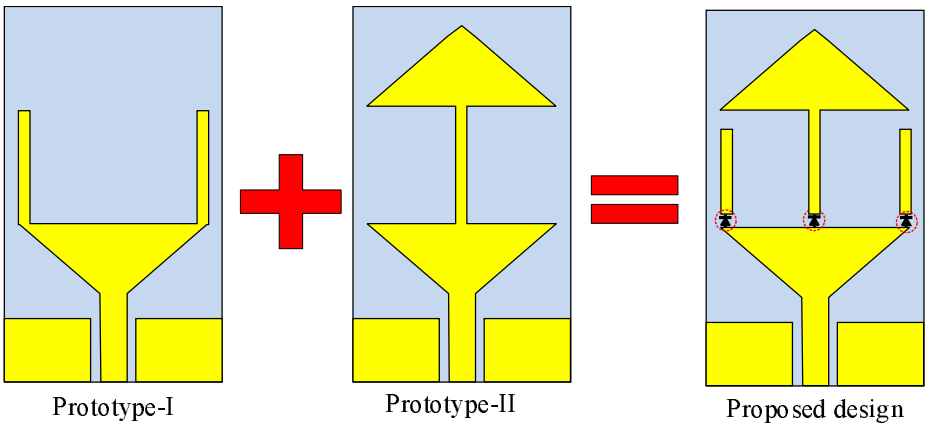

Figure 4.5: Design methodology of the proposed antenna

4.1.3 Results and Discussion

Various antenna performance, including S-parameters, radiation pattern, gain, and efficiency of the proposed antenna are presented in this section. Numerical analysis of the proposed antenna is done using the finite element method solver Higher Frequency Structure Simulator (HFSS) using standard bonding conditions. A 50 Ω SMA connector was utilized to excite antenna to minimize the connector effects on the antenna. The RLC-lumped component equivalent model of the HPND-4005 diode was utilized in such a way that in ON-state, the diode acts as a series combination of a 0.15nH inductor and 4.7Ω resistor. In contrast, in OFF-state, it acts as a series combination of 0.15nH with a parallel combination of 0.017pF and 7kΩ resistance. Detailed schematic of the diode equivalent model along with the biasing circuit, is depicted in Figure 4.6.

4.1.3.1 Measurement Setup

A sample prototype of the antenna is fabricated on the specified FR4 epoxy. Figure 4.7 depicts the top and bottom sides of the fabricated prototype. A commercially available 50Ω SMA connector is used to feed the antenna. The biasing circuit is etched on the backside of the antenna and connected to antenna geometry employing a pad. A 1KΩ

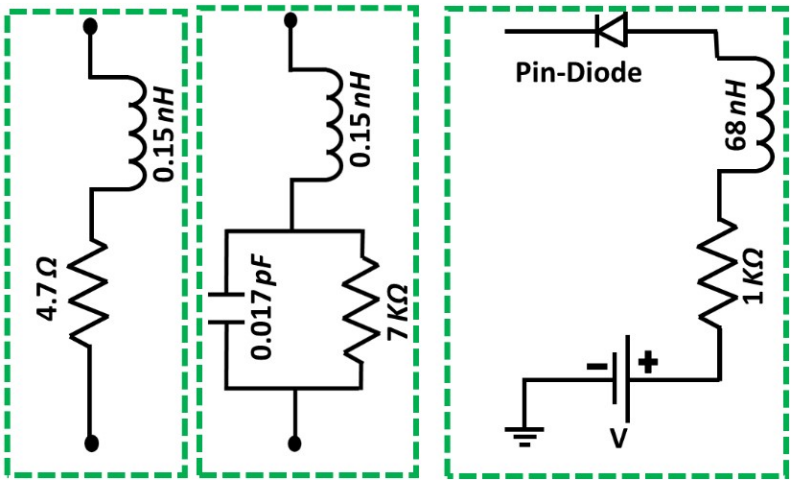

Figure 4.6: Equivalent electrical circuit of pin diode

resistance is connected to limit the source voltage. An inductor of value 68nH is used to block the unnecessary RF current, as shown in Figure 4.7 (b). Vector Network Analyzer (VNA) HP-8720D with a frequency range of 50 MHz to 13.5 GHz was utilized to measure the scattering parameters of the proposed antenna. The fabricated prototype of the presented work is placed 50 cm away from the ETS-Lindgren (EMCO) type broadband horn antenna (Model No. 3115) and maximum of 8 GHz in an anechoic chamber to measure the far-field parameters, including gain and radiation pattern.

4.1.3.2 Return Loss

For simplicity, different cases represent the switching state of the diode. The ON-state of the diode is labelled as '1' while OFF-state is labelled as '0'. Consequently, all diodes in OFF-state are represented as case-000, and so on. Figure 4.8 presents the S-parameters comparison among simulated and measured values. For case-000, sleeves are electrically disconnected from the main radiator, the only lower part is effective. Therefore, the antenna exhibits a wide impedance bandwidth of 3.71 GHz (3.54-7.25 GHz) with S_{11} <-10dB, as depicted in Figure 4.8 (a). Case-001 and case-100

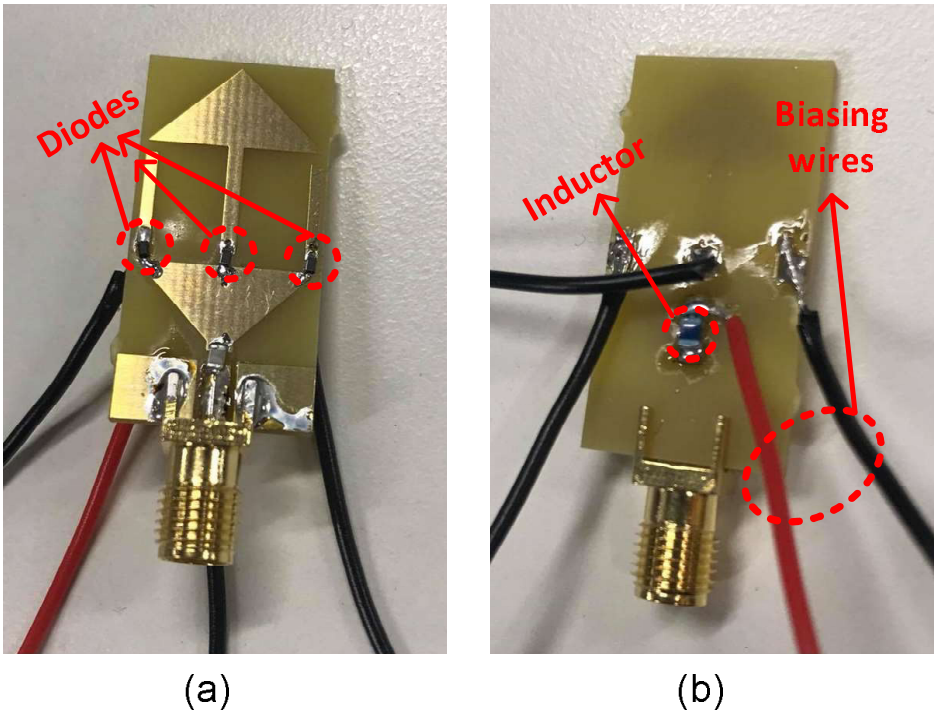

Figure 4.7: Fabricated prototype of the proposed antenna used for testing (a) top-view (b) bottom-view.

produce similar results because only a single side sleeve is connected in both cases. Similarly, case-011 and case-110 also produce the same results. Case-100 and case-110 are considered from the aforementioned four cases . For case-001, the side sleeve is connected, and antenna starts resonating in dual-band mode with an impedance bandwidth of 0.61 GHz (2.95-3.56 GHz) and 3.3 GHz (4.5-7.8 GHz), respectively. Similarly, for case-010, the middle sleeve is connected to the main radiator, and antenna shows dual resonant bands with an impedance bandwidth of 0.21 GHz (2.35-2.56 GHz) and 4.2 GHz (4.4-8.6 GHz). Good agreement between simulated and measured results is observed for both case-001 and case-010, as depicted in Figure 4.8 (b) and 4.8 (c), respectively.

Similarly, for case-101, the antenna starts resonating at a single band due to the theory mentioned above. The antenna resonates at 3.51 GHz with bandwidth ranging from 3.02–4.21 GHz. Noteworthily, for both case-100 and case-101, the antenna covers the

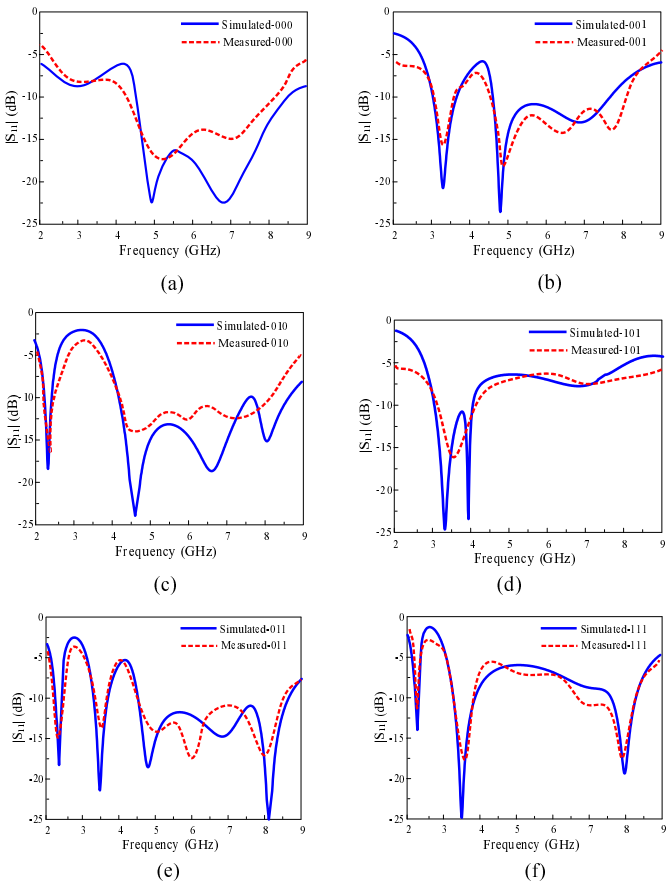

Figure 4.8: Return loss comparison among various diode states (a) Case-000 (b) Case-001 (c) Case-010 (d) Case-101 (e) Case-011 (f) Case-111

3.5 GHz band, which is one promising band to be used for the 5G applications. In case-011, the antenna possesses tri-band mode showing |S11|<-10dB impedance bandwidths of 2.07-2.39 GHz, 3.41-3.9 GHz, and 4.52-8.63 GHz. Finally, when all diodes are switched ON, i.e., for case-111, the antenna starts resonating in tri-band mode with lower resonance at 2.25 GHz, 3.46 GHz and 8 GHz with impedance bandwidth ranging 2.09-2.41GHz, 3.34-4.3 GHz and 7.19-8.75 GHz, as depicted in Figure 4.8 (f). In general, a strong agreement between simulated and measured results is observed. However, the deviation between the corresponding results may be minimized by reducing the fabrication errors. Table 4.1 shows the comparison between measured and simulated results for different states of PIN diodes.

Table 4.1: Summary of the measured and simulated results of the proposed antenna

Switching. Mode	**Operational Mode**	**Simulated Bands (GHz)**	**Measured Bands (GHz)**	**Simulated Peak Gain (dBi)**	**Measured Peak Gain (dBi)**
000	Wideband	3.54–7.25	3.52–7.01	3.37	3.31
001	Dual band	2.95–3.56 4.5–7.8	2.9–3.53 4.45–8.53	2.16,3.7	2.01, 3.24
010	Dual band	2.35–2.56 4.4–8.6	2.3–2.62 4.32–8.11	2.11 3.41	2.04 3.27
011	Tri-band	2.07–2.39 3.41–3.9 4.52–8.63	2.05–2.43 3.35–3.87 4.47–8.43	2.1, 2.3 3.35	1.99, 2.16 3.21
101	Single band	3.02–4.21	3.1–4.4	2.5	2.35
111	Tri-band	2.1–2.38 3.3–4.27 7.89–8.75	2.09–2.41 3.34–4.3 7.19–8.75	2.01, 2.2 3.29	1.96, 2.06 3.1

4.1.3.3 Radiation Pattern, Gain and Efficiency

The radiation pattern of the proposed frequency reconfigurable antenna is depicted in Figure 4.9. For all possible switching cases the antenna possesses monopole like radiation pattern in principle E-Plane ($\theta = 0^{\circ}$) while nearly omnidirectional radiation pattern is observed in H-Plane ($\theta = 90^{\circ}$) at all resonating frequencies below 7 GHz, as depicted in Figure 4.9 (a-e). On the other hand, above 7 GHz the proposed antenna possesses bi-directional radiation pattern in H-Plane, while a slightly tilted bi-directional radiation pattern is observed in E-Plane having beam pointing toward $\Phi = \pm 46^{\circ}$.

Figure 4.10 illustrates the comparison among simulated and measured gain for various

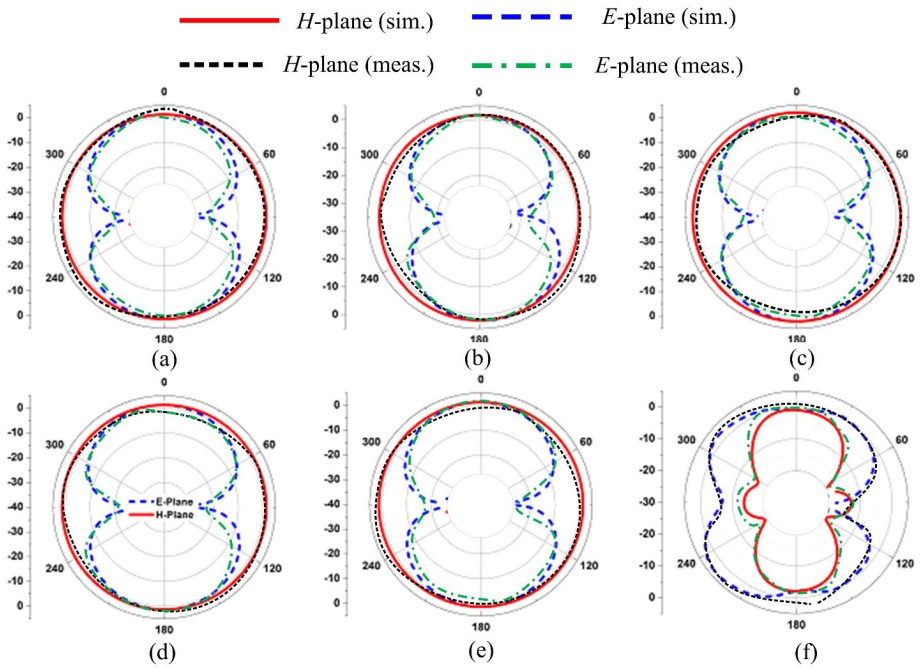

Figure 4.9: Simulated radiation of proposed antenna at various frequencies for various switching state (a) 4.8GHz case-000 (b) 6.77GHz case-000 (c) 8.1GHz case-001 (d) 2.45GHz case-010 (e) 3.5GHz case-101 (f) 2.2GHz case-111 (g) 8GHz case-111.

diode cases. The antenna possesses an average peak gain of > 2 dBi for band ranging 3-10 GHz while an average gain of > 1.9 dBi is observed for 2-3 GHz band spectrum. Note that in non-resonating band the value of gain drops below -5dB, which helps suppress non-resonating bands. Finally, the numerically calculated efficiency of the presented antenna is depicted in Figure 4.10, it can be seen that for all the PIN mode combinations, the antenna possesses efficiency >80% in bandpass region while in band-stop region the efficiency decreases to 25%.

4.1.4 Comparison with state-of-the-art-work

Table 4.2 presents the comparison of proposed antenna with state-of-the-art works for similar applications. It can be observed that the proposed antenna offers a compact size as compared to other works. Although the work reported in [198] had a small electrical size, it only supports dual-band operational mode. Thus, the proposed antenna features

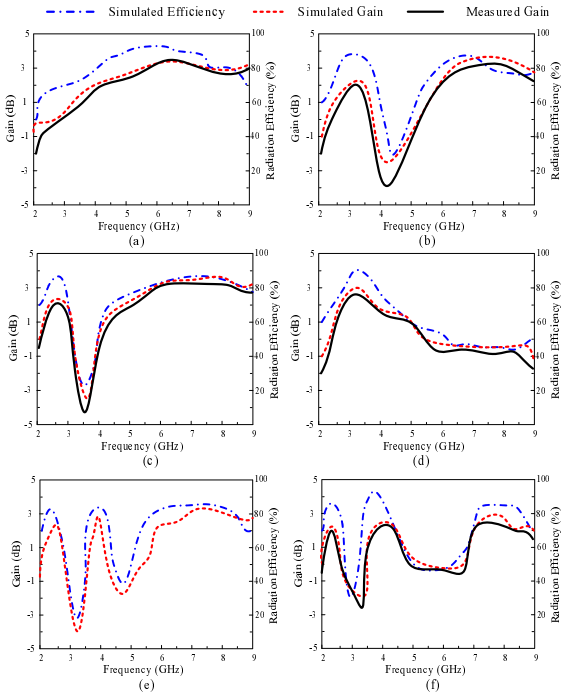

Figure 4.10: Simulated radiation of proposed antenna at various frequencies for various switching state (a) 4.8GHz case-000 (b) 6.77GHz case-000 (c) 8.1GHz case-001 (d) 2.45GHz case-010 (e) 3.5GHz case-101 (f) 2.2GHz case-111 (g) 8GHz case-111.

a potential candidate for heterogeneous applications like ISM bands, including WLAN, WiMAX, 5G-sub-6 GHz, and ultra wideband (UWB) systems.

Table 4.2: Performance comparison of the proposed antenna with state-of-the-art-works

Ref.	**Physical Size** (mm^2)	**Electrical Length** $(\lambda_0 \times \lambda_0)$	**Switching Technique**	**Operational bands per mode**	**Operational Region**
[196]	2300	0.52×0.47	5 PIN diodes	Single band	3 – 5 GHz
[197]	675	0.3×0.28	3 PIN diodes	Single, Dual and Triband	2 – 6 GHz
[198]	476	0.12×0.17	3 PIN diodes	Dual band	1.5 – 6 GHz
[199]	1855	0.29×0.43	Copper tape	Single and Dual band	2 – 6 GHz
[200]	1443	0.3×0.31	Copper tape	Single and Dual band	2 – 6 GHz
[201]	2250	0.37×0.33	2 PIN diodes	Dual and Tri band	2 – 6 GHz
[202]	2400	0.36×0.54	Copper tape	Tri, Quad and Penta-band	2 – 9 GHz
[203]	3900	0.48×0.5	6 Varactors	Dual and Tri band	2 – 6 GHz
[204]	528	0.23×0.13	3 PIN diodes	Single and Dual band	2 – 6 GHz
Presented Work	450	0.21×0.11	3 PIN diodes	Single, Dual Tri and Wideband	2 – 9 GHz

4.2 Frequency Reconfigurable Patch Slot Antenna for 5G Applications

4.2.1 Introduction

Among various types of antennas proposed for sub-6 GHz applications, most of the reported work are related to reconfigurable antennas where RF PIN diode for the purpose of frequency reconfigurability was widely studied by the researchers, thus results in various single band, dual band, and multiple band reconfigurable antennas.

In [212], a wideband antenna was designed for WWAN and LTE applications, the antenna comprises of simple structure and show good performance over wide operational band. However, it has drawbacks including large dimension, low gain and difficulty to achieve the reconfigurability. In [213], a compact wideband monopole antenna was converted into triband antenna for ISM and 5G-sub-6 GHz applications. Although the antenna offers compact size with advantage of flexibility, but it does not support frequency reconfiguration. In [214, 215, 216, 217, 218], several single band frequency reconfigurable antennas were proposed to operate in frequency band spectrum ranges 2 – 4.5 GHz. Although antenna reported in [214, 215, 216] offers a very high gain, but these works suffer from wide dimension along with multiple layer structures, leading to increased complexity. On the other hand, although the work reported in [217, 218] offers compact size, and they cover very limited bandwidth, hence, not suitable for wideband operations.

A compact frequency reconfigurable antenna for LTE and WLAN applications was presented in [219, 220]. Conventional rectangular patch antenna was modified by using Defected Ground Structure (DGS), while three PIN diodes were incorporated in [219], and in [220] various slots and asymmetric feed were utilized along with two PIN diodes, to achieve frequency reconfigurability. Although these compact antennas have simple

geometrical configuration, and their operational bandwidth was narrow. A dual to triband and a dual band to quad band frequency reconfigurable antenna were presented in [221] and [222], respectively. Etching slots in radiator and ground plane were utilized to achieve resultant antennas. Although antenna covers large number of bands, they suffer from various drawbacks including larger dimension, narrow bandwidths and complex geometrical structure. In [223], the presented flexible antenna offers wideband and two dual-band operational mode with relatively simple structure, however, it has large dimension and limited operational bandwidth.

Therefore, to overcome the aforementioned challenges, a compact frequency reconfigurable antenna was proposed in this section. The antenna radiator composed of triangular radiator with V-shaped slots and 2 PIN diodes were utilized to achieve frequency reconfigurability. The presented work shows a good combination of compact size, multimode operation, simple geometrical configuration, wide operational region and reasonable gain.

4.2.2 Antenna Design and Numerical Analysis

4.2.2.1 Antenna Geometry

Geometrical configuration of proposed antenna is illustrated in Figure 4.11 (a-c). The antenna was designed using ROGERS RT/droid 6010 having dielectric loss tangent (tan δ) of 0.0023, relative permittivity (ε_r) of 10.2 and 1.9 mm thickness (H). The overall dimension of the reconfigurable antenna was $A_X \times A_Y$. It can be seen from Figure 4.11 (a) that the proposed monopole antenna consists of a triangle shaped radiator with a dimension of $P_X \times P_Y$ having a feed line of dimension $F_X \times F_Y$. Two V-shaped slots were etched to notch the desire bands from wide bandwidth, the total length of the long slot is $2 \times L_1$, whereas the length of shorter slot is $2 \times L_2$. The width of both slots had a dimension of d while the gap between two slots is g. Truncated ground plane of

length G_X was used to achieve wideband operational bandwidth. Table 4.3 illustrates the length of the various parameters of the antenna.

Table 4.3: Dimension of the various parameters length of the proposed antenna

Parameter	**Value**	**Parameter**	**Value**	**Parameter**	**Value**
A_x	30mm	A_y	30mm	H	1.9mm
G_x	12mm	F_x	30mm	F_y	1.9mm
P_x	15.55mm	P_y	30mm	g	1mm
d	1mm	L_1	12.72mm	L_2	9.9mm
C_1	100pF	I	68nH	C_{DC}	100pF

4.2.2.2 Simulation Setup

The simulations of the proposed frequency reconfigurable antenna were performed using HFSS. For frequency reconfigurability two RF PIN diodes D_1 and D_2 were utilized by SKYWORKS having model number SMP1345-079LF. Two capacitor C_1 and C_2 were utilized to connect the pad with radiator physically and to block any current flow from biasing pads to radiator. Capacitor C_{DC} was utilized to stop the flow of current toward connector which may affect the performance of the antenna. The pads for diode are connected by means of via to biasing pads presented at the back side of the antenna, as depicted in Figure 4.11 (b). Inductor I was utilized to stop the unwanted RF-current from the source V_{DC}. The biasing voltage was provided from the backside of antenna to mitigate the effects of DC-wires on the performance of the antenna.

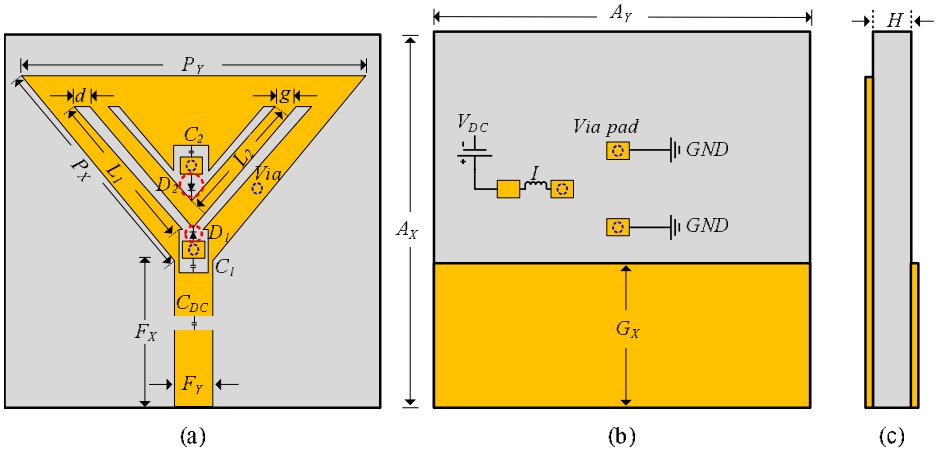

Figure 4.11: Geometrical configuration of proposed antenna (a) top-view (b) bottom-view (c) side-view

4.2.2.3 Design Methodology

The proposed reconfigurable antenna was originally inspired from conventional quarter-wave rectangular monopole antenna. The length (L_R) of the rectangular monopole antenna could be estimated by using the following equation provided in [205].

$$L_R = \frac{C_o}{4f_c\sqrt{\varepsilon_{eff}}} \tag{4.6}$$

Here C_o represents the speed of light in free space, f_c represents the central frequency; for presented case it was selected to be 4 GHz, whereas, ε_{eff} is the effective dielectric constant of the substrate whose value can be find by using the following relation:

$$\varepsilon_{eff} \approx \frac{\varepsilon_R + 1}{2} + \frac{\varepsilon_R - 1}{2}(1 + 12\frac{A_Y}{H})^{-0.5} \tag{4.7}$$

Here A_Y is the width of the substrate.

The resultant antenna exhibits resonance at 3.8 GHz having impedance bandwidth of 850 MHz ranging 3.55 – 4.4 GHz, as depicted in Figure 4.12. Although the antenna offers a wide impedance bandwidth but still it does not cover the targeted 5G-sub-6

GHz band (3.1 – 4.5 GHz) allocated globally. Thus, perturbation techniques were utilized to widen the impedance bandwidth of the antenna. Contrary to common techniques including DGS and slots to achieve wideband behavior, this design employed truncation of radiator corner to widen the bandwidth. Both lower corners were truncated using equilateral triangle which results in increasing the effective length of radiator, thus causing the shifting of resonance toward lower end, as depicted in Figure 4.12 . Moreover, truncation of the corner causes more current to flow from feedline to the radiator and due to triangular shape the current uniformly distribute itself on the surface of the radiator [224]. The increase in flow and uniform distribution of current causes the improvement in impedance mismatching at lower frequencies thus significantly enhances the impedance bandwidth of the antenna. The resultant antenna exhibits the wide impedance bandwidth of 2.2 GHz ranging 2.35 – 4.55 GHz which correspond to 62.8% of central frequency, as depicted in Figure 4.11. It is noteworthy here that beside 5G-sub-6-GHz band spectrum the antenna also covers 2.4 GHz WLAN band, 2.45 GHz ISM band, 2.5 GHz WiMAX band, more than 90% of S-band (2-4 GHz), thus making it suitable for multiple applications.

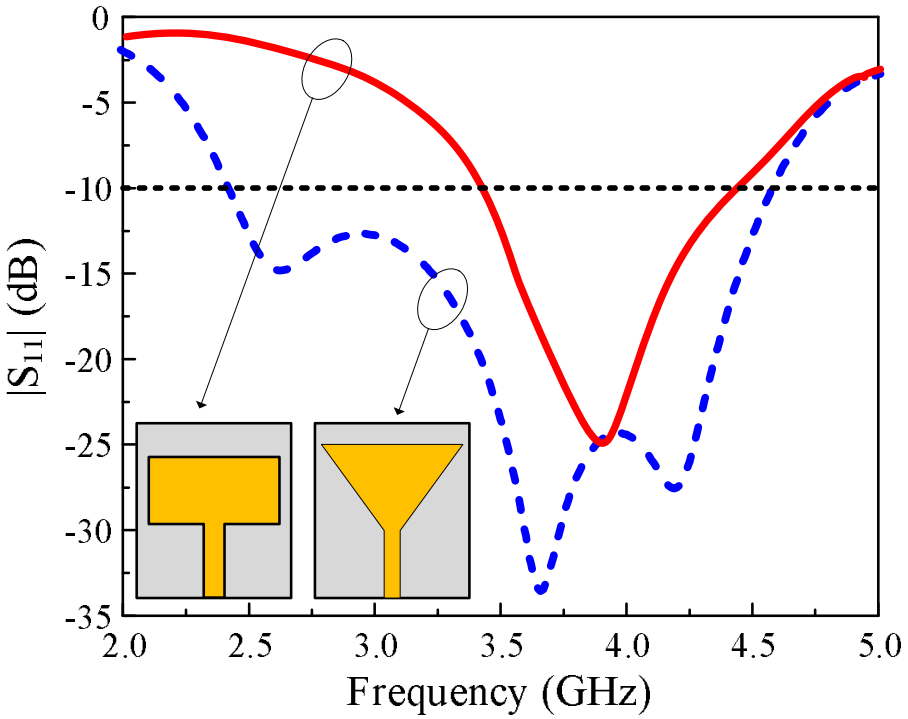

Figure 4.12: Return loss comparison among rectangular shape monopole with and without truncated corners

4.2.2.4 Design of Band Notch Antenna

To overcome the problem of band congestion, the wideband antenna designed in Section 4.2.2.3 was transformed to a notch band antenna. Usage of additional filters are the common way to notch the desire bands [225]. However, it may need additional matching circuits to match the impedance of the filter with wideband antenna [60]. Furthermore, it also requires large area to fit the whole circuit allowing very limited space for other components [226]. Therefore, researcher adopted the various techniques including etching slots [227], loading meta materials [228], insertion of Split Ring Resonator (SSR) [229] and stub loading techniques [230] to notch the desire bands, thus eliminating the need of any additional filter.

Furthermore, to avoid complex geometrical configuration in the proposed work a simple yet effective technique to achieve notch band was adopted, i.e. etching the slot in the

radiator. One challenge is to select the shape and position to place the slot, therefore, the shape and position of the slot must be chosen carefully to achieve a high value VSWR to minimize the interference of the notch bands [231]. Consequently, two V-shaped slots were used to achieve dual notch bands, the effective length (L_S) of the slot for desire frequency (f_d) can be calculated by using the following relation provided in [232]:

$$L_{s(n)} = \frac{c_o}{2f_{d(n)}\sqrt{\varepsilon_{eff}}} \tag{4.8}$$

Here (n) = 1,2 which shows the number of slot while $\varepsilon_{eff} \approx (\varepsilon_r + 1)/2$. Moreover, for the proposed work $L_{S1} = 2 \times L_1$ while $L_{S2} = 2 \times L_2$, as depicted in Figure 4.11(a). Figure 4.13 (a-b) illustrates the comparison among simulated values of return loss and VSWR for wideband antenna and antenna with single and dual notch. It could be observed that with single V-shaped slot the antenna mitigates the band spectrum of 2.47 – 3.11 GHz having maximum value of S_{11} = -0.78dB and peak VSWR of 27.85 at 2.82 GHz. Similarly, when two slots were etched corresponding to dual notch bands, the antenna mitigates the band spectrum of 2.48 – 2.96 GHz and 3.47 – 3.76 GHz having peak VSWR of 22.17 and 10.63, respectively. To have a deeper analysis of the slot to mitigate the desire frequency current distribution plots were presented in Figure 4.14 (a-b). It could be observed from Figure 4.14 (a) that for first notch band the maximum current is around the bigger V-shaped slots which causes the mitigation of lower band. Similarly, the maximum current was observed along smaller V-shaped slot for second notch band which cause its mitigation from the resonating band spectrum.

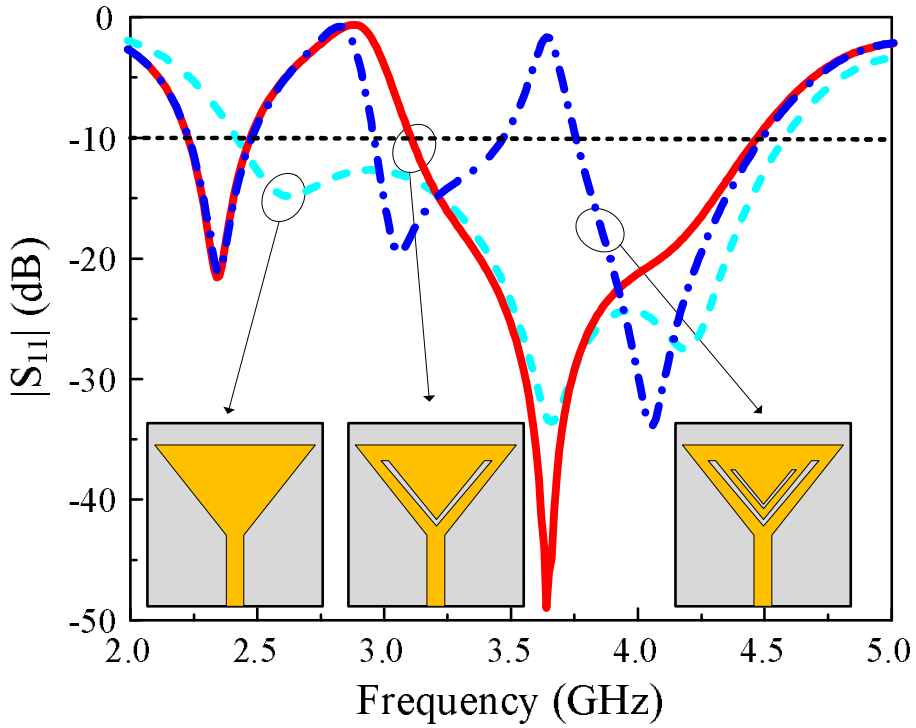

Figure 4.13: Return loss comparison among rectangular shape monopole with and without truncated corners

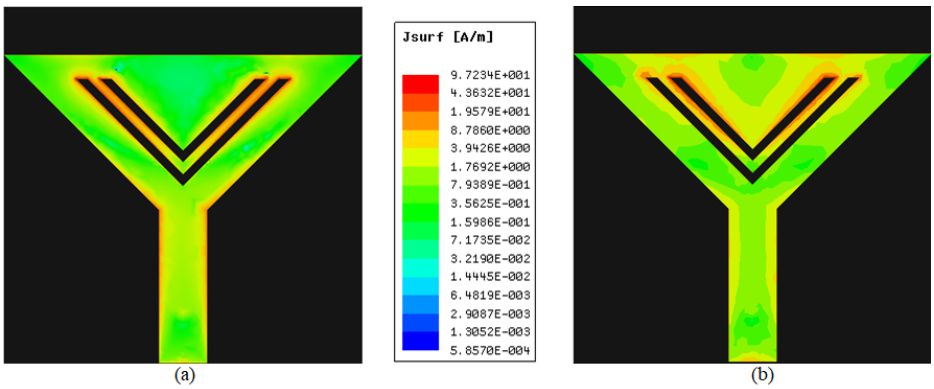

Figure 4.14: Return loss comparison among rectangular shape monopole with and without truncated corners

4.2.2.5 Numerical Analysis

Figure 4.15 depicts the equivalent circuit of the UWB antenna along with UWB antenna with single and dual notch band. The equivalent model of the UWB antenna was

designed using series connected combination of RLC component, where each group of RLC component shows the independent single resonance. The operational region of each resonance overlaps due to closely spaced thus results in a UWB antenna [208]. Similarly, the notch bands occurred due to presence of V-shaped slots were also model using a RLC group, where the LC equivalent notch resonant frequency f_o is given by [233]:

$$f_o = \frac{1}{2\pi}\sqrt{\frac{1}{L_{eq}C_{eq}}} \tag{4.9}$$

Where C_{eq} is the total equivalent capacitance and can be obtained by summing up the capacitances generated by individual leg of the V-shaped slot. L_{eq} is the equivalent inductance generated by the etched slot and can be calculated by using the following relation provided in [234]:

$$L_{eq} = 0.0002E(2.303\log_{10}(\frac{4E}{D}) - \theta)\mu H \tag{4.10}$$

Where E was assumed to be the finite length of a wire of rectangular cross section equals to the notch area, D is the length approximately equals to the cross section of the slot and θ is the angle between the legs of the V-shaped slot.

As the current distribution is perturbed due to slots on the radiating patch, therefore the path of the current is elongated. The length of the current path exhibits the series inductance, whereas the etched gaps of the slots accumulates the charge, hence determines series capacitance. Collectively, this behavior can be represented by the equivalent lumped element circuit with LC configuration. The equivalent lumped element parallel RLC circuit for the proposed antenna is illustrated in Figure 4.15. L_{Si}, C_{Si}, and R_{Si} represent the inductance, capacitance, and radiation resistance for the radiating mode at each resonant frequency band, respectively. The lumped effect of the slots causing the resonant frequency is represented as series combination of all lumped elements with an inductive patch antenna and ground plane as a capacitive load. Both inductive

and capacitive effects as well as feeding effects are considered for higher order modes generation and thus significantly contributes to the input impedance of the antenna.

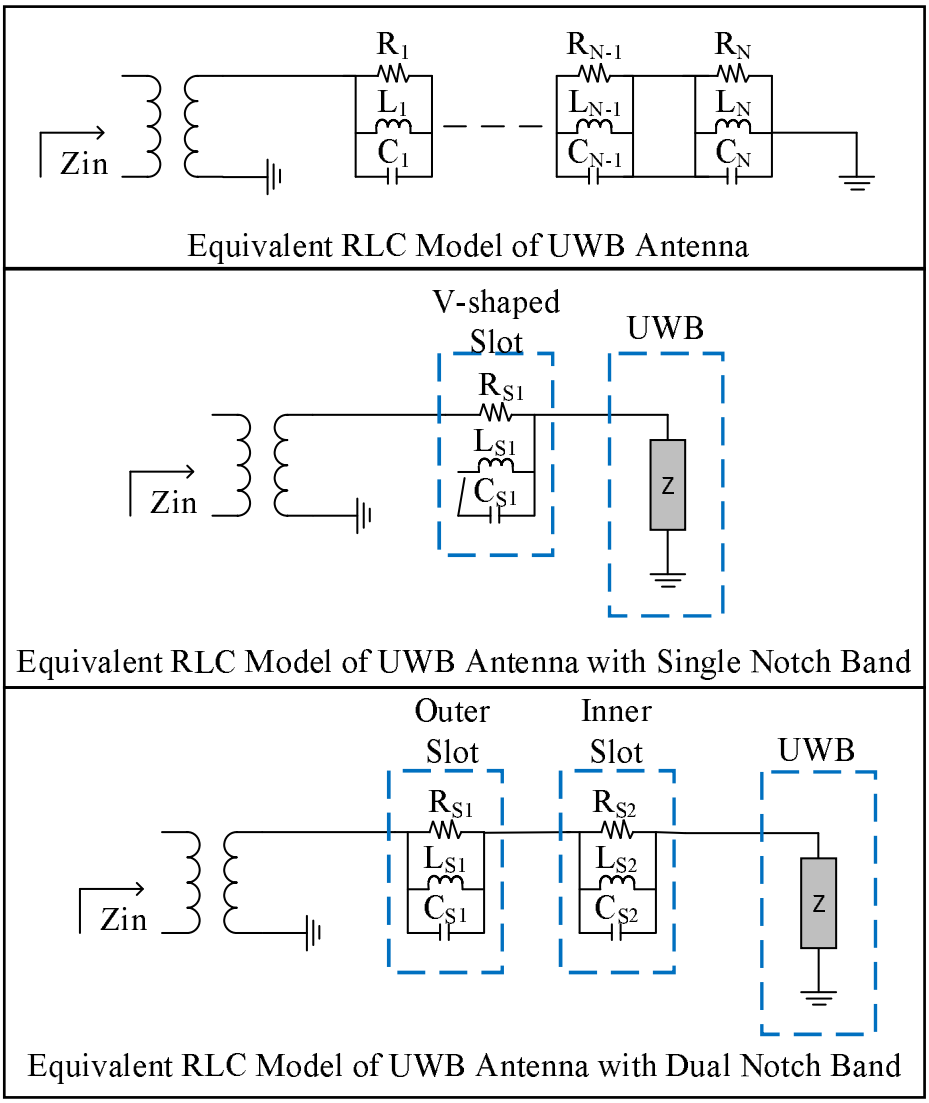

Figure 4.15: RLC equivalent model of UWB antenna with and without notch bands

4.2.2.6 Parametric Analysis

Parametric analysis of the key parameters of antenna were performed to have a closer look at their effects on the performance of antenna, as depicted in Figure 4.16. It could be observed from Figure 4.16 (a), when the length of truncated corner was changed from 15.55 mm to 12.73 mm, all the resonances were shifted toward the higher side.

An increment in bandwidth was observed for third while the bandwidth of the first resonance decreases considerably, as depicted in Figure 4.16(a). On the other hands, when the value of P_X was increased from 15.55 mm to 18.35 mm, all resonances shifts toward lower side along with decrement in bandwidth of the third resonance. The increase / decrease in the bandwidth is due to the amount of current passes from feedline to radiator while the shift in resonance toward lower / higher frequency is due to change in the effective length of the radiator, as discussed earlier. It is noteworthy that the notched frequencies remain unchanged for both higher and lower variations, as depicted in Figure 4.16 (a).

Figure 4.16 (b) illustrates the effects of variation in the dimension of L_1. It could be observed that when the value of L_1 is increased from 12.72mm to 14.15mm the first notch band shifts from 2.8GHz to 2.55GHz, also the bandwidth of the first resonance decreases while the bandwidth of the second resonance increases as depicted in Figure 4.16 (b). On the other hand, when the value of L_1 was decreased to 11.32mm the notch band shifted to 3.1 GHz along with increased bandwidth at first resonance and decreased bandwidth at the second resonance. A similar phenomenon was also observed for the second notch band by varying the dimension of L_2 as shown in Figure 4.16 (c). It is noteworthy that the second notch band and third resonance remain conserved for all variation in L_1 while the first notch and first resonance remain conserved for all variation in L_2. Thus, the presented antenna becomes a potential candidate for the application where independently controllable notch bands antennas are required [208, 233].

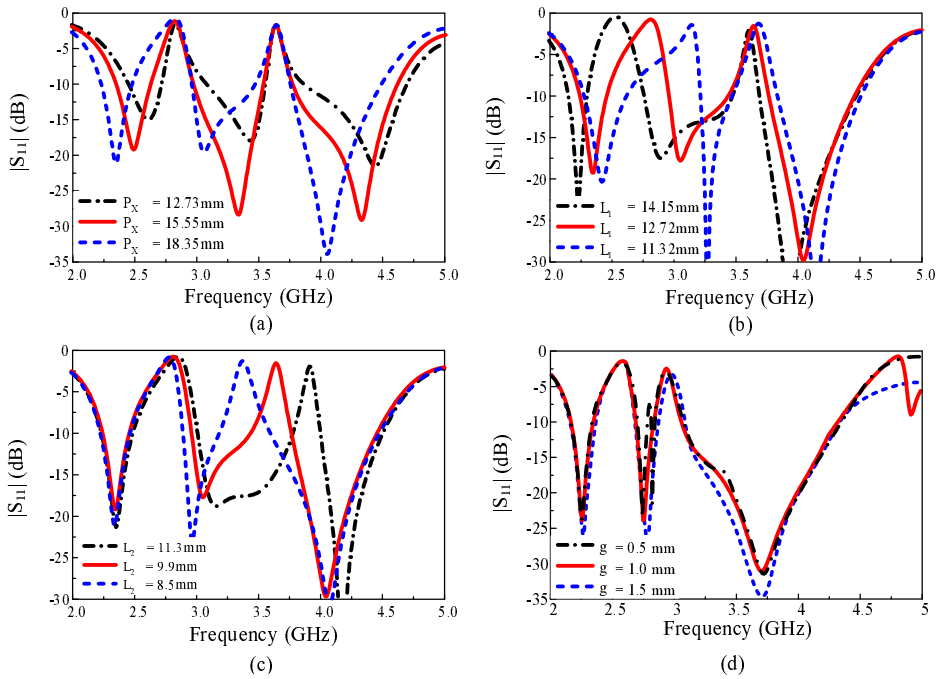

Figure 4.16: Parametric analysis of the various parameters of the antenna (a) P_X (b) L_1 (c) L_2 (d) g

4.2.2.7 Design Procedure

Figure 4.17 depicts the flow chart of the design procedure of the proposed antenna. Initially, a quarter wave rectangular monopole antenna was designed. Various parameters of monopole including length and width of radiator, feedline and truncated ground plane were optimized to get maximum bandwidth. Afterwards, lower corners of the monopole radiator were truncated by using equilateral triangle such that the hypogenous of the triangle is P_X. The hypotenuse of triangular slot and width of radiator were further optimized to get the ultra-wide bandwidth. The resultant antenna shows impedance bandwidth of 62.8%. In the next step, two triangular slots having overall length of $2 \times L_1$ and $2 \times L_2$ were etched from radiator to achieve two notch bands from the already designed ultra-wideband antenna. The length and width slot along with separation between them were well tuned to achieve desire notch bands.

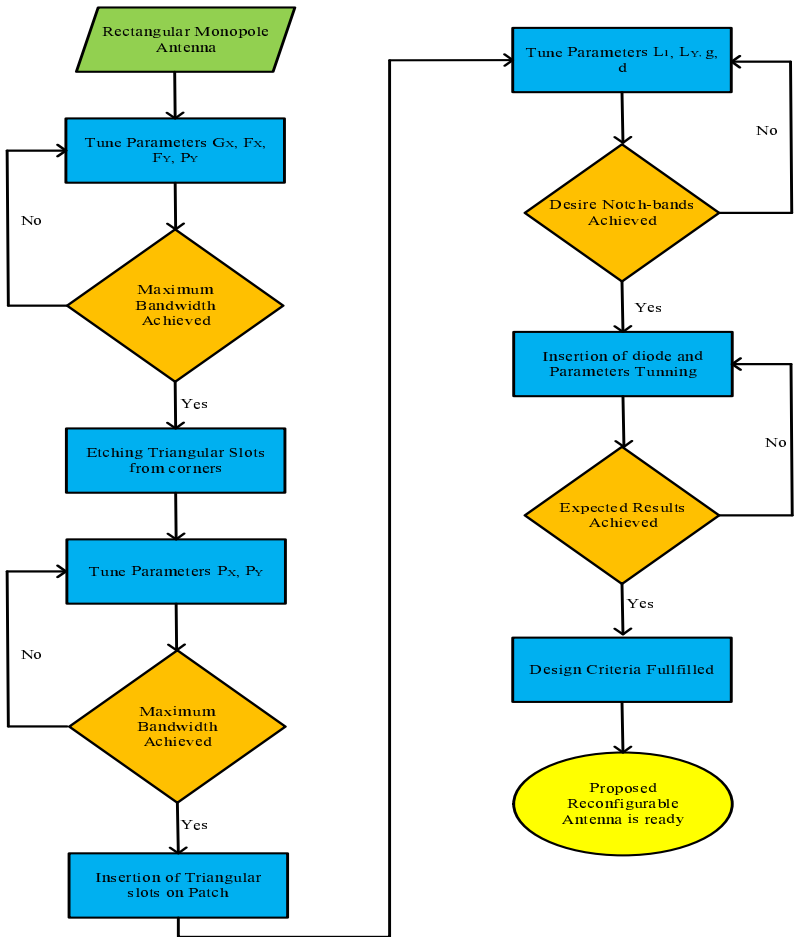

Figure 4.17: Flow chart of the design methodology of proposed antenna

The resultant antenna exhibits tri band operational mode along with two notch bands where the value of S_{11} is greater than -2dB. Finally, two RF-PIN diodes were inserted at the center of the slots, such that when diode is in ON-state the slot become inactive while in OFF-state the slot become active and notch band is achieved. Biasing circuits were designed at the backside of the antenna to minimize the effects of basing components and wires. A final tuning of various parameters was performed due to addition of diodes, capacitors and inductor to achieve the desire frequency reconfigurable antenna having dual-band, tri-band and wideband operational mode.

4.2.3 Results and Discussion

Figure 4.18 shows the prototype of the proposed antenna, the portable Vector Network Analyzer (VNA) was used to measure the return loss. The far-field characteristics of the antenna are measured through a commercial ORBIT/FR far-field measurement system in a shielded RF anechoic chamber. The horn antenna utilized for transmission is an SGH-series horn (SGH-15 by Millitech Co.), with 24 dBi standard gain.

4.2.3.1 Return Loss

Figure 4.19 presents the comparison among predicted and measured return loss. It could be observed that antenna either operates in wideband mode, two dual band modes, and tri band mode, as depicted in Figure 4.19 (a-d). When both diodes $D_1$and D_2 were in ON state, which refers to case-11, the antenna act as wideband antenna having S_{11} < -10dB impedance predicted bandwidth of 2.29 – 4.47 GHz whereas, the measured bandwidth was observed to be 2.25 – 4.53 GHz, as depicted in Figure 4.19 (a). When either the diode D_1 or D_2 was kept in ON-state while keeping the other diode in OFF-state the antenna exhibits dual band mode, as depicted in Figure 4.19 (b-c). The predicted bandwidth of the proposed antenna for case-01 was observed to be 2.3 – 2.65 GHz and 3 – 4.5 GHz while for case-10 it was observed to be 2.1 – 2.4 GHz and 2.92 – 4.37 GHz.

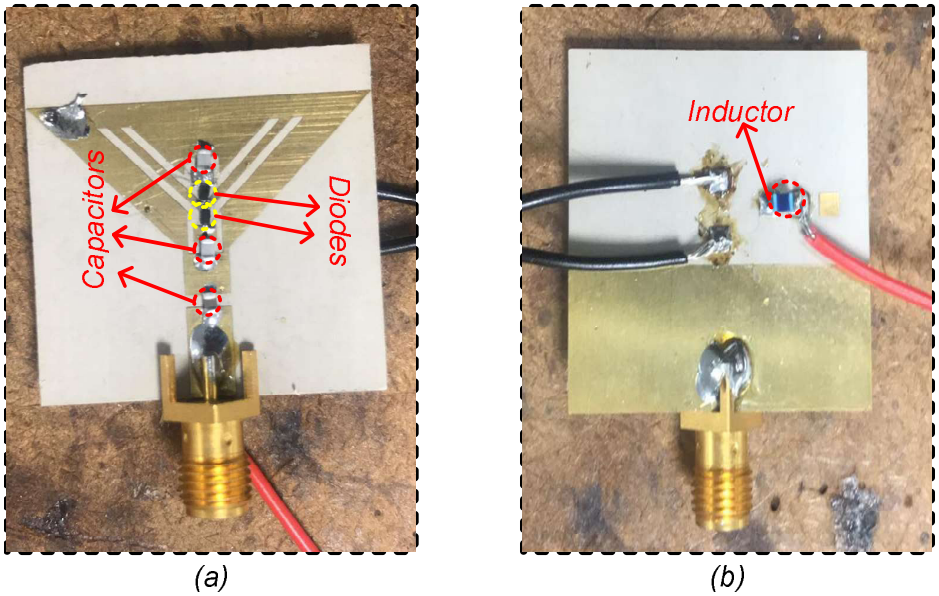

Figure 4.18: Fabricated prototype of the proposed antenna (a) top-view (b) bottom-view

On the other hand, the measured S_{11} < -10dB bandwidth for case-01 was observed to be 2.1 – 2.78 GHz and 3.09 – 4.57 GHz, as depicted in Figure 4.19 (b), while for case-10 it was observed to be 1.86 – 2.5 GHz and 3.03 – 4.47 GHz, as depicted in Figure 4.19 (c). At last, when both diodes were kept in OFF-state, referring to case-00, the antenna exhibits triband operational mode having predicted passbands of 2.17 – 2.35 GHz, 2.64 – 2.85 GHz, and 3.09 – 4.34 GHz. The measured impedance bandwidths for case-00 were reported to be 1.93 – 2.4 GHz, 2.62 – 2.97 GHz, and 3.2 – 4.65GHz, as depicted in Figure 4.19 (d). In general, a strong agreement was observed between simulated and measured results, while the small discrepancy between the results were owing to fabrication and measurement setup tolerance. The comparison of simulated and measured bandwidth and peak gain is shown in Table 4.4

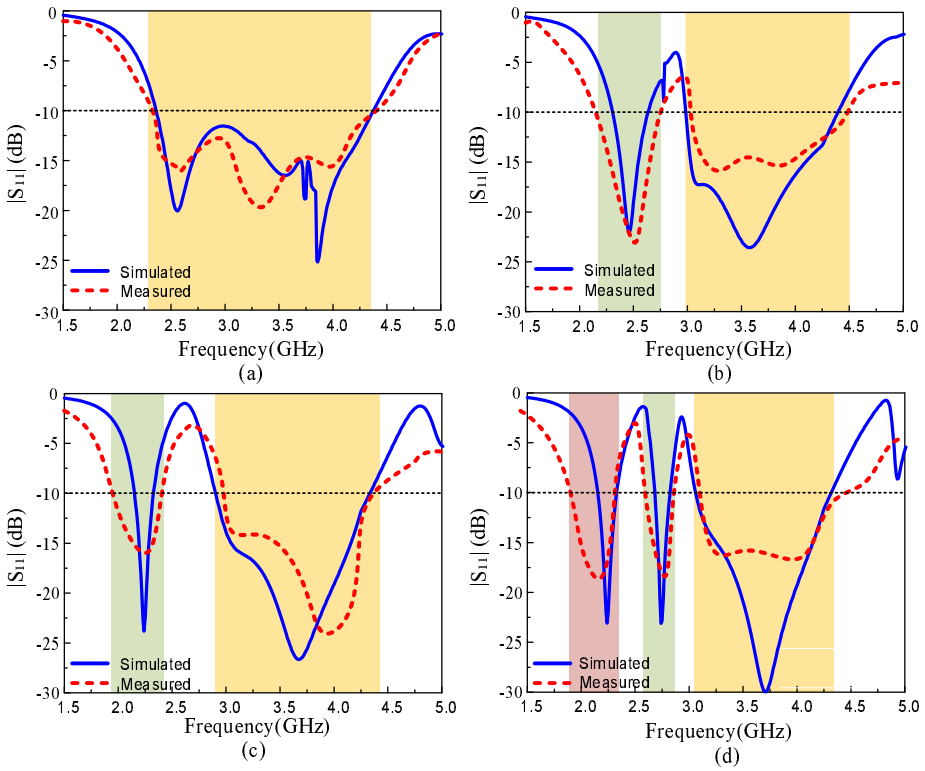

Figure 4.19: Return loss comparison among simulated and measured results (a) case-11 (b) case-01 (c) case-10 (d) case-00

4.2.3.2 Radiation Pattern

Figure 4.20 illustrates the comparison among simulated and measured radiation pattern of the proposed antenna at resonating frequencies for various switching states. It could be observed from Figure 4.20 that for all resonating frequencies the presented antenna exhibits omni-directional radiation pattern in principle H-plane $(\theta = 90°)$, as depicted in Figure 4.20. On the other hand, for all resonating frequencies the antenna exhibits a monopole like bi-directional radiation pattern in principle E-Plane $(\theta = 0°)$, as depicted in Figure 4.20. Moreover, it could also be observed for all switching state that the proposed work exhibits strong agreement between simulated and measured results.

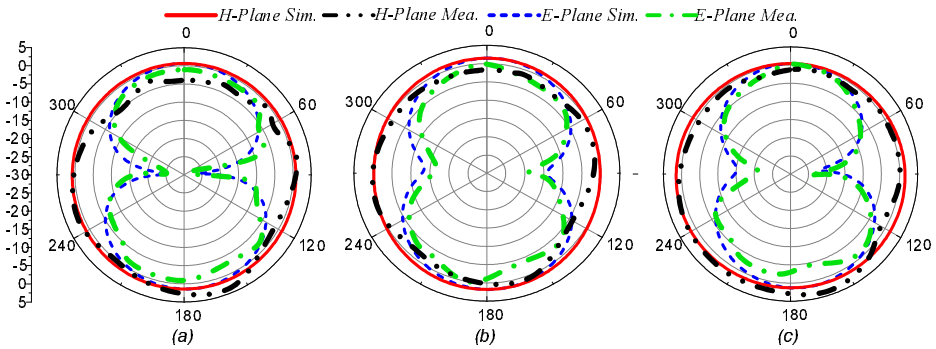

Figure 4.20: Radiation pattern comparison among simulated and measured results for case-00 (a) 2.24 GHz (b) 2.74 GHz (c) 3.71GHz

Table 4.4: Comparison among simulated and measured values for various switching states

Switching. State	**Simulated Bandwdith (GHz)**	**Measured Bandwdith (GHz)**	**Simulated Peak Gain (dBi)**	**Measured Peak Gain (dBi)**
Case-00	2.29-4.47	2.25 – 4.53	3.86	3.8
Case-01	2.3 – 2.65 3-4.5	2.1 – 2.78 3.09 – 4.57	2.44 3.91	2.39 3.82
Case-10	2.1 – 2.4 2.92-4.37	1.86-2.5 3.03-4.47	2.21 3.89	1.89 3.82
Case-11	2.17-2.35 2.64-2.85 3.19-4.34	1.93-2.4 2.62-2.93 3.19-4.65	2.26 2.01 3.9	2.17 1.96 3.79

4.2.3.3 Gain and Efficiency

Figure 4.21 illustrated the comparison among predicted and measured gain of the proposed reconfigurable antenna. It could be observed from Figure 4.21 (a), when both diodes are in ON-state the antenna exhibits a gain of < 2.5 dB in the operational

band along with radiation efficiency of < 90%. On the other hand, it could be observed from Figure 4.21 (b-d) that antenna in multiband mode shows the gain of < 2.4 dB in passband regions along with radiation efficiency of < 89% while for band stop region the gain and radiation efficiency of the proposed antenna decreases up to -8 dB and 22%, respectively. A strong agreement between simulated and measured results shows the performance stability of the antenna.

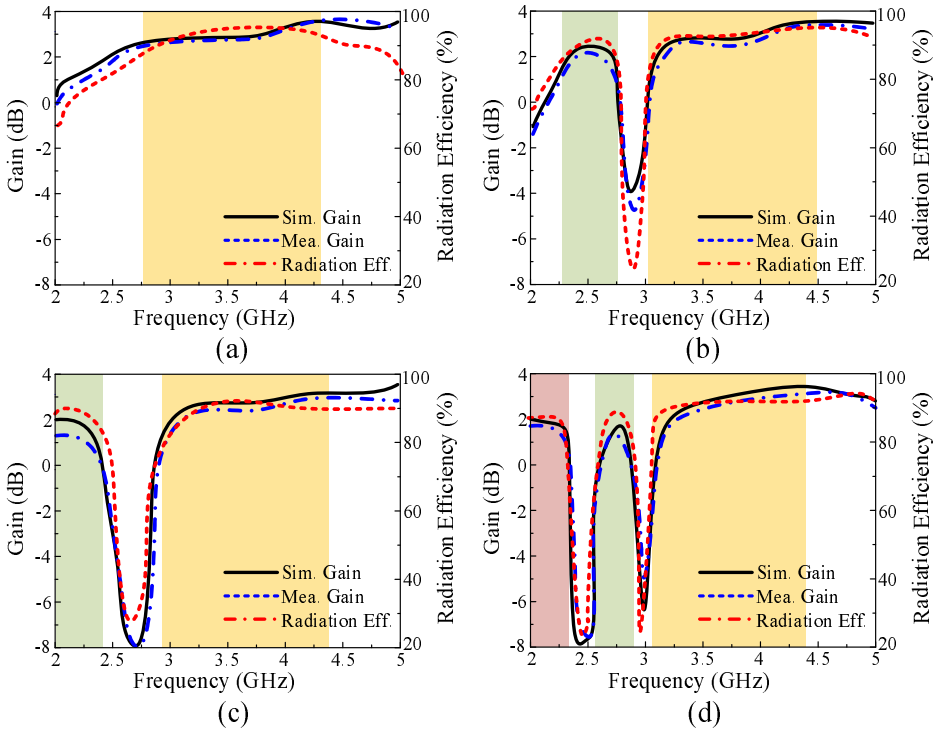

Figure 4.21: Comparison among simulated and measured gain along with predicted radiation efficiency (a) case-11 (b) case-01 (c) case-10 (d) case-00

4.2.4 Comparison with state-of-the-artwork

Table 4.5 presents the comparison of the proposed work with state-of-the-artwork for similar applications. It could be observed clearly that proposed antenna over perform the related work by providing best combination of compact size, multimode operation, wide operational region, relatively high gain and simple geometrical structure.

Table 4.5: Comparison of proposed antenna with state of the artwork for similar applications

Ref.	**Dimension** (mm^2)	**Operation Mode**	**Reconfig. Technique**	**Operational Region (GHz)**	**Peak Gain (dBi)**
[212]	65 × 10	Wideband	N.A	1.6-2.2	2.45
[213]	25 × 30	Triband	N.A	2.35-5.5	3.75
[214]	100 × 100	Single band	PIN-diode (2)	2.2-3.8	6.5
[215]	70 × 70	Single Band	Varactor (2)	2.6-3.8	5.92
[216]	50 × 50	Single Band	Mechanical	2-4.5	5.5
[217]	27 × 27	Single Band	Varactor (1)	1.4 – 2.6	2.48
[218]	14 × 36	Single Band	PIN-diode (2)	2-2.6	N.R
[219]	27 × 25	Single and Dual Band	PIN-diode (2)	2-6	2.8
[220]	20 × 16	Single and Dual Band	PIN-diode (2)	2-6	3.13
[221]	50 × 45	Dual and Triband	PIN-diode (2)	2-5.5	5.8
[222]	30 × 28	Dual and Quadband	PIN-diode (1)	1.5-11	3.1
[223]	50 × 33	Wide and Dualband	PIN-diode (2)	2-3.75	3.2
This work	30 × 30	Wide,dual and triband	PIN-diode (2)	1.8-4.5	3.72

4.3 A Compact Octa-Band Frequency Reconfigurable Antenna

4.3.1 Introduction

In last decade, reconfigurable antenna gains considerable amount of attention [235, 236]. Reconfigurable antennas provide the ability to vary polarization, frequency, and pattern as per users demand [237, 238, 239, 240]. They are preferred over multiband and wideband antennas because they lead to a better solution against the band congestion problems [194, 241]. In the literature, researchers utilized PIN diodes, radio frequency microelectromechanical systems (RF MEMS), optical switches, and varactors diodes to achieve frequency reconfigurability.

PIN diodes are widely used in frequency reconfigurable antennas due to ease of switching between different frequencies by simply controlling the biasing voltage [242]. Typically diodes are used to control current path in an antenna geometry to achieve multi-band operations [243, 244, 245, 246, 247]. In [243, 244], three PIN diodes were placed in the defected ground to switch between three different frequencies. Although the reported antenna were compact, their supported frequency bands were not sufficient for multi-band applications. Another tri-band frequency reconfigurable antenna was presented in [245], where a single diode is placed in the radiator of the monopole antenna. The antenna can switch between dual-band and single-band operating modes, despite its large dimension.

In [246], the hexa-band frequency reconfigurable antenna was proposed, and the antenna shows a compact size with dual operational mode. In [247, 248], octa-band antennas were presented, and the design reported in [248] had the advantage of compact size than that reported in [247], whereas the latter achieve dual and tri-band operational mode by utilizing less number of diodes. Therefore, a compact antenna having more

number of frequency bands while utilizing a minimum number of diodes is still a design challenge for researchers. This motivates us to design a novel frequency reconfigurable antenna. The major contributions of this work are as follow: (1) The proposed antenna has compact size when compared with designs reported in literature. (2) The antenna geometry comprises a simple structure, which minimizes the fabrication losses. (3) By utilizing only two diodes, the antenna resonates at eight different frequencies having four different dual-modes.

4.3.2 Design Methodology

The front, back, and side view of the proposed frequency reconfigurable antenna are depicted in Figure 4.22 (a-c), with all important dimensions labelled by different alphabets. The antenna geometry is engraved on the top side of ROGERS TMMR-4 having dielectric constant (ε_r) of 4.2 and loss tangent (θ) 0.002. The bottom side of the antenna consists of the Defected Ground Structure (DGS). The standard copper cladding of 0.035 mm is used for both the radiator and the DGS. Monopole antenna, owing the advantage of a wider band as compared to other types of antennas, is designed in first step. The length of the monopole antenna can be calculated using the analytical equations given by:

$$L_p = \frac{c}{4f_p\sqrt{\varepsilon_{eff}}} \tag{4.11}$$

Where c is the speed of light which is $3\times10^8 ms^{-1}$, f_p is the central resonating frequency, which is given by:

$$f_p = \frac{c}{\lambda_g\sqrt{\varepsilon_{eff}}} \tag{4.12}$$

Where λ_g is the guided wavelength and ε_{eff} is the effective dielectric constant which is

given by:

$$\varepsilon_{eff} \approx \frac{\varepsilon_r + 1}{2} + \frac{\varepsilon_r + 1}{2}(1 + 12\frac{L_x}{H})^{-0.5} \tag{4.13}$$

where ε_r is the dielectric constant of the substrate, L_x is the width of the monopole, and H is the thickness of the substrate.

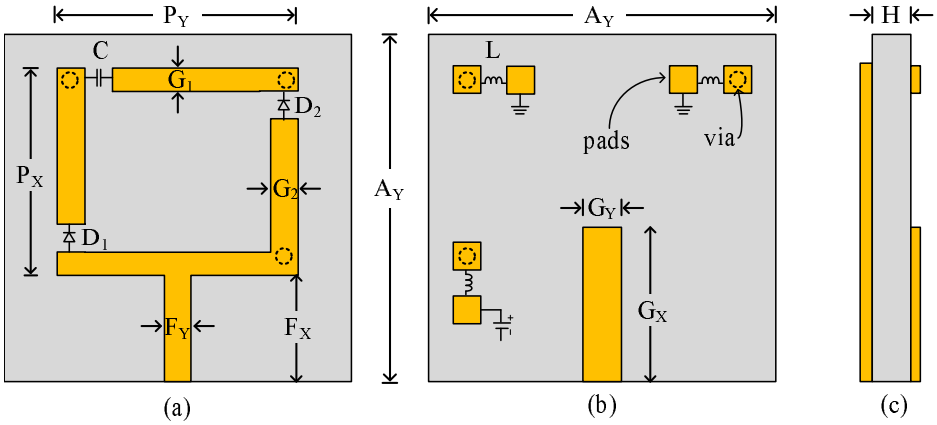

Figure 4.22: Proposed frequency reconfigurable antenna (a) top-view (b) bottom-view (c) side-view. The metal traces are shown with yellow colour

The optimized length of the monopole designed at the operating frequency of 3.5 GHz is found to be 18 mm, which is approximately equal to $\lambda_g/4$, as shown in Figure 4.23. The overall dimensions of the antenna are: 26mm $\times$ 2mm $\times$ 1.524mm. The prototype was simulated with ANSYS Higher Frequency Structure Simulator (HFSS), the magnitude of reflection coefficients is plotted in Figure 4.24. To further miniaturize the dimension of the conventional monopole, a rectangular slot of dimension $(P_y - 2G_y) \times (P_x - 2G_x)$ is inserted in the radiator – this new antenna is referred to as Prototype-II. The introduction of this slot increases the effective area of the antenna and thus shifts the resonance toward the lower side. Moreover, the introduction of this slot also introduces an upper band, as depicted in Figure 4.24.

To shift the resonance frequency back to 3.5 GHz, the dimensions of the antenna are optimized. After a detailed parametric study, optimum dimensions are used in the

Prototype-III, which are shown in Figure 4.23 (c). The Prototype-III resonates at 3.5 GHz and it can be seen from Figure 4.23 (a-c) that this prototype has physical area of 324 mm^2, which is 44% smaller compared to the conventional monopole antenna that has an area of 572mm^2.

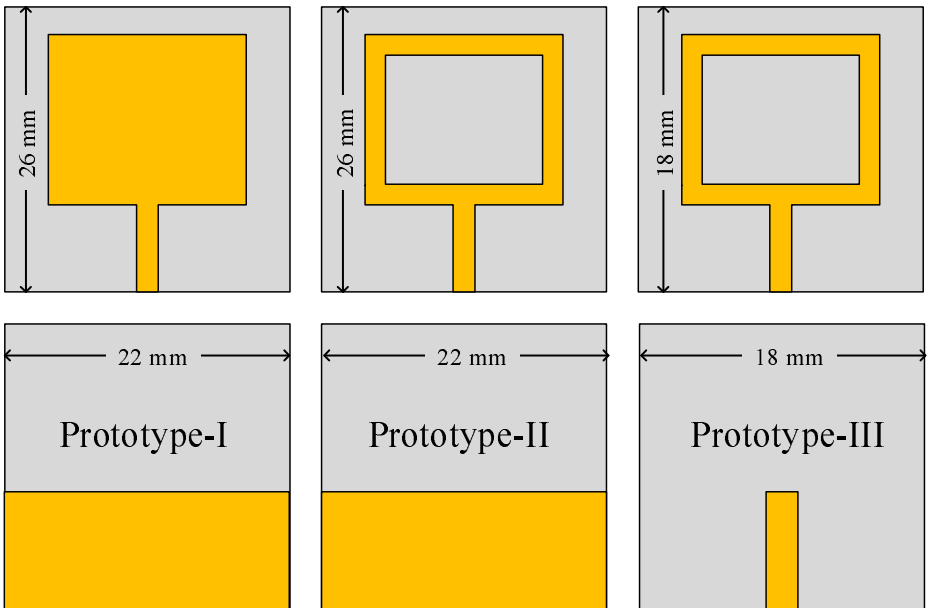

Figure 4.23: Design evolution of the proposed antenna.

In the last step, two RF-PIN diodes (SC-79 by Skyworks) were utilized to achieve frequency reconfiguration. The lumped elements were used in ANSYS HFSS to design an equivalent model of PIN diode. The positions of the diodes are optimized to get desire results while a DC block 100pF capacitor is also used to physically disconnect the upper part of the radiator, as shown in Figure 4.22 (a). The optimized dimensions of the proposed antenna are as follow: $A_x = 18mm; A_y = 18mm; P_x = 13mm; P_y = 16mm; G_x = 4mm; G_y = 2mm; G_1 = 2.75mm; G_2 = 0.5mm; F_x = 4mm; F_y = 2mm; H = 1.524mm; C = 100pF$.

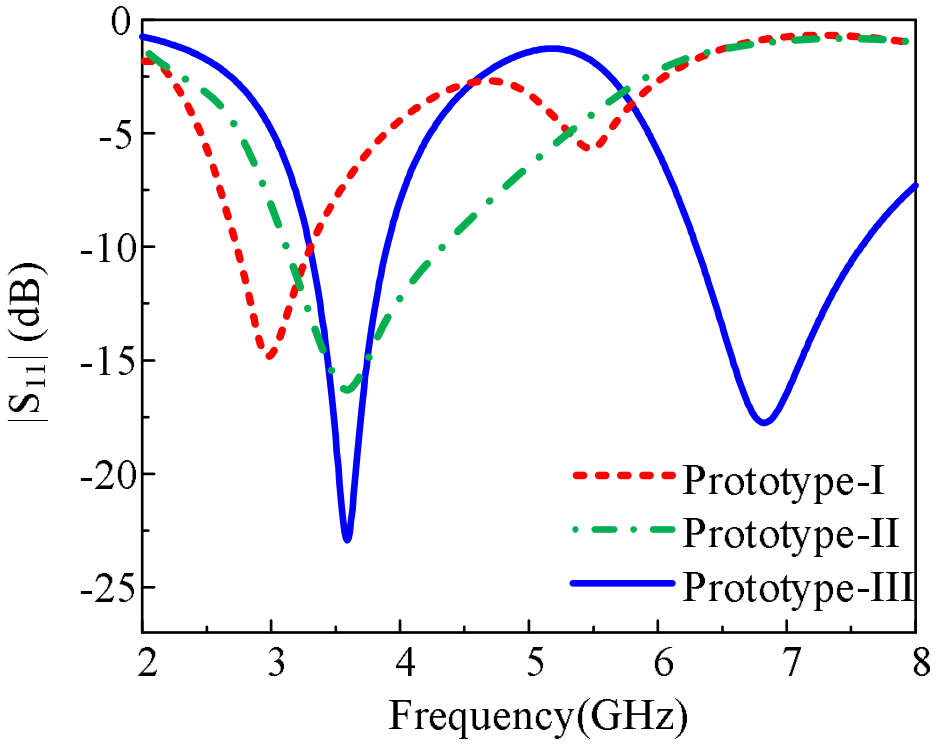

Figure 4.24: The magnitude of reflection coefficient of three different prototypes designed and simulated with electromagnetic solver

4.3.3 Results and Discussion

4.3.3.1 Simulation and Measurement Setup

The simulations of the proposed antenna were carried out using electromagnetic solver (EM) HFSS using appropriate conditions. Furthermore, to minimize the effect of the connector on antenna performance, commercially available SMA is modelled and used at the antenna feed for numerical analysis. The equivalent electrical model of the PIN-diode utilized for simulation was presented in the Figure 4.25. For ON-state the PIN-diode behaves like a series combination of inductor and resistor, while for OFF-state the diode behaves like a series combination of inductor with parallel combination of resistor and capacitor, as depicted in Figure 4.25 (a) and (b), respectively.

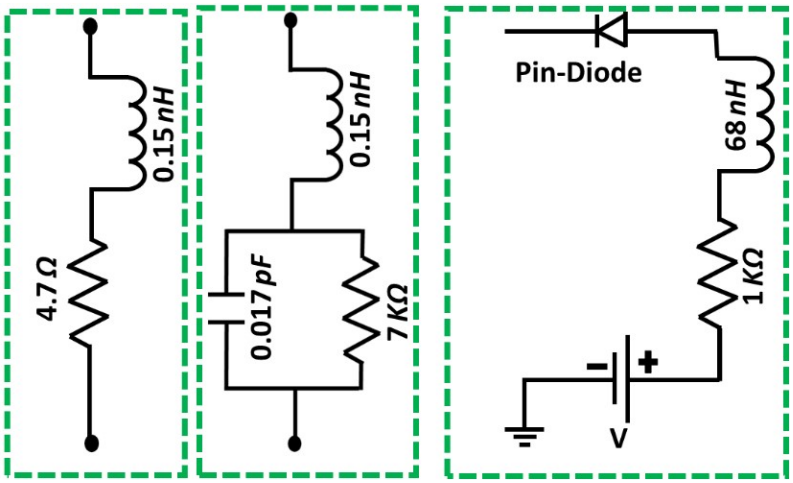

Figure 4.25: Electrical equal model of PIN diode (a) ON-state (b) OFF-state (c) biasing circuit

For ease of understanding diode OFF-state is represented by '0' while diode ON-state is represented by '1'. Figure 4.26 illustrates the fabricated prototype of the proposed antenna utilized for measurement purpose. Vector Network Analyzer (VNA) (Model no. E5063A with range of 500 MHz to 18 GHz, by Keysight Tech.) was utilized to measure the return loss of the proposed work. The broadband horn antenna (1 – 18 GHz) was utilized for the measurements of far-field parameters including radiation pattern and gain.

4.3.3.2 Return Loss

Figure 4.27 presents the comparison of magnitude of reflection coefficient of the proposed antenna for various switching states. For case-00 the antenna resonates at two frequencies of 4.6 GHz and 7.2 GHz with respective predicted bandwidth of 1020 MHz and 840 MHz, as depicted in Figure 4.27 (a), while measured values shows the impedance bandwidth of 1390 MHz and 1010 MHz for resonating frequency of 4 GHz and 6.85 GHz, respectively. It could also be observed from Figure 4.27 (a) that for case-01 antenna resonates at 4.1 GHz and 7 GHz with respective impedance bandwidths of

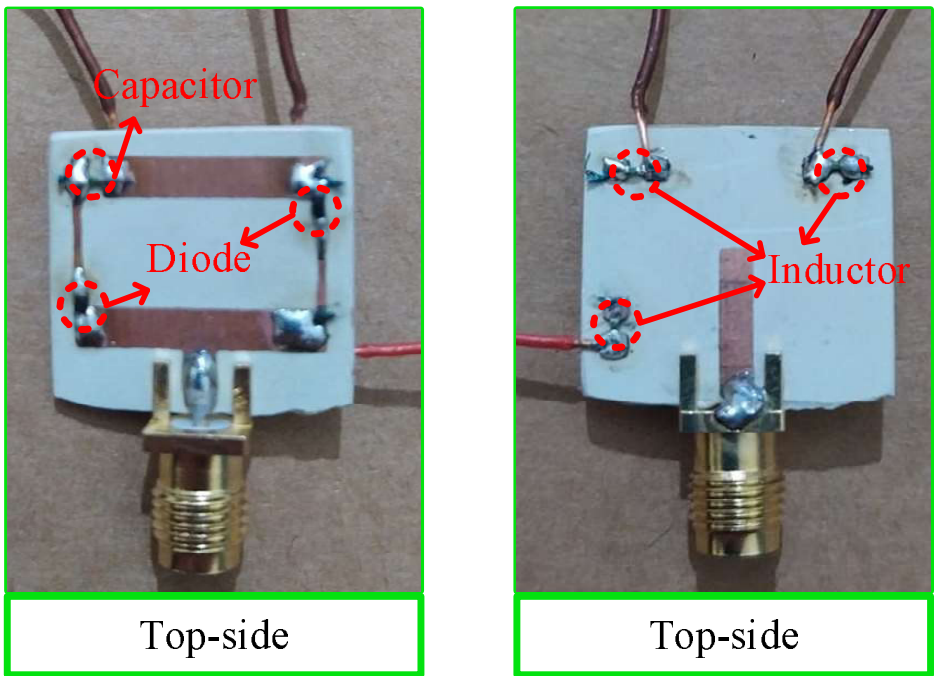

Figure 4.26: The fabricated prototype of proposed antenna utilized for measurements

760 MHz and 1090 MHz. On the other hand, the measured value shows the resonating frequencies of 4 GHz and 6.85 GHz having respective bandwidth of 870 MHz and 1210 MHz, as depicted in Figure 4.27(a).

It could observed from Figure 4.27 (b) that antenna start resonating at 4.4 GHz and 6.92 GHz for case-10, where antenna exhibits the simulated bandwidths of 810 MHz and 1400 MHz while measured impedance bandwidths were observed to be 1100 MHz and 1520 MHz, respectively. At last, for case-11, the simulated $|S_{11}|$ > -10 dB bandwidths were observed to be 560 MHz and 1350 MHz at the resonating frequencies of 3.5GHz and 6.87 GHz, respectively. The measured results shows that the antenna exhibits impedance bandwidths of 920 MHz and 1240 MHz for respective resonating frequencies of 3.55 GHz and 7 GHz, as depicted in Figure 4.27 (b). In general, predicated and measured return loss shows a strong agreement between each other, while a little discrepancy was due to fabrication and measurement tolerance.

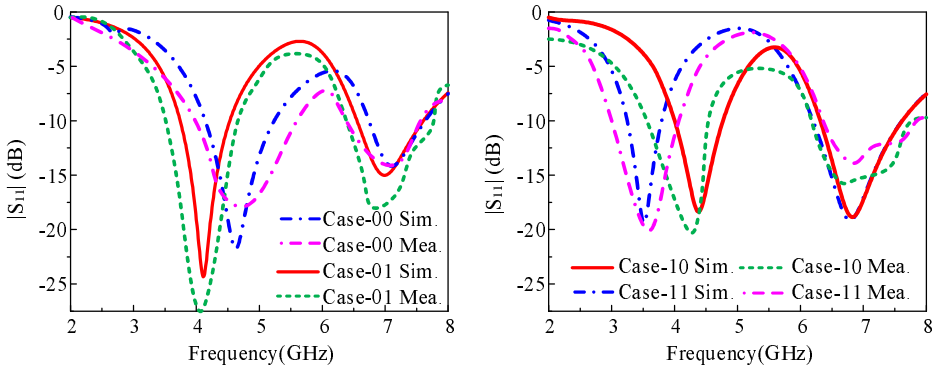

Figure 4.27: The magnitude of reflection coefficient for various switching cases of the proposed antenna

4.3.3.3 Far-Field Analysis

Figure 4.28 (a-f) depicts the comparison among predicted and measured radiation pattern at the various frequencies. The antenna exhibits an omni-directional radiation pattern in principle E-Plane $(\theta = 0^{\circ})$ for lower pass band frequencies, while a slightly distorted omni-directional radiation pattern was observed for higher passband frequencies, as depicted in Figure 4.28 (b) and (f). Regarding principle H-Plane $(\theta = 90^{\circ})$ the antenna exhibits an an 8-shaped bidirectional radiation pattern was observed for all selected resonating frequencies. In general, a strong agreement was observed between simulated and measured results for all selected frequencies, as depicted in Figure 4.28.

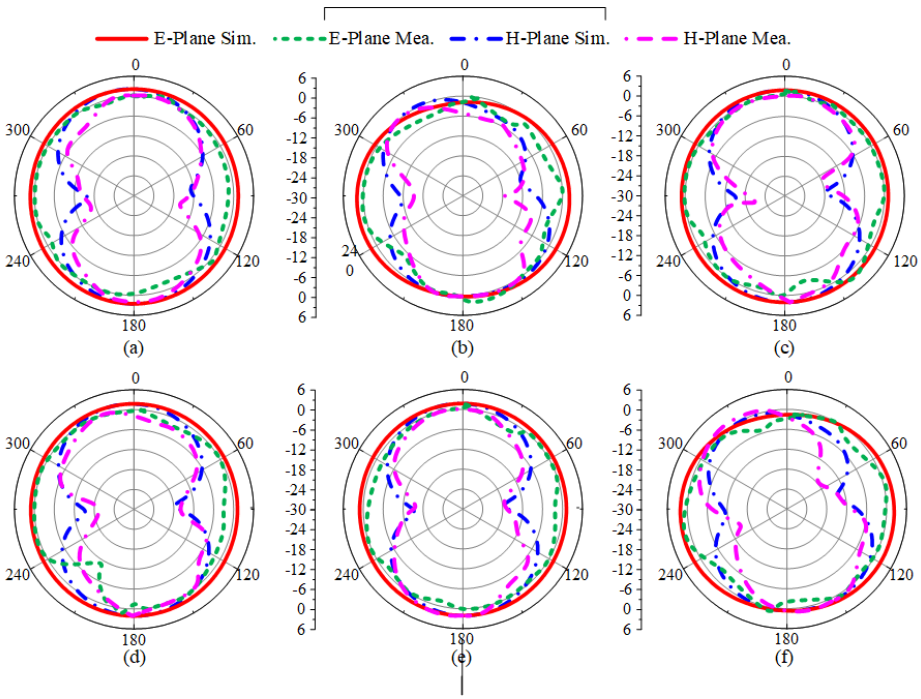

Figure 4.28: Comparison among predicted and measured radiation pattern (a) case-00 (b) case-00 (c) case-01 (d) case-10 (e) case-11 (f) case-11

Figure 4.29 (a-b) presents the comparison among simulated and measure peak gain of the proposed antenna along with numerically calculated radiation efficiency. It could be observed from the Figure 4.29 that in all switching states the peak gain of antenna varies from 2-3 dB in lower pass band while the gain varies from 3-4 dB in upper pass band. The measured peak gain of the antenna for possible switching states of diode was also in good agreement with simulated results. It could also observed, that the antenna exhibits efficiency of more than 80% in both passbands, as depicted in Figure 4.29. Thus its performance stability makes it a potential candidate for compact devices requiring multiband reconfigurable antenna.

Table 4.6: Performance Comparison with Existing works

Ref.	**Dimension** (mm^2)	**Number of diodes**	**Operational Mode**	**Total No of bands**
[243]	400	3	Single band	3
[244]	675	3	Single band	3
[245]	1855	1	Single & Dual band	3
[246]	528	3	Single & Dual band	6
[247]	2250	2	Dual & Tri-band	8
[248]	476	3	Dual band	8
This Work	324	2	Dual band	8

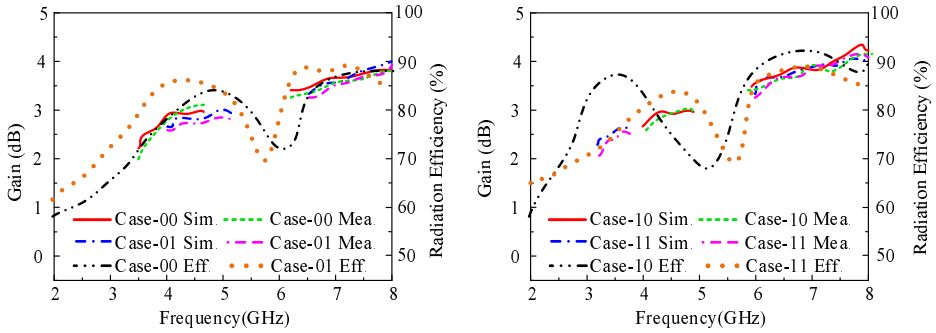

Figure 4.29: Comparison among simulated and measured gain along with radiation efficiency

4.3.4 Comparison with state of the art work

Table 4.6 presents the comparison of presented work with recently reported antennas for similar applications. It could be observed that the proposed work offers more bands as compared to reported works in [243, 244, 245, 246] along with advantage of compact size. Compared to the work presented in [247, 248], although the number of bands are equal to them, the presented antenna offers physical compact size. Thus, it can be deduced that presented antenna outperforms the related work by offering simple structure along with compact size and a large number of bands.

4.4 Summary

The three different antenna structures for frequency reconfiguration were explained in this chapter. First of all, a CPW-fed reconfigurable triangular monopole antenna for wideband operation mode was designed. The proposed antenna resonates at various frequencies of 2.1 GHz, 2.25 GHz, 2.45 GHz, 3.3 GHz, 3.5 GHz, and 8 GHz. Secondly, a reconfigurable wideband triangle shaped monopole antenna to cover 5G sub-6-GHz band was presented. Two V-shaped slots were utilized to achieve two notch bands, PIN diodes were used for reconfigurablity. In the last, compact frequency reconfigurable antenna was proposed that operates in eight different frequencies in four dual-band modes. All these proposed antennas achieves strong agreement between simulated and measured results along with acceptable gain, omnidirectional radiation pattern, and high efficiency.

Chapter 5

Design of Reconfigurable Antennas on Flexible Substrates

5.1 Introduction

In this modern era, usage of flexible/semi-flexible devices increases exponentially due to their numerous advantages over rigid devices, which are not limited to the durability, low weight, flexibility, portability, and energy efficient. Antenna, being responsible for transmitting and receiving signal, plays a major role in designing a compact communication system. Obviously, flexible devices will require flexible antennas. Researchers are looking for flexible antenna with high radiation efficiency, compact size, wide bandwidth, high gain, low complexity and robust impedance matching requirements.

5.2 A Flexible Antenna with Frequency and Radiation Pattern Reconfigurability

5.2.1 Introduction

Multifunctional antennas become popular in wireless communication systems as they can reduce the overall number of the antennas and thus reduce the undesired mutual coupling and other drawbacks required to larger antenna dimensions [249]. Reconfigurable antennas allow ease of integration of numerous radio frontends into on system. The common operational mode of the reconfigurable antennas is on-demand frequency, polarization, and pattern reconfigurability [60, 250]. The various techniques deployed to achieve reconfigurability include electrical, material, and mechanical methods by utilizing PIN diodes, optical switches, metasurface, micro fluids, mechanical switches, and so on [251]. Besides, researchers also design compound type reconfigurable antennas where a combination of more than one reconfigurability could be found, e.g., a frequency and pattern reconfigurability or frequency and polarization reconfigurability at the same time [252, 253, 254].

The demand for flexible electronics increases rapidly owing to their advantages of conformability, lightweight, and durability over rigid antennas. Therefore, a natural demand for flexible, planar compact antennas, and easy integration with a modern flexible device has emerged [255]. Moreover, the compact dimension of flexible devices and overcrowded band spectrum allocation for various wireless communications require flexible and reconfigurable antennas. In this context, numerous works have been reported in the literature. However, existing works have a set of larger dimensions along with the limit of only pattern reconfigurability [256, 257] or frequency reconfigurability [227, 258]. A frequency and radiation pattern reconfigurable antenna based on the center-shorted technique was presented in [259]. Two groups of varactors diodes were

used for tunning the frequency and switching between broadside and monopole-like radiation pattern. Another low profile hybrid reconfigurable antenna by using the PIN diodes was explained in [260]. The antenna structure consists of slits and patch that were connected using PIN diodes. An antenna array was designed in [261] for frequency and radiation pattern reconfiguration. An independent biasing voltage is designed for pattern reconfigurability. A compact frequency and radiation pattern reconfigurable antenna for wireless communications was explained in [262]. To cover the the 5G application, a novel frequency and radiation pattern reconfigurable antenna was presented in [263]. The proposed antenna consists of the two patches and the different states of the transistors resonate the antenna at the required frequency. Moreover, these hybrid reconfigurable antennas [259, 260, 261, 262, 263] have the drawbacks of rigid structure, large antenna size, and complex biasing structure which prevents their applications from flexible electronics. A frequency and radiation pattern reconfigurable antenna to cover 1.9 and 2.4 GHz bands was explained in [264]. The proposed antenna is flexible but it has complex antenna structure and used excessive PIN diodes.

In this Section, a frequency and pattern reconfigurable antenna is designed and realized using diode biasing. Two inverted L-shaped stubs are imprinted on the top side of a triangular monopole antenna. By changing the state of diodes, these stubs can be electrically connected and disconnected with the radiator. When either of the stubs is connected to the radiator, a relative phase difference occurs at both ends of the radiator. This changes the direction of the electromagnetic radiations, thus pattern reconfigurability could be achieved. Moreover, due to the reactive load introduced by the stubs, the effective length of the antenna is changed and hence the frequency reconfigurability is achieved. A simple yet effective technique is exploited for these features. Moreover, a simpler geometrical structure, less PIN diodes, and compact size emphasize the novelty of the proposed antenna as compared to the state-of-the-art works.

5.2.2 Antenna Design and Methodology

Figure 5.1 shows the top, back, and side view of the geometrical configuration of the proposed flexible and compound reconfigurable antenna. The antenna geometry is imprinted on the top side of the ROGERS 5880LZ substrate having a dielectric constant ε_r of 2.1 and tangent loss (tan θ) of 0.002, while the thickness (H) of the substrate is 0.254mm. The antenna consists of a coplanar waveguide (CPW) fed semicircular patch of radius R connected with a triangular radiator. Next, two inverted L-shaped stubs having the longest arm length S_L, shortest arm length S_W and width S_G is connected to the triangular radiator using two RF PIN diodes D_1 and D_2 by SKYWORKS© having model number SMP-1345 SC-79. Two capacitors C_1 and C_2 of 100 pF capacitance are inserted to block DC current to flow towards the SMA connector. On the backside of the substrate, small biasing pads were engraved to provide the required voltage and current to switch the state of diodes, while the two inductors L_1 and L_2 of 68nH were inserted to block unnecessary RF currents. The optimized parameters of the proposed antenna are as follows (unit: mm): $W = 40; L = 50; h = 0.254; L_g = 18; W_g = 5; g = 0.5; W_F = 3; L_F = 5; w_1 = 24.1; w_2 = 2; L_1 = 21.3; L_2 = 5$.

5.2.2.1 Design of the Compact Flexible Monopole Antenna

The proposed flexible antenna is originally derived from a conventional quarter-wave rectangular monopole antenna. The resonating frequency of the monopole antenna can be estimated by [265].

$$f_r = \frac{c}{4L_o\sqrt{\varepsilon_{eff}}} \tag{5.1}$$

Where c is the velocity of light, L_o is the effective length of the rectangular radiator and ε_{eff} is the effective dielectric constant for $A/h < 1$, which can be computed as:

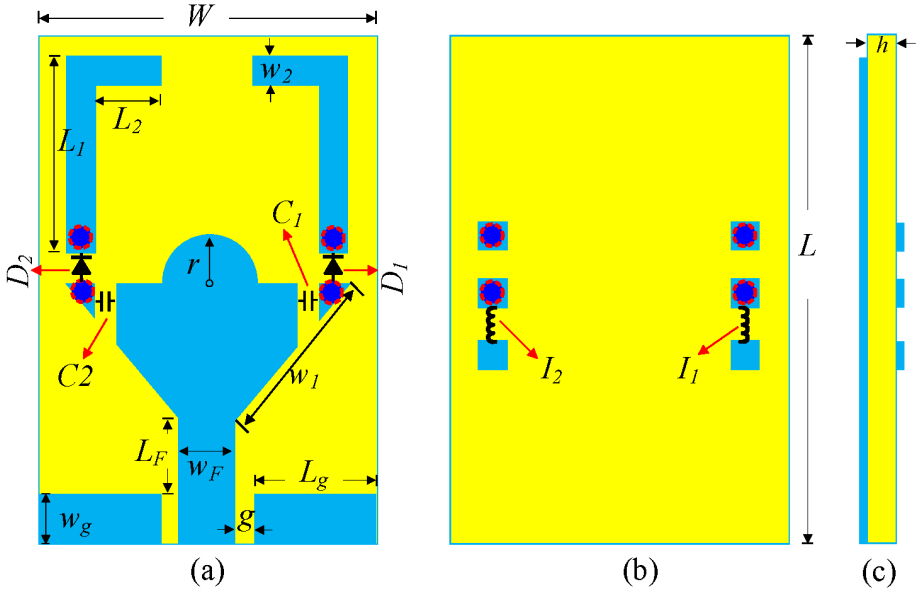

Figure 5.1: The proposed antenna (a) front view (b) back view (c) side view

$$\varepsilon_{eff} = \frac{\varepsilon_r + 1}{2} + \frac{\varepsilon_r - 1}{2}\left[(1 + 12\frac{h}{w})^{-0.5} + 0.04(1 - \frac{w}{h})^2\right] \tag{5.2}$$

ε_r is the relative permittivity and h is the thickness of the substrate, while A is the width of the radiator. Next, to enhance the bandwidth of the conventional monopole, the lower edges of the radiator were truncated. The effects of truncation of the corner of the radiator on the performance of the antenna are well discussed in [266] . In the end, a semicircular patch having radius r is loaded with a triangular patch to provide an additional path for the flow of current, which consequently improved the impedance mismatching, as depicted in Figure 5.2.

5.2.2.2 Design of the Compound Reconfigurable Antenna

Next, the flexible antenna designed above is utilized to design a compound reconfigurable antenna by loading two inverted L-shaped stubs at the upper corners of the triangular radiator. The insertion of the stub at either end of the radiator generates a respective phase difference between two ends of the radiator, which resulted in pattern

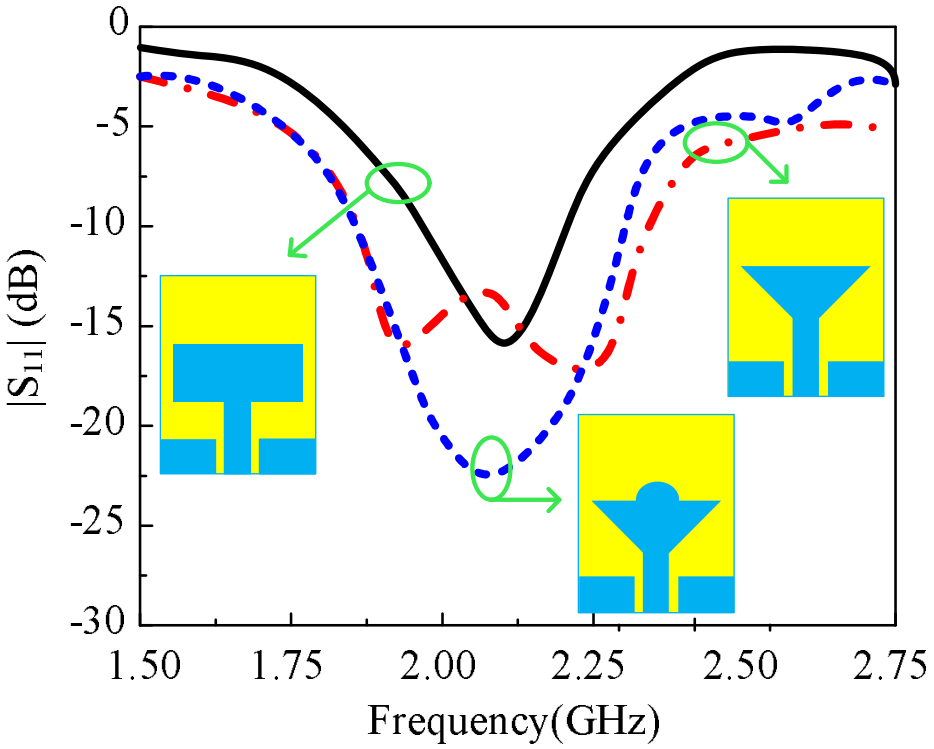

Figure 5.2: Extraction of the wideband antenna from conventional monopole

reconfigurability, as depicted in Figure 5.3. The phase difference Φ generated due to the presence of the stub can be calculated by:

$$\Phi \approx \frac{2\pi c L_t}{f} \tag{5.3}$$

Here $\pi \approx 22/7$, c is the velocity of light, f is the resonating frequency of the antenna, and L_t is the effective length of the stub, which can be calculated by:

$$L_t \approx L_1 + L_2 \tag{5.4}$$

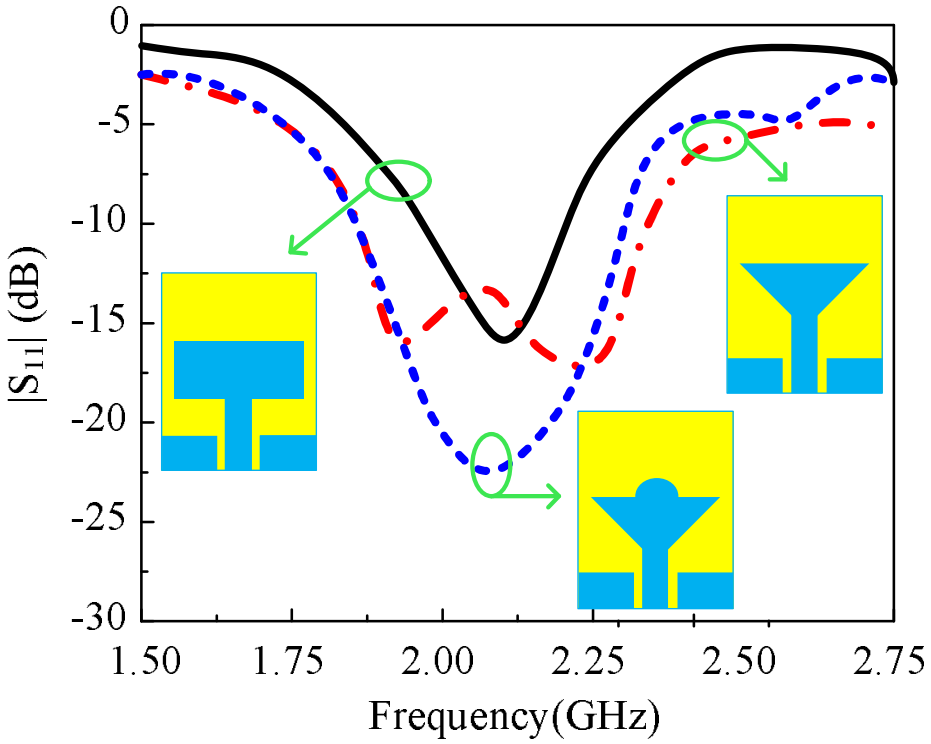

Figure 5.3: Effect of stub loading on the radiation patterns of the antenna

Noteworthily, due to the insertion of the stub, the surface charges redistribute itself and flow more toward the stub, which forces the electromagnetic waves to propagate in a specific direction resulting in the deformation of the radiation pattern in that specific direction, as illustrated in Figure 5.3. Next, the reactance loaded at the end of the radiator due to the insertion of the stub increases the effective area of the radiator, which results in the generation of additional resonance at a lower frequency, as depicted in Figure 5.4. Moreover, when both ends were loaded with stubs, the maximum surface charge distribution is along with the stubs while less amount of charges are distributed on the triangular patch. Therefore, the resonance is mainly due to stubs, and the antenna starts representing only at a lower frequency. Then two PIN diodes are inserted between stubs and triangular patch to achieve on-demand frequency and pattern reconfigurability as shown previously in the final proposed design (See Figure 5.1).

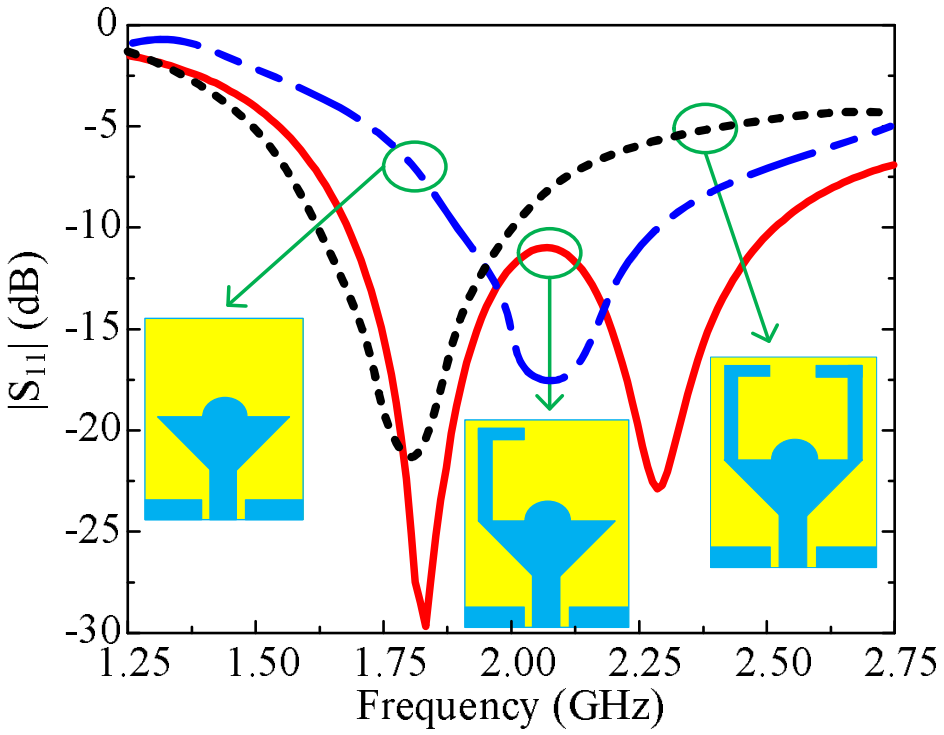

Figure 5.4: S-parameters comparison of various steps involved in antenna designing

5.2.3 Results and Discussion

The simulation of the proposed antenna was done using Higher Frequency Structure Simulator (HFSS) electromagnetic solver. The equivalent electrical model of the diode was constructed by utilizing lumped elements in such a way that for ON-state, the diode behaves like a series combination of 0.7 nH inductor with 5Ω resistor. While for OFF-state, the diode behaves like a series combination of 0.7 nH inductor along with a parallel combination of 5 kΩ resistor and 0.2 pF capacitor. Figure 5.5 illustrates the equivalent model of diode along with the biasing circuit use to provide pure DC-current to switch the state of the diode. Additionally, to validate the findings, a prototype of the proposed antenna is fabricated and tested as shown in Figure 5.6. The reflection coefficient of the proposed antenna was measured by portable vector network analyzer (Anritsu S820E). The antenna and propagation kit (ME1310) from Keysight Technologies was used to measure the radiation pattern of the antenna prototype.

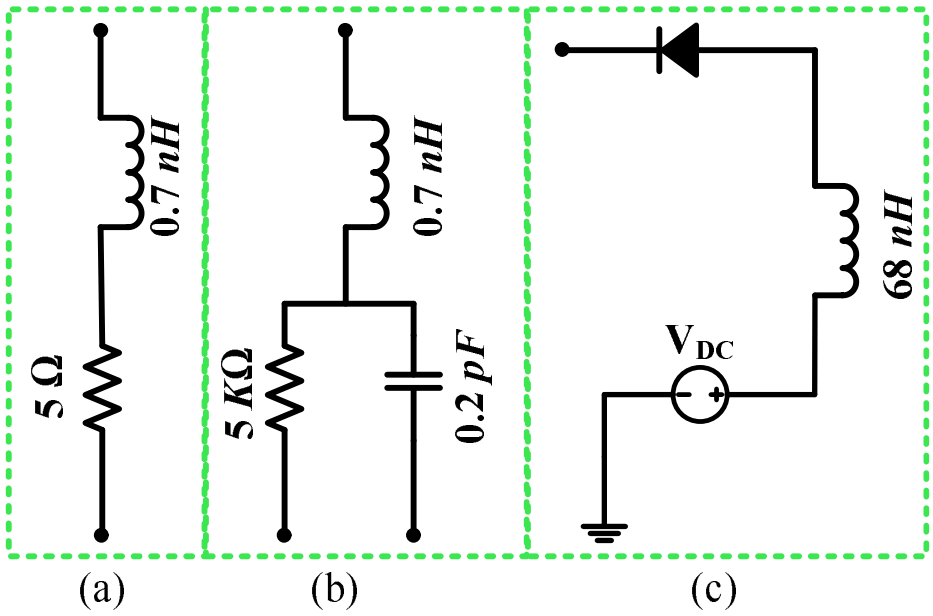

Figure 5.5: Equivlaent model of diode for (a) ON-state (b) OFF-state (c) biasing circuit

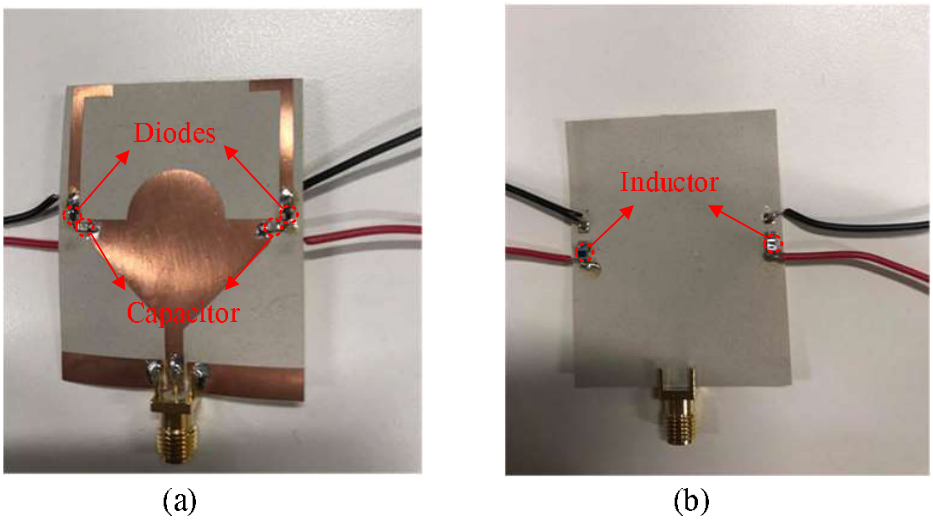

Figure 5.6: Fabricated prototype of the proposed antenna: (a) Top view (b) bottom view

5.2.3.1 Reflection Coefficient

Figure 5.7 presents the simulated and measured reflection coefficient of the proposed antenna for different switching cases of the diode. For case-00 (both diodes are in OFF-state), the simulated results show that the antenna exhibits an impedance bandwidth of

410 MHz (1.91-2.32 GHz), while the measured results show that the antenna exhibits impedance bandwidth of 480 MHz ranging from 1.81-2.29 GHz. When either of the diode D_1 or D_2 is OFF (case-01 or case-10), a simulated impedance bandwidth of 830 MHz (1.68-2.51 GHz) is achieved. On the other hand, the measured value for case-01 is noted to be 910 MHZ (1.64-2.55 GHz), and that for case-10 was 920 MHz ranging 1.635-2.555 GHz. The minor discrepancy between case-01 and case-10 is due to the imperfect fabrication and measurement system. For case-00 (both diodes are in OFF-state), the antenna starts resonating at 1.8 GHz having simulated and measured impedance bandwidth of 400 MHz (1.65-2.05 GHz) and 460 MHz (1.63-2.09 GHz), respectively. In general, good agreement among simulated and measured scattering parameter results was observed due to negligible effect of the biasing circuit as it is printed on the backside of the substrate.

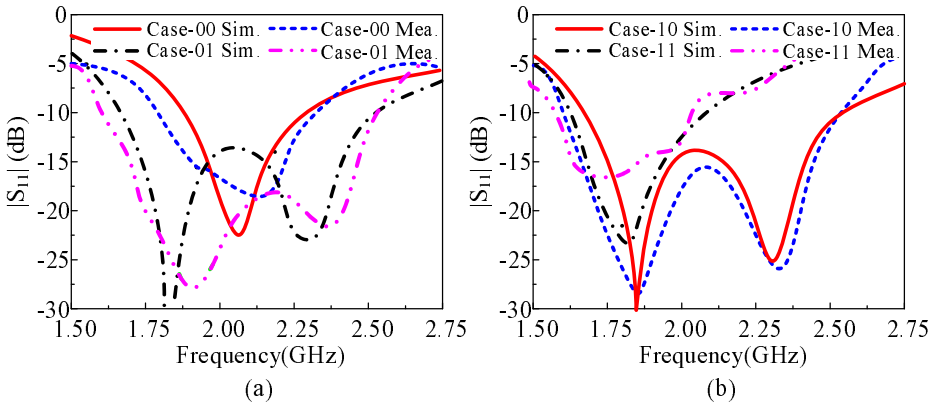

Figure 5.7: Comparison between measured and simulated s-parameters

5.2.3.2 Conformability Analysis

For any flexible device, the antenna should maintain characteristics for non-conformal and conformal condition, therefore the presented antenna is bent along X-axis, and Y-axis and its characteristics are analyzed. For simulation purposes, the antenna is wrapped on a cylinder of radius 25 mm, which is chosen by keeping in mind that the edges of the antenna do not touch each other (Figure 5.8 (a)). For measurements, a

flexible foam having a similar radius was chosen and the fabricated prototype was attached to it, as depicted in Figure 5.8 (b). The S-parameters of the antenna with different switching states under the conformal condition are shown in Figure 5.9. Strong agreement along simulated and measured results was observed for all switching states. Moreover, the similar results for conformal and non-conformal condition pronounce the potential of proposed work for both rigid and flexible devices.

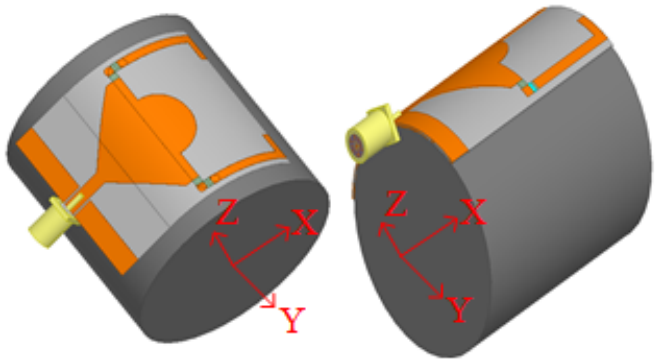

(a)

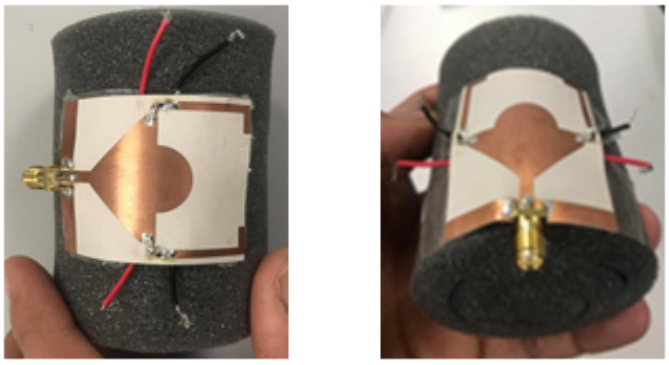

(b)

Figure 5.8: System of the structure used for conformability analysis: (a) Simulation setup and (b) Measurement setup.

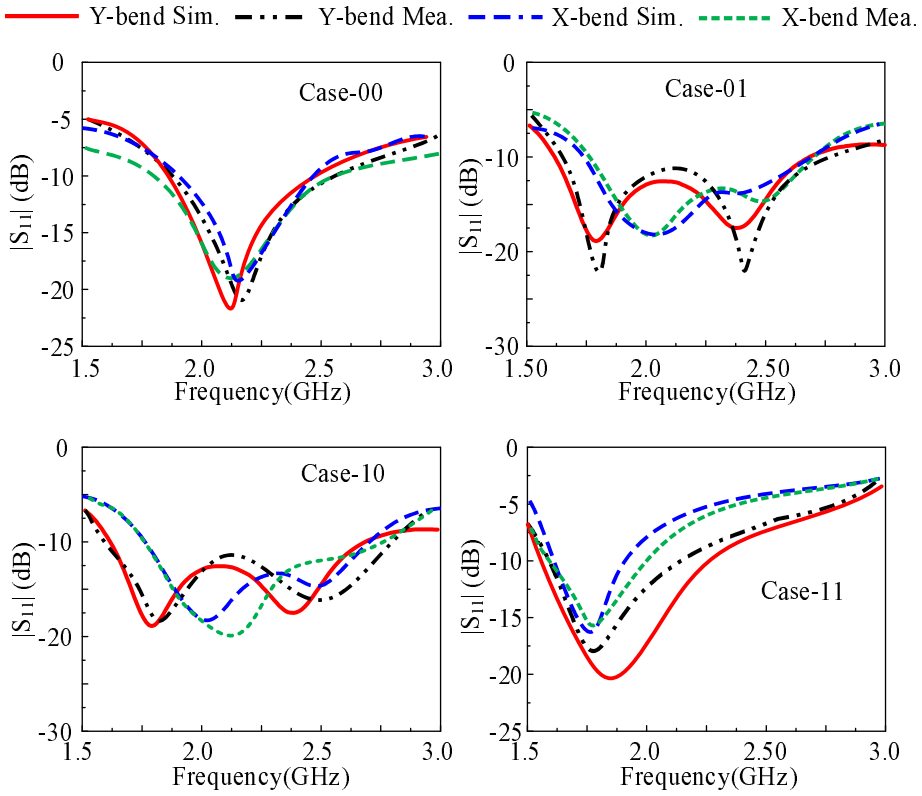

Figure 5.9: Comparison between measured and simulated s-parameters

5.2.3.3 Far-Field Analysis of Conformal and Non-Conformable Antenna

Figure 5.10 presents the comparison among simulated and measured radiation patterns of the antenna for possible switching states of diodes at various frequencies. It can be observed from Figure 5.10 (a) and 5.10 (b) that for case-00 (at 2.1 GHz) and case-11 (at 1.8 GHz), the antenna exhibits omnidirectional radiation pattern in principle E-plane ($\theta = 0°$), and a bi-directional radiation pattern is observed in H-plane ($\theta = 90°$). Moreover, the value of simulated gain at 2.1 GHz and 1.8 GHz is observed to be 2.1 dBi and 1.8 dBi, respectively. While the measured values for these frequencies were observed to be 2 dBi and 1.62 dBi for case-00 and case-11, respectively. On the other hand, for case-10 and case-11, the radiation pattern of the proposed antenna gets deviated from the original form and points toward $90°$ and -$90°$ as depicted in Figure 5.10 (c) and 5.10 (d), respectively. Moreover, at the selected frequency of 2.1 GHz,

for both case-01 and case-10, the simulated gain of the antenna is 2.98 dBi while the measured value is observed to 2.82 dBi.

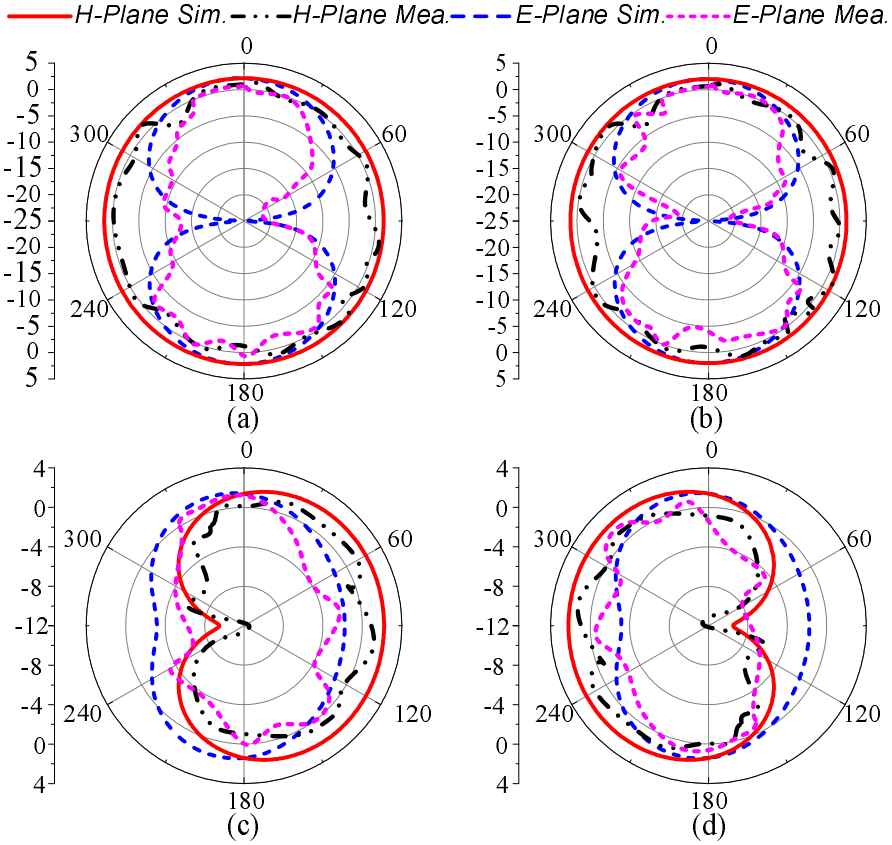

Figure 5.10: Comparison among simulated and measured radiation pattern (a) 2.1 GHz [case-00], (b) 1.8 GHz [case-11], (c) 2.1 GHz [case-01], (d) 2.1 GHz [case-10].

Figure 5.11 presents the radiation pattern of the proposed antenna under bend condition along the X-axis and Y-axis. For brevity, only the measured results of case-01 and case-10 were reported at the selected frequency of 2.1 GHz. When being bent along Y-axis, the antenna exhibits identical results as of without bending. On the other hand, when the antenna was bent along X-axis, a little deviation is observed, as depicted in Figure 5.11 (c-d), which is mainly due to large variation in the flow of current when the antenna was bent along the X-axis. The simulated value of the gain under conformal condition was observed to 3.04 dBi while measured results show that the antenna exhibits a gain of 2.8 dBi. In general, the antenna exhibits a good agreement between

simulated results for both conformal and non-conformal cases, which confirms the stability of the proposed work, thus making it a potential candidate for both conformal and non-conformal applications.

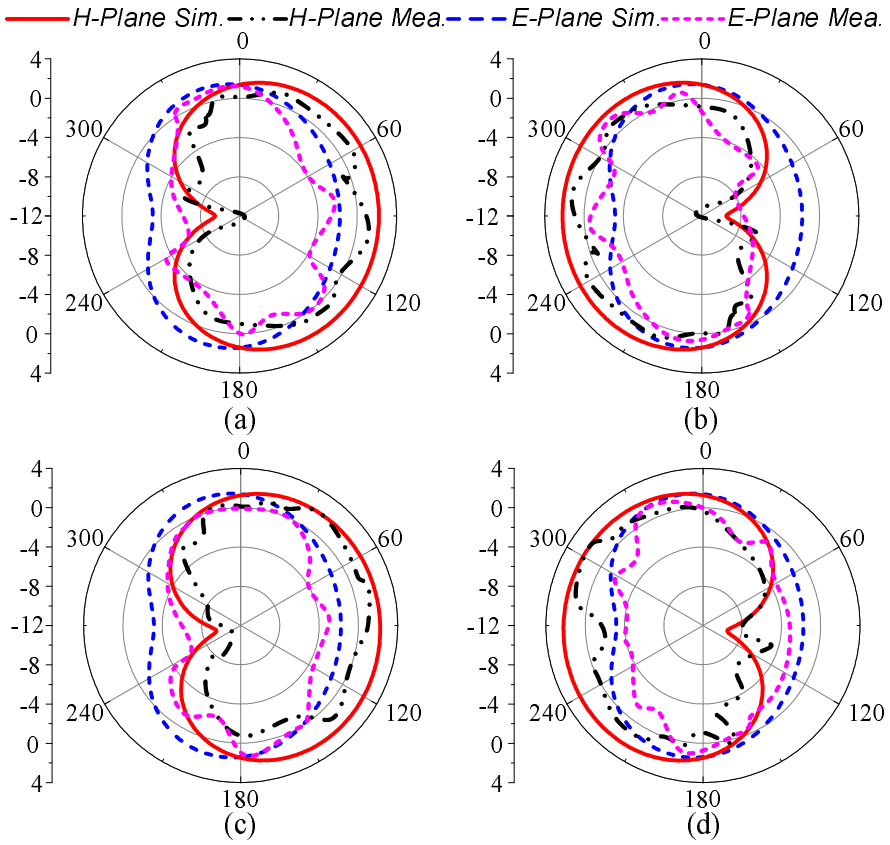

Figure 5.11: Comparison among simulated and measured radiation pattern of the antenna under bend condition at 2.1 GHz (a) bend along Y-axis [case-10], (b) bent along Y-axis, [case-01] (c) bent along X-axis [case-10], (d) bent along X-axis [case-01]

5.2.3.4 Comparison with state-of-the-art-work

The performances of the proposed antenna (in terms of overall size, reconfigurability type, flexibility, RF switch type used for reconfigurability, and frequency bandwidth) have been compared with state-of-the-art antennas in Table 5.1. The antenna over-performs the reported antennas due to its smaller size, discrete RF switch type with the advantages of flexibility, and both frequency and pattern reconfigurability.

Table 5.1: Comparison of the proposed work with the state of the art-work

Ref.	**Antenna Size** (mm^2)	**Reconfigurable Type**	**Material Type**	**RF Switch**	**Frequency (GHz)**
[256]	35×25	Radiation pattern	Flexible	2 PIN diodes	2.4-2.48
[258]	50×33	Frequency	Flexible	2 PIN diodes	2.18-2.58
[259]	85×85	Frequency & Radiation pattern	Solid	6 Varactors diodes	2.68-3.51
[260]	50×50	Frequency & Radiation pattern	Solid	4 PIN diodes	4.5/4.8 5.2/5.8
[261]	151×160	Frequency & Radiation pattern	Solid	6 Varactors diodes	2.15-2.38
[262]	23×31	Frequency & Radiation pattern	Solid	3 PIN diodes	3.1-6.8
[263]	112×52	Frequency & Radiation pattern	Solid	18 NMOS transistors	28/38
This work	40×50	Frequency & Radiation pattern	Flexible	2 PIN diodes	1.65-2.51

5.3 A Compact Dual Band Flexible Antenna for 900 and 2450 MHz band Applications

5.3.1 Introduction

Industrial, Medical and Scientific (ISM) frequency band spectrum are the one of the most used frequency bands. ISM bands are used in cellular radios, cordless phone, Near Field Communication (NFC), Bluetooth, and Wi-Fi [267, 268]. Beside these, hyperthermia therapy uses 2.45 GHz ISM band frequency to cure the cancer [269]. Moreover, ISM bands are also used in industries for induction heating, softening plastic, welding of plastic and microwave heat treating [270].

Researchers have designed several single and dual band flexible antennas for 900 MHz and 2450 MHz, which are the most common used ISM bands [205, 271, 272, 273, 274, 275, 276, 277, 278]. For an instant, a compact flexible fractal antenna was presented in [205] for 2450 MHz application, although the reported work offers wide bandwidth, compact size and high gain but it does not cover 900 MHz. A dual band flexible antenna of 100 mm $\times$ 60 mm was presented in [271]. The antenna offers dual band operational with a wide bandwidth, but its performance was adversely affected by bending. A miniaturized dual band antenna for ISM band applications was proposed in [273], however, it had several drawbacks, including rigid structure and narrow bandwidth. Another compact antenna was presented in [274], where varactors tunning was utilized to shift the frequency from 2.45 GHz to 900 MHz. However, this work also suffers from rigid structure and narrow bandwidth at both bands.

In [276], an antenna was presented for 900, 1800 and 2450 MHz band applications. The antenna consists of simple geometrical structure along with compact size of 43.5 mm $\times$ 48 mm. However, the antenna suffers from rigid structure, narrow bandwidth and low gain. The Paper substrate based dual band flexible antenna was presented in

[277]. It offers wide operational bandwidth, but having a large dimension and negative gain at lower resonance. Contrary to this, a dual band flexible antenna based on felt substrate was presented in [278], the antenna offers compact size along with reasonable gain at the cost of structural complexity due to vias and unsatisfactory performance in conformable condition.

Thus, there is still a need of compact flexible antenna, having wide operational bandwidth, simple geometrical structure and high gain. Therefore, a dual band flexible antenna was presented in this Section having the following key features:

• To the best of our knowledge, it is the compact size flexible antenna as compared to the reported work in literature.

• The proposed antenna offers wide bandwidth at both frequencies of 900 MHz and 2450 MHz along with reasonable gain for said frequencies.

• The antenna exhibits a strong comparison of performance parameters between predicted and measured results in both bent and unbent condition, thus making the proposed work a potential candidate for both conformal and non-conformable devices.

5.3.2 Antenna Design and Methodology

5.3.2.1 Antenna Design

Figure 5.12 illustrates the geometrical configuration of the proposed dual band flexible antenna. The antenna was designed utilizing the flexible material by ROOGERS Corp., RT-5880 having relative permittivity (ε_r) of 2.2 and loss tangent (tan θ) of 0.0002. The substrate had a thickness H while the overall dimension of the substrate was (length $\times$ width) $A_X \times A_Y$. The radiator of the proposed antenna was embedded on the top side of substrate, which consist of titled W-shaped serpentine structure feed a microstrip line having dimension of $F_X \times F_Y$. The backside of the substrate was consisting of partial ground plane of length G_X. A rectangular shaped slot was etched form a ground plane

initially and afterword a capacitor was loaded at the center of the slot by means of two small stubs of thickness g. The simulations were carried out using HFSS, while CST Studio Suit was utilized to perform the conformability tests.

The optimized parameters of the proposed antenna are $A_X = 78mm; A_Y = 40mm; H = 0.254mm; G_X = 28mm; G_Y = 15mm; G_1 = 10mm; G_2 = 14mm; g = 2mm; F_X = 3.5mm; F_Y = 44mm; X_1 = 14mm; X_2 = 14mm; X_3 = 5mm; X_4 = 14mm; X_5 = 4mm; Y_1 = 30mm; Y_2 = 36mm.$

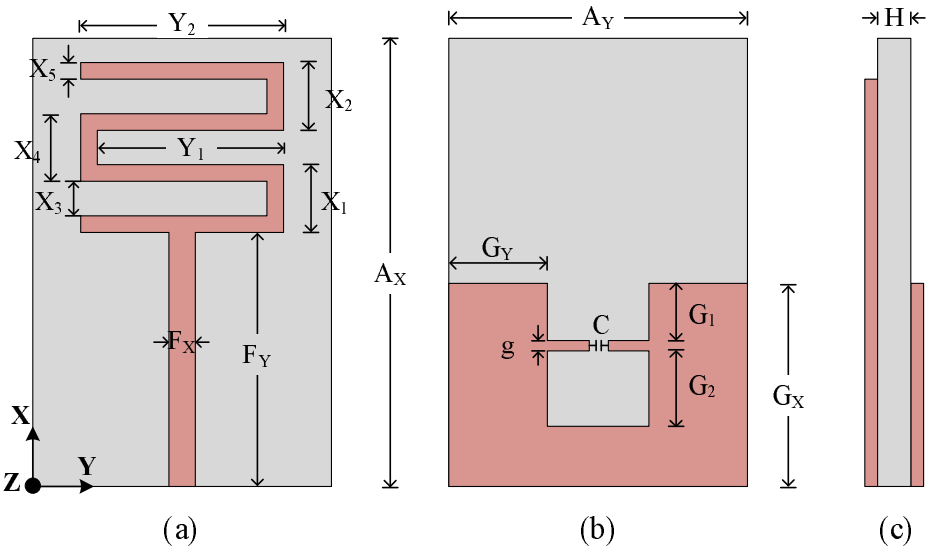

Figure 5.12: The proposed antenna (a) top-view (b) back-view (c) side-view

5.3.2.2 Design Methodology

Figure 5.13 illustrates the various steps, involve in designing of the proposed antenna, and their corresponding return loss. The antenna designing was divided in to four major parts: (1) antenna design at 2.45GHz, (2) lower the resonating frequency, (3) impedance matching at the lower resonating frequency, (4) capacitor loading to achieve dual band behavior.

In the first step, a simple quarter wave monopole antenna was designed for the central frequency of 2450MHz. The length (F_Y) of the transmission line can be estimated

using the relation provided.

$$F_Y = \frac{c}{2f_c\sqrt{\varepsilon_{eff}}} \tag{5.5}$$

Here f_c is the desire central frequency, c is the free space speed of light ($\approx 3\times10^8 ms^{-1}$) and ε_{eff} is the effective dielectric constant which can be estimated:

$$\varepsilon_{eff} = \frac{\varepsilon_r + 1}{2} \tag{5.6}$$

Here ε_r is the dielectric constant of the substrate. The length and width of the ground plane can also be expressed as the integral part of the wavelength by:

$$G_N = \frac{c}{x_n f_c\sqrt{\varepsilon_{eff}}} \tag{5.7}$$

For length (G_X) of the substrate $x_n \approx$ 4.5 and for width (A_Y) of the substrate $x_n \approx$ 3. The resultant antenna shows resonance around 2.45 GHz having an $|S_{11}|$ > -10dB impedance bandwidth of 240 MHz ranging 2.37 – 2.61 MHz, as depicted in Figure 5.13 (b).

In step 2, serpentine structure was utilized to achieve lower resonance without effecting the overall size of the antenna. A tilted W-shaped serpentine structure was constructed, where the total effective length of the serpentine can be estimated by:

$$L_T = x_o\frac{c}{f_c\sqrt{\varepsilon_{eff}}} \tag{5.8}$$

Here L_T is the total effective length of the serpentine, for the presented antenna it was expressed as $L_T = 4 \times Y_2 + X_1 + X_2 + X_4$, where x_o is the fractional part of the wavelength at the desire frequency and for presented case x_o ≈0.55. The resultant antenna although shows a resonance at the lower frequency around the 900 MHz, but the return loss of the resultant antenna was very low. Thus, to improve the return loss of

the antenna Defected Ground Structure (DGS) was utilized.

In the third step, a rectangular slot was etched from the center of the ground plane, which results in a U -shaped ground plane, as depicted in Figure 5.13 (a).The resultant antenna shows a good impedance matching at the lower frequency of 875 MHz having an impedance bandwidth of 200 MHz ranging 775 – 975 MHz. The desire lower band of 900 MHz was covered by the antenna, but at the higher desire band of 2450MHz the return loss is still very low. Thus, to overcome this a capacitor was loaded in the middle of slot in ground plane, as depicted in Figure 5.13 (a). The presence of capacitor introduces additional capacitor load, which nullify the inductive load due to transmission line and results in the higher resonance. The final antenna exhibits a dual band behavior having resonance around 900 MHz and 2450 MHz having a respective impedance bandwidth of 200 MHz and 570 MHz, as illustrated in Figure 5.13 (b).

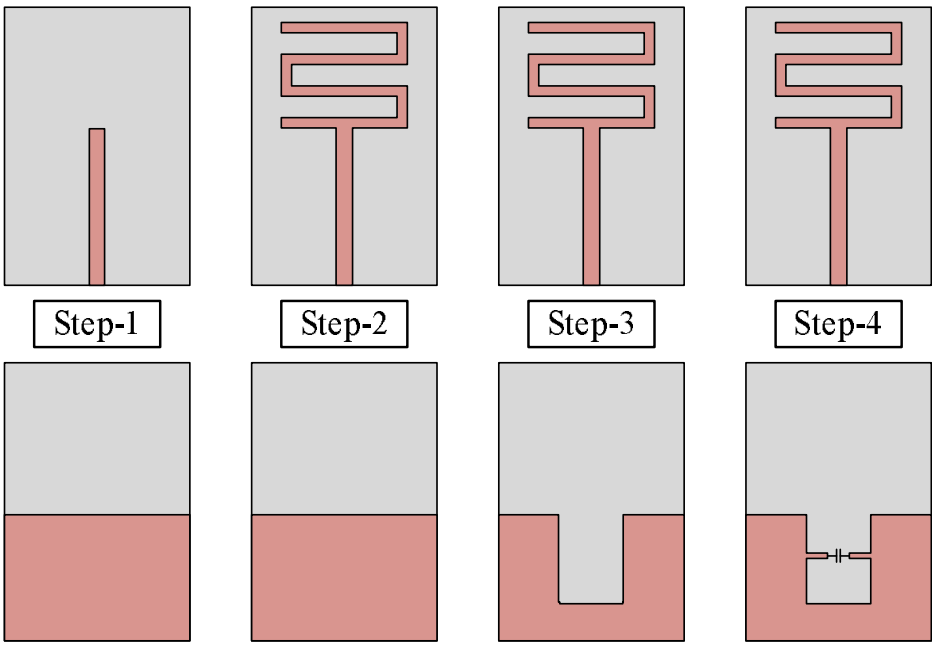

(a)

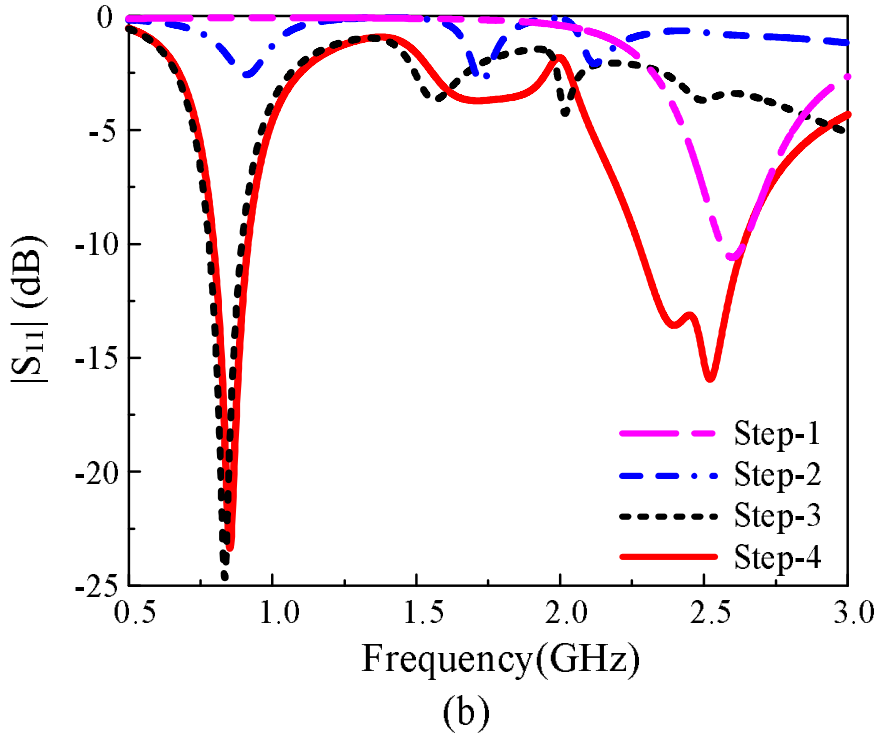

(b)

Figure 5.13: (a) Geometrical configuration of various antennas involve in designing of proposed antenna (b) return loss comparison among various antennas

5.3.3 Results and Discussion

5.3.3.1 Scattering Parameters

Figure 5.14 illustrates the fabricated prototype of the antenna under conformal and non-conformable condition along with the comparison among predicted and measured results. Figure 5.14 (a-b) presets the top and bottom view of the fabricated prototype used for measurments. Commercially available 50-Ω SMA connector was used for excitation of antenna. E5063A ENA Network analyzer having frequency range of 500 MHz – 18 GHz was used for measuring return loss of the antenna. Figure 5.14 (e) presents the comparison among simulated and measured results of antenna under normal condition, the antenna shows a good agreement between both results while exhibiting wideband of 220 MHz (760 – 980 MHz) and 570 MHz (2200 – 2770 MHz) at the resonating frequencies of 900 MHz and 2450 MHz, respectively.

Figure 5.14 (c) depicts the simulation setup for the conformability analysis of the antenna along X-axis and Y-axis, while Figure 5.14 (d) illustrates the measurments setup for the bending analysis of the proposed dual band antenna. For both X and Y-axis, the antenna exhibits good agreement between each other as well as a strong agreement between simulated and measured results, as depicted in Figure 5.14 (f). The measured bandwidths of the antenna while bend along X-axis are 245 MHz (750 – 995 MHz) and 720 MHz (2130 – 2850 MHz) while for bend along Y-axis the measured bandwidths are 270 MHz (728 – 998 MHz) and 585 MHz (2230 – 2815 MHz) at the resonating frequencies of 900 MHz and 2450 MHz, respectively.

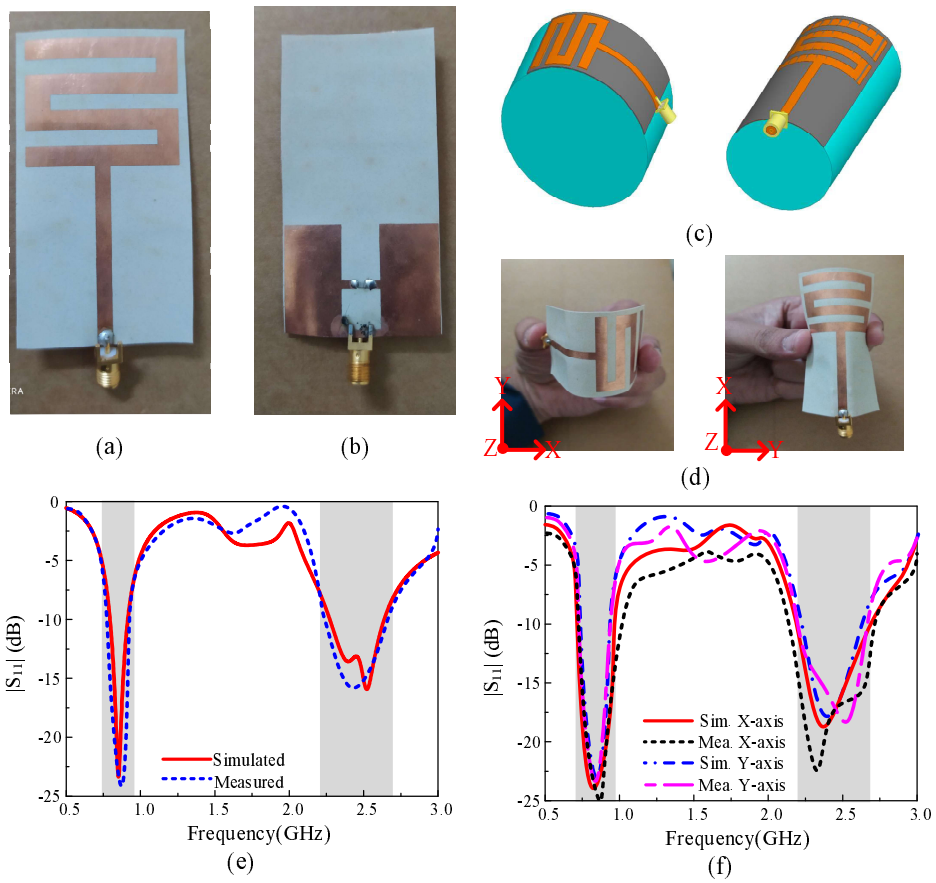

Figure 5.14: Fabricated prototype of the proposed antenna (a) top-view (b) bottom view; Setup for bending analysis (c) simulated (d) measured; (e) comparison among simulated and measured results (f) comparison among results under bending condition

5.3.3.2 Radiation Pattern

Figure 5.15 (b-c) depicts the comparison among simulated and measured radiation pattern at the respective frequencies of 900 MHz and 2450 MHz. It could be observed from the Figure 5.15 (b-c) that antenna exhibits nearly omni-directional radiation pattern in principle H-Plane $(\theta = 0°)$ while a slightly distorted bi directional radiation pattern was observed in principle E-Plane $(\theta = 90°)$. The measured radiation pattern results show a strong agreement with simulated one, as depicted in Figure 5.15(b-c), stating the performance stability of the proposed antenna.

5.3.3.3 Gain and Efficiency

Figure 5.15 (d) illustrates the comparison among numerically calculated and measured gain of the proposed antenna. At the low pass band region, the numerically calculated gain was reported to be 1.99 dB while the measured value show a peak gain of 1.85 dB. On the other hand, higher pass band exhibits a simulated peak gain of 2.27 dB while measured value shows a gain of 2.2 dB. The little difference between simulated and measured value is infect due to fabrication tolerance and random error in measurement setup. Moreover, the antenna exhibits simulated efficiency > 85% for both passbands.

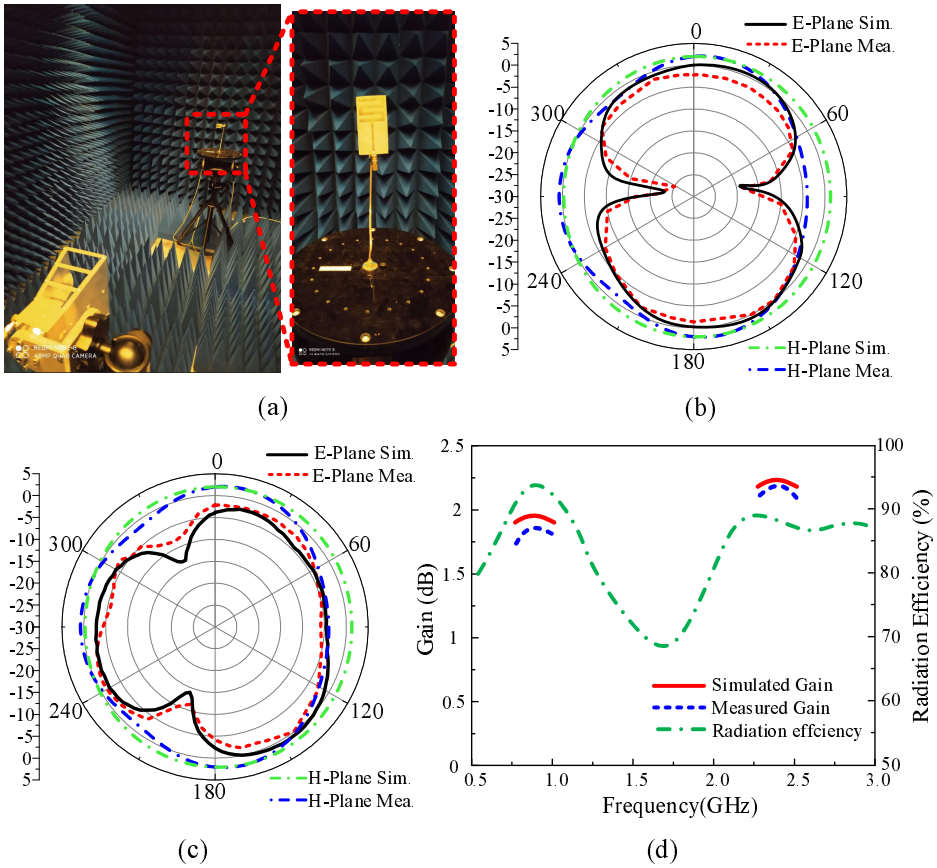

Figure 5.15: (a) Measurements setup for far-field analysis; predicted and simulated and measured radiation pattern at (b) 900 MHz (c) 2450 MHz; (d) simulated and measured gain

5.3.4 Comparison with state-of-the-art-work

Table 5.2 presents the comparison of the proposed antenna with reported work in literature. It could be observed that proposed work offer compact size as compared to [271, 272, 275, 276, 277, 278], although antenna presented in [273, 274] offered compact size as compared to proposed work but they have set back of rigid body along with narrow bandwidth. Thus, it can be concluded that the proposed antenna outperforms other related work and become a potential candidate for the present and future communication systems.

Table 5.2: Performance Comparison with Existing works

Ref.	**Dimension** (mm^2)	**Impedance Bandwidth (MHz)**	**Peak Gain (dBi)**	**Flexibility**
[205]	30×25	450	2.4	Yes
[271]	100×60	200 / 350	1.6 / 1.9	Yes
[272]	115×90	580 / 640	1.25 / 1.53	Yes
[273]	15×15	30 / 70	5.34 / 4.49	No
[274]	65×46	40 / 70	N.R	No
[275]	70×80	70 / 800	N.R	No
[276]	44×48	30 / 40	1.9 / 2.7	No
[277]	90×100	200 / 70	1.3 / 2.4	Yes
[278]	60×60	150 / 250	1.5 / 2.4	Yes
This work	78×40	220 / 570	1.85 / 2.2	Yes

5.4 Summary

In this chapter, we present two novel flexible antenna designs for flexible wearable applications. The first design is hybrid frequency and radiation pattern reconfigurable

antenna. The proposed antenna shows the good simulated and measurement results, which makes it applicable for 3G, 4G, LTE, GSM, and ISM bands. The second design is capacitor loaded dual-band antenna for ISM applications. The negligible deviation of resonance for conformal and non-conformal case makes it suitable for both rigid and flexible devices.

Chapter 6

Conclusion and Recommendation for Future Works

6.1 Conclusion

In the era of modern wireless communication, mobile, connectivity, audio communication, and data transfer are the important part of everyone's life. As antenna is vital part of every communication system, which helps to connect different portable devices. The design and concept of the antenna has been changed due to the advancement of modern electronics devices. The devices with fixed antenna properties face challenges in modern environment where frequency of operation, radiation pattern or polarisation is required to change according to the system requirements. However, the idea of antenna reconfiguration has helped to cope up the above-mentioned challenges and leads to new possibilities. This research problem motivated us to find the scope by using the reconfigurable antenna instead of fixed performance type for current and future modern wireless devices. Reconfigurable antennas possess some properties like more compact, cover multiple wireless bands, and reduce the complexity. It is best idea to use the reconfigurable antennas for the improvement of system efficiency. There are various

techniques and methods have been designed in the literature to tune the three properties (frequency, radiation pattern, and polarization) of an antenna to make it reconfigurable. However, there are some limitations like large antenna size, tunning range, complex biasing circuit that remain and affect the efficiency of an antenna. The research goals were achieved by designing several antenna prototypes that aimed multiple band coverage, compact size, and stable antenna efficiencies at all switching states.

This thesis presents the detailed design methodology, analysis and prototypes of different reconfigurable antennas for multiple wireless applications. The proposed antennas provide the compact size, multiple frequency bands, and hybrid reconfigurable capabilities, suitable for mobile stations and wearable electronic devices.

First of all, two PIFA antennas were designed. The first design illustrated the frequency reconfigurable PIFA antenna, which is proposed for GSM$850/900$, and UMTS 2100 frequency bands. Two PIN diodes with different states are applied to generate the required frequencies. The different parameters of proposed antenna are optimized. The proposed antenna is fabricated, and measurements results showed good agreement with simulated results in terms of return loss, radiation pattern, gain and efficiency. The measurements results meet the requirements of several wireless standards. The main feature of the first design is its highly compact size, while retaining a performance comparable with existing designs. In the second design, a novel dual frequency band and polarization-reconfigurable antenna is proposed. By using four PIN diodes, 800 MHz and 1.4 GHz operation is achieved for both horizontal and vertical polarizations. Simulation results showed that return loss, radiation pattern, antenna gain, and E-field distribution of the proposed reconfigurable antenna met conventional requirements. In particular, the second design achieves a reflection coefficient of -10 dB in both designed frequency bands, which is highly desirable in adverse impedance changing environments.

Secondly, three different frequency reconfigurable antennas were proposed. In first

design, a compact multiband frequency reconfigurable antenna is presented. The antenna contains a CPW-fed triangular monopole antenna generating wideband operational mode. Two rectangular stubs are loaded to achieve frequency reconfigurability between wideband, narrowband, and dual-band mode. Then, a rectangular stub loaded to an inverted triangular patch is utilized to provide frequency reconfigurability between dual-band and wideband mode. Finally, both antennas are joined together to form the proposed multi-mode frequency reconfigurable antenna. The antenna offers a wideband mode of 3-8GHz along with narrow bands at various frequencies of 2.1 GHz, 2.25 GHz, 2.45 GHz, 3.3 GHz, 3.5 GHz, and 8 GHz. The antenna achieves strong agreement between simulated and measured results along with acceptable gain, omnidirectional radiation pattern, and high efficiency. Moreover, the comparison to the related work shows that the proposed antenna outperforms existing antennas in the literature, thus making it a strong candidate for heterogeneous applications that requires a compact multi-band and multi-mode antenna. The second design presents a compact frequency reconfigurable antenna. Initially to cover 5G sub-6-GHz band a wideband triangle shaped monopole antenna was designed which was originally inspired from rectangular monopole antenna. Afterwards, two V-shaped slots were utilized to achieve two notch bands, their length could be adjusted independently to achieve desire notch bands. At the end, two RF-PIN diodes were inserted at the middle of slot such that when diodes are in Off-state they active the slot and thus result in notching the band. The overall size of antenna was $0.19\lambda_o \times 0.19\lambda_o \times 0.0081\lambda_o$, where λ_o correspond to the free space wavelength at lowest resonating frequency. The proposed work either operates in wideband mode, two different dual-band modes or in tri-band, depending upon the state of the diodes. Strong agreement between simulation and measured results, along with reasonable gain in pass bands and very low gain in band stop region makes the proposed antenna suitable candidate for 2.1 GHz 4G-LTE band, 2.45 GHz ISM band, 5G-sub-6-GHz band and S-band satellite applications. In the last design, another

compact frequency reconfigurable antenna was proposed that operates in eight different frequencies in four dual-band modes. The operating modes are controlled using two PIN diodes introduced in the radiating element. The presented antenna is characterized by the good adaptation for all provided frequencies, higher efficiency values in the whole range of frequencies, and a similar radiation pattern in all diode cases, which makes it a promising candidate for various wireless applications.

Finally, this thesis concludes with two flexible antenna designs for wearable applications. The first design presents a hybrid frequency and pattern reconfigurable antenna. The geometrical structure of the proposed antenna consists of a semicircular patch loaded on a triangular radiator along with two inverted L-shaped stubs, which are utilized to achieve compound reconfigurability using diodes. The antenna comprises of a simple structure along with a compact size of $0.29\lambda_o \times 0.24\lambda_o \times 0.001\lambda_o$. The frequency of the proposed antenna can be switched from 2.1 GHz to 1.8 GHz by switching the state of both diodes in OFF and ON-state, respectively. Moreover, when one diode is in ON-state and the other in OFF-state, the antenna shows a wide impedance bandwidth of 1.65-2.5 GHz along with tilted radiation patterns in the E-plane. The strong agreement between simulated and measured results for both conformal and non-conformal conditions makes the proposed work a promising candidate for the applications operating in 3G, 4G, LTE, GSM, and ISM bands. In second design, a dual-band capacitor loaded DGS flexible antenna for ISM applications is presented. The combination of serpentine, DGS and additional capacitor loading results in dual resonance at 850 MHz and 2520 MHz with a compact size of $0.22\lambda \times 0.11\lambda \times 0.0007\lambda$. The presented antenna shows a good agreement between simulated and measured for both conformal and non-conformal scenarios. Furthermore, the negligible deviation of resonance for conformal and non-conformal case makes the presented work a promising candidate for both rigid and flexible devices.

6.2 Recommendation for Future Works

The reconfigurable antennas have attractive features and provide flexibility in adjusting the functionality of the system, minimizing overall system volume and circuit complexity. It is desired to use the reconfigurable antenna to increase the system capacity, spectrum and energy efficiency. To make an antenna reconfigurable and change its three main properties (resonance frequency, radiation pattern and polarization), different methods and novel design ideas have been proposed in the literature. However, there is still some imperfection, which adversely affects the performance of the reconfigurable antennas. These imperfections include large antenna size, limited gain, and non-linear behaviour of RF switches, narrow bandwidth, complex impedance matching circuit, complicated biasing circuit and finite overall performance.

1. These work can be enhanced by using varactor diode or with MEMS for wearable electronic technology.

2. Hybrid reconfigurable can be implemented in the future. Pattern reconfiguration helps to achieve the narrow beam for 5G applications, and polarization reconfiguration is highly recommended to avoid the propagation loss in portable devices.

3. The proposed antenna designs can be implemented for array configuration by using some microwave circuits to attain the wide range of applications.

4. Due to implementation of 5G/6G in the future, the modern wireless technology and advanced electronics systems will require huge demand of reconfigurable antenna for different applications like IoT devices, massive MIMO, cognitive radios, and vehicle-to-vehicle communication. The reconfigurable antennas will provide the easiness for different wireless services simultaneously, flexibility, and more functionality.

References

[1] G. A. Norton, "Apparatus for wave changing in radiosignaling," Feb. 2 1926, uS Patent 1,571,405.

[2] H. Friis, C. Feldman, and W. Sharpless, "The determination of the direction of arrival of short radio waves," *Proceedings of the Institute of Radio Engineers*, vol. 22, no. 1, pp. 47–78, 1934.

[3] E. Bruce and A. Beck, "Experiments with directivity steering for fading reduction," *Proceedings of the Institute of Radio Engineers*, vol. 23, no. 4, pp. 357–371, 1935.

[4] H. T. Friis and C. B. Feldman, "A multiple unit steerable antenna for short-wave reception," *Proceedings of the Institute of Radio Engineers*, vol. 25, no. 7, pp. 841–917, 1937.

[5] W. Ernst, "Antenna tunable in its length," Apr. 7 1942, uS Patent 2,278,601.

[6] R. Antennas, "Bell systems technical journal, vol. 26, apr., 1947," *to*, vol. 317, p. 219, 1947.

[7] W. Rotman and A. Maestri, "An electromechanically scannable trough waveguide array," in *IRE International Convention Record*, vol. 8. IEEE, 1966, pp. 67–83.

[8] E. Matthews, C. Cuccia, and M. Rubin, "Technology considerations for the use of multiple beam antenna systems in communication satellites," *IEEE Transactions on Microwave Theory and Techniques*, vol. 27, no. 12, pp. 998–1004, 1979.

[9] D. H. Schaubert, F. G. Farrar, S. T. Hayes, and A. R. Sindoris, "Frequency-agile, polarization diverse microstrip antennas and frequency scanned arrays," Jan. 4 1983, uS Patent 4,367,474.

[10] J. T. Bernhard and C. Balanis, "Reconfigurable antennas (synthesis lectures on antennas and propagation)," *Morgan and Claypool*, 2006.

[11] R. L. Haupt and M. Lanagan, "Reconfigurable antennas," *IEEE Antennas and Propagation Magazine*, vol. 55, no. 1, pp. 49–61, 2013.

[12] D. Rodrigo, L. Jofre, and B. A. Cetiner, "Circular beam-steering reconfigurable antenna with liquid metal parasitics," *IEEE Transactions on Antennas and Propagation*, vol. 60, no. 4, pp. 1796–1802, 2012.

[13] X. Bai, M. Su, Y. Liu, and Y. Wu, "Wideband pattern-reconfigurable cone antenna employing liquid-metal reflectors," *IEEE Antennas and Wireless Propagation Letters*, vol. 17, no. 5, pp. 916–919, 2018.

[14] M. Alam and A. Abbosh, "Beam-steerable planar antenna using circular disc and four pin-controlled tapered stubs for wimax and wlan applications," *IEEE Antennas and Wireless Propagation Letters*, vol. 15, pp. 980–983, 2015.

[15] G. Ruvio, M. J. Ammann, and Z. N. Chen, "Wideband reconfigurable rolled planar monopole antenna," *IEEE Transactions on Antennas and Propagation*, vol. 55, no. 6, pp. 1760–1767, 2007.

[16] Y. Tawk, J. Costantine, K. Avery, and C. Christodoulou, "Implementation of a cognitive radio front-end using rotatable controlled reconfigurable antennas," *IEEE Transactions on Antennas and Propagation*, vol. 59, no. 5, pp. 1773–1778, 2011.

[17] J.-C. Langer, J. Zou, C. Liu, and J. Bernhard, "Micromachined reconfigurable out-of-plane microstrip patch antenna using plastic deformation magnetic actuation," *IEEE Microwave and Wireless Components Letters*, vol. 13, no. 3, pp. 120–122, 2003.

[18] J. T. Bernhard, E. Kiely, and G. Washington, "A smart mechanically actuated two-layer electromagnetically coupled microstrip antenna with variable frequency, bandwidth, and antenna gain," *IEEE Transactions on Antennas and Propagation*, vol. 49, no. 4, pp. 597–601, 2001.

[19] S. Cheng, Z. Wu, P. Hallbjorner, K. Hjort, and A. Rydberg, "Foldable and stretchable liquid metal planar inverted cone antenna," *IEEE Transactions on antennas and propagation*, vol. 57, no. 12, pp. 3765–3771, 2009.

[20] T. Aboufoul, A. Alomainy, and C. Parini, "Reconfiguring uwb monopole antenna for cognitive radio applications using gaas fet switches," *IEEE Antennas and Wireless Propagation Letters*, vol. 11, pp. 392–394, 2012.

[21] N. Haider, D. Caratelli, and A. Yarovoy, "Recent developments in reconfigurable and multiband antenna technology," *International Journal of Antennas and Propagation*, vol. 2013, 2013.

[22] T. J. Jung, I.-J. Hyeon, C.-W. Baek, and S. Lim, "Circular/linear polarization reconfigurable antenna on simplified rf-mems packaging platform in k-band," *IEEE Transactions on Antennas and Propagation*, vol. 60, no. 11, pp. 5039–5045, 2012.

[23] A. Tagantsev, V. Sherman, K. Astafiev, J. Venkatesh, and N. Setter, "Ferroelectric materials for microwave tunable applications," *Journal of Electroceramics*, vol. 11, no. 1-2, pp. 5–66, 2003.

[24] R. Mishra, S. Pattnaik, and N. Das, "Tuning of microstrip antenna on ferrite substrate," *IEEE Transactions on Antennas and Propagation*, vol. 41, no. 2, pp. 230–233, 1993.

[25] D. Pozar and V. Sanchez, "Magnetic tuning of a microstrip antenna on a ferrite substrate," *Electronics Letters*, vol. 24, no. 12, pp. 729–731, 1988.

[26] A. D. Brown, J. L. Volakis, L. C. Kempel, and Y. Botros, "Patch antennas on ferromagnetic substrates," *IEEE Transactions on Antennas and Propagation*, vol. 47, no. 1, pp. 26–32, 1999.

[27] Y. Yashchyshyn and J. W. Modelski, "Rigorous analysis and investigations of the scan antennas on a ferroelectric substrate," *IEEE Transactions on Microwave Theory and Techniques*, vol. 53, no. 2, pp. 427–438, 2005.

[28] M. F. Iskander, Z. Yun, Z. Zhang, R. Jensen, and S. Redd, "Design of a low-cost 2-d beam-steering antenna using ferroelectric material and cts technology," *IEEE Transactions on Microwave Theory and Techniques*, vol. 49, no. 5, pp. 1000–1003, 2001.

[29] G. Lovat, P. Burghignoli, and S. Celozzi, "A tunable ferroelectric antenna for fixed-frequency scanning applications," *IEEE Antennas and Wireless Propagation Letters*, vol. 5, pp. 353–356, 2006.

[30] M. Rutschlin and V. Sokol, "Reconfigurable antenna simulation: Design of reconfigurable antennas with electromagnetic simulation," *IEEE Microwave Magazine*, vol. 14, no. 7, pp. 92–101, 2013.

[31] W. Hu, M. Ismail, R. Cahill, J. Encinar, V. Fusco, H. Gamble, D. Linton, R. Dickie, N. Grant, and S. Rea, "Liquid-crystal-based reflectarray antenna with electronically switchable monopulse patterns," *Electronics Letters*, vol. 43, no. 14, 2007.

[32] W. Hu, R. Cahill, J. A. Encinar, R. Dickie, H. Gamble, V. Fusco, and N. Grant, "Design and measurement of reconfigurable millimeter wave reflectarray cells with nematic liquid crystal," *IEEE Transactions on Antennas and Propagation*, vol. 56, no. 10, pp. 3112–3117, 2008.

[33] S. Bildik, S. Dieter, C. Fritzsch, W. Menzel, and R. Jakoby, "Reconfigurable folded reflectarray antenna based upon liquid crystal technology," *IEEE Transactions on Antennas and Propagation*, vol. 63, no. 1, pp. 122–132, 2014.

[34] T. S. Teeslink, D. Torres, J. L. Ebel, N. Sepulveda, and D. E. Anagnostou, "Reconfigurable bowtie antenna using metal-insulator transition in vanadium dioxide," *IEEE Antennas and Wireless Propagation Letters*, vol. 14, pp. 1381–1384, 2015.

[35] D. Zhao, L. Lan, Y. Han, F. Liang, Q. Zhang, and B.-Z. Wang, "Optically controlled reconfigurable band-notched uwb antenna for cognitive radio applications," *IEEE Photonics Technology Letters*, vol. 26, no. 21, pp. 2173–2176, 2014.

[36] P. Alizadeh, C. Parini, and K. Rajab, "Optically reconfigurable unit cell for ka-band reflectarray antennas," *Electronics Letters*, vol. 53, no. 23, pp. 1526–1528, 2017.

[37] S. Pendharker, R. Shevgaonkar, and A. Chandorkar, "Optically controlled frequency-reconfigurable microstrip antenna with low photoconductivity," *IEEE Antennas and Wireless Propagation Letters*, vol. 13, pp. 99–102, 2014.

[38] C. G. Christodoulou, Y. Tawk, S. A. Lane, and S. R. Erwin, "Reconfigurable antennas for wireless and space applications," *Proceedings of the IEEE*, vol. 100, no. 7, pp. 2250–2261, 2012.

[39] Y. Tawk, A. R. Albrecht, S. Hemmady, G. Balakrishnan, and C. G. Christodoulou, "Optically pumped frequency reconfigurable antenna design," *IEEE Antennas and Wireless Propagation Letters*, vol. 9, pp. 280–283, 2010.

[40] C. J. Panagamuwa, A. Chauraya, and J. Vardaxoglou, "Frequency and beam reconfigurable antenna using photoconducting switches," *IEEE Transactions on Antennas and Propagation*, vol. 54, no. 2, pp. 449–454, 2006.

[41] T. Aboufoul, C. Parini, X. Chen, and A. Alomainy, "Pattern-reconfigurable planar circular ultra-wideband monopole antenna," *IEEE Transactions on Antennas and Propagation*, vol. 61, no. 10, pp. 4973–4980, 2013.

[42] S. Shelley, J. Costantine, C. G. Christodoulou, D. E. Anagnostou, and J. C. Lyke, "Fpga-controlled switch-reconfigured antenna," *IEEE Antennas and Wireless Propagation Letters*, vol. 9, pp. 355–358, 2010.

[43] J. Costantine, Y. Tawk, J. Woodland, N. Flaum, and C. G. Christodoulou, "Reconfigurable antenna system with a movable ground plane for cognitive radio," *IET Microwaves, Antennas & Propagation*, vol. 8, no. 11, pp. 858–863, 2014.

[44] Z. Jiang and F. Yang, "Reconfigurable sensing antennas integrated with thermal switches for wireless temperature monitoring," *IEEE Antennas and Wireless Propagation Letters*, vol. 12, pp. 914–917, 2013.

[45] J. Costantine, Y. Tawk, and C. G. Christodoulou, "Motion-activated reconfigurable and cognitive radio antenna systems," *IEEE Antennas and Wireless Propagation Letters*, vol. 12, pp. 1114–1117, 2013.

[46] A. Abbas, N. Hussain, M.-J. Jeong, J. Park, K. S. Shin, T. Kim, and N. Kim, "A rectangular notch-band uwb antenna with controllable notched bandwidth and centre frequency," *Sensors*, vol. 20, no. 3, p. 777, 2020.

[47] Y. Cai, Y. J. Guo, and T. Bird, "A frequency reconfigurable printed yagi-uda dipole antenna for cognitive radio applications," *IEEE Transactions on Antennas and Propagation*, vol. 60, no. 6, pp. 2905–2912, 2012.

[48] D. Rodrigo, J. Romeu, and L. Jofre, "Interference rejection using frequency and pattern reconfigurable antennas," in *Proceedings of the 2012 IEEE International Symposium on Antennas and Propagation*. IEEE, 2012, pp. 1–2.

[49] L. Ge and K.-M. Luk, "Frequency-reconfigurable low-profile circular monopolar patch antenna," *IEEE Transactions on Antennas and Propagation*, vol. 62, no. 7, pp. 3443–3449, 2014.

[50] C. Sun, H. Zheng, L. Zhang, and Y. Liu, "A compact frequency-reconfigurable patch antenna for beidou (compass) navigation system," *IEEE Antennas and Wireless Propagation Letters*, vol. 13, pp. 967–970, 2014.

[51] N. Behdad and K. Sarabandi, "A varactor-tuned dual-band slot antenna," *IEEE Transactions on Antennas and Propagation*, vol. 54, no. 2, pp. 401–408, 2006.

[52] B. A. Cetiner, G. R. Crusats, L. Jofre, and N. Biyikli, "Rf mems integrated frequency reconfigurable annular slot antenna," *IEEE Transactions on Antennas and Propagation*, vol. 58, no. 3, pp. 626–632, 2009.

[53] C.-Y. Chiu, J. Li, S. Song, and R. D. Murch, "Frequency-reconfigurable pixel slot antenna," *IEEE Transactions on Antennas and Propagation*, vol. 60, no. 10, pp. 4921–4924, 2012.

[54] G. Xu, H.-L. Peng, C. Sun, J.-G. Lu, Y. Zhang, and W.-Y. Yin, "Differential probe fed liquid crystal-based frequency tunable circular ring patch antenna," *IEEE Access*, vol. 6, pp. 3051–3058, 2017.

[55] L. Liu and R. Langley, "Liquid crystal tunable microstrip patch antenna," *Electronics Letters*, vol. 44, no. 20, pp. 1179–1180, 2008.

[56] S. A. Aghdam, "A novel uwb monopole antenna with tunable notched behavior using varactor diode," *IEEE Antennas and Wireless Propagation Letters*, vol. 13, pp. 1243–1246, 2014.

[57] A. K. Horestani, Z. Shaterian, J. Naqui, F. Martín, and C. Fumeaux, "Reconfigurable and tunable s-shaped split-ring resonators and application in band-notched uwb antennas," *IEEE Transactions on Antennas and Propagation*, vol. 64, no. 9, pp. 3766–3776, 2016.

[58] M. U. Memon and S. Lim, "Frequency-tunable compact antenna using quarter-mode substrate integrated waveguide," *IEEE Antennas and Wireless Propagation Letters*, vol. 14, pp. 1606–1609, 2015.

[59] S. Somarith, K. Hyunseong, and L. Sungjoon, "Frequency reconfigurable and miniaturized substrate integrated waveguide interdigital capacitor (siw-idc) antenna," *IEEE Transactions on Antennas and Propagation*, vol. 62, no. 3, pp. 1039–1045, 2013.

[60] W. A. Awan, N. Hussain, S. A. Naqvi, A. Iqbal, R. Striker, D. Mitra, and B. D. Braaten, "A miniaturized wideband and multi-band on-demand reconfigurable antenna for compact and portable devices," *AEU-International Journal of Electronics and Communications*, p. 153266, 2020.

[61] W. Lin, S.-L. Chen, R. W. Ziolkowski, and Y. J. Guo, "Reconfigurable, wideband, low-profile, circularly polarized antenna and array enabled by an artificial magnetic conductor ground," *IEEE Transactions on Antennas and Propagation*, vol. 66, no. 3, pp. 1564–1569, 2018.

[62] Y.-M. Cai, S. Gao, Y. Yin, W. Li, and Q. Luo, "Compact-size low-profile wideband circularly polarized omnidirectional patch antenna with reconfigurable polarizations," *IEEE Transactions on Antennas and Propagation*, vol. 64, no. 5, 2016.

[63] B. Wu, M. Okoniewski, and C. Hayden, "A pneumatically controlled reconfigurable antenna with three states of polarization," *IEEE Transactions on Antennas and Propagation*, vol. 62, no. 11, pp. 5474–5484, 2014.

[64] H. Zhu, S. Cheung, X. Liu, and T. Yuk, "Design of polarization reconfigurable antenna using metasurface," *IEEE Transactions on Antennas and Propagation*, vol. 62, no. 6, pp. 2891–2898, 2014.

[65] F. Wu and K. M. Luk, "Wideband tri-polarization reconfigurable magneto-electric dipole antenna," *IEEE Transactions on Antennas and Propagation*, vol. 65, no. 4, pp. 1633–1641, 2017.

[66] K. X. Wang and H. Wong, "A reconfigurable cp/lp antenna with cross-probe feed," *IEEE Antennas and Wireless Propagation Letters*, vol. 16, pp. 669–672, 2016.

[67] Y. Kim, N.-G. Kim, J.-M. Kim, S. H. Lee, Y. Kwon, and Y.-K. Kim, "60-ghz full mems antenna platform mechanically driven by magnetic actuator," *IEEE Transactions on Industrial Electronics*, vol. 58, no. 10, pp. 4830–4836, 2011.

[68] D. R. López, "Reconfigurable pixel antennas for communications," Ph.D. dissertation, Universitat Politècnica de Catalunya (UPC), 2013.

[69] Y.-Y. Bai, S. Xiao, C. Liu, X. Shuai, and B.-Z. Wang, "Design of pattern reconfigurable antennas based on a two—element dipole array model," *IEEE Transactions on Antennas and Propagation*, vol. 61, no. 9, pp. 4867–4871, 2013.

[70] P.-Y. Qin, Y. J. Guo, and C. Ding, "A beam switching quasi-yagi dipole antenna," *IEEE Transactions on Antennas and Propagation*, vol. 61, no. 10, pp. 4891–4899, 2013.

[71] S. S. Nair and M. J. Ammann, "Reconfigurable antenna with elevation and azimuth beam switching," *IEEE Antennas and Wireless Propagation Letters*, vol. 9, pp. 367–370, 2010.

[72] P.-Y. Qin, Y. J. Guo, A. R. Weily, and C.-H. Liang, "A pattern reconfigurable u-slot antenna and its applications in mimo systems," *IEEE Transactions on Antennas and Propagation*, vol. 60, no. 2, pp. 516–528, 2011.

[73] S.-J. Ha and C. W. Jung, "Reconfigurable beam steering using a microstrip patch antenna with a u-slot for wearable fabric applications," *IEEE Antennas and Wireless Propagation Letters*, vol. 10, pp. 1228–1231, 2011.

[74] M. Jusoh, T. Sabapathy, M. F. Jamlos, and M. R. Kamarudin, "Reconfigurable four-parasitic-elements patch antenna for high-gain beam switching application," *IEEE Antennas and Wireless Propagation Letters*, vol. 13, pp. 79–82, 2014.

[75] M. H. Nemati, R. Kazemi, and I. Tekin, "Pattern reconfigurable patch array for 2.4 ghz wlan systems," *Microwave and Optical Technology Letters*, vol. 56, no. 10, pp. 2377–2381, 2014.

[76] M. Nor, S. Rahim, M. I. Sabran, P. J. Soh, and G. Vandenbosch, "Dual-band, switched-beam, reconfigurable antenna for wlan applications," *IEEE Antennas and Wireless Propagation Letters*, vol. 12, pp. 1500–1503, 2013.

[77] S. Lim and H. Ling, "Design of electrically small, pattern reconfigurable yagi antenna," *Electronics Letters*, vol. 43, no. 24, pp. 1326–1327, 2007.

[78] C. Kittiyanpunya and M. Krairiksh, "A four-beam pattern reconfigurable yagi-uda antenna," *IEEE Transactions on Antennas and Propagation*, vol. 61, no. 12, pp. 6210–6214, 2013.

[79] I. Lim and S. Lim, "Monopole-like and boresight pattern reconfigurable antenna," *IEEE Transactions on Antennas and Propagation*, vol. 61, no. 12, pp. 5854–5859, 2013.

[80] C. won Jung, M.-j. Lee, G. Li, and F. De Flaviis, "Reconfigurable scan-beam single-arm spiral antenna integrated with rf-mems switches," *IEEE Transactions on Antennas and Propagation*, vol. 54, no. 2, pp. 455–463, 2006.

[81] R. Guzmán-Quirós, J. L. Gómez-Tornero, A. R. Weily, and Y. J. Guo, "Electronically steerable 1-d fabry-perot leaky-wave antenna employing a tunable high impedance surface," *IEEE Transactions on Antennas and Propagation*, vol. 60, no. 11, pp. 5046–5055, 2012.

[82] R. O. Ouedraogo, E. J. Rothwell, and B. J. Greetis, "A reconfigurable microstrip leaky-wave antenna with a broadly steerable beam," *IEEE Transactions on Antennas and Propagation*, vol. 59, no. 8, pp. 3080–3083, 2011.

[83] E. Ojefors, S. Cheng, K. From, I. Skarin, P. Hallbjorner, and A. Rydberg, "Electrically steerable single-layer microstrip traveling wave antenna with varactor diode based phase shifters," *IEEE Transactions on Antennas and Propagation*, vol. 55, no. 9, pp. 2451–2460, 2007.

[84] D. K. Karmokar, K. P. Esselle, and S. G. Hay, "Fixed-frequency beam steering of microstrip leaky-wave antennas using binary switches," *IEEE Transactions on Antennas and Propagation*, vol. 64, no. 6, pp. 2146–2154, 2016.

[85] Z.-L. Lu, X.-X. Yang, and G.-N. Tan, "A wideband printed tapered-slot antenna with pattern reconfigurability," *IEEE Antennas and Wireless Propagation Letters*, vol. 13, pp. 1613–1616, 2014.

[86] N. Nguyen-Trong, L. Hall, and C. Fumeaux, "A dual-band dual-pattern frequency-reconfigurable antenna," *Microwave and Optical Technology Letters*, vol. 59, no. 11, pp. 2710–2715, 2017.

[87] S. N. M. Zainarry, N. Nguyen-Trong, and C. Fumeaux, "A frequency-and pattern-reconfigurable two-element array antenna," *IEEE Antennas and Wireless Propagation Letters*, vol. 17, no. 4, pp. 617–620, 2018.

[88] P. K. Li, Z. H. Shao, Q. Wang, and Y. J. Cheng, "Frequency-and pattern-reconfigurable antenna for multistandard wireless applications," *IEEE Antennas and Wireless Propagation Letters*, vol. 14, pp. 333–336, 2014.

[89] N. K. Sahu and A. K. Sharma, "An investigation of pattern and frequency reconfigurable microstrip slot antenna using pin diodes," in *2017 Progress In Electromagnetics Research Symposium-Spring (PIERS)*. IEEE, 2017, pp. 971–976.

[90] L. Han, C. Wang, W. Zhang, R. Ma, and Q. Zeng, "Design of frequency-and pattern-reconfigurable wideband slot antenna," *International Journal of Antennas and Propagation*, vol. 2018, 2018.

[91] H. A. Majid, M. K. A. Rahim, M. R. Hamid, and M. F. Ismail, "Frequency and pattern reconfigurable slot antenna," *IEEE Transactions on Antennas and Propagation*, vol. 62, no. 10, pp. 5339–5343, 2014.

[92] M. Ye and P. Gao, "Back-to-back f semicircular antenna with frequency and pattern reconfigurability," *Electronics Letters*, vol. 51, no. 25, pp. 2073–2074, 2015.

[93] B. Liang, B. Sanz-Izquierdo, E. A. Parker, and J. C. Batchelor, "A frequency and polarization reconfigurable circularly polarized antenna using active ebg structure for satellite navigation," *IEEE Transactions on Antennas and Propagation*, vol. 63, no. 1, pp. 33–40, 2014.

[94] G. Yi, C. Huang, X. Ma, W. Pan, and X. Luo, "A low profile polarization reconfigurable dipole antenna using tunable electromagnetic band-gap surface," *Microwave and Optical Technology Letters*, vol. 56, no. 6, pp. 1281–1285, 2014.

[95] C. Ni, M. S. Chen, Z. X. Zhang, and X. L. Wu, "Design of frequency-and polarization-reconfigurable antenna based on the polarization conversion metasurface," *IEEE Antennas and Wireless Propagation Letters*, vol. 17, no. 1, pp. 78–81, 2017.

[96] N. Nguyen-Trong, L. Hall, and C. Fumeaux, "A frequency-and polarization-reconfigurable stub-loaded microstrip patch antenna," *IEEE Transactions on Antennas and Propagation*, vol. 63, no. 11, pp. 5235–5240, 2015.

[97] J. Liu, J. Li, and R. Xu, "Design of very simple frequency and polarisation reconfigurable antenna with finite ground structure," *Electronics Letters*, vol. 54, no. 4, pp. 187–188, 2018.

[98] M. A. Rahman, E. Nishiyama, and I. Toyoda, "A frequency diversity reconfigurable antenna with circular polarization switching capability," in *2017 IEEE International Symposium on Antennas and Propagation & USNC/URSI National Radio Science Meeting*. IEEE, 2017, pp. 1367–1368.

[99] M. S. Kumar and Y. K. Choukiker, "Frequency and polarization reconfigurable antenna using blc feed network," in *2017 IEEE International Conference on Antenna Innovations & Modern Technologies for Ground, Aircraft and Satellite Applications (iAIM)*. IEEE, 2017, pp. 1–4.

[100] A. Narbudowicz, X. Bao, and M. J. Ammann, "Omnidirectional microstrip patch antenna with reconfigurable pattern and polarisation," *IET Microwaves, Antennas & Propagation*, vol. 8, no. 11, pp. 872–877, 2014.

[101] C. Gu, S. Gao, H. Liu, Q. Luo, T.-H. Loh, M. Sobhy, J. Li, G. Wei, J. Xu, F. Qin *et al.*, "Compact smart antenna with electronic beam-switching and reconfigurable polarizations," *IEEE Transactions on Antennas and Propagation*, vol. 63, no. 12, pp. 5325–5333, 2015.

[102] K. Yang, A. Loutridis, X. Bao, G. Ruvio, and M. Ammann, "Printed inverted-f antenna with reconfigurable pattern and polarization," in *2016 10th European Conference on Antennas and Propagation (EuCAP)*. IEEE, 2016, pp. 1–5.

[103] W. Lin, H. Wong, and R. W. Ziolkowski, "Circularly polarized antenna with reconfigurable broadside and conical beams facilitated by a mode switchable feed network," *IEEE Transactions on Antennas and Propagation*, vol. 66, no. 2, pp. 996–1001, 2017.

[104] A. Chen, X. Ning, L. Wang, and Z. Zhang, "A design of radiation pattern and polarization reconfigurable antenna using metasurface," in *2017 IEEE Asia Pacific Microwave Conference (APMC)*. IEEE, 2017, pp. 108–111.

[105] X. Yi, L. Huitema, and H. Wong, "Polarization and pattern reconfigurable cuboid quadrifilar helical antenna," *IEEE Transactions on Antennas and Propagation*, vol. 66, no. 6, pp. 2707–2715, 2018.

[106] N. Nguyen-Trong, A. T. Mobashsher, and A. M. Abbosh, "Reconfigurable shorted patch antenna with polarization and pattern diversity," in *2018 Australian Microwave Symposium (AMS)*. IEEE, 2018, pp. 27–28.

[107] D. Rodrigo, B. A. Cetiner *et al.*, "Frequency, radiation pattern and polarization reconfigurable antenna using a parasitic pixel layer," *IEEE Transactions on Antennas and Propagation*, vol. 62, no. 6, pp. 3422–3427, 2014.

[108] Y. P. Selvam, L. Elumalai, M. G. N. Alsath, M. Kanagasabai, S. Subbaraj, and S. Kingsly, "Novel frequency-and pattern-reconfigurable rhombic patch antenna with switchable polarization," *IEEE Antennas and Wireless Propagation Letters*, vol. 16, pp. 1639–1642, 2017.

[109] L. Ge, Y. Li, J. Wang *et al.*, "A low-profile reconfigurable cavity-backed slot antenna with frequency, polarization, and radiation pattern agility," *IEEE Transactions on Antennas and Propagation*, vol. 65, no. 5, pp. 2182–2189, 2017.

[110] M. Hamid, P. Gardner, P. S. Hall, and F. Ghanem, "Vivaldi antenna with integrated switchable band pass resonator," *IEEE Transactions on Antennas and Propagation*, vol. 59, no. 11, pp. 4008–4015, 2011.

[111] N. Nguyen-Trong and C. Fumeaux, "Reconfigurable half-mode substrate-integrated cavity antenna arrays," in *12th European Conference on Antennas and Propagation (EuCAP 2018)*, 2018.

[112] E. J. Rodrigues, H. W. Lins, and A. G. D'Assunção, "Reconfigurable circular ring patch antenna for uwb and cognitive radio applications," in *The 8th European Conference on Antennas and Propagation (EuCAP 2014)*. IEEE, 2014, pp. 2744–2748.

[113] W. Y. Sam and Z. b. Zakaria, "Design of reconfigurable integrated substrate integrated waveguide (siw) filter and antenna using multilayer approach," *International Journal of RF and Microwave Computer-Aided Engineering*, vol. 28, no. 9, p. e21561, 2018.

[114] K. Yan, P. Yang, F. Yang, X. Wang, and J. Wang, "Multi-band antenna design for full metal casing mobile handset," in *2017 Sixth Asia-Pacific Conference on Antennas and Propagation (APCAP)*. IEEE, 2017, pp. 1–3.

[115] I. Serhsouh, M. Himdi, H. Lebbar, and H. Vettikalladi, "Reconfigurable siw antenna for fixed frequency beam scanning and 5g applications," *IEEE Access*, vol. 8, pp. 60 084–60 089, 2020.

[116] G.-P. Gao, B. Hu, and J.-S. Zhang, "Design of a miniaturization printed circular-slot uwb antenna by the half-cutting method," *IEEE Antennas and Wireless Propagation Letters*, vol. 12, pp. 567–570, 2013.

[117] R. J. Fontana, "Recent system applications of short-pulse ultra-wideband (uwb) technology," *IEEE Transactions on Microwave Theory and Techniques*, vol. 52, no. 9, pp. 2087–2104, 2004.

[118] F. Fereidoony, S. Chamaani, and S. A. Mirtaheri, "Uwb monopole antenna with stable radiation pattern and low transient distortion," *IEEE Antennas and Wireless Propagation Letters*, vol. 10, pp. 302–305, 2011.

[119] K. G. Thomas and M. Sreenivasan, "A simple ultrawideband planar rectangular printed antenna with band dispensation," *IEEE Transactions on Antennas and Propagation*, vol. 58, no. 1, pp. 27–34, 2009.

[120] M. G. N. Alsath and M. Kanagasabai, "Compact uwb monopole antenna for automotive communications," *IEEE Transactions on Antennas and Propagation*, vol. 63, no. 9, pp. 4204–4208, 2015.

[121] T. Li, H. Zhai, L. Li, C. Liang, and Y. Han, "Compact uwb antenna with tunable band-notched characteristic based on microstrip open-loop resonator," *IEEE Antennas and Wireless Propagation Letters*, vol. 11, pp. 1584–1587, 2012.

[122] D. E. Anagnostou, M. T. Chryssomallis, B. D. Braaten, J. L. Ebel, and N. Sepúlveda, "Reconfigurable uwb antenna with rf-mems for on-demand wlan rejection," *IEEE Transactions on Antennas and Propagation*, vol. 62, no. 2, pp. 602–608, 2013.

[123] S. Nikolaou, N. D. Kingsley, G. E. Ponchak, J. Papapolymerou, and M. M. Tentzeris, "Uwb elliptical monopoles with a reconfigurable band notch using mems switches actuated without bias lines," *IEEE Transactions on Antennas and Propagation*, vol. 57, no. 8, pp. 2242–2251, 2009.

[124] P. Kim and Y. Jeong, "A coupled line impedance transformer for high termination impedance with a bandpass filtering response," *Journal of Electromagnetic Engineering and Science*, vol. 18, no. 1, pp. 41–45, 2018.

[125] T. L. Wu, Y. M. Pan, P. F. Hu, and S. Y. Zheng, "Design of a low profile and compact omnidirectional filtering patch antenna," *IEEE Access*, vol. 5, pp. 1083–1089, 2017.

[126] K. S. Ryu and A. A. Kishk, "Uwb antenna with single or dual band-notches for lower wlan band and upper wlan band," *IEEE Transactions on Antennas and Propagation*, vol. 57, no. 12, pp. 3942–3950, 2009.

[127] M. Roozbahani, A. Kalteh, and R. Fallahi, "A novel uwb elliptical slot antenna with band notch characteristics," *Progress in Electromagnetics Research, PIER*, vol. 82, pp. 127–136, 2008.

[128] W. Choi, K. Chung, J. Jung, and J. Choi, "Compact ultra-wideband printed antenna with band-rejection characteristic," *Electronics Letters*, vol. 41, no. 18, pp. 990–991, 2005.

[129] J.-W. Jang and H.-Y. Hwang, "An improved band-rejection uwb antenna with resonant patches and a slot," *IEEE Antennas and Wireless Propagation Letters*, vol. 8, pp. 299–302, 2009.

[130] C. R. Medeiros, J. R. Costa, and C. A. Fernandes, "Compact tapered slot uwb antenna with wlan band rejection," *IEEE Antennas and Wireless Propagation Letters*, vol. 8, pp. 661–664, 2009.

[131] J. Kim, C. Cho, and J. Lee, "5.2 ghz notched ultra-wideband antenna using slot-type srr," *Electronics Letters*, vol. 42, no. 6, pp. 315–316, 2006.

[132] K. Bahadori and Y. Rahmat-Samii, "A miniaturized elliptic-card uwb antenna with wlan band rejection for wireless communications," *IEEE Transactions on Antennas and Propagation*, vol. 55, no. 11, pp. 3326–3332, 2007.

[133] F. Zhu, S. Gao, A. T. Ho, R. A. Abd-Alhameed, C. H. See, T. W. Brown, J. Li, G. Wei, and J. Xu, "Multiple band-notched uwb antenna with band-rejected elements integrated in the feed line," *IEEE Transactions on Antennas and Propagation*, vol. 61, no. 8, pp. 3952–3960, 2013.

[134] K.-H. Kim, Y.-J. Cho, S.-H. Hwang, and S.-O. Park, "Band-notched uwb planar monopole antenna with two parasitic patches," *Electronics Letters*, vol. 41, no. 14, pp. 783–785, 2005.

[135] L. Peng and C.-L. Ruan, "Uwb band-notched monopole antenna design using electromagnetic-bandgap structures," *IEEE Transactions on Microwave Theory and Techniques*, vol. 59, no. 4, pp. 1074–1081, 2011.

[136] W. Liu and Y.-Z. Yin, "Dual band-notched antenna with the parasitic strip for uwb," *Progress In Electromagnetics Research*, vol. 25, pp. 21–30, 2011.

[137] M. S. Alam and A. Abbosh, "Reconfigurable band-rejection antenna for ultra-wideband applications," *IET Microwaves, Antennas & Propagation*, vol. 12, no. 2, pp. 195–202, 2017.

[138] S. Lakrit, S. Das, A. El Alami, D. Barad, and S. Mohapatra, "A compact uwb monopole patch antenna with reconfigurable band-notched characteristics for wi-max and wlan applications," *AEU-International Journal of Electronics and Communications*, vol. 105, pp. 106–115, 2019.

[139] A. H. Nazeri, A. Falahati, and R. Edwards, "A novel compact fractal uwb antenna with triple reconfigurable notch reject bands applications," *AEU-International Journal of Electronics and Communications*, vol. 101, pp. 1–8, 2019.

[140] V. G. Veselago, "The electrodynamics of substances with simultaneously negative values of img align= absmiddle alt= ϵ eps/img and μ," *Physics-Uspekhi*, vol. 10, no. 4, pp. 509–514, 1968.

[141] H. Zhu, K. L. Chung, X. Sun, S. Cheung, and T. I. Yuk, "Cp metasurfaced antennas excited by lp sources," in *Proceedings of the 2012 IEEE International Symposium on Antennas and Propagation*. IEEE, 2012, pp. 1–2.

[142] X. Chen and Y. Zhao, "Dual-band polarization and frequency reconfigurable antenna using double layer metasurface," *AEU-International Journal of Electronics and Communications*, vol. 95, pp. 82–87, 2018.

[143] J. Hu, G. Q. Luo, and Z.-C. Hao, "A wideband quad-polarization reconfigurable metasurface antenna," *IEEE Access*, vol. 6, pp. 6130–6137, 2017.

[144] S. Chaimool, T. Hongnara, C. Rakluea, P. Akkaraekthalin, and Y. Zhao, "Design of a pin diode-based reconfigurable metasurface antenna for beam switching applications," *International Journal of Antennas and Propagation*, vol. 2019, 2019.

[145] A. Ahmad, F. Arshad, S. I. Naqvi, Y. Amin, H. Tenhunen, and J. Loo, "Flexible and compact spiral-shaped frequency reconfigurable antenna for wireless applications," *IETE Journal of Research*, vol. 66, no. 1, pp. 22–29, 2020.

[146] M. U. HASSAN, F. Arshad, S. I. Naqvi, Y. Amin, and H. Tenhunen, "A compact flexible and frequency reconfigurable antenna for quintuple applications." *Radioengineering*, vol. 26, no. 3, 2017.

[147] S. M. Saeed, C. A. Balanis, and C. R. Birtcher, "Inkjet-printed flexible reconfigurable antenna for conformal wlan/wimax wireless devices," *IEEE Antennas and Wireless Propagation Letters*, vol. 15, pp. 1979–1982, 2016.

[148] K. Saraswat and A. R. Harish, "Flexible dual-band dual-polarised cpw-fed monopole antenna with discrete-frequency reconfigurability," *IET Microwaves, Antennas & Propagation*, vol. 13, no. 12, pp. 2053–2060, 2019.

[149] S. M. Saeed, C. A. Balanis, C. R. Birtcher, A. C. Durgun, and H. N. Shaman, "Wearable flexible reconfigurable antenna integrated with artificial magnetic conductor," *IEEE Antennas and Wireless Propagation Letters*, vol. 16, pp. 2396–2399, 2017.

[150] R. B. Simorangkir, Y. Yang, K. P. Esselle, and B. A. Zeb, "A method to realize robust flexible electronically tunable antennas using polymer-embedded conductive fabric," *IEEE Transactions on Antennas and Propagation*, vol. 66, no. 1, pp. 50–58, 2017.

[151] H. F. Abutarboush and A. Shamim, "A reconfigurable inkjet-printed antenna on paper substrate for wireless applications," *IEEE Antennas and Wireless Propagation Letters*, vol. 17, no. 9, pp. 1648–1651, 2018.

[152] E. A. Kadir, "A reconfigurable mimo antenna system for wireless communications," in *2017 4th International Conference on Electrical Engineering, Computer Science and Informatics (EECSI)*. IEEE, 2017, pp. 1–4.

[153] A. Kantemur, J. Tak, P. Siyari, A. H. Abdelrahman, M. Krunz, and H. Xin, "A novel compact reconfigurable broadband antenna for cognitive radio applications," *IEEE Transactions on Antennas and Propagation*, 2020.

[154] E. Al Abbas, A. T. Mobashsher, and A. Abbosh, "Polarization reconfigurable antenna for 5g cellular networks operating at millimeter waves," in *2017 IEEE Asia Pacific Microwave Conference (APMC)*. IEEE, 2017, pp. 772–774.

[155] A. Ghaffar, X. J. Li, and B.-C. Seet, "Compact dual-band broadband microstrip antenna at 2.4 ghz and 5.2 ghz for wlan applications," in *2018 IEEE Asia-Pacific Conference on Antennas and Propagation (APCAP)*. IEEE, 2018, pp. 198–199.

[156] H. F. AbuTarboush, R. Nilavalan, and T. Peter, "Pifa based reconfigurable multiband antenna for wireless applications," in *2010 International Conference on Electromagnetics in Advanced Applications*. IEEE, 2010, pp. 232–235.

[157] J.-H. Lim, G.-T. Back, Y.-I. Ko, C.-W. Song, and T.-Y. Yun, "A reconfigurable pifa using a switchable pin-diode and a fine-tuning varactor for uspcs/wcdma/wimax/wlan," *IEEE Transactions on Antennas and Propagation*, vol. 58, no. 7, pp. 2404–2411, 2010.

[158] Y. Li, Z. Zhang, J. Zheng, Z. Feng, and M. F. Iskander, "A compact hepta-band loop-inverted f reconfigurable antenna for mobile phone," *IEEE Transactions on Antennas and Propagation*, vol. 60, no. 1, pp. 389–392, 2011.

[159] H. A. Majid, M. K. A. Rahim, M. R. Hamid, and M. Ismail, "A compact frequency-reconfigurable narrowband microstrip slot antenna," *IEEE Antennas and Wireless Propagation Letters*, vol. 11, pp. 616–619, 2012.

[160] M. Choi, H. Wi, B. Mun, Y. Yoon, H. Lee, and B. Lee, "A compact frequency reconfigurable antenna for lte mobile handset applications," *International Journal of Antennas and Propagation*, vol. 2015, 2015.

[161] S. Lee, H. Jung, and Y. Sung, "A reconfigurable antenna for lte/wwan mobile handset applications," *IEEE Antennas and Wireless Propagation Letters*, vol. 14, pp. 48–51, 2014.

[162] X. Liu, X. Yang, and F. Kong, "A frequency-reconfigurable monopole antenna with switchable stubbed ground structure," *Radioengineering*, vol. 24, no. 2, pp. 449–454, 2015.

[163] P. K. Li, Z. H. Shao, Q. Wang, and Y. J. Cheng, "Frequency-and pattern-reconfigurable antenna for multistandard wireless applications," *IEEE Antennas and Wireless Propagation Letters*, vol. 14, pp. 333–336, 2014.

[164] Y. Xu, Y.-W. Liang, and H.-M. Zhou, "Small-size reconfigurable antenna for wwan/lte/gnss smartphone applications," *IET Microwaves, Antennas & Propagation*, vol. 11, no. 6, pp. 923–928, 2017.

[165] X. Zhang, M. Tian, A. Zhan, Z. Liu, and H. Liu, "A frequency reconfigurable antenna for multiband mobile handset applications," *International Journal of RF and Microwave Computer-Aided Engineering*, vol. 27, no. 9, p. e21143, 2017.

[166] P. T. Minh, N. T. Duc, P. X. Vu, N. T. Chuyen, and V. Van Yem, "Low profile frequency reconfigurable pifa antenna using defected ground structure," *REV Journal on Electronics and Communications*, vol. 7, no. 1-2, 2017.

[167] Y. I. Abdulraheem, G. A. Oguntala, A. S. Abdullah, H. J. Mohammed, R. A. Ali, R. A. Abd-Alhameed, and J. M. Noras, "Design of frequency reconfigurable multiband compact antenna using two pin diodes for wlan/wimax applications," *IET Microwaves, Antennas & Propagation*, vol. 11, no. 8, pp. 1098–1105, 2017.

[168] M. A. Madi, M. Al-Husseini, and M. Y. Mervat, "Frequency tunable cedar-shaped antenna for wifi and wimax," *Progress In Electromagnetics Research*, vol. 72, pp. 135–143, 2018.

[169] P. Wang, Y. Shao, D. Huang, and M. A. Basit, "A compact coupled-fed loop antenna for mobile lte smartphones," *International Journal of Antennas and Propagation*, vol. 2018, 2018.

[170] F. A. Asadallah, J. Costantine, and Y. Tawk, "A multiband compact reconfigurable pifa based on nested slots," *IEEE antennas and wireless propagation letters*, vol. 17, no. 2, pp. 331–334, 2018.

[171] H. I. Azeez, H.-C. Yang, and W.-S. Chen, "Wearable triband e-shaped dipole antenna with low sar for iot applications," *Electronics*, vol. 8, no. 6, p. 665, 2019.

[172] T. Khan, M. Rahman, A. Akram, Y. Amin, and H. Tenhunen, "A low-cost cpw-fed multiband frequency reconfigurable antenna for wireless applications," *Electronics*, vol. 8, no. 8, p. 900, 2019.

[173] K.-C. Lin, C.-H. Lin, and Y.-C. Lin, "Simple printed multiband antenna with novel parasitic-element design for multistandard mobile phone applications," *IEEE Transactions on Antennas and Propagation*, vol. 61, no. 1, pp. 488–491, 2012.

[174] C.-T. Lee and K.-L. Wong, "Planar monopole with a coupling feed and an inductive shorting strip for lte/gsm/umts operation in the mobile phone," *IEEE Transactions on Antennas and Propagation*, vol. 58, no. 7, pp. 2479–2483, 2010.

[175] J.-H. Lu and Y.-S. Wang, "Internal uniplanar antenna for lte/gsm/umts operation in a tablet computer," *IEEE Transactions on Antennas and Propagation*, vol. 61, no. 5, pp. 2841–2846, 2013.

[176] K.-L. Wong and M.-T. Chen, "Small-size lte/wwan printed loop antenna with an inductively coupled branch strip for bandwidth enhancement in the tablet computer," *IEEE Transactions on Antennas and Propagation*, vol. 61, no. 12, pp. 6144–6151, 2013.

[177] K.-L. Wong and T.-W. Weng, "Small-size triple-wideband lte/wwan tablet device antenna," *IEEE Antennas and Wireless Propagation Letters*, vol. 12, pp. 1516–1519, 2013.

[178] J.-H. Lu and J.-L. Guo, "Small-size octaband monopole antenna in an lte/wwan mobile phone," *IEEE Antennas and Wireless Propagation Letters*, vol. 13, pp. 548–551, 2014.

[179] D.-A. Lee and Y. Sung, "Reconfigurable pifa/loop antenna for mobile handset applications," *Microwave and Optical Technology Letters*, vol. 56, no. 9, pp. 2034–2037, 2014.

[180] J. H. Lee and Y. Sung, "Reconfigurable hexa-band planar inverted-f antenna using a pin diode for mobile handset," *Microwave and Optical Technology Letters*, vol. 55, no. 8, pp. 1926–1928, 2013.

[181] Y. Sung, "A frequency-reconfigurable antenna for internal mobile handset applications," *Microwave and Optical Technology Letters*, vol. 56, no. 6, pp. 1366–1371, 2014.

[182] S. C. Del Barrio, M. Pelosi, G. F. Pedersen, and A. Morris, "Challenges for frequency-reconfigurable antennas in small terminals," in *2012 IEEE Vehicular Technology Conference (VTC Fall)*. IEEE, 2012, pp. 1–5.

[183] S. Padmanathan, A. A. Al-Hadi, P. J. Soh, and M. F. Jamlos, "Reconfigurable antennas for mimo applications: An overview," in *2015 IEEE Student Conference on Research and Development (SCOReD)*. IEEE, 2015, pp. 193–197.

[184] P. Chakrapani and S. Raghavan, "Reconfigurable antenna for wireless communication bands," in *2015 2nd International Conference on Electronics and Communication Systems (Icecs)*. IEEE, 2015, pp. 364–367.

[185] A. C. Mak, C. R. Rowell, R. D. Murch, and C.-L. Mak, "Reconfigurable multiband antenna designs for wireless communication devices," *IEEE Transactions on Antennas and Propagation*, vol. 55, no. 7, pp. 1919–1928, 2007.

[186] Y. Park and Y. Sung, "A reconfigurable antenna for quad-band mobile handset applications," *IEEE Transactions on Antennas and Propagation*, vol. 60, no. 6, pp. 3003–3006, 2012.

[187] S. Yang, C. Zhang, H. K. Pan, A. E. Fathy, and V. K. Nair, "Frequency-reconfigurable antennas for multiradio wireless platforms," *IEEE Microwave Magazine*, vol. 10, no. 1, pp. 66–83, 2009.

[188] H.-R. Chuang and L.-C. Kuo, "3-d fdtd design analysis of a 2.4-ghz polarization-diversity printed dipole antenna with integrated balun and polarization-switching circuit for wlan and wireless communication applications," *IEEE Transactions on Microwave Theory and Techniques*, vol. 51, no. 2, pp. 374–381, 2003.

[189] M. Agiwal, A. Roy, and N. Saxena, "Next generation 5g wireless networks: A comprehensive survey," *IEEE Communications Surveys & Tutorials*, vol. 18, no. 3, pp. 1617–1655, 2016.

[190] A. Ghaffar, X. J. Li, W. A. Awan, and N. Hussain, "A compact dual-band antenna based on defected ground structure for ism band applications," in *WSA 2020; 24th International ITG Workshop on Smart Antennas*. VDE, 2020, pp. 1–2.

[191] T. Ali, N. Fatima, and R. C. Biradar, "A miniaturized multiband reconfigurable fractal slot antenna for gps/gnss/bluetooth/wimax/x-band applications," *AEU-International Journal of Electronics and Communications*, vol. 94, pp. 234–243, 2018.

[192] A. J. Alazemi, B. Avser, and G. M. Rebeiz, "Low-profile tunable multi-band lte antennas with series and shunt tuning devices," *AEU-International Journal of Electronics and Communications*, vol. 110, p. 152855, 2019.

[193] M. Borhani, P. Rezaei, and A. Valizade, "Design of a reconfigurable miniaturized microstrip antenna for switchable multiband systems," *IEEE Antennas and Wireless Propagation Letters*, vol. 15, pp. 822–825, 2015.

[194] A. Ghaffar, X. J. Li, B.-C. Seet, W. A. Awan, and N. Hussain, "Compact multiband frequency reconfigurable antenna for 5g communications," in *2019 29th International Telecommunication Networks and Applications Conference (ITNAC)*. IEEE, 2019, pp. 1–3.

[195] W. Hong and K. Sarabandi, "Low-profile, multi-element, miniaturized monopole antenna," *IEEE Transactions on Antennas and Propagation*, vol. 57, no. 1, pp. 72–80, 2009.

[196] H. A. Majid, M. K. A. Rahim, M. R. Hamid, and M. Ismail, "A compact frequency-reconfigurable narrowband microstrip slot antenna," *IEEE Antennas and Wireless Propagation Letters*, vol. 11, pp. 616–619, 2012.

[197] L. Han, C. Wang, X. Chen, and W. Zhang, "Compact frequency-reconfigurable slot antenna for wireless applications," *IEEE Antennas and Wireless Propagation Letters*, vol. 15, pp. 1795–1798, 2016.

[198] A. Iqbal, A. Smida, L. F. Abdulrazak, O. A. Saraereh, N. K. Mallat, I. Elfergani, and S. Kim, "Low-profile frequency reconfigurable antenna for heterogeneous wireless systems," *Electronics*, vol. 8, no. 9, p. 976, 2019.

[199] S. Ullah, S. Hayat, A. Umar, U. Ali, F. A. Tahir, and J. A. Flint, "Design, fabrication and measurement of triple band frequency reconfigurable antennas for portable wireless communications," *AEU-International Journal of Electronics and Communications*, vol. 81, pp. 236–242, 2017.

[200] A. Iqbal and O. A. Saraereh, "A compact frequency reconfigurable monopole antenna for wi-fi/wlan applications," *Progress In Electromagnetics Research*, vol. 68, pp. 79–84, 2017.

[201] Y. I. Abdulraheem, G. A. Oguntala, A. S. Abdullah, H. J. Mohammed, R. A. Ali, R. A. Abd-Alhameed, and J. M. Noras, "Design of frequency reconfigurable multiband compact antenna using two pin diodes for wlan/wimax applications," *IET Microwaves, Antennas & Propagation*, vol. 11, no. 8, pp. 1098–1105, 2017.

[202] T. Khan, M. Rahman, A. Akram, Y. Amin, and H. Tenhunen, "A low-cost cpw-fed multiband frequency reconfigurable antenna for wireless applications," *Electronics*, vol. 8, no. 8, p. 900, 2019.

[203] M. A. Madi, M. Al-Husseini, and M. Y. Mervat, "Frequency tunable cedar-shaped antenna for wifi and wimax," *Progress In Electromagnetics Research*, vol. 72, pp. 135–143, 2018.

[204] I. Shah, S. Hayat, A. Basir, M. Zada, S. Shah, and S. Ullah, "Design and analysis of a hexa-band frequency reconfigurable antenna for wireless communication," *AEU-International Journal of Electronics and Communications*, vol. 98, pp. 80–88, 2019.

[205] W. A. Awan, N. Hussain, and T. T. Le, "Ultra-thin flexible fractal antenna for 2.45 ghz application with wideband harmonic rejection," *AEU-International Journal of Electronics and Communications*, vol. 110, p. 152851, 2019.

[206] N. Hussain, S. I. Naqvi, W. A. Awan, and T. T. Le, "A metasurface-based wideband bidirectional same-sense circularly polarized antenna," *International Journal of RF and Microwave Computer-Aided Engineering*, 2020.

[207] A. H. Nazeri, A. Falahati, and R. Edwards, "A novel compact fractal uwb antenna with triple reconfigurable notch reject bands applications," *AEU-International Journal of Electronics and Communications*, vol. 101, pp. 1–8, 2019.

[208] W. A. Awan, A. Zaidi, N. Hussain, A. Iqbal, and A. Baghdad, "Stub loaded, low profile uwb antenna with independently controllable notch-bands," *Microwave and Optical Technology Letters*, vol. 61, no. 11, pp. 2447–2454, 2019.

[209] A. J. Alazemi, B. Avser, and G. M. Rebeiz, "Low-profile tunable multi-band lte antennas with series and shunt tuning devices," *AEU-International Journal of Electronics and Communications*, vol. 110, p. 152855, 2019.

[210] C. A. Balanis, *Advanced Engineering Electromagnetics*. John Wiley & Sons, 2012.

[211] M. A. Matin, *Ultra Wideband Communications: Novel Trends-Antennas and Propagation*. BoD–Books on Demand, 2011.

[212] A. Affandi, R. Azim, M. M. Alam, and M. T. Islam, "A low-profile wideband antenna for wwan/lte applications," *Electronics*, vol. 9, no. 3, p. 393, 2020.

[213] A. Zaidi, W. A. Awan, N. Hussain, and A. Baghdad, "A wide and tri-band flexible antennas with independently controllable notch bands for sub-6-ghz communication system." *Radioengineering*, vol. 29, no. 1, 2020.

[214] G. Jin, C. Deng, J. Yang, Y. Xu, and S. Liao, "A new differentially-fed frequency reconfigurable antenna for wlan and sub-6ghz 5g applications," *IEEE Access*, vol. 7, pp. 56 539–56 546, 2019.

[215] Y.-M. Cai, K. Li, Y. Yin, S. Gao, W. Hu, and L. Zhao, "A low-profile frequency reconfigurable grid-slotted patch antenna," *IEEE Access*, vol. 6, pp. 36 305–36 312, 2018.

[216] G. Feng, C. Guo, and J. Ding, "Frequency-reconfigurable slot antenna using metasurface," in *2018 International Conference on Microwave and Millimeter Wave Technology (ICMMT)*. IEEE, 2018, pp. 1–3.

[217] X. Zhao and S. Riaz, "A dual-band frequency reconfigurable mimo patch-slot antenna based on reconfigurable microstrip feedline," *IEEE Access*, vol. 6, pp. 41 450–41 457, 2018.

[218] M. Soltanpour and M. Fakharian, "Compact filtering slot antenna with frequency agility for wi-fi/lte mobile applications," *Electronics Letters*, vol. 52, no. 7, pp. 491–492, 2016.

[219] L. Han, C. Wang, X. Chen, and W. Zhang, "Compact frequency-reconfigurable slot antenna for wireless applications," *IEEE Antennas and Wireless Propagation Letters*, vol. 15, pp. 1795–1798, 2016.

[220] T. Ali and R. C. Biradar, "A compact hexagonal slot dual band frequency reconfigurable antenna for wlan applications," *Microwave and Optical Technology Letters*, vol. 59, no. 4, pp. 958–964, 2017.

[221] Y. I. Abdulraheem, G. A. Oguntala, A. S. Abdullah, H. J. Mohammed, R. A. Ali, R. A. Abd-Alhameed, and J. M. Noras, "Design of frequency reconfigurable multiband compact antenna using two pin diodes for wlan/wimax applications," *IET Microwaves, Antennas & Propagation*, vol. 11, no. 8, pp. 1098–1105, 2017.

[222] T. Ali, M. M. Khaleeq, and R. C. Biradar, "A multiband reconfigurable slot antenna for wireless applications," *AEU-International Journal of Electronics and Communications*, vol. 84, pp. 273–280, 2018.

[223] K. Saraswat and A. R. Harish, "Flexible dual-band dual-polarised cpw-fed monopole antenna with discrete-frequency reconfigurability," *IET Microwaves, Antennas & Propagation*, vol. 13, no. 12, pp. 2053–2060, 2019.

[224] A. Abbas, N. Hussain, M.-J. Jeong, J. Park, K. S. Shin, T. Kim, and N. Kim, "A rectangular notch-band uwb antenna with controllable notched bandwidth and centre frequency," *Sensors*, vol. 20, no. 3, p. 777, 2020.

[225] M. J. Jeong, N. Hussain, H.-U. Bong, J. W. Park, K. S. Shin, S. W. Lee, S. Y. Rhee, and N. Kim, "Ultrawideband microstrip patch antenna with quadruple band notch characteristic using negative permittivity unit cells," *Microwave and Optical Technology Letters*, vol. 62, no. 2, pp. 816–824, 2020.

[226] X. Yang, H. Luyen, S. Xu, and N. Behdad, "Design method for low-profile, harmonic-suppressed filter-antennas using miniaturized-element frequency selective surfaces," *IEEE Antennas and Wireless Propagation Letters*, vol. 18, no. 3, pp. 427–431, 2019.

[227] N. Hussain, W. A. Awan, S. I. Naqvi, A. Ghaffar, A. Zaidi, S. A. Naqvi, A. Iftikhar, and X. J. Li, "A compact flexible frequency reconfigurable antenna for heterogeneous applications," *IEEE Access*, vol. 8, pp. 173 298–173 307, 2020.

[228] S. Ur Rahman, Q. Cao, Y. Wang, and H. Ullah, "Design of wideband antenna with band notch characteristics based on single notching element," *International Journal of RF and Microwave Computer-Aided Engineering*, vol. 29, no. 2, p. e21541, 2019.

[229] S. Luo, Y. Chen, D. Wang, Y. Liao, and Y. Li, "A monopole uwb antenna with sextuple band-notched based on srrs and u-shaped parasitic strips," *AEU-International Journal of Electronics and Communications*, p. 153206, 2020.

[230] M. S. Khan, S. A. Naqvi, A. Iftikhar, S. M. Asif, A. Fida, and R. M. Shubair, "A wlan band-notched compact four element uwb mimo antenna," *International Journal of RF and Microwave Computer-Aided Engineering*, p. e22282, 2020.

[231] J. Park, M. Jeong, N. Hussain, S. Rhee, S. Park, and N. Kim, "A low-profile high-gain filtering antenna for fifth generation systems based on nonuniform metasurface," *Microwave and Optical Technology Letters*, vol. 61, no. 11, pp. 2513–2519, 2019.

[232] N. Hussain, M. Jeong, J. Park, S. Rhee, P. Kim, and N. Kim, "A compact size 2.9-23.5 ghz microstrip patch antenna with wlan band-rejection," *Microwave and Optical Technology Letters*, vol. 61, no. 5, pp. 1307–1313, 2019.

[233] A. Iqbal, A. Smida, N. K. Mallat, M. T. Islam, and S. Kim, "A compact uwb antenna with independently controllable notch bands," *Sensors*, vol. 19, no. 6, p. 1411, 2019.

[234] J. Ghimire and D.-Y. Choi, "Design of a compact ultrawideband u-shaped slot etched on a circular patch antenna with notch band characteristics for ultrawideband applications," *International Journal of Antennas and Propagation*, vol. 2019, 2019.

[235] W. A. Awan, A. Zaidi, N. Hussain, S. Khalid, A. Baghdad *et al.*, "Characterization of dual band mimo antenna for 25 ghz and 50 ghz applications," in *2018 International Conference on Computing, Electronic and Electrical Engineering (ICE Cube)*. IEEE, 2018, pp. 1–4.

[236] ——, "Frequency reconfigurable patch antenna for millimeter wave applications," in *2019 2nd International Conference on Computing, Mathematics and Engineering Technologies (iCoMET)*. IEEE, 2019, pp. 1–5.

[237] A. H. Naqvi and S. Lim, "Design of polarization reconfigurable antenna using liquid metal," in *2018 International Symposium on Antennas and Propagation (ISAP)*. IEEE, 2018, pp. 1–2.

[238] A. Ghaffar, X. J. Li, and B.-C. Seet, "Dual frequency band and polarization reconfigurable antenna for mobile devices," in *2017 IEEE 17th International Conference on Communication Technology (ICCT)*. IEEE, 2017, pp. 696–700.

[239] A. Zaidi, A. Baghdad, W. A. Awan, A. Ballouk, A. Badri *et al.*, "Cpw fed wide to dual band frequency reconfigurable antenna for 5g applications," in *2019 International Conference on Wireless Technologies, Embedded and Intelligent Systems (WITS)*. IEEE, 2019, pp. 1–3.

[240] A. H. Naqvi and S. Lim, "A beam-steering antenna with a fluidically programmable metasurface," *IEEE Transactions on Antennas and Propagation*, vol. 67, no. 6, pp. 3704–3711, 2019.

[241] S. A. Naqvi and M. S. Khan, "Design of a miniaturized frequency reconfigurable antenna for rectenna in wimax and ism frequency bands," *Microwave and Optical Technology Letters*, vol. 60, no. 2, pp. 325–330, 2018.

[242] W. A. Awan, A. Ghaffar, N. Hussain, and X. J. Li, "A frequency reconfigurable flexible antenna for multiple mobile applications," in *2019 IEEE Asia-Pacific Microwave Conference (APMC)*. IEEE, 2019, pp. 813–815.

[243] M. Borhani, P. Rezaei, and A. Valizade, "Design of a reconfigurable miniaturized microstrip antenna for switchable multiband systems," *IEEE Antennas and Wireless Propagation Letters*, vol. 15, pp. 822–825, 2015.

[244] L. Han, C. Wang, X. Chen, and W. Zhang, "Compact frequency-reconfigurable slot antenna for wireless applications," *IEEE Antennas and Wireless Propagation Letters*, vol. 15, pp. 1795–1798, 2016.

[245] S. Ullah, S. Hayat, A. Umar, U. Ali, F. A. Tahir, and J. A. Flint, "Design, fabrication and measurement of triple band frequency reconfigurable antennas for portable wireless communications," *AEU-International Journal of Electronics and Communications*, vol. 81, pp. 236–242, 2017.

[246] I. Shah, S. Hayat, A. Basir, M. Zada, S. Shah, and S. Ullah, "Design and analysis of a hexa-band frequency reconfigurable antenna for wireless communication," *AEU-International Journal of Electronics and Communications*, vol. 98, pp. 80–88, 2019.

[247] Y. I. Abdulraheem, G. A. Oguntala, A. S. Abdullah, H. J. Mohammed, R. A. Ali, R. A. Abd-Alhameed, and J. M. Noras, "Design of frequency reconfigurable multiband compact antenna using two pin diodes for wlan/wimax applications," *IET Microwaves, Antennas & Propagation*, vol. 11, no. 8, pp. 1098–1105, 2017.

[248] A. Iqbal, A. Smida, L. F. Abdulrazak, O. A. Saraereh, N. K. Mallat, I. Elfergani, and S. Kim, "Low-profile frequency reconfigurable antenna for heterogeneous wireless systems," *Electronics*, vol. 8, no. 9, p. 976, 2019.

[249] T. T. Le, H.-Y. Park, and T.-Y. Yun, "Simple reconfigurable circularly polarized antenna at three bands," *Sensors*, vol. 19, no. 10, p. 2316, 2019.

[250] A. H. Naqvi and S. Lim, "Microfluidically polarization-switchable metasurfaced antenna," *IEEE Antennas and Wireless Propagation Letters*, vol. 17, no. 12, pp. 2255–2259, 2018.

[251] N. Ojaroudi Parchin, H. Jahanbakhsh Basherlou, Y. I. Al-Yasir, R. A. Abd-Alhameed, A. M. Abdulkhaleq, and J. M. Noras, "Recent developments of reconfigurable antennas for current and future wireless communication systems," *Electronics*, vol. 8, no. 2, p. 128, 2019.

[252] P. K. Li, Z. H. Shao, Q. Wang, and Y. J. Cheng, "Frequency-and pattern-reconfigurable antenna for multistandard wireless applications," *IEEE Antennas and Wireless Propagation Letters*, vol. 14, pp. 333–336, 2014.

[253] J. Liu, J. Li, and R. Xu, "Design of very simple frequency and polarisation reconfigurable antenna with finite ground structure," *Electronics Letters*, vol. 54, no. 4, pp. 187–188, 2018.

[254] W. Lin, H. Wong, and R. W. Ziolkowski, "Circularly polarized antenna with reconfigurable broadside and conical beams facilitated by a mode switchable feed network," *IEEE Transactions on Antennas and Propagation*, vol. 66, no. 2, pp. 996–1001, 2017.

[255] B. Mohamadzade, R. B. Simorangkir, S. Maric, A. Lalbakhsh, K. P. Esselle, and R. M. Hashmi, "Recent developments and state of the art in flexible and conformal reconfigurable antennas," *Electronics*, vol. 9, no. 9, p. 1375, 2020.

[256] X. He, P. Gao, Z. Zhu, S. You, and P. Wang, "A flexible pattern reconfigurable antenna for wlan wireless systems," *Journal of Electromagnetic Waves and Applications*, vol. 33, no. 6, pp. 782–793, 2019.

[257] M.-C. Tang, B. Zhou, Y. Duan, X. Chen, and R. W. Ziolkowski, "Pattern-reconfigurable, flexible, wideband, directive, electrically small near-field resonant parasitic antenna," *IEEE Transactions on Antennas and Propagation*, vol. 66, no. 5, pp. 2271–2280, 2018.

[258] K. Saraswat and A. R. Harish, "Flexible dual-band dual-polarised cpw-fed monopole antenna with discrete-frequency reconfigurability," *IET Microwaves, Antennas & Propagation*, vol. 13, no. 12, pp. 2053–2060, 2019.

[259] N. Nguyen-Trong, L. Hall, and C. Fumeaux, "A frequency-and pattern-reconfigurable center-shorted microstrip antenna," *IEEE Antennas and Wireless Propagation Letters*, vol. 15, pp. 1955–1958, 2016.

[260] Y. P. Selvam, M. Kanagasabai, M. G. N. Alsath, S. Velan, S. Kingsly, S. Subbaraj, Y. R. Rao, R. Srinivasan, A. K. Varadhan, and M. Karuppiah, "A low-profile frequency-and pattern-reconfigurable antenna," *IEEE Antennas and Wireless Propagation Letters*, vol. 16, pp. 3047–3050, 2017.

[261] S. N. M. Zainarry, N. Nguyen-Trong, and C. Fumeaux, "A frequency-and pattern-reconfigurable two-element array antenna," *IEEE Antennas and Wireless Propagation Letters*, vol. 17, no. 4, pp. 617–620, 2018.

[262] A. Iqbal, A. Smida, N. K. Mallat, R. Ghayoula, I. Elfergani, J. Rodriguez, and S. Kim, "Frequency and pattern reconfigurable antenna for emerging wireless communication systems," *Electronics*, vol. 8, no. 4, p. 407, 2019.

[263] M. K. Shereen, M. I. Khattak, M. Al-Hasan *et al.*, "A frequency and radiation pattern combo-reconfigurable novel antenna for 5g applications and beyond," *Electronics*, vol. 9, no. 9, p. 1372, 2020.

[264] Z. Zhu, P. Wang, S. You, and P. Gao, "A flexible frequency and pattern reconfigurable antenna for wireless systems," *Progress In Electromagnetics Research*, vol. 76, pp. 63–70, 2018.

[265] C. A. Balanis, *Antenna Theory: Analysis and Design*. John wiley & sons, 2016.

[266] A. Abbas, N. Hussain, M.-J. Jeong, J. Park, K. S. Shin, T. Kim, and N. Kim, "A rectangular notch-band uwb antenna with controllable notched bandwidth and centre frequency," *Sensors*, vol. 20, no. 3, p. 777, 2020.

[267] J. Buckley, K. G. McCarthy, L. Loizou, B. O'Flynn, and C. O'Mathuna, "A dual-ism-band antenna of small size using a spiral structure with parasitic element," *IEEE Antennas and Wireless Propagation Letters*, vol. 15, pp. 630–633, 2015.

[268] M. Usluer, B. Cetindere, and S. C. Basaran, "Compact implantable antenna design for mics and ism band biotelemetry applications," *Microwave and Optical Technology Letters*, vol. 62, no. 4, pp. 1581–1587, 2020.

[269] S. A. Naqvi and M. S. Khan, "Design of a miniaturized frequency reconfigurable antenna for rectenna in wimax and ism frequency bands," *Microwave and Optical Technology Letters*, vol. 60, no. 2, pp. 325–330, 2018.

[270] A. Basir, A. Bouazizi, M. Zada, A. Iqbal, S. Ullah, and U. Naeem, "A dual-band implantable antenna with wide-band characteristics at mics and ism bands," *Microwave and Optical Technology Letters*, vol. 60, no. 12, pp. 2944–2949, 2018.

[271] A. Hassan, S. Ali, G. Hassan, J. Bae, and C. H. Lee, "Inkjet-printed antenna on thin pet substrate for dual band wi-fi communications," *Microsystem Technologies*, vol. 23, no. 8, pp. 3701–3709, 2017.

[272] S. Ahmed, F. A. Tahir, and H. M. Cheema, "A flexible low cost fractal-slot multiband antenna for wireless applications," in *2015 9th European Conference on Antennas and Propagation (EuCAP)*. IEEE, 2015, pp. 1–4.

[273] M. Haerinia and S. Noghanian, "A printed wearable dual-band antenna for wireless power transfer," *Sensors*, vol. 19, no. 7, p. 1732, 2019.

[274] S. Masihi, M. Panahi, A. Bose, D. Maddipatla, A. Hanson, B. Narakathu, B. Bazuin, and M. Atashbar, "Rapid prototyping of a tunable and compact microstrip antenna by laser machining flexible copper tape," in *2019 IEEE International Conference on Flexible and Printable Sensors and Systems (FLEPS)*. IEEE, 2019, pp. 1–3.

[275] Y. Zhao, Y. Lv, T. Si, G. Du, M. Li, and Y. Yu, "Design of a miniaturized dual-frequency monopole antenna for applications in iot," in *2019 6th International Conference on Systems and Informatics (ICSAI)*. IEEE, 2019, pp. 1051–1055.

[276] P. Forouzannezhad, A. Jafargholi, and A. Jahanbakhshi, "Multiband compact antenna for near-field and far-field rfid and wireless portable applications," *IET Microwaves, Antennas & Propagation*, vol. 11, no. 4, pp. 535–541, 2016.

[277] S. Kim and M. M. Tentzeris, "Parylene coated waterproof washable inkjet-printed dual-band antenna on paper substrate," *International Journal of Microwave and Wireless Technologies*, vol. 10, no. 7, pp. 814–818, 2018.

[278] F. Khajeh-Khalili, F. Haghshenas, and A. Shahriari, "Wearable dual-band antenna with harmonic suppression for application in medical communication systems," *AEU-International Journal of Electronics and Communications*, vol. 126, p. 153396, 2020.